Modelling tumourigenesis and the stress response in *Drosophila melanogaster*

By Rhoda Katerina Anne Stefanatos

Submitted in fulfillment of the requirements for the Degree of Doctor of Philosophy

Beatson Institute for Cancer Research

College of Medical, Veterinary and Life science

University of Glasgow

September 2013

Abstract

Cancer is a complex group of heterogeneous diseases. Intensive research spanning almost 50 years has greatly broadened our understanding of how cancer forms and disseminates around the human body. Despite this, many open questions remain. In this time, there has been a rise in the use of alternative cancer models. One such cancer model is *Drosophila melanogaster*.

In this thesis I utilize *Drosophila* to: demonstrate a role of *Drosophila p120ctn* in the stress response and negative regulation of immune signalling; uncover novel mediators of *Apc* driven intestinal hyperplasia in the adult *Drosophila* midgut; and describe the role of the innate immune response in control of tumour burden in tumour bearing larvae.

p120ctn is the founding member of the p120ctn family of proteins and is essential for adherens junction formation and stability in mammalian epithelia. It is required for vertebrate development and is deregulated in many epithelial cancers. In *Drosophila*, a single p120ctn family member (*dp120ctn*) is not required for the formation of adherens junctions, development or homeostasis. I demonstrate that *dp120ctn* null adult flies are sensitive to specific stressors and possess a differential transcriptional profile reminiscent of infected flies. Additionally, combination of loss of *dp120ctn* with null mutations in polarity tumour suppressors resulted in increased tumour burden. Suggesting that *dp120ctn* may have conserved tumour suppressor activity.

Adenomatous polyposis coli (*Apc*) is frequently mutated in human colorectal cancer. *Apc* loss in the mouse intestine leads to rapid tumourigenesis. Here, we have uncovered novel regulators of the *Apc* phenotype in the adult *Drosophila* midgut and describe a paracrine signalling cross-talk required for *Apc* driven hyperplasia.

The systemic response to a growing tumour is poorly understood and cancer associated inflammation has paradoxical effects on tumour progression. Using *Drosophila* larval models of cancer we characterized the relationship between a growing tumour and the innate immune system. We demonstrate that larvae mount an immune response that requires activation of Toll signalling in the fat body and expression of Egr/TNF in the haemocytes to orchestrate tumour cell death and restrict tumour burden.

Table of Contents

List of Tables

List of Figures

Acknowledgements

I would first like to acknowledge my supervisor Dr Marcos Vidal. Marcos, I thank you for giving me the opportunity to do my PhD in your lab and for your mentorship these past 4 years. Thank you for giving me the freedom to work on so many projects in the lab and giving me both support and guidance when experiments did not go as planned. I hope the lab goes from strength to strength.

I would next like to thank Dr Julia Cordero for taking me under her wing when I joined the lab. Thank you for giving me the opportunity to work along side you and for teaching me everything I know about the fly gut. Thank you for always giving me honest and constructive advice. I know that you are going to make a great mentor and I wish you every success in the future.

A heartfelt thanks goes out to my friend and colleague Dr Federica Parisi. Working with you so closely over the last year has brought a lot of laughter but also great science. I have learned a lot from you, namely that everything can be beautiful even a graph? No but seriously as friends we have supported each other in good and bad moments and as colleagues we push each other to be better. I know that this will continue.

I was not on this roller-coaster alone. I had the pleasure of spending the last four years with the soon to be Dr Juanita Macagno. You have been a fantastic bench mate, making fun of me all the time. I would not change a minute. I sincerely wish you all the best.

I would also like to thank the rest of the Vidal lab: Dr Alessandro Scopelliti, Ale thanks for always giving me useful comments and never complaining about how much noise I make; our newly joined S.O Dr Yachuan Yu, I look forward to working with you in the next few months. A very big thank you goes out to our previous S.O Karen Strathdee who has been a great colleague and supportive friend over the last four years. Thank you for all your help, advice and for always putting a smile back on my face. I thank all my friends at the Beatson who have made the last four years so great.

To all my friends all over the world I love you: Alberto, Rach, Vassia, Tito, Matthew and everyone I have no space to mention, thank you for being in my life. To my little sister, Dimitroula I hope you are proud of your big sister

because I am proud of you, love you always. To my Dad, I love you and miss you. To my Auntie Ruth, thank you for always taking an interest in my work.

Finally, I would like to dedicate this thesis to my mum. Mum, you are my best friend and you have made me who I am. What I have achieved is because of you. You have inspired, loved and taken care of me.

Author's Declaration

I declare that I am the sole author of this thesis. All research presented here is my own except where explicit reference is made to the contribution of others. This work has not been submitted for any other degree at the University of Glasgow or any other institution.

Rhoda Katerina Anne Stefanatos

Publications arising from this work

Cordero JB*, **Stefanatos RKA***, Myant K, Vidal M, Sansom OJ (2012) Non-autonomous crosstalk between the Jak/Stat and Egfr pathways mediates Apc1-driven intestinal stem cell hyperplasia in the *Drosophila* adult midgut. *Development* **139:** 4524-4535

Parisi F*, **Stefanatos RKA***, Strathdee K, Vidal M (2013) A systemic relay between *Drosophila* macrophages and adipose tissue restrains tumour growth via apoptosis. Under Review

Stefanatos RKA, Bauer, Christin Vidal M (2013) p120 catenin is required for the stress response in *Drosophila*. Accepted

* Equal contribution

Abbreviations

˚C	Degrees centigrade
♀	Female
♂	Male
aa	amino acid(s)
AMPs	Antimicrobial peptides
ANOVA	Analysis of Variance
Apc	Adenomatous polyposis coli
AttA	Attacin A
AttB	Attacin B
AttC	Attacin C
AttD	Attacin D
BSA	Bovine serum albumin
Caspase	Cysteine-aspartic protease
CC3	Cleaved caspase 3
CO2	Carbon dioxide
d	day(s)
DAPI	4',6-diamidino-2-phenylindole
dau	daughterless
Def	Defensin
DGRC	Drosophila Genetic Resource Center
DIAP1	Drosophila Inhibitor of Apoptosis Protein 1
DIF	Dorsal related immunity factor
dlg	discs large
DNA	Deoxyribonucleic acid
dp120ctn	*Drosophila* p120 catenin
dpp	decapentaplegic
DptB	Diptericin B
Drs	Drosomycin
DSHB	Developmental Studies Hybridoma Bank
DTT	dithiothreitol
Dv	Dorsal vessel
EBs	Enteroblasts
ECs	Enterocytes
EDTA	Ethylenediaminetetraacetic acid
ee	Enteroendocrine cells
EGF	Epithelial growth factor
EGFR	Epidermal growth factor receptor
Egr	Eiger
EGTA	Ethyleneglycoltetraacetic acid
esg	escargot
ey	eyeless
FADD	Fas-Associated protein with Death Domain
FLP	Flippase
FRT	Flippase recognition target
GFP	Green fluorescent protein

h/hr	hour(s)
H_20_2	Hydrogen peroxide
he	hemese
hid	head involution defective
hml	hemolectin
imd	immune deficiency
InR	Insulin Receptor
IP	immunoprecipitation
IR	RNA interference line
Ird5	immune response deficient 5
ISCs	Intestinal stem cells
JNK	c-Jun N-terminal kinase
kb	Kilobase Pairs
kDa	kilo Dalton
KO	Knock out
lgl/lg(2)l	lethal giant larvae
MAPK	Mitogen activated protein kinase
MARCM	Mosaic analysis with a repressible cell marker
mins	minutes
ml	microlitre
mM	millimolar
mm	micrometre
MMP1	Matrix metalloproteinase 1
MOPS	3-(N-morpholino)propanesulfonic acid
Mtk	Metchnikowin
MyoIA	Myosin IA
NaCl	Sodium chloride
NF-κB	Nuclear factor kappa-light-chain-enhancer of activated B cells
n°	number
p120ctn	p120 catenin
PAGE	Polyacrylamide gel electrophoresis
PBS	phosphate buffered saline
PBS-T	phosphate buffered saline triton X-100
PGRP-	Peptidoglycan recognition protein
PIPES	piperazine-N,N′-bis(2-ethanesulfonic acid)
ppl	pumpless
PVDF	Polyvinylidene Fluoride
Pvf1	PDGF- and VEGF-related factor 1
Pvr	PDGF- and VEGF-related receptor
qPCR	Quantitative Polymerase chain reaction
Ras	Rat sarcoma
Rel	Relish
RFP	Red fluorescent protein
RNA	Ribonucleic acid
RNAi	RNA interference
ROS	Reactive oxygen species
scrib	scribble

SDS	sodium dodecyl sulfate
SEM	Standard error of the mean
SPE	Spätzle processing enzyme
Spn4	Serpin 42Da
spz	Spätzle
TAH	Tumour associated haemocytes
TBL	Tumour bearing larvae
TBS	Tris-buffered saline
TBST	Tris-buffered saline Tween 20
TLR	Toll-like receptor
TNF	Tumour necrosis factor
TNFR	Tumour necrosis factor receptor
ts	Temperature sensitive
tub	tubulin
UAS	upstream activating sequence
Ubi	ubiquitin
VDRC	Vienna Drosophila RNAi Center
VEGFR	Vascular endothelial growth factor receptor
Vg	Vestigial
wt	wild type

1 Introduction

1.1 Cancer

Cancer is a complex family of diseases, which can affect nearly every organ and system in the human body. For a tumour to establish itself it must integrate several "hallmarks" of cancer (Hanahan and Weinberg, 2011). These include the ability to sustain proliferative signalling while at the same time becoming insensitive to apoptotic signals (Hanahan and Weinberg, 2011). This occurs when cells acquire activating mutations in oncogenes and deactivating mutations in tumour suppressor genes. Tumour progression is a complex and multistep process that is affected by interactions with the surrounding normal tissue and the immune system (Hanahan and Weinberg, 2011). Once a primary tumour has exhausted its site of origin, tumour cells undergo further changes in order to invade and metastasize to a new location within the body (Hanahan and Weinberg, 2011). It is these latter phases of cancer progression that are the most lethal. During this process tumour cells engage in local invasion where they drive remodelling of the extracellular matrix (Hanahan and Weinberg, 2011). Invasive cells will enter a local blood or lymphatic vessel in order to reach other sites in the body. The cells will exit the vessel and form "micro-metastases" and eventually secondary tumours (Hanahan and Weinberg, 2011). Despite intensive studies in cell culture and in mouse models, many open questions remain. More recently, non-mammalian models like zebrafish and *Drosophila melanogaster* are been utilized to investigate aspects of tumourigenesis and tumour progression (White et al., 2013, Gonzalez, 2013).

1.2 *Drosophila* as a model organism

Drosophila melanogaster, also known as the fruit or vinegar fly, has been utilized as a model organism for over 100 years and has contributed greatly to the understanding of genetics and development (Schneider, 2000). Currently, *Drosophila* is one of the most characterized and widely used animal models. *Drosophila* research is providing insights into our understanding of ageing, neurodegenerative diseases, immunity, diabetes, addiction and cancer (Adams et al., 2000, Chan and Bonini, 2000, Vidal and Cagan, 2006, Stefanatos and

Vidal, 2011, Valanne et al., 2011). A key to its popularity is the array of available tools for genetic manipulation. Temporal and spatial control of gene expression through the use of the yeast derived GAL4/UAS system, as well as the creation of genetically distinct mosaic clones allow in detail analysis of complicated and dynamic events (Brand and Perrimon, 1993, Theodosiou and Xu, 1998, Lee and Luo, 2001). There is remarkable conservation of signalling pathways between flies and humans despite the evolutionary distance. Moreover, the *Drosophila* genome is significantly less redundant than the human genome making the genetic dissection of pathways simpler (Adams et al., 2000).

1.2.1 The *Drosophila* Life Cycle

The *Drosophila melanogaster* life cycle consists of an embryonic stage, followed by a larval stage, a pupa stage (metamorphosis) and finally the adult stage (Fig 1.1). This life cycle takes approximately 10 days at 25°C. Adult *Drosophila* live around 70 days at 25°C and in that time can produce hundreds of offspring. Adult female flies become sexually mature within 8-12 hrs and each female can lay around 300 eggs. The embryos hatch 16 hrs after deposition and the hatched larvae proceed to eat for the next 5 days and undergo two molting stages. The mature third instar larvae wander out of the food and look for a dry place to pupate. After pupariation during metamorphosis, some larval tissues are remodeled and others removed completely as the adult fly develops. Many of the structures that will make up the adult fly are derived from epithelial mitotic sacs known as the imaginal discs (Lewis I. Held, 2002, Weigmann et al., 2003).

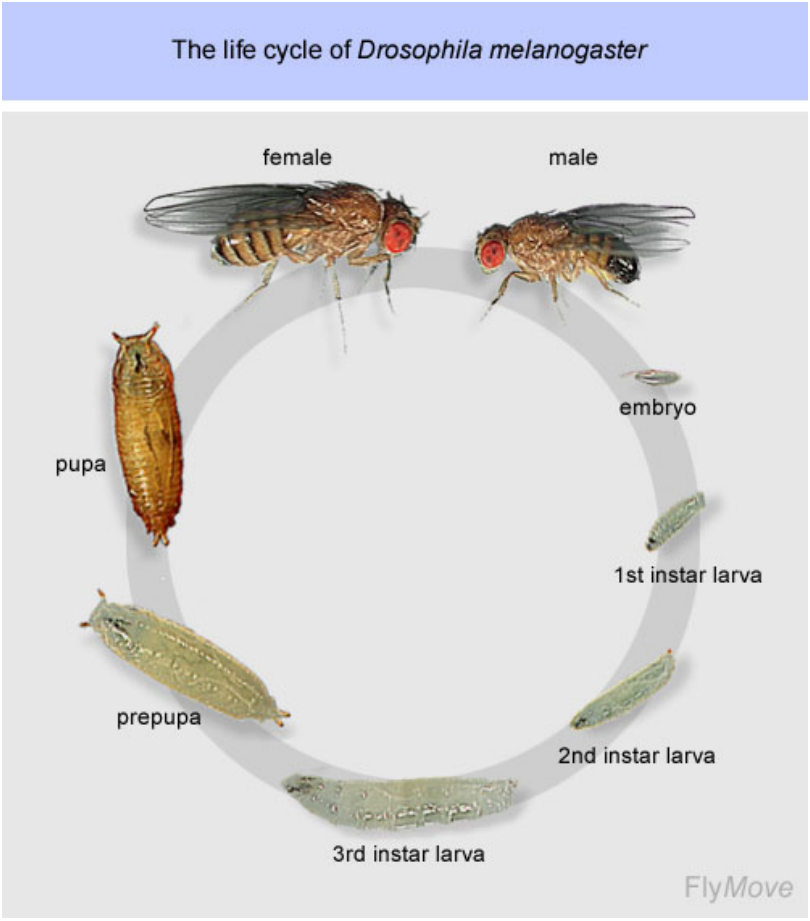

Figure 1.1 The life cycle of *Drosophila melanogaster*.

Picture depicting the life cycle of *Drosophila melanogaster*. From egg to adult fly, development takes 10 days at 25°C. Taken from (Weigmann et al., 2003).

1.2.2 *Drosophila* Genetics and Husbandry

Drosophila melanogaster are one of the cheapest laboratory animals to culture, as they require very little space and starting equipment. They can be kept in either vials or bottles that contain an agar set yeast-sugar medium (see Chapter 2) that they eat and lay eggs on to. They are cold and oxygen sensitive and can be cultured at temperatures varying from 18-29°C using incubators or dedicated "Fly rooms".

The *Drosophila* genome contains around 15,000 genes arranged on just 4 chromosomes. They are the X (1^{st}), 2^{nd}, 3^{rd} and 4^{th} chromosomes that are divided by the centromeres into left and right arms. *Drosophila* were historically used to uncover the nature of genes this led to the isolation of many mutants from the natural population. Mutagenic agents such as X-ray irradiation, Ethyl methanesulphonate and transposable *P*-elements have been used over the years to isolate new mutants and therefore discover new genes required for development of *Drosophila*. The ability to easily generate mutants allowed researchers to do large screens looking for aberrations in patterning and morphology in the early embryo as well as in the adult stage of development. This painstaking work is responsible for much of our understanding of *Drosophila* development. In the early 1990's two more tools were added to the *Drosophila* tool kit, the GAL4/UAS and the FLP-FRT systems are in later sections.

Experimental crosses are normally performed at 25°C using virgin females and males from stock cultures that carry mutations or transgenes that we want to combine. As it would be highly impractical to genotype all the progeny every time you perform a cross, we use phenotypic markers, such as curly wings or eye colour and shape, that are associated to the gene or transgene we are interested in so that we the progeny of interest can be identified by the presence or absence of these phenotypic markers. These stock cultures are a very important part of any *Drosophila* laboratory and the flies need to be transferred to new food every 2-3 weeks. However, if any disasters do occur there are major stock centers that hold and maintain many thousands of essential *Drosophila* stocks from which stocks can be ordered. Another very important tool in *Drosophila* genetics are the "Balancer Chromosomes". Balancer chromosomes are chromosomes that carry multiple inversions and rearrangements and therefore cannot recombine with wild type chromosomes. They normally also carry one or

multiple dominant markers and recessive lethal markers making them indispensable for maintaining mutants stocks and for following complicated genetic combinations.

1.2.3 Targeted gene expression in *Drosophila* using the Gal4/UAS system

Gal4 is a yeast transcriptional activator that binds to an upstream activating sequence (UAS), which contains Gal4 binding sites. Using this system, it is possible to express any cloned gene that is flanked by UAS (Brand and Perrimon, 1993). It is a binary system, where the Gal4 and the UAS target gene are expressed by different transgenic flies that must be combined through mating to drive expression (Brand and Perrimon, 1993) (Fig 1.2).

1.2.3.1 Extensions of the Gal4/UAS system: Gal80.

The Gal80 repressor binds to Gal4 transcriptional activation domain and blocks its activity (Ma and Ptashne, 1987). Thus, expression of Gal80 can be used to prevent Gal4-driven expression. Temperature sensitive variants of Gal80 protein ($Gal80^{ts}$) allow temporal control over Gal4/UAS expression through changes in temperature (Matsumoto et al., 1978, McGuire et al., 2003). At the permissive temperature Gal80 becomes inactive and allows Gal4 to activate the transcription.

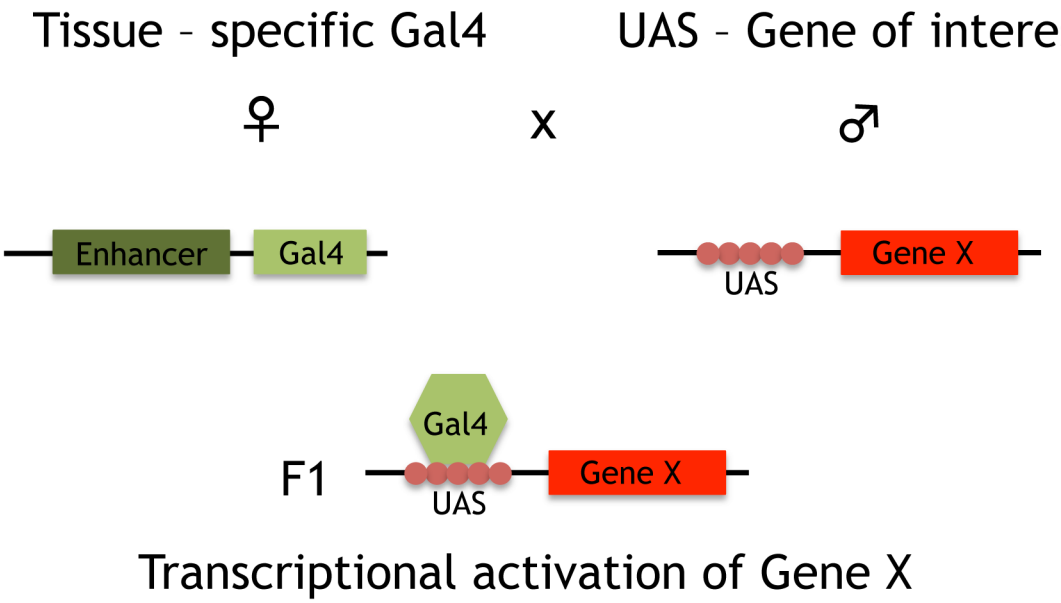

Figure 1.2 The Gal4/UAS system for targeted gene expression.

Schematic describing the Gal4/UAS system for targeted gene expression. The system consists of two components: the yeast transcriptional activator Gal4 (green hexagon) and the Upstream Activating Sequence (UAS) (red circles) element containing eukaryotic elements which are bound by Gal4 to activate gene expression. Placing Gal4 downstream of a tissue specific enhancer element (dark green rectangle) results in tissue specific expression of Gal4. Placing a UAS upstream of any gene will result in expression of this gene in tissues also expressing Gal4.

1.2.4 The FLP/FRT system

In *Drosophila,* we can create genetically distinct clones of cells using the yeast derived site-specific recombinase FLP coupled with FLP recombination targets (FRT) (Dang and Perrimon, 1992, Theodosiou and Xu, 1998) (Fig 1.3). This system works having identical FRT recombination sites for the FLP to act on. There are FRT sites on each on the major arms of 3 of the 4 chromosomes. The introduction of this system allowed the analysis of mutations in clones of cell that could be engineered in a specific tissue, by controlling the expression of the FLP by placing downstream of a tissue specific enhancer, and at a specific developmental time point, by using a temporally regulated enhancer, allowing a much more sophisticated functional dissection of essential genes. This simple method can also be used to overexpress UAS transgenes in a subset of cells in an otherwise wild type animal. This type of experiment can be very useful when trying to look for genes that may cooperate or are required for a mutant phenotype, enhancers or suppressors.

1.2.4.1 Mosaic analysis with a repressible marker (MARCM)

The MARCM system is an extension of the FLP/FRT system with which we can uniquely mark homozygous mutant clones (Fig 1.4, see legend for more details) (Lee and Luo, 2001) and utilizes the Gal4 repressor Gal80 (Fig 1.4, see legend for more details). This is important as it means that you can easily score clone size and number by expressing GFP or RFP to mark the cells your interested in. This system has successfully been used to screen for genes with a role in oncogenic cooperation and interactions with the tumour microenvironment. In this thesis, we have utilized a temperature sensitive form of the Gal4 repressor Gal80 to understand the contribution of different signalling pathways to pre-established *Apc1* dependent hyperproliferation in the *Drosophila* midgut.

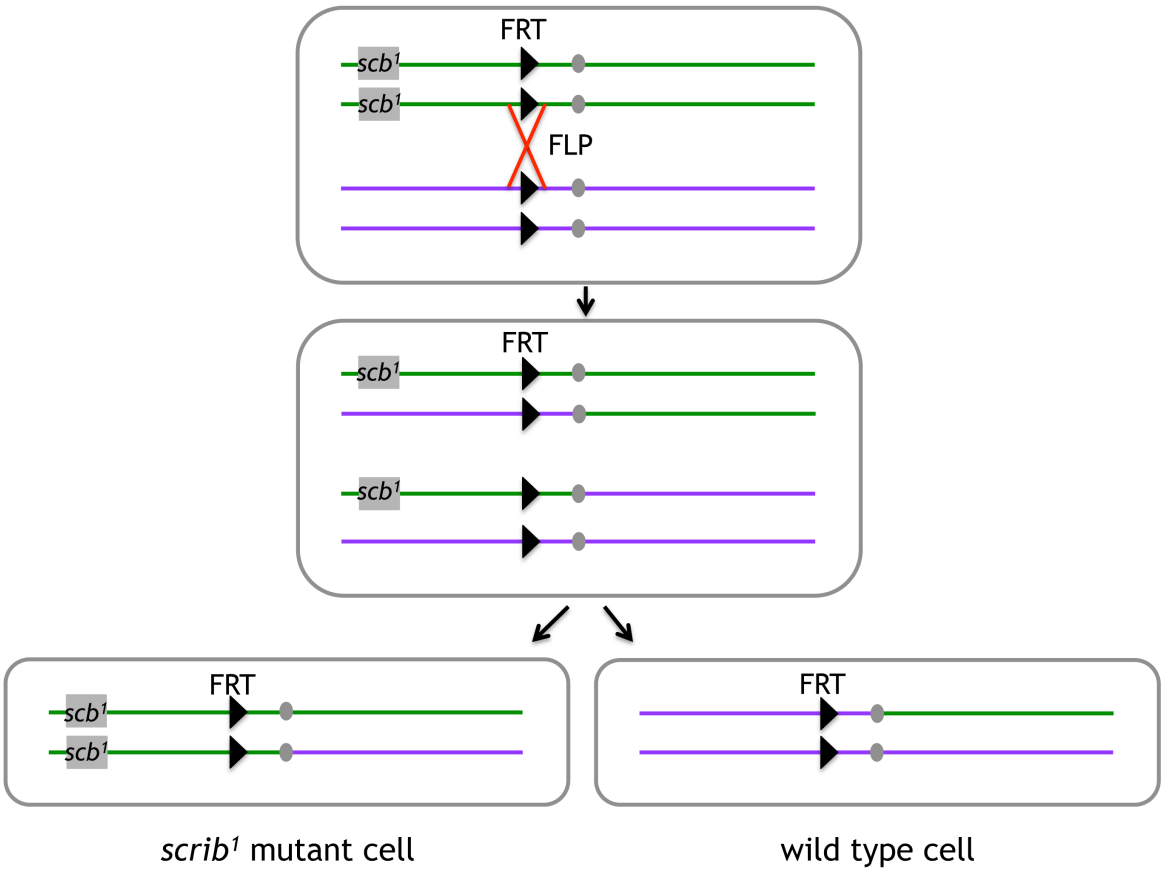

Figure 1.3 The FLP/FRT system

Schematic diagram depicting how use of the FLP/FRT system allows creation of in this case *scribble* (*scrib*) mutant cells. In this diagram you can see both 3rd chromosomes (Green and Purple line) of *Drosophila* carrying one copy of a mutant allele for the *scribble* gene (grey box) and FRT sites at identical positions (black arrowhead). After DNA replication, the FLP recombinase mediates recombination of the region of the chromosome distal to the FRT site. In this example, mitosis leads to the formation of a *scribble* mutant cell and a wild type cell in a fly that will be heterozygous for *scribble*. This is important for probing the roles of genes that have essential functions but are haplosufficient.

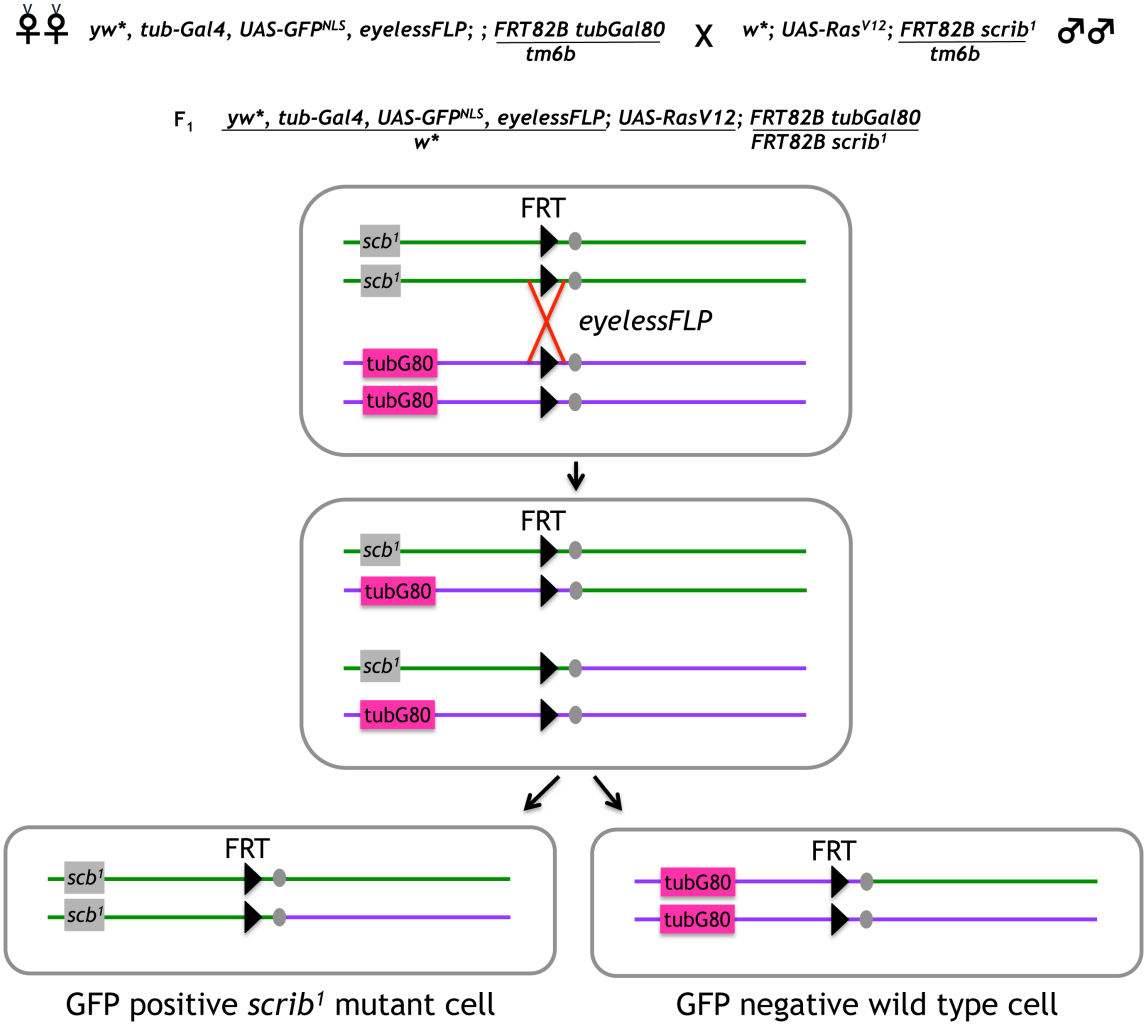

Figure 1.4 Mosaic analysis with a repressible marker system (MARCM)

Crossing scheme and schematic diagram depicting how the addition of the Gal4 repressor Gal80 (see Fig 1.2) to the FLP/FRT system (see Fig 1.3) allows creation of *scribble* (*scrib*^{1}) mutant cells which will also be marked with GFP (*UAS-GFP*^{NLS}) and over express oncogenic *Ras* (*UAS-Ras*^{V12}) specifically in the eye (eyeless (eye specific gene) FLP. In this diagram you can see both 3rd chromosomes (Green and Purple line) of the F_1 carrying either a copy of a mutant allele for the *scribble* gene (grey box) or Gal80 under control of the tubulin enhancer (magenta box) distal to FRT sites (black arrowhead). After DNA replication, the FLP recombinase mediates recombination of the region of the chromosome distal to the FRT site. In this example, mitosis leads to the formation of a GFP positive *scribble* mutant cell expressing oncogenic *Ras* and a GFP negative type cell in the eye of flies that will be otherwise wild type. It is important to note that all the cells carry all the transgenes and mutations however only cells in which the

eyeless promoter is active will recombination occur and only in those cells where Gal80 is no longer present will GFP and oncogenic Ras be expressed.

1.2.5 The *Drosophila* Imaginal Discs

In the *Drosophila* larvae, each imaginal disc is located in a specific location along the length of the animal (Lewis I. Held, 2002). As the larval stage progresses the imaginal discs proliferate and become locked in a developmental fate (Lewis I. Held, 2002). This is orchestrated by specific and discrete expression of several morphogens. By the late 3rd instar larval stage each imaginal disc is a highly folded monolayer of columnar pseudo-stratified epithelium with a layer of squamous epithelium known as the "peripodial membrane" (Lewis I. Held, 2002). During metamorphosis (pupa stage) stage the imaginal discs elongate and evert to form the adult structures that they are programmed to produce (Lewis I. Held, 2002).

1.2.5.1 The Wing Imaginal Disc

Each *Drosophila* larvae contains a pair wing imaginal discs that will form the adult wings and body wall during metamorphosis (Lewis I. Held, 2002). The wing disc is divided along the anterior/posterior and dorsal/ventral axes (Lewis I. Held, 2002). These boundaries are defined by expression of *Decapentaplegic* (*Dpp*) (A/P) and Vestigial (*Vg*) (D/V) (Lewis I. Held, 2002). As wing development and cell fate is highly controlled we are able to use these discreet patterns of expression together with the Gal4/UAS system to overexpress or down-regulate genes within specific compartments (Brand and Perrimon, 1993).

1.2.6 The Adult *Drosophila* Intestine

The adult *Drosophila* intestinal tract is a simple tube made up of a monolayer epithelium surrounded by a layer of visceral muscle and trachea (Cordero and Sansom, 2012). The trachea represent the respiratory system of *Drosophila* and are a network of tubular chitin that delivers oxygen around the fly (Campos-Ortega, 1985.). The *Drosophila* gut can be divided into 3 main regions, the foregut, midgut and hindgut (Buchon et al., 2013). The midgut, which is the main site of digestion, is lined by a semipermeable peritrophic matrix that regulates the passage of material from the lumen to the enterocytes below (Buchon et al., 2013). The midgut is made up of large absorptive Enterocytes (ECs), small Enteroendocrine cells (ee), pluripotent intestinal stem cells (ISCs)

and transient Enteroblasts (EBs) (Ohlstein and Spradling, 2006, Micchelli and Perrimon, 2006). The midgut can also be subdivided into the anterior, middle and posterior midgut (Buchon et al., 2013). Most studies including the work in this thesis focus on the posterior midgut (Buchon et al., 2013).

1.2.7 The *Drosophila* Immune system

The *Drosophila* Immune system comprises of only an innate immune response that includes both systemic and local responses to bacterial and fungal infection (Charroux and Royet, 2010). Pathogenic infection induces a systemic response that is accompanied by striking changes in gene transcription. These transcriptional changes are regulated by the Toll and Immune deficiency (Imd) signalling pathways (De Gregorio et al., 2001, De Gregorio et al., 2002). Activation of these pathways is required for resistance to bacterial and fungal infection (Lemaitre et al., 1996, Rutschmann et al., 2002).

At the cellular level the *Drosophila* immune response is carried out by the haemocytes that phagocytize bacteria and the fat body that produces antimicrobial peptides (AMPs) and secretes them into the haemolymph (Lemaitre and Hoffmann, 2007). The *Drosophila* genome encodes for around 20 AMPs belonging to seven classes. Analysis of their promoter regions of has shown Toll, Imd or Toll and Imd transcriptional regulation of these genes (Boman et al., 1972, Bangham et al., 2006, Lemaitre and Hoffmann, 2007). AMPs are small cationic peptides whose mechanism of action is still unknown but increasing the genetic dose of these peptides has been shown to promote resistance to infection (Tzou et al., 2002).

1.2.7.1 The Toll pathway

The *Drosophila* Toll pathway is an evolutionary conserved signalling pathway that is required for resistance to fungal and gram-positive bacterial infection (Valanne et al., 2011) (Fig 1.5). The pathway is activated when a cleaved Spätzle dimer binds to the Toll receptor (Lemaitre et al., 1996, Valanne et al., 2011, Shia et al., 2009). Once activated, the Toll receptor binds to the Myd88 adaptor that interacts with tube and pelle, leading to the phosphorylation and eventual degradation of cactus, a negative regulator of the pathway (Valanne et

al., 2011). Once cactus has been degraded, the Rel/NF-κB like transcription factors Dorsal and Dorsal related immunity factor (DIF) translocate to the nucleus where they activate transcription of many antimicrobial genes (Lemaitre and Hoffmann, 2007, Valanne et al., 2011). In *Drosophila*, the specificity of Toll activation to gram-positive bacteria and fungi is achieved through recognition proteins that activate Spätzle processing enzyme (SPE) to cleave Spätzle (Michel et al., 2001). This ensures that Toll signalling is only activated during infection with gram-positive bacteria or fungi.

1.2.7.2 The Imd pathway

The *Drosophila* Imd pathway was named after the *imd* immune deficient mutants (Lemaitre et al., 1995) (Fig 1.5). Imd signalling is induced upon infection with gram-negative bacteria (Gottar et al., 2002). The membrane bound peptidoglycan recognition protein LC (PGRP-LC) is activated by binding of peptidoglycan (Gottar et al., 2002). Once activated PGRP-LC interacts with Imd at the cell surface. Imd is then bound by the FADD adaptor intracellularly (Lemaitre and Hoffmann, 2007). FADD recruits the Dredd caspase that will cleave phosphorylated Relish and allow nuclear translocation of the Rel domain to activate transcription of antimicrobial peptides like *Diptericin* and *Attacin* (Lemaitre and Hoffmann, 2007). This cascade also requires the IKK signalling complex composed of IKKβ/Kenny (Key) and IKKγ/ird5 that phosphorylates Relish (Lemaitre and Hoffmann, 2007). This is postulated to happen upon activation of IKK by the MAP3K TAK1 and the adaptor TAB2 and may be dependent on FADD or *Drosophila* Inhibitor of Apoptosis 2 (DIAP2) (Lemaitre and Hoffmann, 2007). Mutations in any of these canonical components of Imd signalling results in phenotypes that phenocopy that of the original *imd* mutants (Lemaitre et al., 1995). Although Imd signalling is not fully understood, it is known that Imd signalling is carefully regulated (Lemaitre et al., 1997, Boutros et al., 2002). Many positive regulators and negative regulators have been identified and are thought to limit the response to infection (Kleino et al., 2008). This is in accordance with the expression patterns observed for Imd specific AMPs (Lemaitre et al., 1997). The *Drosophila* Imd signalling pathway closely resembles the mammalian TNFR signalling pathway as they share many components (Lemaitre and Hoffmann, 2007).

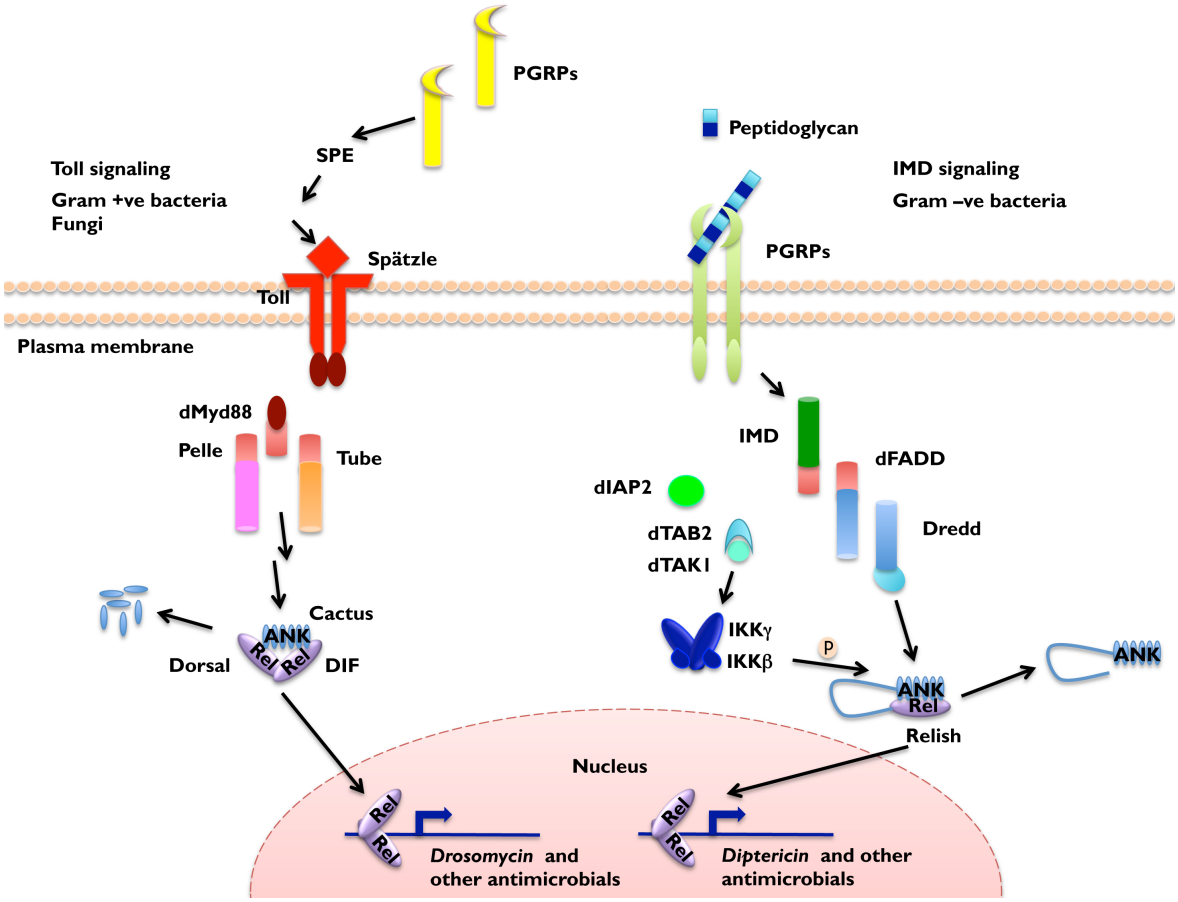

Figure 1.5 The Toll and IMD pathways

The Toll signalling pathway (analogous to the mammalian Toll like Receptor signalling pathway) is activated when the ligand Spätzle binds the Toll receptor upon infection with gram +ve bacteria. This leads to the release of the NF-κB like transcription factors Dorsal and DIF to translocate to the nucleus and induce many Toll regulated antimicrobial genes. The Immune Deficiency (Imd) pathway (that shares many components with the mammalian TNFR signalling pathway) is activated upon infection with gram –ve bacteria. Pattern recognition receptors detect the presence of bacterial peptidoglycan that leads to cleavage of the NF-κB like transcription factor relish allowing it to translocate to the nucleus and induce many Imd regulated antimicrobial genes (PGRP-Pattern recognition receptor protein). See text for more details.

1.2.7.3 The Drosophila haemolymph

Drosophila haemolymph is analogous to mammalian blood (Parisi and Vidal, 2011). However unlike in mammals there is no vasculature in *Drosophila*. Instead, the fly possesses an open circulatory system where the organs are bathed in the haemolymph that contains haemocytes (blood cells), nutrients and factors secreted by the peripheral tissues and is pumped around by the *Drosophila* heart or Dorsal Vessel (DV) (Bate and Martinez-Arias, 1993, Meister and Lagueux, 2003). The haemocytes originate from the procephalic mesoderm and are important for embryonic development, metamorphosis and innate immunity (Meister and Lagueux, 2003, Wood and Jacinto, 2007). They compose of three classes, the plasmatocytes, the lamellocytes and the crystal cells. The plasmatocytes, analogous to mammalian macrophages or monocytes, are responsible for phagocytosis of apoptotic cells and microorganisms and act as immune surveillance cells (Meister and Lagueux, 2003, Wood and Jacinto, 2007). The lamellocytes, which have a flat and spread morphology, are important for a process called encapsulation that is induced when parasitoid wasps lay their eggs in the larvae (Lemaitre and Hoffmann, 2007). Finally the crystal cells are important for melanization at sites of injury.

1.2.7.4 The Drosophila Fat body

The *Drosophila* fat body is a storage and secretory tissue. It is analogous to the mammalian liver and adipose tissue (Boman et al., 1972). It is part of the systemic immune response and is the site of antimicrobial peptide (AMPs) production (Boman et al., 1972).

1.3 *Drosophila* as a model in Cancer research

Drosophila models of cancer have been successfully utilized to model diverse aspects of tumour progression (Vidal and Cagan, 2006, Stefanatos and Vidal, 2011, Rudrapatna et al., 2012, Gonzalez, 2013). The use of *Drosophila* to model cancer allows *in vivo* analysis of genetically defined tumours in a highly tractable and well established invertebrate model (Vidal and Cagan, 2006, Stefanatos and Vidal, 2011, Rudrapatna et al., 2012, Gonzalez, 2013).

Although not widely appreciated, early fruit fly research reported the development of hereditary tumours (Stark, 1918, Harshbarger and Taylor, 1968, Gateff, 1978) and the first tumour suppressor was isolated in *Drosophila* (Stern and Bridges, 1926). This discovery provided early evidence for the existence of tumour suppressor genes and predates the discovery of mammalian tumour suppressors by many decades. Recent studies in ageing flies demonstrated the presence of tumours in a significant proportion of adult flies (Salomon and Jackson, 2008). Moreover, many components of signalling pathways like the Wnt, TGF-β and Notch pathways that are often miss-regulated in cancer were first discovered in *Drosophila* (Greenwald, 1998, Raftery and Sutherland, 1999, Cadigan and Peifer, 2009). Thus, *Drosophila* is a powerful model for cancer research.

1.3.1 The *scribble* group of polarity tumour suppressors

The *scribble* (*scrib*) group of polarity regulators includes *scrib*, *discs large* (*dlg*) and *lethal giant larvae* (*lgl*) (Bridges and Brehme, 1944, Mechler et al., 1985, Bilder et al., 2000, Bilder and Perrimon, 2000). These proteins define apico-basal polarity in *Drosophila* epithelia and are well conserved (Bilder and Perrimon, 2000, Bilder et al., 2000, Dow et al., 2003, Lohia et al., 2012). Loss of function mutations in any of these genes results in loss of apico-basal polarity and neoplastic overgrowth of the brain and imaginal discs of developing larvae (Bilder and Perrimon, 2000, Bilder et al., 2000, Humbert et al., 2008). Homozygous mutant larvae become arrested at the larval stage and die as giant larvae (Woods and Bryant, 1991, Bilder et al., 2000). In order to build more relevant models of cancer, Mosaic Analysis with a Repressible Cell Marker system (MARCM) which allows the establishment of homozygous mutant cell clones within a heterozygous and thus normal tissue, was used to create clones of cells mutant for *scrib* group tumour suppressors specifically in the eye imaginal disc (Brumby and Richardson, 2003). Alone these mutant clones rapidly disappear from the epithelium through JNK dependent apoptosis (Brumby and Richardson, 2003). However, if the Ras^{V12} oncogene was overexpressed together with loss of *scrib* within the clones, the clones proliferated and formed invasive neoplasia with metastasis that killed the larvae ($eyRas^{V12}$; $scrib^{1}$) (Brumby and Richardson,

2003, Pagliarini and Xu, 2003). These studies together demonstrate the power of *Drosophila* as a tool to uncover novel regulators of invasion and metastasis.

2 Materials and Methods

2.1 Flies

2.1.1 Fly husbandry

Flies were crossed and maintained on standard media in incubators with temperatures varying from 18°C to 29°C with a controlled 12hr-light: 12hr-dark cycle. Fly were anaesthetised using CO_2, pushed using paintbrushes and visualised using a Leica dissection microscope. All experiments were carried out at 25°C unless otherwise stated. Stocks were maintained at 18°C.

Standard Media: 10g Agar, 15g Sucrose, 30g Glucose, 15g Maize meal, 10g wheat germ, 30g treacle and 10g Soya flour per litre of distilled water.

10ml of Nipagin/Methylparaben (Deutscher scientific, Anti-fungal) and 5ml of Propionic acid (Fisher, anti bacterial agent) per litre distilled water were also added to the food mix.

Food was prepared by Beatson Central services according to this recipe.

2.1.2 Fly stocks

Fly stocks were kindly provided to us by our colleagues or obtained from the Bloomington, Drosophila Genome Resource (DGRC) and Vienna Drosophila RNAi Centre (VDRC) stock collections. A full list of stocks and their sources can be found in Table 2.1.

Strain/Genotype/Class	Description	Source/Reference
Control strains		
Canton S	Wild type strain of *Drosophila*	Vidal lab stocks
w^{1118}	allele of white mutant - flies have white eyes.	Vidal lab stocks
Strain/Genotype/Class	**Description**	**Source/Reference**
Mutants		
$Apc1^{Q8}$	loss of function allele, point mutation isolated from screen	(Ahmed et al., 1998)
$Apc1^{x1}$	loss of function allele, point mutation isolated from screen	(Ahmed et al., 1998)
$Apc1^{S76}$	loss of function allele, point mutation isolated from screen	(Ahmed et al., 1998)
$scrib^{1}$	loss of function allele of scribble created by EMS mutagenesis	(Bilder and Perrimon, 2000)
$dlg^{40.2}$	loss of function allele of discs large for PDZ created by p-element excision	(Mendoza-Topaz et al., 2008)
$l(2)gl^{4}$	loss of function allele of lethal giant larvae, natural mutation isolated from population	(Bridges and Brehme, 1944)
egr^{1}	loss of function allele of eiger created by p-element excision	(Igaki et al., 2002)
egr^{3}	loss of function allele of eiger created by p-element excision	(Igaki et al., 2002)

relE20	loss of function allele of relish created by p-element excision	(Hedengren et al., 1999)
p120^{308}	p120 catenin null allele created by p-element excision	(Myster et al., 2003)
Strain/Genotype/Class	**Description**	**Source/Reference**
Gal4 drivers		
esg-Gal4,UAS-GFP/+; tubGal80ts/+	temperature regulated GAL80 repressor combined with Gal4 driver for escargot driving GFP. Drives expression in ISCs and EBs	Hayashi, Shigeo (RIKEN Center for Developmental Biology)
MyoIA-Gal4/+; UAS-GFP, tub-Gal80^{ts}*/+*	temperature regulated GAL80 repressor combined with GAL4 driver for MyoIA driving GFP. Drives expression in ECs	Edgar, Bruce (DKFZ, Heidelberg)
spitz-Gal4^{NP0261}	Gal4 driver insertion in spitz. Recapitulates spitz expression pattern	DGRC - 112114
CG-Gal4	Gal4 driver for cg25c (collagen)- drives expression in the haemocytes, fat body and lymph glands	Bloomington 7011 (Asha et al., 2003)
Hml-Gal4	Gal4 driver for hemolectin drives expression in the haemocytes	Bloomington 30139 (Goto et al., 2001)
He-Gal4	Gal4 driver for hemese drives expression in the haemocytes	Bloomington 8699 (Kurucz et al., 2003)

ppl-Gal4	Gal4 driver for pumpless drives expression in the fat body	Leopold, Pierre (iBV, Nice) (Zinke et al., 1999)
Strain/Genotype/Class	**Description**	**Source/Reference**
UAS-Transgenes		
UAS-DER$^{DN\ (EGFR)}$	UAS Transgene expressing a dominant negative form of EGFR	Freeman, Matthew (MRC LMB, Cambridge)
UAS-GFP	UAS Transgene expressing GFP	Bloomington 6874
UAS-wg	UAS Transgene expressing wingless	Bloomington 5918
UAS-egr^{venus}	UAS Transgene expressing eiger fused with a Venus fluorescent tag	Davis,G (UCSF)
UAS-Toll	UAS Transgene expressing Toll fused with a Venus fluorescent tag	Bloomington 30899
Strain/Genotype/Class	**Description**	**Source/Reference**
RNA interference lines (RNAi)		
UAS-STAT-IR	UAS RNA interference transgene for STAT	VDRC - 43866
UAS-domeless-IR	UAS RNA interference transgene for domeless	VDRC - 2612
UAS-Max-IR	UAS RNA interference transgene for Max	Gallant, Peter (UZH, Zurich) 5(Steiger et al., 2008)
UAS-Myc-IR	UAS RNA interference transgene for Myc	VDRC - 2947
UAS-Apc1-IR (II)	UAS RNA interference transgene for Apc1	VDRC - 51468
UAS-Apc1-IR (III)	UAS RNA interference transgene for Apc1	VDRC - 51469

UAS-spitz-IR	UAS RNA interference transgene for spitz	VDRC - 3920
UAS-eiger-IR	UAS RNA interference transgene for eiger	VDRC - 108814
UAS-spätzle-IR	UAS RNA interference transgene for spätzle	VDRC - 105017
UAS-Myd88-IR	UAS RNA interference transgene for Myd88	VDRC - 19691
UAS-dlg-IR	UAS RNA interference transgene for discs large	VDRC - 41134
UAS-Pvr-IR	UAS RNA interference transgene for Pvr (PDGF and VEGF receptor homolog)	VDRC - 105353
Strain/Genotype/Class	**Description**	**Source/Reference**
MARCM lines		
y,w,hsFlp/+; UAS-CD8-gfp, tub-gal4/+; FRT82B, tub-gal80/tm6b	MARCM line	Bilder, David (UC, Berkeley)
FRT82B UAS-LacZ	FRT82B recombination site carrying UAS Transgene expressing bacterial LacZ	Cagan Lab stocks

Table 2.1: Fly stocks used in this study

2.1.3 Backcrossing

In order to isogenize mutant flies into control backgrounds mutants were backcrossed to wild type strains for 10 generations.

2.1.4 RNA interference

RNA interference (RNAi) was first discovered in *Caenorhabditis elegans* (*C.elegans*). In *Drosophila*, it is now routinely used for gene knockdown. It allows gene silencing through the use of specific RNA sequences that target mRNA for degradation.

2.1.5 MARCM analysis

In order to measure ISC proliferation in the posterior midgut we generated recombinant clones using the MARCM technique that allows the analysis of homozygous mutant populations of cells within a wild type tissue (Lee and Luo, 2001). Crosses were maintained at 22°C. 3-5 day old adult females of the desired genotypes were selected and subjected to three 30 min heat shocks at 37°C in one day with a break of 2 hours after each heat shock to induce clones. Flies were then incubated at 25°C and their guts dissected for analysis two weeks after clone induction.

2.1.6 Regression experiments

In order to assay the effect of knockdown of specific genes on hyper proliferation in the midgut we employed a temperature sensitive Gal4 repressor ($Gal80^{ts}$) in combination with either an ISC/EB Gal4 driver (*esg-*$Gal4^{ts}$) or the MARCM system.

esg-$Gal4^{ts}$: Adults were kept at 22ºC for 5 days. Midguts were dissected at this time point or flies were transferred to 29ºC for a further 7 days to allow expression of RNAi transgenes and then analyzed.

MARCM clones: Clones were induced and flies were incubated at 22ºC for 14 days. After the first 14 days all flies were switched to 29ºC and midguts were

dissected after 1 day (15 day-old clones; 15d), 7 days (21 day-old clones; 21d) and 14 days (28 day-old clones; 28d) of incubation at 29ºC.

2.1.7 Lifespan analysis

Flies were collected using CO_2 anaesthesia within 12 hours of eclosion and allowed to mate at 25°C for 2 days at a density of 20 flies per vial. Flies were transferred to new vials and placed at either 25°C or 29°C. Every 2-3 days the flies were transferred to fresh food and the number of dead flies was counted.

2.1.8 Fly collection for stress assays

For all stress tests flies were collected and aged using the same method. Flies were collected using CO_2 anaesthesia within 12 hours of eclosion and allowed to mate at 25°C for 2 days at a density of 20 flies per vial. They were separated into males and females and allowed to age at 25°C for a further 4 days.

2.1.9 Heat shock stress assay

Flies were transferred into empty vials and placed in a water bath set at 37°C. Dead flies were counted at 15min intervals. The experiment was terminated when all flies were dead.

2.1.10 Starvation assay

Flies were transferred into vials containing 5ml of 1% agar and placed in a 25°C incubator. Dead flies were counted at 12hr intervals. The experiment was terminated when all flies were dead.

2.1.11 Osmotic stress assay

Flies were transferred into vials containing 5ml of 1% agar and then placed in a 25°C incubator for overnight starvation. Flies were then transferred to vials with 5ml of standard medium containing 6% NaCl. Media was changed daily and dead

flies were counted at 12hr intervals. The experiment was terminated when all flies were dead.

2.1.12 H_2O_2 feeding assay

Flies were transferred into vials containing 5ml of 1% agar and then placed in a 25°C incubator for overnight starvation. Flies were then transferred to vials with 5ml of 1% agar containing 5% Sucrose and 1% H_2O_2. Media was changed daily and dead flies were counted at 12hr intervals. The experiment was terminated when all flies were dead.

2.1.13 Paraquat feeding assay

Flies were transferred put into vials containing 5ml of 1% agar and then placed in a 25°C incubator for overnight starvation. Flies were then transferred to vials containing filter paper (Whatman) soaked in 300µl of 5% Sucrose plus 20µM Paraquat and maintained at 25°C. Dead flies were counted at 12hr intervals. The experiment was terminated when all flies were dead.

2.2 Immunofluorescence of *Drosophila* tissues

2.2.1 Fixation and antibody staining

Adult and larval tissues were dissected in PBS and fixed 30–45 min in 4% para-formaldehyde (Polysciences, Inc.) using two nº 5 forceps (Dumont) and Leica dissection microscope. After fixation, three 15 min washes in PBS + 0.3% TritonX-100 (PBST) were performed. Samples were incubated overnight at 4°C in primary antibodies and DAPI (1:1000) in PBST+3% Bovine Serum Albumin (BSA) (Sigma). Samples were then washed as before and incubated with secondary antibodies (Invitrogen – Life technologies) in PBST for 1-2hrs at room temperature. Samples were mounted on polylysine glass slides (Thermo Scientific) with 13mm x 0.12mm spacers (Electron Microscopy Sciences) and Vectashield mounting media (Vector Laboratories, Inc.). For dissection of wild types wing discs spacers were not used to keep the tissue flat. For Wg staining tissues were fixed in PEM-FA (0.1 M PIPES, 2 mM EGTA, 1.0 mM $MgSO_4$, 3.7% formaldehyde, pH 7.0) for 20 min

and then washed with PBST (Lin et al., 2008). From here the standard staining protocol described above was used.

2.2.2 Antibodies

Antibody	Description	Dilution	Source/Ref
Primary Antibodies			
anti-GFP	Chicken, polyclonal against full length eGFP	1:4000	abcam - ab13970
anti-Delta	Mouse, monoclonal against extracellular domain of Delta	1:30	Developmental Studies Hybridoma Bank (DSHB)– C594.9B
anti-Pros	Mouse, monoclonal against Prospero protein	1:20	DHSB
anti-Arm	Mouse, monoclonal against N-terminal domain of Armadillo	1:3	DHSB- MR1A
anti-pH3S10	Rabbit, polyclonal against Ser10 phosphorylated Histone H3	1:100	Cell signalling - 9701
anti-pH3S28	Rabbit, polyclonal against Ser28 phosphorylated Histone H3	1:100	Cell signalling - 9713
anti-Myc	Guinea pig, polyclonal against *Drosophila* Myc	1:100 pre-absorbed	Morata, G (SIC-UAM, Madrid)
anti-βgal	Rabbit, polyclonal against β-gal	1:1000	Cappel Antibodies
anti-Pdm1	Rabbit, polyclonal against Pdm-1 (nubbin)	1:500	Chia, W (King's College, London)
anti-CC3	Rabbit, polyclonal against large cleaved caspase 3 fragment at Asp175	1:200	Cell signalling – 9661L(lot-36)
anti-MMP1	Mouse, monoclonal against catalytic domain of MMP1	1:10	DHSB – 3B8D12
anti-p1	Mouse, monoclonal against nimrod (marks all plasmatocytes)	1:5	Ando, I (Kurucz et al., 2007)

Antibody	Description	Dilution	Source/Ref
Secondary Antibodies			
anti-chi-IgG-488	Goat, polyclonal against chicken IgG, conjugated to Alexa Fluor 488	1:200	Invitrogen - A11039
anti-ms-IgG-488	Goat, polyclonal against mouse IgG, conjugated to Alexa Fluor 488	1:200	Invitrogen - A11029
anti-ms-IgG-594	Goat, polyclonal against mouse IgG, conjugated to Alexa Fluor 594	1:100	Invitrogen - A11032
anti-rb-IgG-594	Goat, polyclonal against rabbit IgG, conjugated to Alexa Fluor 594	1:100	Invitrogen - A11037
anti-gp-IgG-594	Goat, polyclonal against guinea pig IgG, conjugated to Alexa Fluor 594	1:100	Invitrogen - A11076
anti-rb-IgG-Cy5	Donkey, polyclonal against rabbit IgG, conjugated to Alexa Fluor 488	1:50	Jackson Laboratories - 711-176-152
Phalloidin - 647	High affinity F-Actin probe, conjugated to Alexa Fluor 647	1:40	Invitrogen - A22287
anti-ms-HRP	Rabbit, polyclonal against mouse IgG conjugated to HRP	1:5000	Abcam - 97046

Table 2.2: Primary and Secondary Antibodies used in this study.

2.2.3 Microscopy and Image processing

2.2.3.1 Light and Fluorescent light microscopy

All images of 3rd instar larvae were taken using a Leica M205 FA stereomicroscope.

2.2.3.2 Confocal microscopy

All confocal imaging was performed in the Beatson Advanced Imaging Resource (BAIR) using the Zeiss 710 LSM confocal microscope. Raw data was stored as LSM files. Confocal stacks were processed using Image J (National Institutes of Health) and Adobe Photoshop.

2.3 Quantifications

2.3.1.1 Quantification of pH3^{+ve} cells

In order to quantify the level of proliferation in the posterior midgut of different genotype, the total number of the cells in the posterior midgut was counted. For each genotype at least 10 posterior midguts were analysed.

2.3.1.2 Quantification of number of cells per clone

In order to quantify the level of proliferation within clones in the posterior midgut of different genotypes, the total number of cells per clone in the posterior midguts was counted using DAPI positivity. For each genotype at least 30 clones were counted.

2.3.1.3 Quantification of larval Haemocyte number

In order to quantify the number of circulating haemocytes in different genotypes, larvae were washed three times in PBS to remove any food debris. 5 larvae per genotype were then opened and turned inside out using two nº 5 forceps (Dumont) in 200µl of PBS. The sample was gently pipetted to ensure equal distribution and avoid clustering. 10µl were loaded into each end of a Bright Line haemocytometer. The total number of haemocytes in 10 squares was

counted and was used to calculate the average total number of haemocytes. The average total number of haemocytes was calculated per larva. These experiments were performed at least in triplicate for each genotype i.e. a minimum of 15 larvae per genotype.

2.3.1.4 Quantification of total DAPI positive volume

In order to compare the sizes of tumours from different genotypes, tumour Volume was quantified as the total volume of DAPI from individual series of confocal images. This was carried out using Volocity 3D image analysis software. For each tumour 40-50 images were taken at around 2.55µm per image step depending on the size of the tumour. At least 10 tumours were analysed for each genotype.

2.3.1.5 Quantification of percentage Cleaved Caspase 3 positivity

In order to quantify the level of tumour cell death I developed a method using the Volocity 3D image analysis software. The percentage tumour cell death was calculated as the cleaved caspase 3 positive tumour volume normalized to the total tumour volume. At least 10 tumours were analysed for each genotype.

2.4 Protein Analysis

2.4.1 Protein Extraction

For Immunoprecipitation experiments 40-60 flies were homogenized in 500ul of 10 mM Tris-HCl, 5mM EDTA, 150mM NaCl, 40mM Sodium pyrophosphate, 1% NP-40, 0.5% sodium deoxycholate, 50 mM NaF, 1 mM sodium orthovanadate, 0.025% SDS, 0.5 mg/ml PMSF, and Protease Inhibitors Complete cocktail (Roche Molecular Biochemicals). Samples were centrifuged 12,000g for 10 mins to pellet adult cuticle debris and the supernatant was transferred to a fresh eppendorf. Protein was quantified using micro BCA Protein assay kit (Pierce).

2.4.2 Immunoprecipitation

1mg of protein sample was incubated with 40μl GFP-trap beads (Chromotek) overnight with rotation at 4°C. Beads were washed 3 times with homogenization buffer. Samples were then boiled at 95°C to release the attached protein in 35μl of loading dye (2xSDS buffer: 50mM TrisCl pH 6.8, 0.01% Bromophenol Blue, 4% SDS, 12% glycerol, 0.1M DTT) for 10mins.

2.4.3 SDS-PAGE and Protein Transfer

Protein extracts were either loaded onto a 10% polyacrylamide gel with a 4% stacking gel or onto a 4-12% Bis Tris pre-cast gel (Invitrogen) and run at 150V for 1 hr in 1X NuPAGE® MOPS SDS running buffer using Invitrogen XCell *SureLock*™ electrophoresis system. 10μl of pre-stained marker (*BIO-RAD* Precision Plus Protein™ Dual Color Standard) was used to estimate protein size. Gels were transferred onto PDVF membrane (Amersham) and blocked with 5% Milk powder TBS-T for 1hr at room temperature. Membranes were incubated with primary antibody overnight at 4°C with shaking. Membranes were then washed 3 times for 10 minutes with TBS-T. Incubation with secondary antibody was performed at room temperature for 1 hour. Membranes were washed as described and bands were visualized using ECL solutions (Amersham).

2.4.4 Liquid Chromatography mass spectrometry

The samples generated from in gel digestion performed by the laboratory of Dr Sara Zanivan contain tryptic peptides that span a broad range of abundances. To measure them with high accuracy and depth, they combine the high resolving power of reverse phase chromatography with the speed and ultra-high resolution achieved in the Orbitrap Elite (Michalski et al., 2012). Data were acquired using the Xcalibur software, which generates .RAW files that were analyzed with the MaxQuant computational package (Cox and Mann, 2008). Using this analysis, they were able to identify 23 unique peptides corresponding to dp120ctn.

2.5 RNA Quantification

2.5.1 RNA extraction from guts

Total RNA was extracted from 6 to 10 midguts per biological replicate. RNA was extracted from each genotype in triplicate. A standard TRIZOL protocol was used to extract RNA that was then treated with DNaseI (Qiagen) to remove any genomic DNA. Phenol-Chloroform extraction was used to purify RNA followed by Ethanol precipitation. RNA was quantified using a NanoDrop Spectrophotometer.

2.5.2 RNA extraction from whole flies, larval tumours and fat bodies

Total RNA was extracted from triplicates of 10 adult females using the Qiagen RNAeasy kit (Qiagen) according to manufacturers instructions.

2.5.3 cDNA synthesis

cDNA synthesis was performed in triplicate for each biological replicate using the High-Capacity cDNA reverse transcription kit (Applied Biosystems – Life Technologies) from 1µg RNA. cDNA synthesis reactions were pooled for each biological replicate.

2.5.4 Quantitative PCR

Expression of the target genes was measured relative to that of *RpL32*, GAPDH or Actin and primers used for qPCR are shown in Table 2.3. A series of 10-fold dilutions of an external standard was used in each run to produce a standard curve. MAXIMA SYBR GREEN Master Mix (Fermentas) was used for gut samples and Quanta SYBR green Master mix (low ROX) was used for whole fly, tumour and fat body samples following manufacturers instructions. Data were extracted and analysed using Applied Biosystems 7500 software version 2.0. Melt curves were used to ensure only one product was produced from each primer pair.

2.5.5 Primers

Target	Primer name	Sequence 5'-3'
RpL32	RpL32 F	AGGCCCAAGATCGTGAAGAA
	RpL32 A	TGTGCACCAGGAACTTCTTGAA
Unpaired	updF	CCACGTAAGTTTGCATGTTG
	updR	CTAAACAGTAGCCAGGACTC
Unpaired2	upd2F	ACTGTTGCATGTGGATGCTG
	upd2R	CAGCCAAGGACGAGTTATCA
Unpaired3	upd3F	AGGCCATCAACCTGACCAAC
	upd3R	ACGCTTCTCCATCAGCTTGC
Actin	act5cF1	GAGCGCGGTTACTCTTTCAC
	act5cR1	CCATCTCCTGCTCAAAGTCG
Drosomycin	drosF1	CTCTTCGCTGTCCTGATGCT
	drosR1	ACAGGTCTCGTTGTCCCAGA
Pvf1	pvf1F1	CAGACCGTTCACCATCATCA
	pvf1R1	AATCCTTGCGATACGACTGG
Puckered	pucF1	CATCTCGCCCAATCTGAACT
	pucR1	CCCACAGAAGATGACGAAGG
socs36E	socs36EF1	ATGACCGTGCACTCGCAAAT
	socs36ER1	CCTCGTAGCGGTCCATCTTG
Insulin receptor	InRF1	GGTGCTGGCATCATAGGTCT
	InRR1	CCTGCCTCTGAGTGATAGAAGG
thor	thorF1	CCAGGAAGGTTGTCATCTCG
	thorR1	TGAAAGCCCGCTCGTAGATA
Defensin	DefF1	CTTCGTTCTCGTGGCTATCG
	DefR1	ATCCTCATGCACCAGGACAT
Metchnikowin	MtkF1	GCTACATCAGTGCTGGCAGAG
	MtkR1	TAAATTGGACCCGGTCTTGG
Mmp1	Mmp1F1	ACGAGTTCGGTCACTCCTTG
	Mmp1R1	CTTGTCGTCCTCGTCCAACT
Spitz	spitzF	TACCAGGCATCGAAGGTTTC
	spitzR	GACCCAGGCTCCAGTCACTA
Vein	veinF	GTGAAGTTGCCTGGATTCGT
	veinR	CTACAGGGAGCGACTGATGC
Keren	kerenF	CGAGCCATCAATCTCCTTGT
	kerenR	AACGATGGCACCTGCTTTAC
Hsp22	hsp22F1	CCGTCAACAAGGATGGCTAC
	hsp22R1	CTCTGATTTTCCCTCCACCA
Attacin A	AttAF1	ATGCTCGTTTGGATCTGACC
	AttAR1	AAAGTTCCGCCAGTTGTGAC
Attacin B	AttBF1	GTCATGGTGCCTCTTTGACC
	AttBR1	CCAGATTGTGTCTGCCATTG
Attacin C	AttCF1	CAACGGTGTTCACAATCTGG
	AttCR1	GGGAGTAGTCCAGTGCAGCTT
Attacin D	AttDF1	AGTGGGGGTCACTAGGGTTC

	AttDR1	GTGGCGTTGAGGTTGAGATT
Diptericin B	DptBF1	GGATTCGATCTGAGCCTCAAC
	DptBR1	ATAGGGTCCACCAAGGTGCT
PGRP-LB	PGRP-LB-F1	TCTCCAATCTCCGATCAGCA
	PGRP-LB-R1	GCGATGGCATGATTTACACC
PGRP-LC	PGRP-LC-F1	CCGAAGCGGAGGATTATACG
	PGRP-LC-R1	GGCGACTGATCACCGTTAGA
PGRP-SB	PGRP-SB1-F1	AGACGATGCCAATGCTCTTG
	PGRP-SB1-R1	ACTTTATCGTGGCCGGTGAT
PGRP-SC	PGRP-SC2F1	CGTGACCATCATCTCCAAGTC
	PGRP-SC2R1	GTAGTTTCCAGCGGTGTGGT
PGRP-SD	PGRP-SD-F1	CAGCTGGTGGAGGGCTATAA
	PGRP-SD-R1	AGTTGGGCCACTGCTGTATC
Spn4	Spn4F1	TCTGGGCGGGTTAAGTGTTT
	Spn4R1	CTTGTGCCGGCTGATGTATT

Table 2.3: Primer pairs used in this study

2.5.6 Microarray analysis

RNA extracted as described in 2.3.2 was sent to the MIAMI microarray facility at the University of Manchester were after quality control testing it was hybridized to the Drosophila Affymetrix chip 2.0. The cel files normalised and analysed in Partek Genomics Suite Software by the Beatson Bioinformatics department. RMA normalisation and log2 transformation of the data was followed by the differential gene expression analysis using t-test. All p-values were corrected for multiple testing using Benjamini & Hochberg step up method that controls the false discovery rate. Finally, the fold change values were considered in ranking genes of interest.

2.5.6.1 Gene enrichment analysis

Gene set enrichment analysis was done using The Database for Annotation, Visualization and Integrated Discovery (DAVID) version 6.7 (Huang et al., 2008).

2.6 Statistics

Unless otherwise stated all experiments have been performed 3 times. All Statistical analyses were performed using Graph Pad Prism 6. Specific statistical tests are described in each figure legend. P-values less than 0.05 were considered statistically significant. Error bars mean ± standard error of the mean (SEM). For survival experiments median survival was calculated by Graph Pad Prism 6 and is an approximation to the closest sampling time.

3 *Drosophila p120 catenin*: a role in the stress response

3.1 Summary

p120ctn is the founding member of the p120ctn family of proteins. It is a ubiquitously expressed core component of adherens junctions and has been shown to be essential for adherens junction formation and stability in mammalian epithelia. It is essential for vertebrate development and is deregulated in many epithelial cancers. In *Drosophila*, there is only one p120ctn family member: *dp120ctn*. dp120ctn is not required for the formation of adherens junctions, development or homeostasis. *dp120ctn* null flies are viable and fertile and display no obvious phenotype. As this gene family is well conserved from invertebrates to vertebrates I hypothesized that although not essential for development *dp120ctn* may be required in certain conditions. To test this I assayed the requirement of *dp120ctn* in stress and oncogenic stress conditions. I found that *dp120ctn* null adult flies were sensitive to Heat shock and display a reduced lifespan that can be rescued by ubiquitous overexpression of *dp120ctn*. Using transcriptomic analysis I analysed normal and stress induced transcription and found that several targets of the *relish*/NF-κB transcription factor were differentially expressed. This aberrant gene expression was rescued by overexpression of dp120ctn and heterozygosity for *relish*.

I also examined the effects of *dp120ctn* loss on tumour burden in null mutants of the *scribble* group of polarity tumour suppressors. I found that tumour burden was increased in larvae carrying both mutations. I have carried out a preliminary analysis on this model and suggest further experiments to understand the role of *dp120ctn* in this tumour model.

Together these results indicate that *dp120ctn* may negatively regulate immune signalling in adult flies and suggests that loss of *dp120ctn* in transformed epithelia may increase tumour burden. This novel role of *dp120ctn* in the regulation of immune signalling may be the ancestral role of *dp120ctn*.

3.2 Introduction

3.2.1 Adherens Junctions

Adherens junctions are cell-cell adhesive junctions, that are centrally required for normal epithelial architecture and their dynamic regulation is pivotal for the development of tissues, organs and animals. Adherens junctions are made up of several different proteins that orchestrate adhesion between cells. Adherens junctions are formed when the extracellular domain or ectodomain of classical cadherins trans-dimerizes with that of an adjacent cell. The cadherin cytoplasmic tail contains a catenin binding domain (CBD) and a highly conserved juxta-membrane domain (JMD) which participates in cytoskeletal organization and intracellular signalling (Takeichi et al., 2000). Catenins, α- and ß-catenin work in concert to link the intracellular domain of classical cadherins to the actin cytoskeleton regulating cell-cell adhesion (Anastasiadis and Reynolds, 2000). α-catenin binds ß-catenin which itself binds to the CBD domain of cadherin and the actin cytoskeleton to tether the junction. p120ctn binds cadherin at the JMD domain and regulates the strength of adhesion.

3.2.2 p120 catenin

p120 catenin (p120ctn) was first characterized as part of a screen for phosphorylated substrates of the transforming tyrosine kinase, Src (Reynolds et al., 1989). p120 catenin is the ubiquitously expressed prototypic member of the p120ctn family which includes ARCVF; p0071 and δ-catenin. The remaining members of the family are expressed at lower levels (Anastasiadis et al., 2000). p120ctn binds the highly conserved juxta-membrane domain (JMD) of classic cadherins to promote adherens junction stability (Reynolds et al., 1989, Reynolds et al., 1994, Anastasiadis et al., 2000).

3.2.3 Structure and function

p120ctn localizes to the plasma membrane, cytoplasm and nucleus. Human p120ctn has 4 alternative start codons which define four isoforms, p120 1 – 4 (Ishiyama et al., 2010). Through alternative splicing of 4 alternative exons, a total of 48 possible isoforms can be produced (Ishiyama et al., 2010). The protein is composed of three main domains, an N-terminal regulatory domain, nine Armadillo (ARM) repeats and a C-terminal domain. The N-terminal regulatory domain contains serine/threonine and tyrosine phosphorylation sites that are acted upon by Src family kinases (SFK), tyrosine phosphatases (PTP) and Serine/Threonine Kinases (Xu et al., 2004, Zondag et al., 2000) to regulate p120ctn function. At the plasma membrane, p120ctn binds E-cadherin at the JMD through its ARM repeats. This interaction can be abolished through modification of two conserved glycine residues contained within the JMD (Thoreson and Reynolds, 2002, Ishiyama et al., 2010). ß-catenin binds E-cadherin at the CBD and is then itself bound by α-catenin which anchors the complex directly to the actin cytoskeleton (Reynolds, 2007). While the connection to the actin cytoskeleton via ß-catenin and α-catenin is essential for cadherin-dependent adhesion, the role of p120ctn is not (Reynolds et al., 1994, Daniel and Reynolds, 1995, Anastasiadis et al., 2000, Ireton et al., 2002, Smith et al., 2012). In the absence of p120ctn, E-cadherin is endocytosed resulting in weaker adhesion as junctions become more dynamic (Thoreson et al., 2000, Ireton et al., 2002, Pece and Gutkind, 2002). Moreover, binding of p120ctn to the JMD of classic cadherins prevents modifications that target cadherins for

degradation (Fujita et al., 2002). Thus, p120ctn can modulate the strength of adhesion.

In the cytoplasm, p120ctn has been shown to regulate Rho GTPases and exert effects on actin fiber contractility (Anastasiadis et al., 2000, Anastasiadis and Reynolds, 2001, Fang et al., 2004).

p120ctn associates with the BTB/POZ transcriptional repressor Kaiso and affects its localization and role in the regulation of transcription (Daniel and Reynolds, 1999, Van Roy and Mccrea, 2005, Daniel, 2007, Dai et al., 2010, Zhang et al., 2010, Zhang et al., 2011, Jones et al., 2012, Jiang et al., 2012). Kaiso also associates with ß-catenin preventing transcription downstream of Wnt signalling activation. When Wnt signalling is induced p120ctn becomes phosphorylated and this increases its affinity for Kaiso. When p120ctn is bound ß-catenin is free to drive transcription (del Valle-Pérez et al., 2011).

3.2.4 p120ctn in development

In order to understand p120ctn function *in vivo* it has been deleted or downregulated in many different models. In *C. elegans* knockdown of the *p120ctn* homologue *JAC-1* has no measurable effects on development but is believed to be a positive regulator of adherens junctions (Pettitt et al., 2003). In *Xenopus*, miss-expression of p120ctn or concomitant knockdown together with δ-catenin leads to gastrulation defects (Paulson et al., 1999, Gu et al., 2009). In the mouse, a *p120ctn* knock out (KO) was lethal. Using conditional knockout models p120ctn has been shown to be required for salivary gland, brain, kidney, vascular and mammary gland development (Davis and Reynolds, 2006, Elia et al., 2006, Oas et al., 2010, Marciano et al., 2011, Kurley et al., 2012).

3.2.5 p120ctn in Cancer

p120ctn is downregulated, mislocalized or misexpressed in many different cancers and correlates with poor prognosis and survival. (Thoreson and Reynolds, 2002, Mayerle et al., 2003, Fei et al., 2009, Vidal et al., 2010, Mortazavi et al., 2010, Talvinen et al., 2010, Miao et al., 2010, Lu, 2010, Dai et al., 2011). p120ctn is a bona fide tumour suppressor in the mouse oesophageal tract and its

deletion results in the establishment of an inflammatory microenvironment. In the mouse intestine, conditional knockdown of p120ctn leads to inflammation and an increased adenoma formation and in the mouse epidermis deletion of p120ctn increases inflammation and tumourigenesis (Perez-Moreno et al., 2006, Perez-Moreno et al., 2008, Smalley-Freed et al., 2011, Smalley-Freed et al., 2010).

3.2.6 *Drosophila* p120 catenin

Drosophila p120ctn (*dp120ctn*) is the single member of the p120ctn family in flies and is ubiquitously expressed with enrichment in the larval and adult central nervous system (CNS) (FlyAtlas.org). The gene contains 4 exons across around 14Kb that gives rise to a 781 amino acid (aa) protein with an approximate molecular weight of 87kDa (Myster et al., 2003). dp120ctn localizes to the cytoplasm and plasma membrane (Myster et al., 2003, Pacquelet et al., 2003). In the cytoplasm it binds and possibly has an inhibitory role on Rho1, the *Drosophila* homologue of the Rho GTPase RhoA, as it preferentially binds to the GDP bound form of Rho1 and could block GDP-GTP exchange keeping the protein inactive (Magie et al., 2002). At the plasma membrane dp120ctn localizes to adherens junctions where, like its vertebrate counterpart, it binds to the conserved JMD of DE-cadherin but in *Drosophila* this interaction does not affect DE-cadherin stability (Pacquelet et al., 2003, Myster et al., 2003). Initial experiments using direct injection of dsRNA against dp120ctn into embryos suggested an essential function for *dp120ctn* (Magie et al., 2002) and there have been reports of mild developmental defects in the developing retina (Larson et al., 2008). Nevertheless, the generation of a null allele for *dp120ctn* through incomplete P-element excision demonstrated that *dp120ctn* is dispensable for development and homeostasis in *Drosophila* (Myster et al., 2003). This finding was further confirmed when re-expression of a mutant dE-cadherin (dE-cad) that cannot bind dp120ctn rescued *shotgun/DE-cadherin* null mutants (Pacquelet et al., 2003). This is in great contrast with the observation that null mutations of either Armadillo (β-catenin) or Shotgun (dE-cad) result in gastrulation defects. Combination of either of these null mutants with loss of *dp120ctn* greatly enhanced the lethality of these alleles mutations suggesting that *dp120ctn* may not have an essential role in adhesion but might be required to modulate it

(Myster et al., 2003). There have been no homologous proteins identified for Kaiso in *Drosophila* and as dp120ctn has not yet been reported to localize to the nucleus it is still unknown if *dp120ctn* plays are role in the nucleus. Despite this dispensability of *dp120ctn* for adhesion, it has been retained in the *Drosophila* genome and can be found in all invertebrates and vertebrates as a single or multi-gene family. This suggests that it may have important ancestral roles (Zhao et al., 2011, Carnahan et al., 2010).

3.2.7 Aims of project

Due to the requirement of *p120ctn* for development in vertebrate models open questions remain about adhesion independent functions of *p120ctn*. I hypothesized that as *dp120ctn* was not required for development in *Drosophila* this would be a tractable model to uncover novel adhesion independent roles of *p120ctn*. I wanted to address if *dp120ctn* could be required in conditions of stress and to incorporate loss of *dp120ctn* with genetically defined models of Cancer in *Drosophila* in order to study the affect on tumour burden.

The majority of the experiments were carried out by myself. I would like to acknowledge assistance from Karen Strathdee with troubleshooting of the IP protocol and from Christin Bauer a visiting student who carried out the salt and H_2O_2 stress tests and helped with qPCR.

3.3 Results

3.3.1 *dp120ctn* mutants are not sensitive to oxidative stress

I hypothesized that while dispensable for development and adult tissue homeostasis, *dp120ctn* could be required in conditions of stress in adult flies. To ensure that I only observed phenotypes associated specifically with loss of *dp120ctn* I initially backcrossed flies carrying the null allele of dp120ctn, $p120ctn^{308}$ with the control background w^{1118} for ten generations to create our experimental line (w^{1118}; $p120^{308}$) (O'Keefe et al., 2007). For all experiments we compared mated w^{1118} male and females with mated w^{1118}; $p120^{308}$ males and females.

Oxidative stress is characterized as an increase in the amount of reactive oxygen species (ROS) in a biological system and has been linked to several pathologies. In order to induce oxidative stress in our system I treated flies with either Paraquat (Sigma) or H_20_2 (Sigma). Paraquat is a herbicide that is readily reduced in cells to give rise to ROS, while H_20_2 is a potent ROS itself. To examine the effects of oxidative stress on controls and *dp120ctn* mutants, I fed overnight starved 7 day old adults with either 20μM Paraquat 5% sucrose or 1% H_20_2 5% sucrose media. These concentrations were chosen as both had been previously demonstrated to induce oxidative stress in *Drosophila*. I compared the survival of controls (w^{1118} -blue line) and *dp120ctn* mutants (w^{1118}; $p120^{308}$-red line) on these two media. I found no difference in survival associated with loss of *dp120ctn* in males or females on either Paraquat or H_20_2 (Fig 3.1A-B and Fig 3.2A-B).

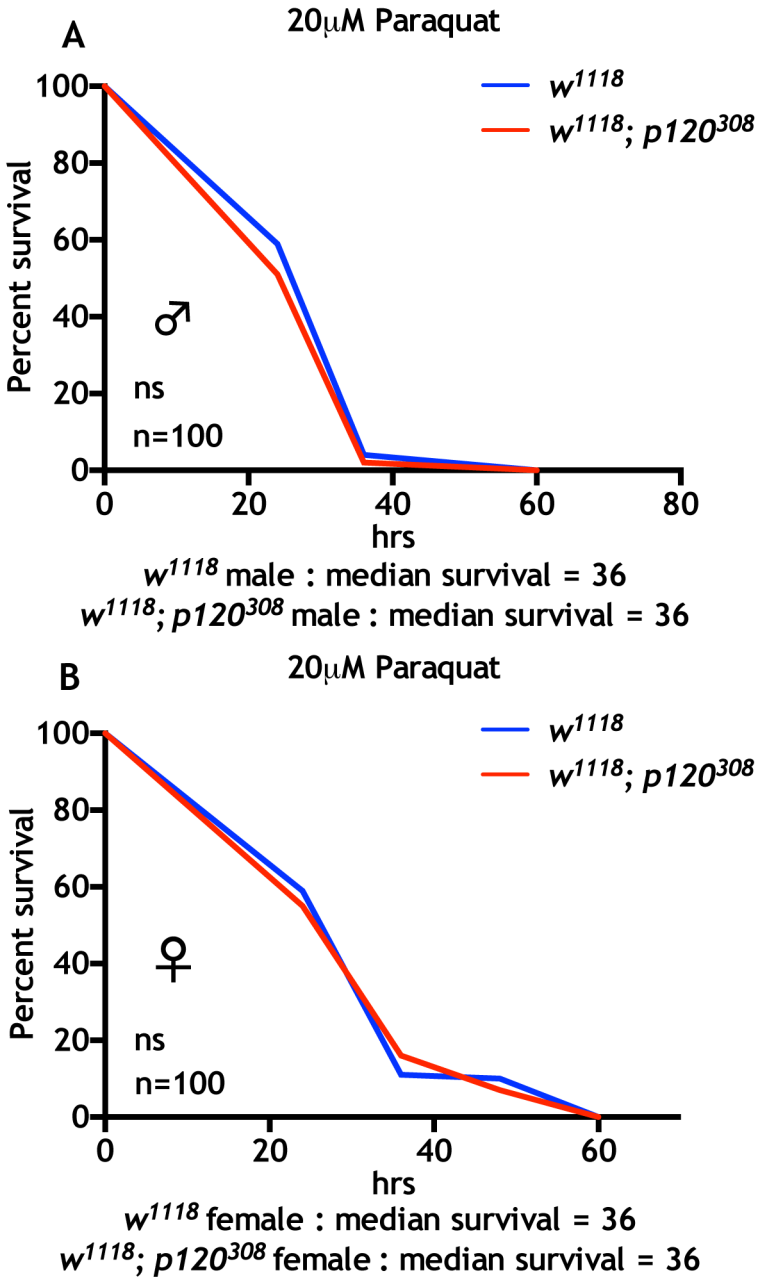

Figure 3.1 *dp120ctn* mutants flies are not sensitive to Paraquat

(A-B) Survival of w^{1118} and w^{1118}; $p120^{308}$ males (A) and females (B) fed a sucrose solution containing 20μM Paraquat. Survival is plotted as adult survival in hours at 25°C. Blue lines indicate w^{1118} controls and red lines w^{1118}; $p120^{308}$. Each curve represents ~100 flies. Median survival is presented for each cohort and *p* value generated using log-rank tests.

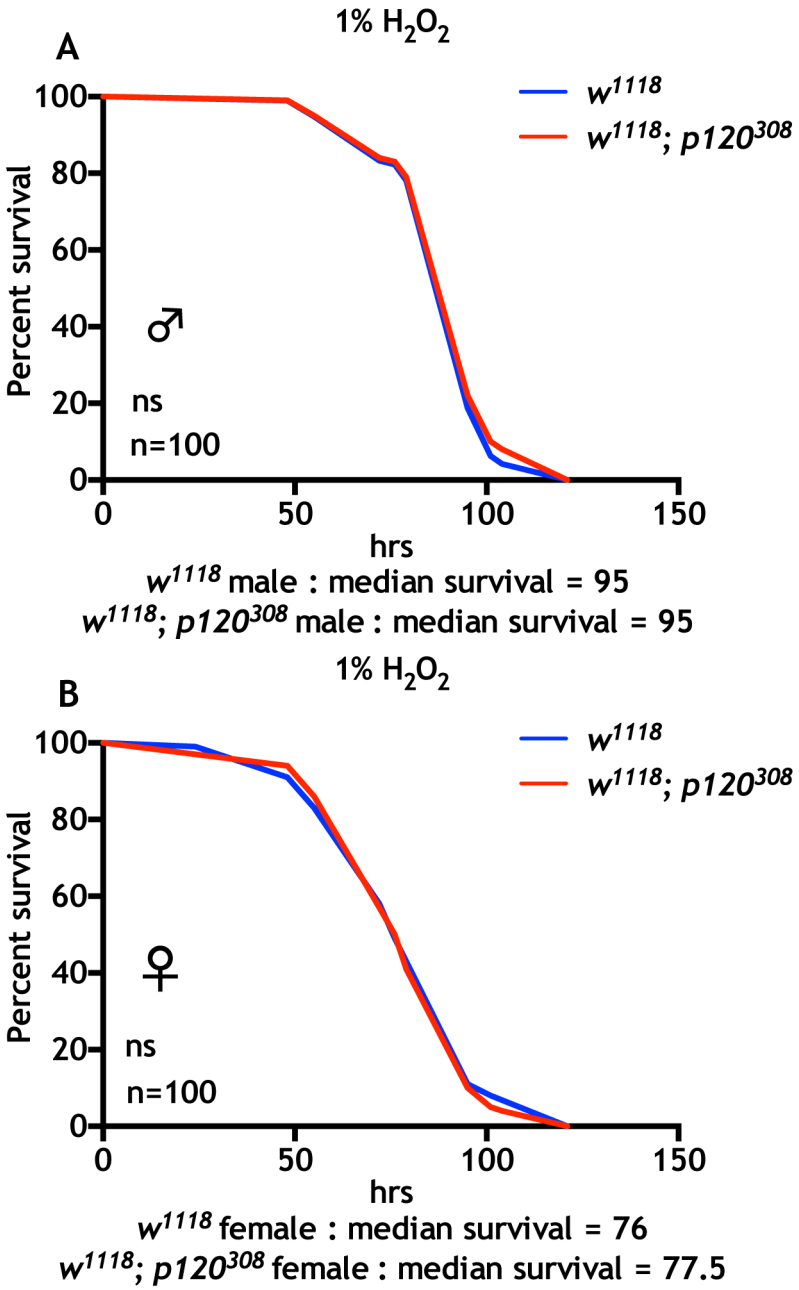

Figure 3.2 *dp120ctn* mutants are not sensitive to H_2O_2

(A-B) Survival of w^{1118} and w^{1118}; $p120^{308}$ males (A) and females (B) on a 1% H_2O_2, 5% Sucrose agar medium. Survival is plotted as adult survival in hours at 25°C. Blue lines indicate w^{1118} controls and red lines w^{1118}; $p120^{308}$. Each curve represents ~100 flies. Median survival is presented for each cohort and *p* value generated using log-rank tests.

3.3.2 *dp120ctn* mutants are not sensitive to osmotic stress

Osmotic stress results in acute changes in water balance. To understand whether *dp120ctn* mutants were more sensitive to an increase in osmotic stress I added sodium chloride (NaCl, Sigma) at a concentration of 6% to normal fly medium and then fed overnight starved 7 day old control (w^{1118}) and *dp120ctn* (w^{1118}; $p120^{308}$) males and females on this media. This concentration of NaCl was chosen as it had been previously been shown to induce acute osmotic stress (Stergiopoulos et al., 2009). I observed that there was a significant difference in survival between control (w^{1118} -blue line) and *dp120ctn* mutant males (w^{1118}; $p120^{308}$-red line) (Fig 3.3A) but this was not mirrored in the case of females which showed no change in median survival in these conditions (Fig 3.3B). These results suggested that *dp120ctn* males were sensitive to increased osmotic stress but females were not.

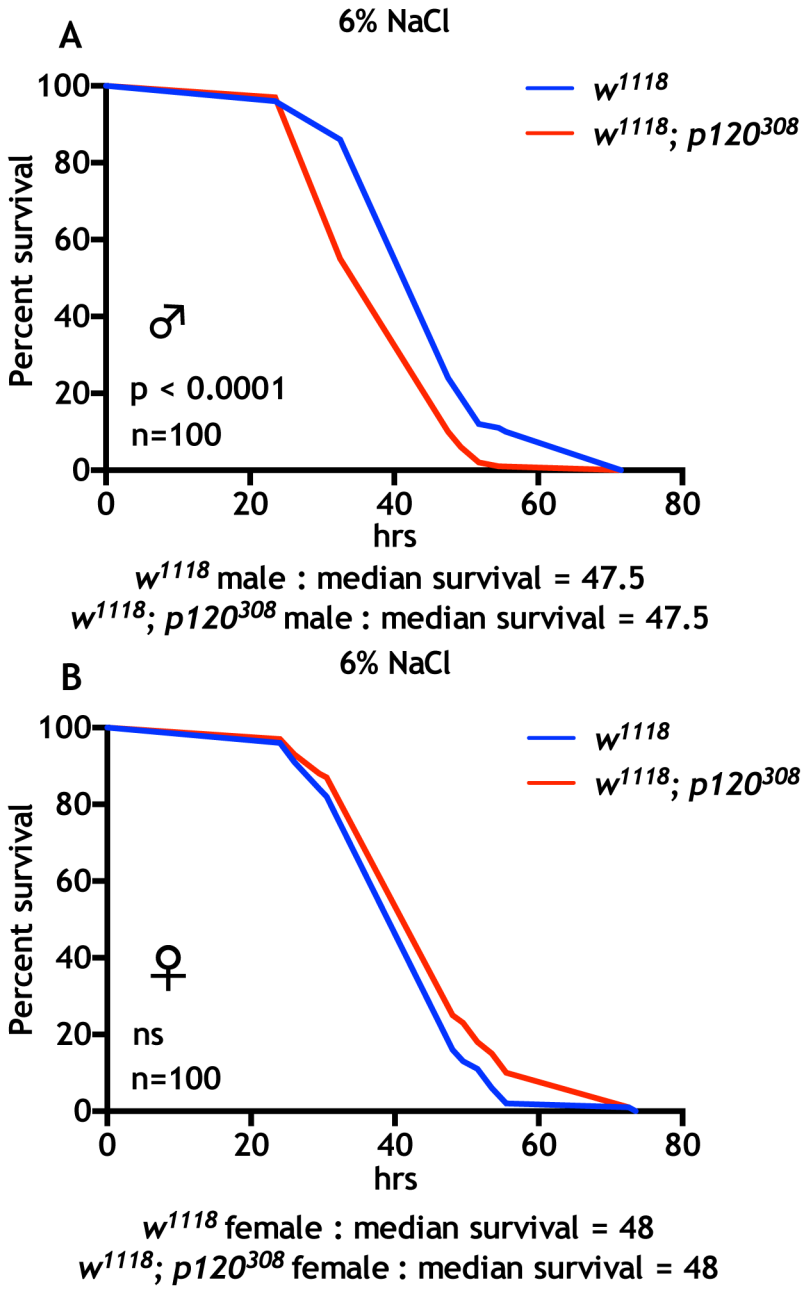

Figure 3.3 *dp120ctn* mutants are not sensitive to osmotic stress

(A-B) Survival of w^{1118} and w^{1118}; $p120^{308}$ males (A) and females (B) on standard medium supplemented with 6% NaCl. Survival is plotted as adult survival in hours at 25°C. Blue lines indicate w^{1118} controls and red lines w^{1118}; $p120^{308}$. Each curve represents ~100 flies. Median survival is presented for each cohort and *p* value generated using log-rank tests.

3.3.3 *dp120ctn* mutants are sensitive to heat shock

Heat shock, where an organism is exposed to temperatures out with normal ambient temperature has been heavily studied and is often used to induce stress conditions. It acts as a stress stimulus that induces transcription of specific genes, namely the Heat Shock proteins. A number of these genes encode protein chaperones that assist with protein folding, localization and targeting of old or misfiled proteins for degradation. Like most invertebrates, *Drosophila* is unable to regulate body temperature and as such prefers temperatures ranging from 18ºC to 29ºC. To induce Heat shock, I placed control and *dp120ctn* mutant flies in a 37ºC water bath. I placed 7 day old flies in empty vials to prevent flies sticking to the food and dying during the experiment. The vials were submerged in order to ensure a constant temperature of the 37ºC inside the vials. The vials were removed every 15 minutes so that the number of dead flies could be scored. We compared the survival of control males and females (w^{1118} -blue line) to *dp120ctn* mutant males and females (w^{1118}; $p120^{308}$-red line). We found that both *dp120ctn* males and females were significantly more sensitive to heat shock stress with nearly a 50% decrease in median survival under these conditions (Fig 3.4A-B). This suggests that *dp120ctn* may be functionally required under heat shock stress conditions.

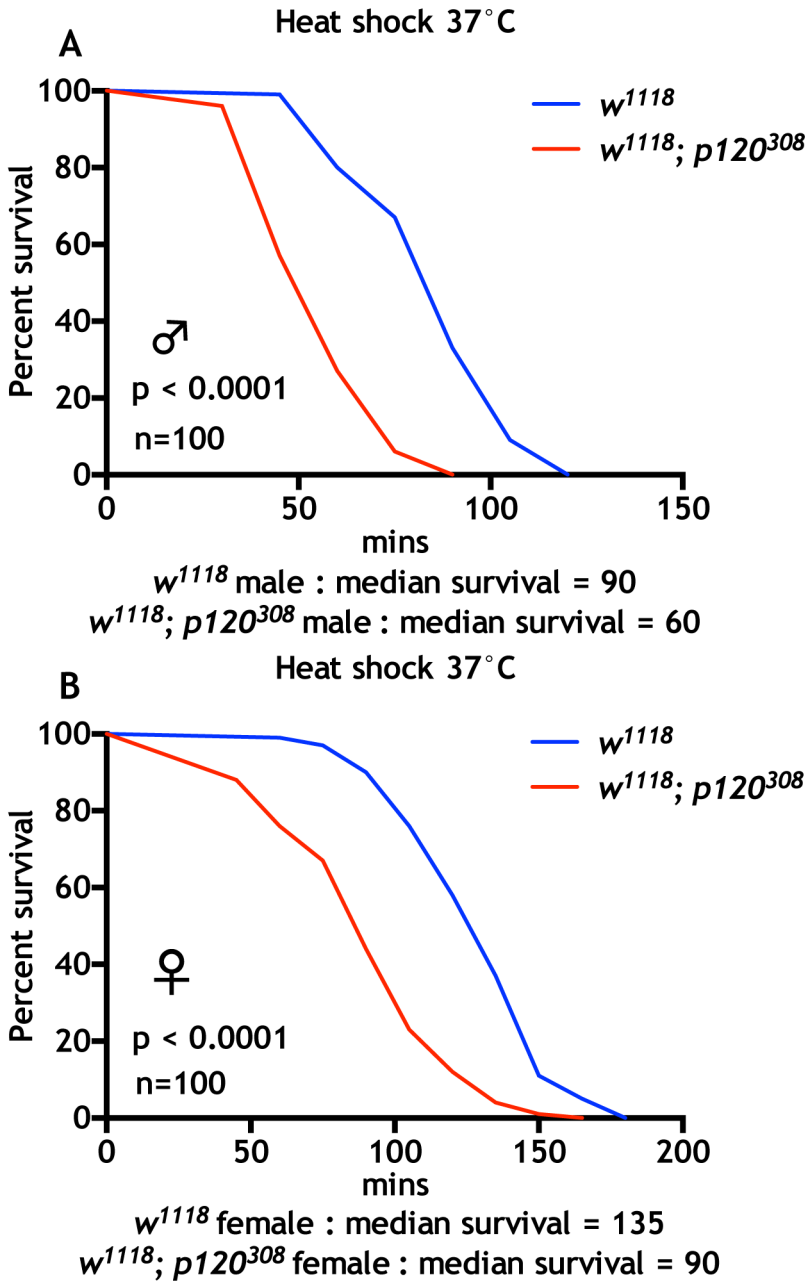

Figure 3.4 *dp120ctn* mutants are sensitive to heat shock

(A-B) Survival of w^{1118} and w^{1118}; $p120^{308}$ males (A) and females (B) under heat shock conditions. Survival is plotted as adult survival in minutes under heat shock at 37°C. Blue lines indicate w^{1118} controls and red lines w^{1118}; $p120^{308}$. Each curve represents ~100 flies. Median survival is presented for each cohort and *p* value generated using log-rank tests.

3.3.4 *dp120ctn* mutants are sensitive to starvation

Animal starvation results in progressive tissue degradation and, if prolonged indefinitely, in death. I wanted to examine whether *dp120ctn* mutant flies were more sensitive to starvation. To induce starvation, I placed 7 day old control and *dp120ctn* mutant males and females in vials containing 5ml of 1% Agar (Detacher) at 25ºC. The agar did not contain any caloric value but was utilized to maintain moisture levels within the vial to prevent desiccation. We measured the survival of control males and females (w^{1118} -blue line) to *dp120ctn* mutant males and females (w^{1118}; $p120^{308}$-red line) and found that both *dp120ctn* mutant males and females were significantly more sensitive to starvation at 25ºC with - nearly a 20% decrease in median survival under these conditions (Fig 3.5A-B). This suggests that *dp120ctn* may be required during starvation stress.

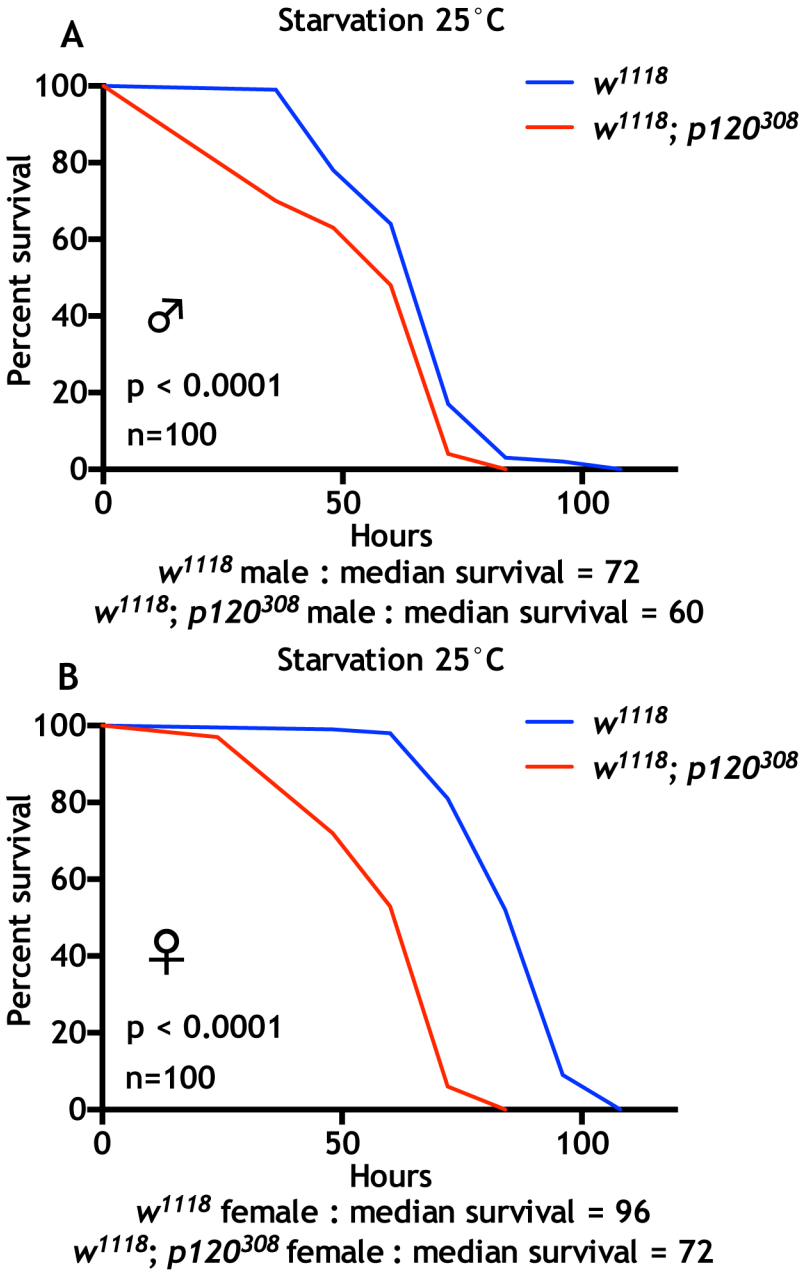

Figure 3.5 *dp120ctn* mutants are sensitive to starvation

(A-B) Survival of w^{1118} and w^{1118}; $p120^{308}$ males (A) and females (B) under Starvation conditions. Survival is plotted as adult survival in hours under Starvation at 25°C. Blue lines indicate w^{1118} controls and red lines w^{1118}; $p120^{308}$. Each curve represents ~100 flies. Median survival is presented for each cohort and *p* value generated using log-rank tests.

3.3.5 *dp120ctn* mutants have a reduced median lifespan

Ageing is characterized by a progressive deterioration of an animal. One consequence of the ageing process is a reduced ability to cope with environmental stress. To ascertain whether *dp120ctn* mutants were less able to deal with environmental stress and thus may have a reduced lifespan I measured the lifespan of control and *dp120ctn* mutant males and females. I collected flies within 12hrs of eclosion to reduce variability. I allowed them to mate for 48 hrs as mated flies are normally used in this type of analysis as female virgin have a different physiology than mated females (Cognigni et al., 2011). Lifespan analysis at 29ºC is often used as an accelerated assay. In accordance with this I first measured lifespan of *dp120ctn* mutants in these conditions. We observed a significant decrease in median lifespan of *dp120ctn* mutants (w^{1118}; $p120^{308}$-red line) when compared with control flies (w^{1118} -blue line) and this was consistent in males and females (Fig 3.6A-B). These results were encouraging and to extend them I repeated the experiment at 25ºC. When I measured lifespan of *dp120ctn* mutant males and females (w^{1118}; $p120^{308}$-red line) at 25ºC I found that they displayed a reduced median survival when compared to controls (w^{1118} -blue line) (Fig 3.7A-B). Additionally, I observed a small but reproducible decrease in the maximum lifespan of *dp120ctn* mutant males and females (Fig 3.87-B). This together with what we had observed at 29ºC suggested that *dp120ctn* maybe required for normal lifespan even in conditions were the flies were not being exposed to an acute stress stimulus.

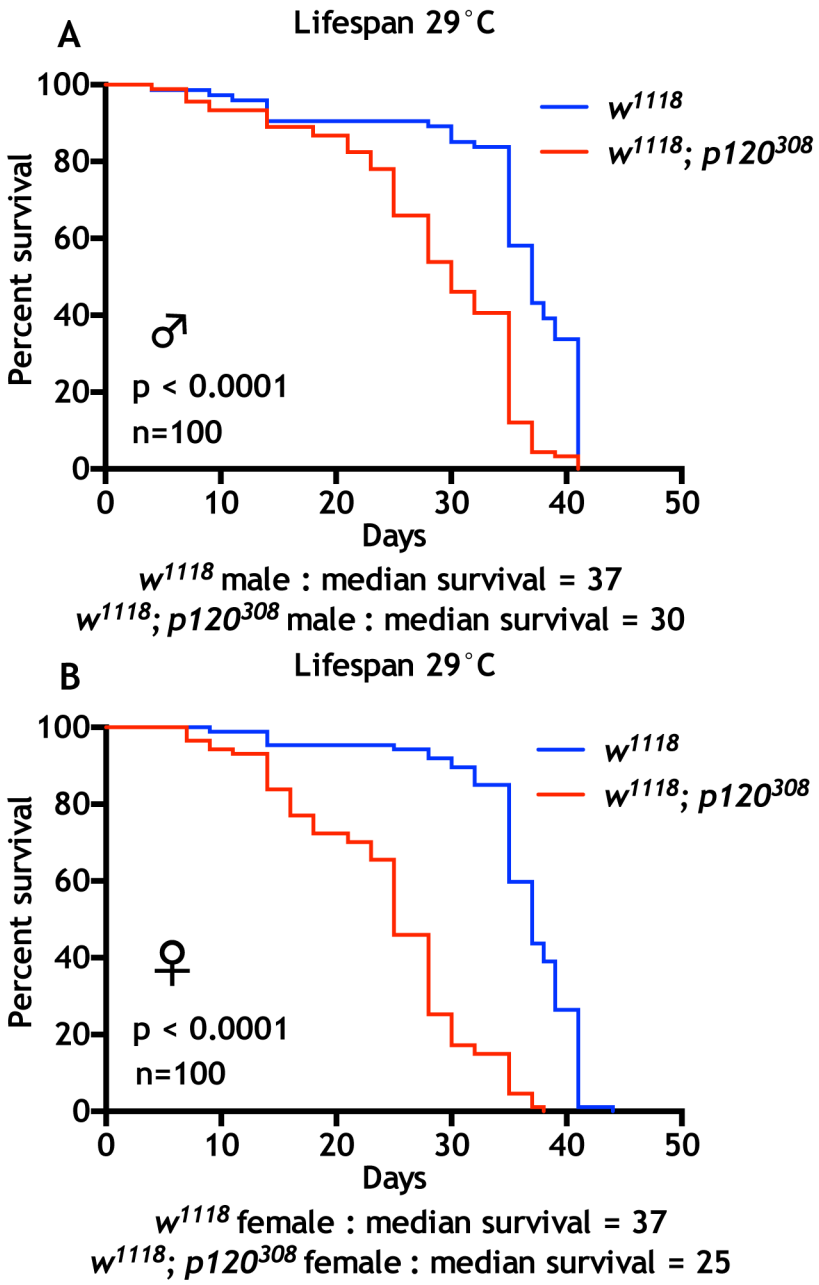

Figure 3.6 *dp120ctn* mutants display a reduced lifespan at 29°C

(A-B) Lifespan of w^{1118} and w^{1118}; $p120^{308}$ males (A) and females (B) at 29°C. Survival is plotted as adult survival in days. Blue lines indicate w^{1118} controls and red lines w^{1118}; $p120^{308}$. Each curve represents ~100 flies. Median survival is presented for each cohort and *p* value generated using log-rank tests.

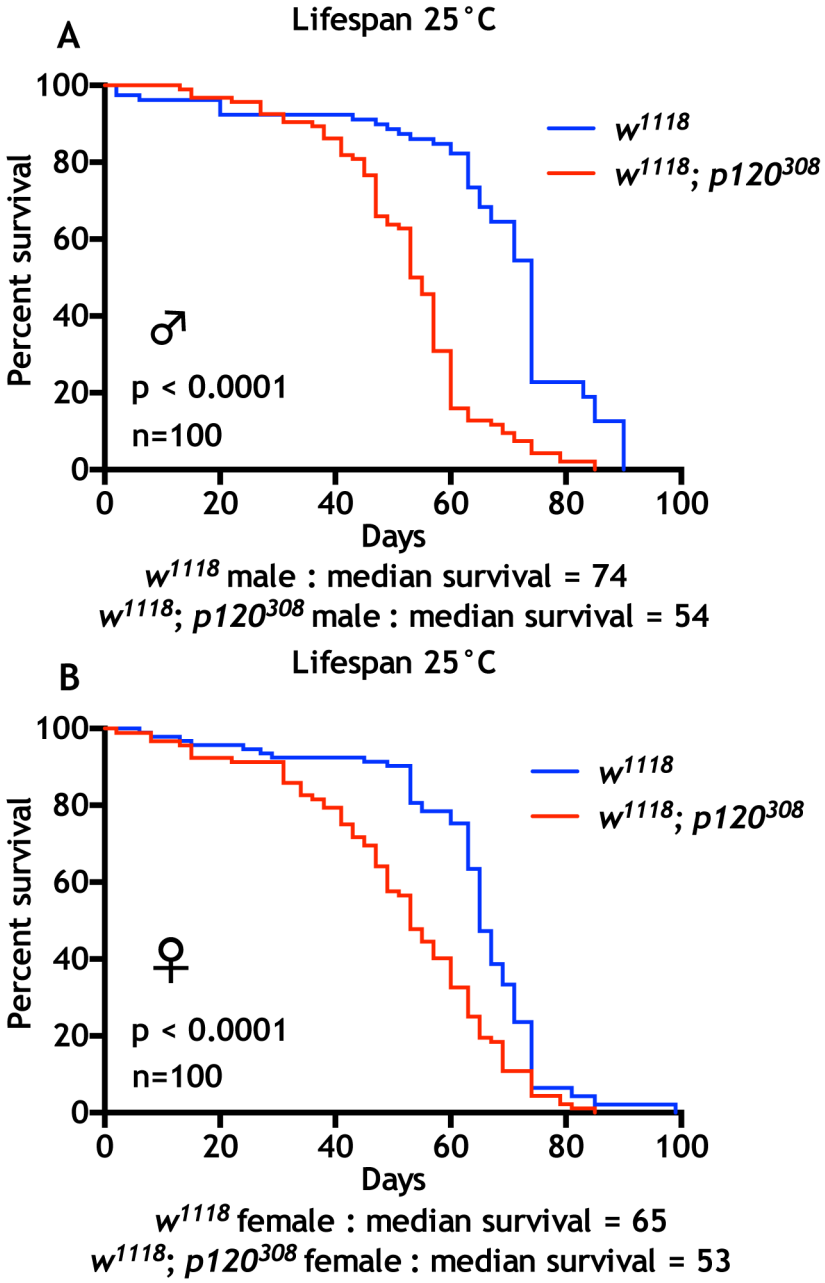

Figure 3.7 *dp120ctn* mutants display a reduced lifespan at 25°C

Lifespan of w^{1118} and w^{1118}; $p120^{308}$ males (A) and females (B) at 25°C. Survival is plotted as adult survival in days. Blue lines indicate w^{1118} controls and red lines w^{1118}; $p120^{308}$. Each curve represents ~100 flies. Median survival is presented for each cohort and *p* value generated using log-rank tests.

3.3.6 Ubiquitous expression of dp120ctn-GFP rescues heat shock sensitivity in *dp120ctn* mutants

As I had isogenized *dp120ctn* null mutants ($p120^{308}$) by backcrossing them to the control strain I was confident that the stress sensitivity I had observed was a result of the absence of dp120ctn. Nevertheless, to further confirm this I attempted to rescue the stress sensitivity phenotype of *dp120tn* mutants by re-expressing dp120 in these mutants. To do this I used a fly expressing a GFP tagged form of *dp120ctn* under the control of the ubiquitin promoter (ubi-p120-GFP) (Myster et al., 2003), which I also backcrossed to the w^{1118} strain and combined with the *dp120ctn* null allele (w^{1118}; $p120^{308}$; *ubiquitin-p120-GFP*).

I first tested if I could rescue the sensitivity to heat shock of *dp120ctn* mutants. I repeated the experiment as before but with the addition of *dp120ctn* mutant flies that were also expressing dp120ctn-GFP ubiquitously (w^{1118}; $p120^{308}$; *ubi-p120-GFP*). When I exposed control (w^{1118}-blue line), *dp120ctn* mutant (w^{1118}; $p120^{308}$-red line) and rescue (w^{1118}; $p120^{308}$; *ubi-p120-GFP*-green line) males and females to heat shock at 37°C, I observed that expression of dp120ctn-GFP completely rescued the sensitivity to heat shock observed in *dp120ctn* mutants (Fig 3.8A-B). Thus confirming that the heat shock sensitivity I observed in *dp120ctn* mutants is specific to loss of *dp120ctn*.

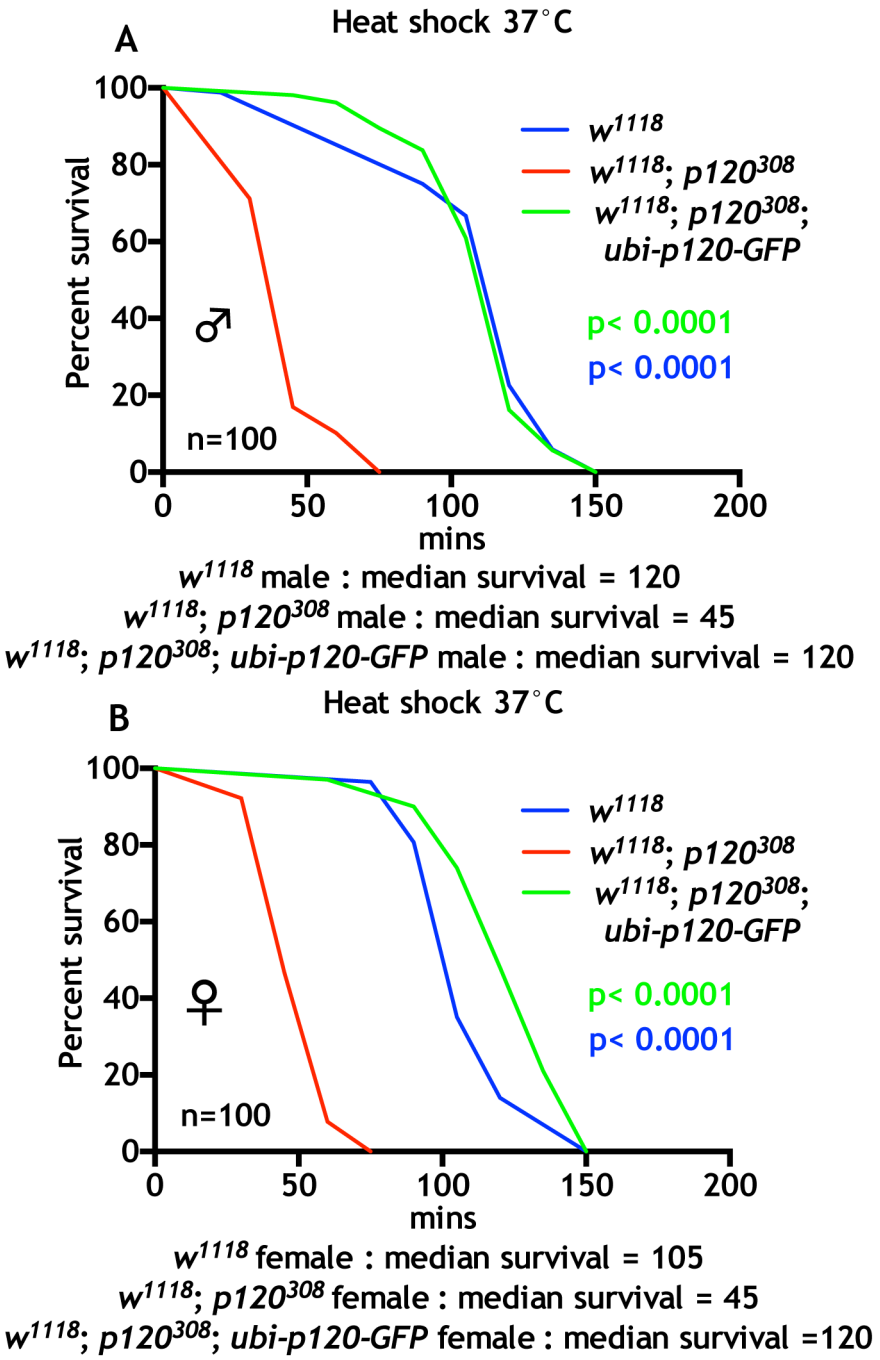

Figure 3.8 Ubiquitous Expression of p120-GFP rescues sensitivity to heat shock in *dp120ctn* flies

(A-B) Survival of w^{1118}, w^{1118}; $p120^{308}$ and w^{1118}; $p120^{308}$; *ubi-p120-GFP* males (A) and females (B) under heat shock conditions. Survival is plotted as adult survival in minutes under heat shock at 37°C. Blue lines indicate w^{1118} controls, red lines w^{1118}; $p120^{308}$ and green lines w^{1118}; $p120^{308}$; *ubi-p120-GFP*. Each curve represents ~100 flies. Median survival is presented for each cohort and *p* values generated using log-rank tests (Green *p* values correspond to comparison

between w^{1118}; $p120^{308}$ (RED) and w^{1118}; $p120^{308}$; *ubi-p120-GFP* (GREEN), blue *p* values correspond to comparison between w^{1118}; $p120^{308}$ (RED) and w^{1118} (BLUE)).

3.3.7 Ubiquitous expression of dp120ctn-GFP partially rescues starvation in *dp120ctn* mutant females.

I next tested if I could rescue the sensitivity of *dp120ctn* mutants to starvation. I measured survival under starvation in control (w^{1118}-blue lines), *dp120ctn* mutant flies (w^{1118}; $p120^{308}$-red lines) and *dp120ctn* mutant flies that also express dp120ctn-GFP ubiquitously (w^{1118}; $p120^{308}$; *ubiquitin-p120-GFP*-greed lines). I observed that expression of dp120ctn-GFP failed to rescue starvation sensitivity of *dp120ctn* mutant males as rescue males had a median survival similar to *dp120ctn* mutant males (Fig 3.9A). When I looked at survival of female rescue flies I observed an intermediate rescue of median survival under starvation (Fig 3.9B). In this case expression of dp120ctn-GFP was not able to rescue stress sensitivity in *dp120ctn* mutants.

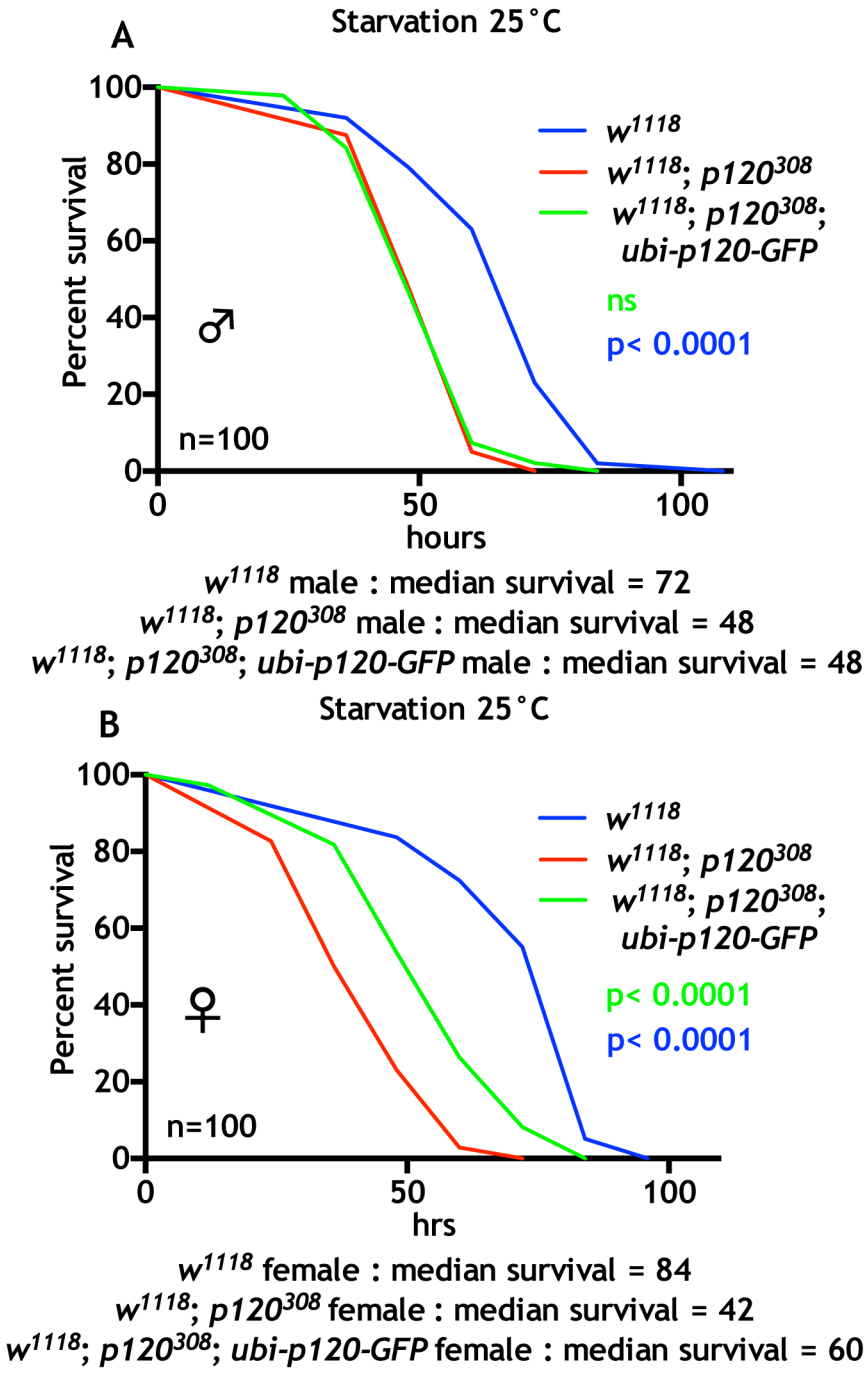

Figure 3.9 Ubiquitous Expression of p120-GFP partially rescues starvation sensitivity in female *dp120ctn* but not male *dp120ctn* mutant flies.

(A-B) Survival of w^{1118}, w^{1118}; $p120^{308}$ and w^{1118}; $p120^{308}$; *ubi-p120-GFP* males (A) and females (B) under starvation conditions. Survival is plotted as adult survival in hours under starvation at 25°C. Blue lines indicate w^{1118} controls, red lines w^{1118}; $p120^{308}$ and green lines w^{1118}; $p120^{308}$; *ubi-p120-GFP*. Each curve represents ~100 flies. Median survival is presented for each cohort and *p* value generated using log-rank tests (Green *p* values correspond to comparison

between *w*^{1118}*; p120*^{308} (RED) and *w*^{1118}*; p120*^{308}*; ubi-p120-GFP* (GREEN), blue *p* values correspond to comparison between *w*^{1118}*; p120*^{308} (RED) and *w*^{1118} (BLUE), ns-non significant).

3.3.8 Ubiquitous expression of dp120ctn-GFP rescues lifespan reduction in *dp120ctn* mutants

I also wanted to examine whether the reduction in median survival observed in *dp120ctn* mutants maintained at 25ºC and 29ºC could be rescued by ubiquitous expression of dp120ctn-GFP. When I compared the survival curves of control males and females (w^{1118}-blue lines) with *dp120ctn* mutant (w^{1118}; $p120^{308}$-red lines) males and females I again observed a significant reduction in median lifespan at both 29ºC and 25ºC (Fig 3.10A-B and Fig 3.11A-B). However, when I compared control flies (w^{1118}-blue line) with *dp120ctn* mutant males and females that were also expressing dp120ctn-GFP ubiquitously (w^{1118}; $p120^{308}$; *ubiquitin-p120-GFP* -green lines) I found that median lifespan was similar to controls at 29ºC and 25ºC (Fig 3.10A-B and Fig 3.11A-B). This confirmed that the reduction in median and maximum lifespan I observed in *dp120ctn* mutants was specific to loss of *dp120ctn*.

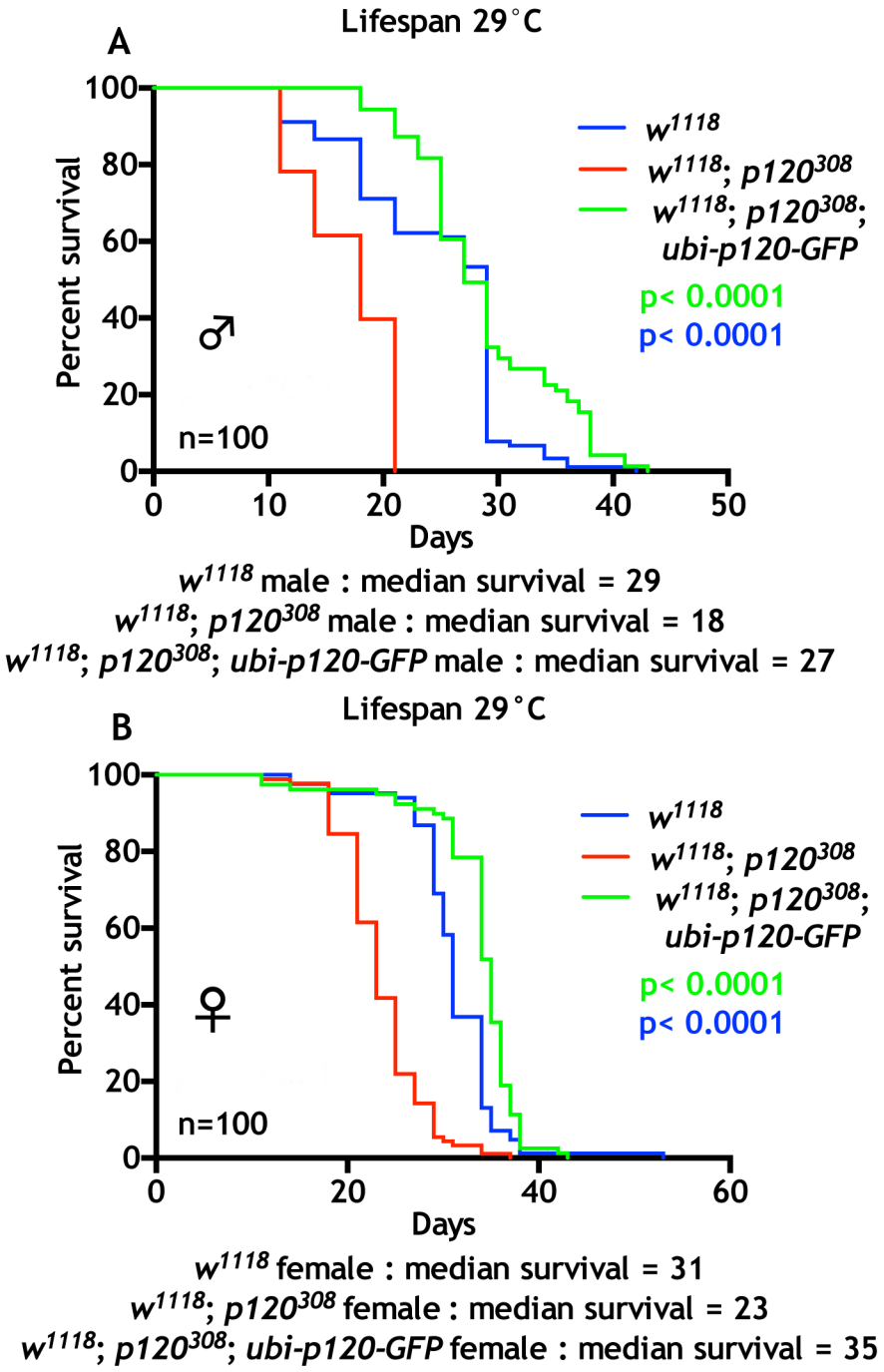

Figure 3.10 Ubiquitous Expression of p120-GFP rescues reduced lifespan of *dp120ctn* mutant flies at 29°C.

(A-B) Lifespan of w^{1118}, w^{1118}; $p120^{308}$ and w^{1118}; $p120^{308}$; *ubi-p120-GFP* males (A) and females (B) at 29°C. Blue lines indicate w^{1118} controls, red lines w^{1118}; $p120^{308}$ and green lines w^{1118}; $p120^{308}$; *ubi-p120-GFP*. Each curve represents ~100 flies. Median survival is presented for each cohort and *p* value generated using log-rank tests (Green *p* values correspond to comparison between w^{1118}; $p120^{308}$

(RED) and *w*^{1118}*; p120*^{308}*; ubi-p120-GFP* (GREEN), blue *p* values correspond to comparison between *w*^{1118}*; p120*^{308} (RED) and *w*^{1118} (BLUE)).

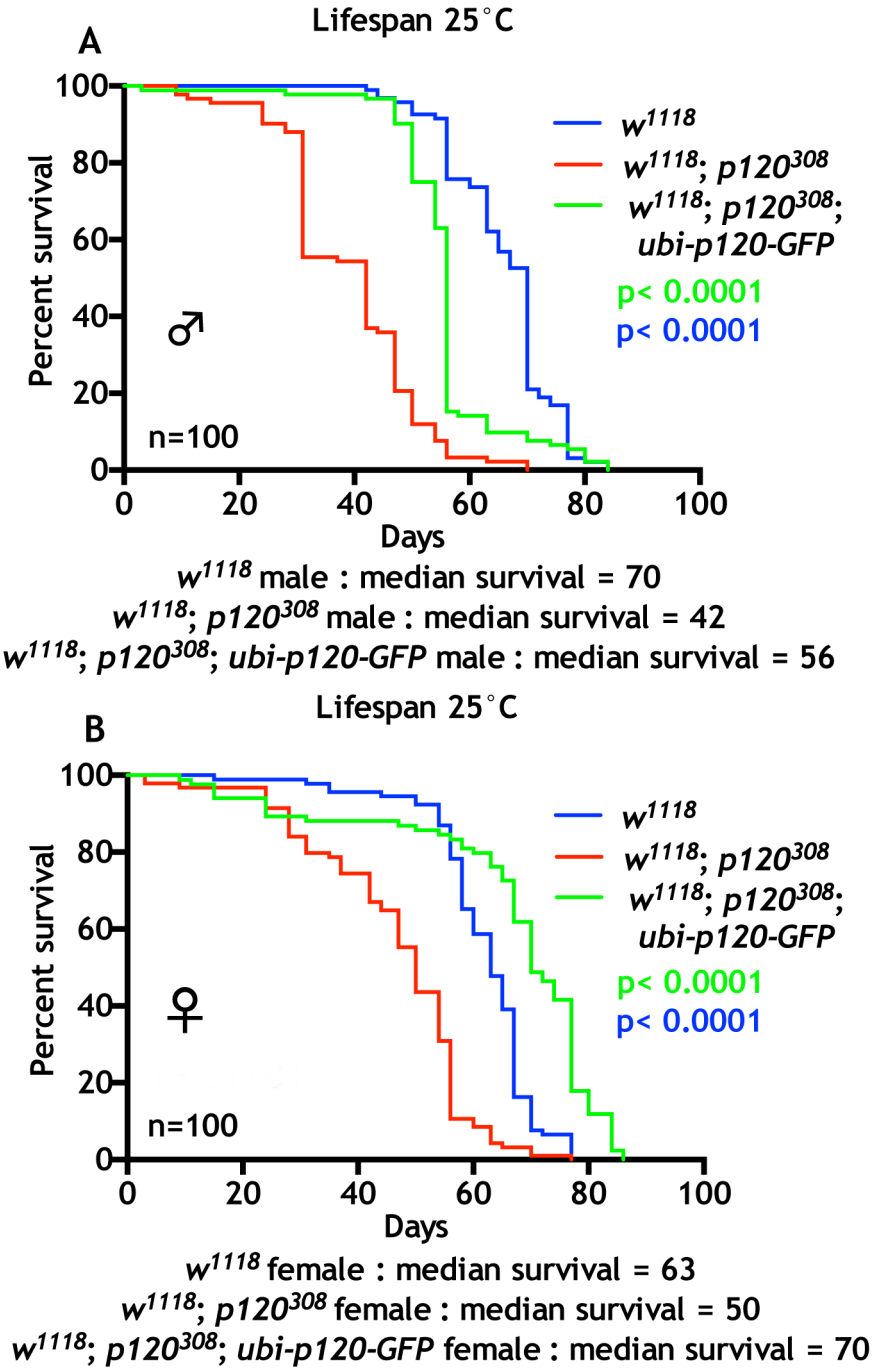

Figure 3.11 Ubiquitous Expression of p120-GFP rescues reduced lifespan of *dp120ctn* mutant flies at 25°C.

(A-B) Lifespan of w^{1118}, w^{1118}; $p120^{308}$ and w^{1118}; $p120^{308}$; *ubi-p120-GFP* males (A) and females (B) at 25°C. Blue lines indicate w^{1118} controls, red lines w^{1118}; $p120^{308}$ and green lines w^{1118}; $p120^{308}$; *ubi-p120-GFP*. Each curve represents ~100 flies. Median survival is presented for each cohort and *p* value generated using log-rank tests (Green *p* values correspond to comparison between w^{1118}; $p120^{308}$

(RED) and *w*^{1118}*; p120*^{308}*; ubi-p120-GFP* (GREEN), blue *p* values correspond to comparison between *w*^{1118}*; p120*^{308} (RED) and *w*^{1118} (BLUE)).

3.3.9 dp120ctn-GFP specifically delocalizes upon heat shock

To address how *dp120ctn* might be affected by stress stimuli I utilized dp120ctn-GFP to analyse localization of the dp120ctn in the *Drosophila* intestinal epithelium. I chose to perform this experiment in this tissue, as the adult intestine is a monolayered epithelium that is easily dissected and contains a variety of differentiated and undifferentiated cells. I dissected midguts from *dp120ctn* mutant flies expressing dp120ctn-GFP (*w^{1118}; $p120^{308}$; ubi-p120-GFP*) before and after 1 hour heat shock at 37°C. I used this genotype so that all the dp120ctn present would be tagged with GFP and to avoid reaching toxic levels of dp120ctn protein. Before heat shock dp120ctn-GFP was localized mostly at the plasma membrane with a diffuse cytoplasmic signal (Fig 3.12A-A'', white arrow). After heat shock dp120ctn-GFP could no longer be found at the plasma membrane of cells and instead the signal was diffuse and cytoplasmic (Fig 3.12B-B'', white arrow). This could be best appreciated in small cells where the cytoplasmic signal was more intense (Fig 3.12B-B'').

This result was very interesting but I wanted to test if it was specific as delocalization of dp120ctn upon heat shock could result from adherens junction disassembly. To address this point I repeated the experiment and stained for the core component *armadillo* (arm/β-catenin). Before heat shock I could observe that Arm was localized to cell membranes together with dp120ctn-GFP (Fig 3.13A-A'', white arrows). After heat shock, arm was still localized to membranes but as I had previously observed dp120ctn-GFP was delocalized and appeared diffuse in the cytoplasm (Fig 3.13B-B'', white arrows).

From these experiments I can say that dp120ctn-GFP becomes specifically delocalized from the plasma membrane upon heat shock and that this is not a result of adherens junction disassembly.

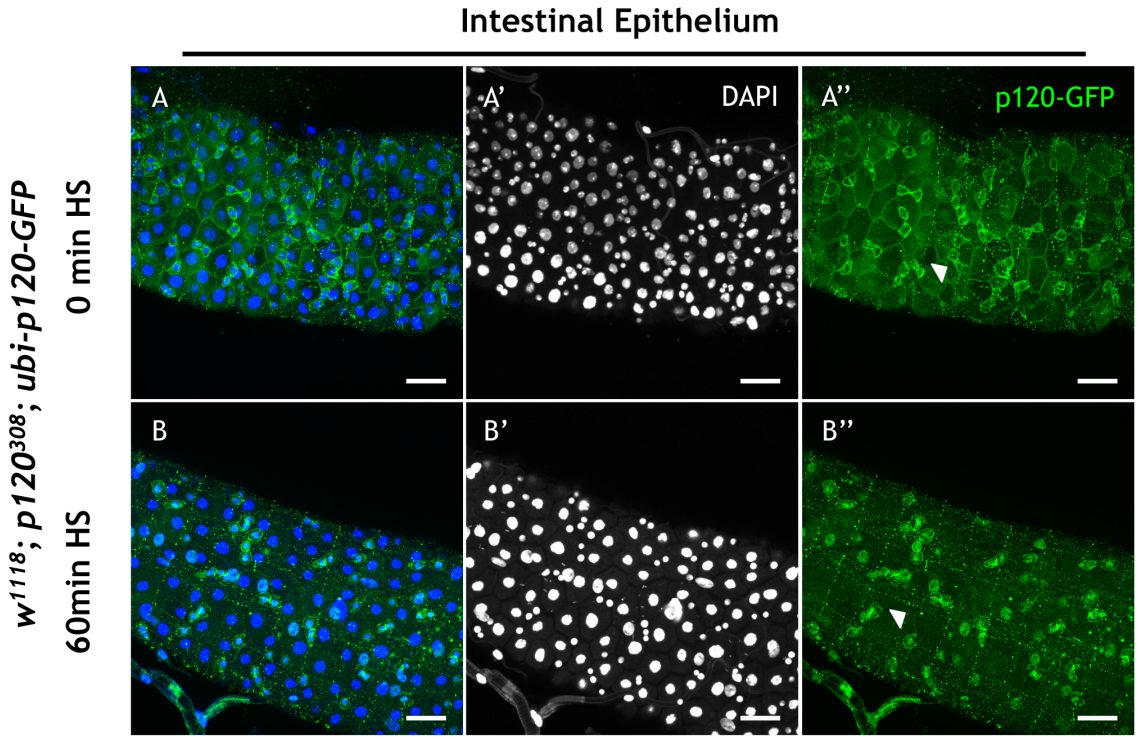

Figure 3.12 p120-GFP delocalizes upon Heat-shock in the *Drosophila* midgut epithelium.

(A-B'') Immunofluorescence of 7 day old midguts from *w*^{1118}; *p120ctn*^{308}; *ubi-p120ctn-GFP* flies before (A-A'') and after 1 hour heat-shock (B-B'') stained with DAPI and GFP. White arrowheads highlight membrane localization of p120-GFP that becomes diffuse after Heat- shock. Scale bar 25μm.

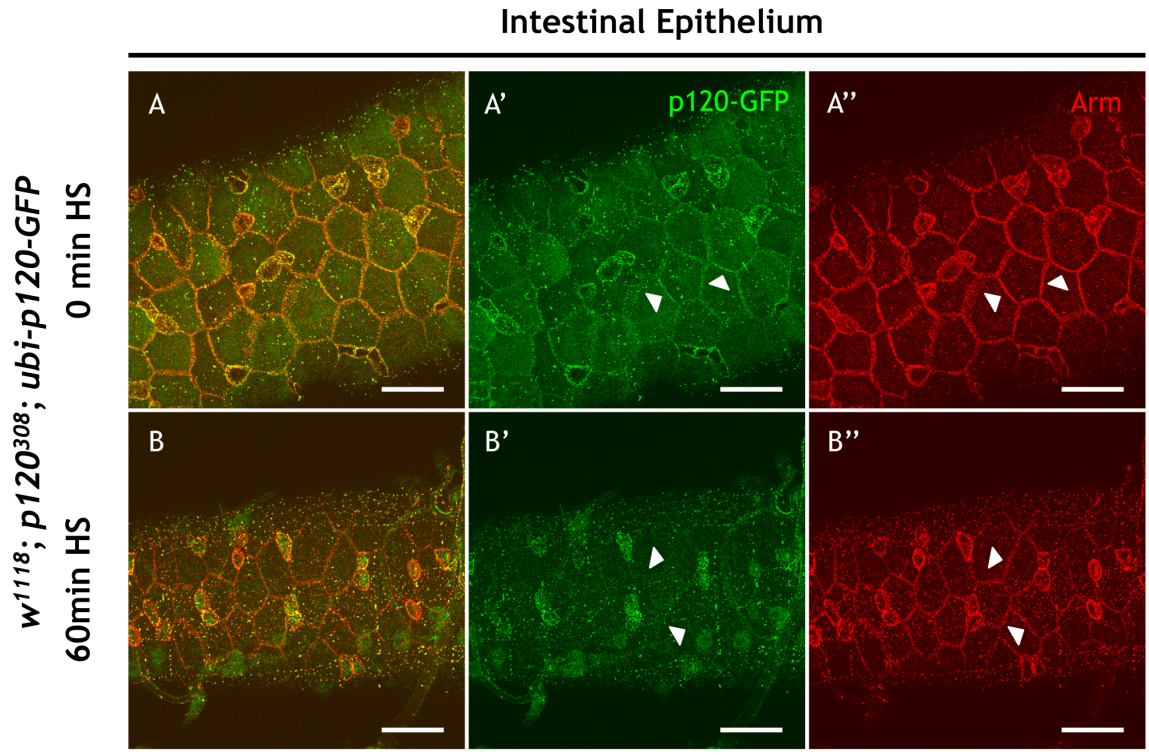

Figure 3.13 Armadillo (β-Catenin) does not delocalize upon Heat-Shock in the *Drosophila* midgut.

(A-B'') Immunofluorescence of 7 day old midguts from *w^{1118}; p120ctn^{308}; ubi-p120ctn-GFP* flies before (A-A'') and after 1 hour heat-shock (B-B'') stained with GFP and Armadillo. White arrowheads highlight membrane localization of p120-GFP that becomes diffuse after heat-shock while Armadillo remains clearly localized to the plasma membrane. Scale bar 25μm.

3.3.10 dp120ctn-GFP is regulated upon heat shock

I next wanted to ascertain if *dp120ctn* was perhaps being regulated as a result of heat shock and that this was leading to the delocalization I had observed. I first tested whether *dp120ctn* transcription was altered upon heat shock. I performed qPCR analysis on RNA from control (w^{1118}) flies and control whole adult flies heat shocked at 37°C for 1 hour and measured the levels of mRNA of *dp120ctn* and the core adherens junction protein *dE-cad*. I did not observe any significant difference in the transcription of these genes suggesting that *dp120ctn* is not regulated at the transcriptional level upon heat shock (Fig 3.14A-B).

Next I looked at *dp120ctn* regulation at the protein level using dp120ctn-GFP. After several failed attempts to visualize dp120ctn-GFP using western blot analysis, I decided to use the GFP tag to perform a GFP immunoprecipitation. Using this technique I analyzed samples from *dp120ctn* rescue flies (w^{1118}; $p120ctn^{308}$; *ubi-p120ctn-GFP*) before and after heat shock treatment. The anticipated size of dp120ctn-GFP is around 113kDa. I observed two distinct bands in both samples, one at around 80kDa and one at around 130kDa (Fig 3.14C) and as you can see from the western blot performed on the sample input dp120ctn-GFP was undetectable by western blot analysis (Fig 3.14D). More interestingly, I could see that there was more of the higher molecular weight band after heat shock treatment. The opposite was true for the lower molecular weight band that seemed to deplete after heat shock. In collaboration with the group of Sara Zanivan in the Beatson bands corresponding to these different molecular weights were cut out and using mass spectroscopy it was confirmed that all 4 bands contained dp120ctn-GFP (Fig 3.14C). Unfortunately due to the location of trypsin cleavage sites within dp120ctn we were not able to distinguish which regions of the protein were missing in the lower molecular weight band (Fig 3.14C). Overall, I concluded that two forms of dp120ctn-GFP are present in the cell and that heat shock affects the relative levels of these forms.

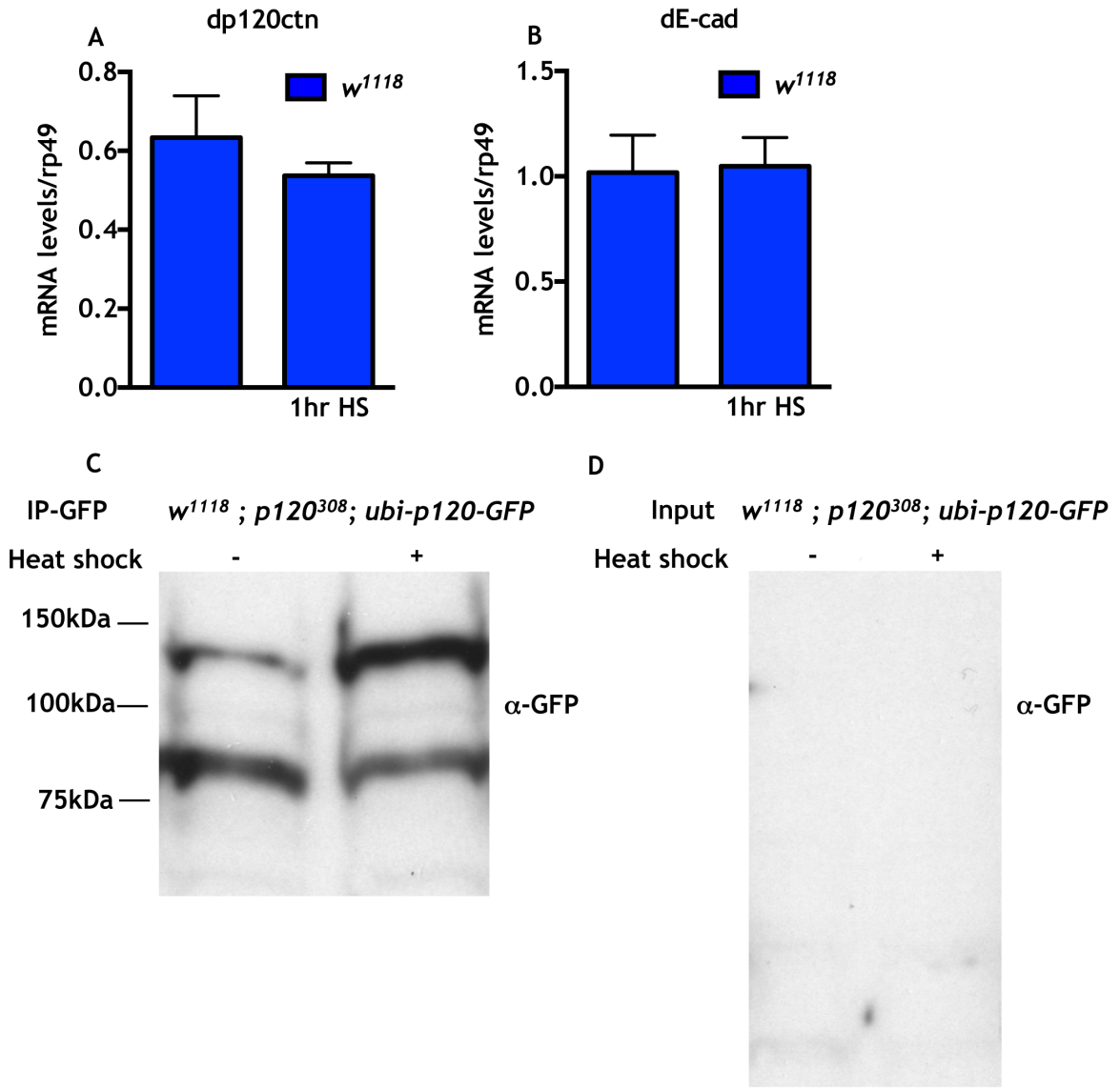

Figure 3.14 dp120ctn-GFP is regulated upon Heat shock.

(A-B) qPCR analysis for *dp120ctn* (A) and *dE-cad* (B) in w^{1118} flies before and after Heat shock. (C) dp120ctn-GFP was immunoprecipitated using GFP-pull down in *dp120ctn* mutant flies expressing dp120ctn-GFP ubiquitously (w^{1118}; $p120^{308}$; *ubi-p120-GFP*). (D) Input was blotted for GFP ubi-p120-GFP was not detected using western blotting methods.

3.3.11 *dp120ctn* mutants possess a differential gene expression profile.

To gain insights into the mechanisms that underlie how *dp120ctn* might be required in response to specific stressors I decided to perform microarray analysis on RNA extracted from control (w^{1118}) and *dp120ctn* mutant (w^{1118}; $p120^{308}$) females. This allowed me to get a global view of transcription in these mutants before and after stress stimulus. I isolated total RNA from control (w^{1118}) and *dp120ctn* mutant (w^{1118}; $p120^{308}$) 7 day old adult female flies in biological triplicates before and after 1 hour Heat shock at 37°C. Samples were purified and then sent to the MIAMI microarray facility at the Paterson Institute where the samples were hybridized to the Affymetrix GeneChip platform. After data collection the Beatson Institute Bioinformatics facility calculated fold change and significance. A cut off of 1.5/-1.5 in fold change and an adjusted p-value of 0.05 was used to select genes for analysis.

I first compared how each genotype responded to the 1 hour heat shock (Fig 3.15A). I could appreciate that although there were many genes equally upregulated and downregulated in response to heat shock there were also many genes that behaved distinctly in each genotype upon heat shock. I found that overall more genes were induced than repressed in both control (w^{1118}) and *dp120ctn* mutant flies (w^{1118}; $p120^{308}$) flies after eat shock (Fig 3.15B-C). When I looked just at those genes that were upregulated I noted that over 60 genes more were upregulated in *dp120ctn* mutant flies (w^{1118}; $p120^{308}$) than in control (w^{1118}) flies (Fig 3.15B). Additionally, only around half the genes induced in control (w^{1118}) and *dp120ctn* mutant flies (w^{1118}; $p120^{308}$) flies were common between both groups. A significant number of genes were also downregulated in response to heat shock but in this case control (w^{1118}) flies downregulated around 70 genes more than *dp120ctn* mutant flies (w^{1118}; $p120^{308}$) and only around half the genes downregulated in control (w^{1118}) flies were also downregulated in *dp120ctn* mutant flies (w^{1118}; $p120^{308}$) (Fig 3.15C). From this first assessment I could conclude that indeed there was a transcriptional response to heat shock in *dp120ctn* mutant flies (w^{1118}; $p120^{308}$), however it did not completely match that of control (w^{1118}) flies. I next wanted to ask whether *dp120ctn* mutant flies ($p120^{308}$) had a distinct transcriptional profile from control flies without any stress stimulus as I had observed a reduction in lifespan at 29°C and 25°C which could be rescued by ubiquitous expression of dp120ctn-GFP (Fig 3.10 and Fig

3.11). When I performed this comparison I found around 700 genes that were differentially expressed in *dp120ctn* mutant flies ($p120^{308}$) (Fig 3.15D). The majority of genes were up- or downregulated between 1.5 and 5 fold where as around only 40 genes were up- or downregulated more than 5 fold in *dp120ctn* mutant flies (w^{1118}; $p120^{308}$) (Fig 3.15D). From this, I could conclude that *dp120ctn* mutant flies possessed a differential transcriptional profile before and after heat shock treatment.

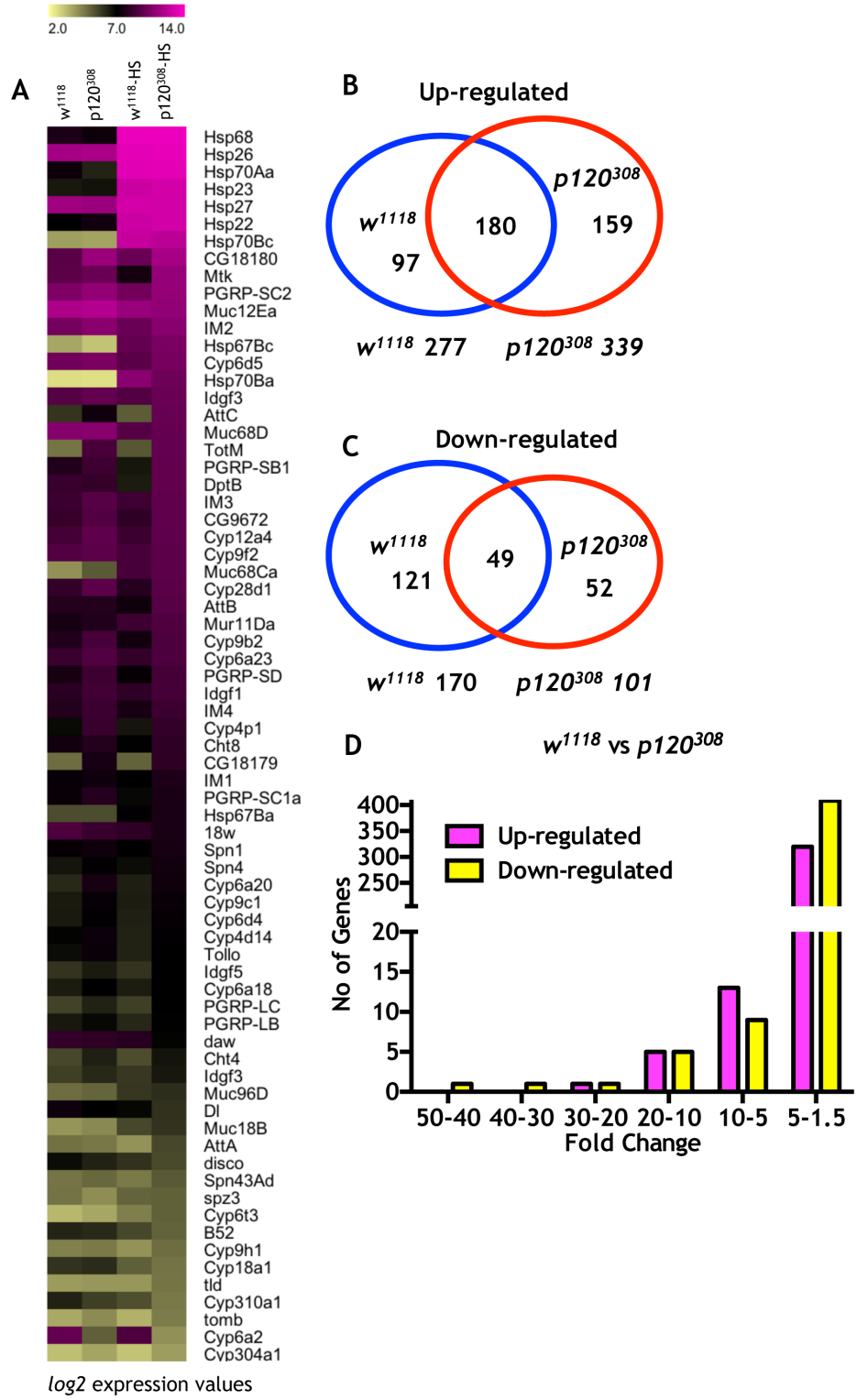

Figure 3.15 Transcriptomic analysis of *dp120ctn* mutants reveals differential gene expression.

(A) Averaged expression profile (*log2* expression values) of selected genes in w^{1118} and w^{1118}; $p120^{308}$ flies before (w^{1118}, w^{1118}; $p120^{308}$) and after 1hr of heat shock (w^{1118}-HS, w^{1118}; $p120^{308}$-HS). (B-C) Diagrams showing the number of genes upregulated and downregulated in w^{1118} and w^{1118}; $p120^{308}$ flies in response to a 1hr heat shock, and their overlap. (D) Graph displaying the numbers of genes up-

or down regulated in each fold change category between w^{1118} and w^{1118}; $p120^{308}$ flies

3.3.12 *dp120ctn* negatively regulates immune signalling.

A careful examination of the data led me to realize that many of the genes that were differentially regulated in *dp120ctn* mutant flies (w^{1118}; $p120^{308}$) were associated with a response to infection. Going back to the literature, I identified two previous studies from *De Gregorio et al* that had investigated the transcriptomic response of adult flies to different immune challenges (De Gregorio et al., 2001, De Gregorio et al., 2002). In these studies *De Gregorio et al* were able to identify around 400 genes that they named *Drosophila* immune-regulated genes (DIRGs) as their transcription was regulated in response to infection with a variety of *Drosophila* pathogens (De Gregorio et al., 2001). They went on to extend this by defining which DIRGs were targets of the Immune deficiency pathway (IMD) or the Toll signalling pathway, that represent the two branches of the innate immune response in *Drosophila*. Each pathway is upstream of the NF-κB like transcription factors *relish* (IMD) and *Dorsal/Dorsal related immune factor* (*Dif*) (Toll) which act to effect transcription in order to respond accordingly to an immune challenge (De Gregorio et al., 2002, Lemaitre and Hoffmann, 2007). I found that several DIRGs were misregulated in *dp120ctn* mutant flies (w^{1118}; $p120^{308}$). To confirm these hits I performed qPCR analysis on from control (w^{1118}), *dp120ctn* mutant flies (w^{1118}; $p120^{308}$) and *dp120ctn* mutant flies ubiquitously expressing dp120ctn-GFP (w^{1118}; $p120^{308}$; *ubi-p120-GFP*) before and after 1 hour heat shock 37°C.

I first looked at Heat shock protein 22 (*Hsp22*) that is induced readily upon heat shock as a control. I found that all flies subjected to heat shock showed highly elevated levels of this gene (Fig 3.16A). I next measured levels of three antimicrobial peptides (AMPs), *Attacin C* (*AttC*), *Attacin D* (*AttD*) and *Diptericin B* (*DptB*) that are all induced in response to infection through the IMD pathway downstream of *relish* (De Gregorio et al., 2002, Lemaitre and Hoffmann, 2007) (Fig 3.16B-D). In all three cases, expression of these genes in *dp120ctn* mutant flies (w^{1118}; $p120^{308}$) was significantly increased even before heat shock treatment (Fig 3.16B-D). Additionally, after heat shock *AttC* and *DptB* were significantly upregulated only in *dp120ctn* mutant flies (w^{1118}; $p120^{308}$) (Fig 3.16B, D). Furthermore, this aberrant expression was completely abolished in *dp120ctn* mutant flies ubiquitously expressing dp120ctn-GFP (w^{1118}; $p120^{308}$; *ubi-p120-GFP*)(Fig 3.16B-D). I also measured the levels of another DIRG, the peptidoglycan recognition protein (PGRP-LB) in the same samples and found that

dp120ctn mutant flies (w^{1118}; $p120^{308}$) expressed significantly higher levels of this gene before heat shock and that this misregulation was rescued in *dp120ctn* mutant flies ubiquitously expressing dp120ctn-GFP (w^{1118}; $p120^{308}$; *ubi-p120-GFP*)(Fig 3.16E). This data strongly supports a role for *dp120ctn* in the negative regulation of the immune response as *dp120ctn* mutants express genes that are normally expressed as part of an immune response.

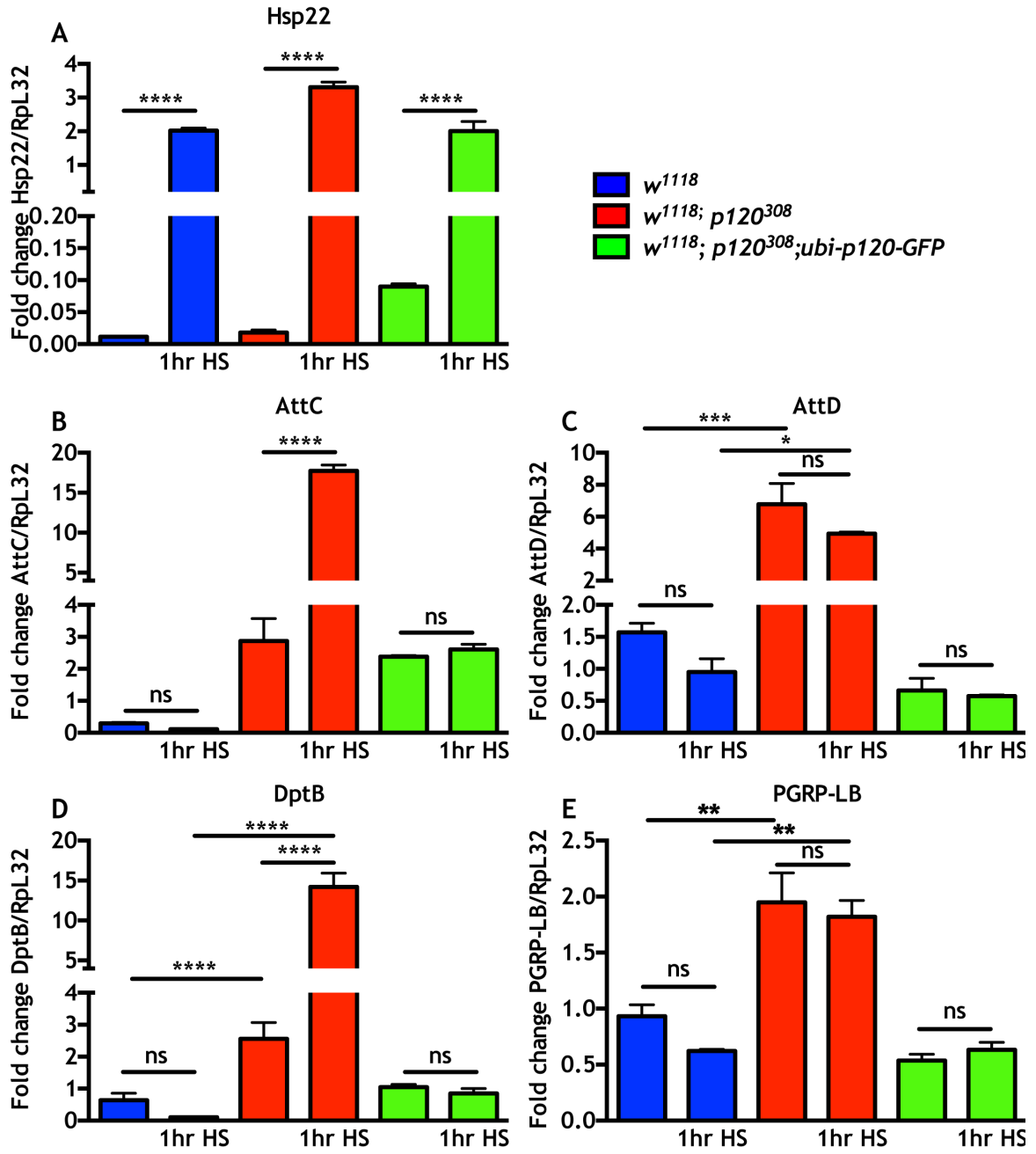

Figure 3.16 Ubiquitous expression of p120ctn-GFP rescues aberrant gene expression in *dp120ctn* mutant flies.

(A-E) qPCR analysis of selected targets in w^{1118}, w^{1118}; $p120^{308}$ and w^{1118}; $p120^{308}$; *ubi-p120-GFP* flies before and after 1hr heat shock (one-way ANOVA with Bonferroni post test correction, ns: non-significant, * $p<0.05$; **$p<0.005$, ***$p<0.001$****$p<0.0001$). Targets B-E have been reported to be regulated by the *relish* transcription factor in response to infection. Here we find that all of these genes are upregulated in *dp120ctn* mutant flies. A smaller subset (B, D) are further upregulated in response to heat shock in *dp120* mutant flies.

3.3.13 Heterozygous loss of *relish* rescues aberrant gene expression in *dp120ctn* mutants.

The DIRGs that I identified as aberrantly expressed in *dp120ctn* mutant flies are regulated by the *relish* NF-κB-like transcription factor (De Gregorio et al., 2001, De Gregorio et al., 2002). Interestingly, it has been described that p120ctn loss in the murine epidermis leads to constitutive activation of NF-κB (De Gregorio et al., 2001, De Gregorio et al., 2002, Perez-Moreno et al., 2006, Perez-Moreno et al., 2008). I wanted to test whether the divergent transcriptional profile I had observed in *dp120ctn* mutant flies was dependent on the NF-κB-like transcription factor *relish*. To do this I combined *dp120ctn* mutant flies with one copy of a null allele of *relish* (*Rel*^{E20}) to half the genetic dose of *relish* (*w*^{1118}*; p120*^{308}*; Rel*^{E20}/+). I extracted total RNA from control (*w*^{1118}), *dp120ctn* mutant (*w*^{1118}*; p120*^{308}) and *dp120ctn* mutant females carrying either one copy of a null allele for *relish* (*RelE20*) (*w*^{1118}*; p120*^{308}*; Rel*^{E20}/+) or a transgene expressing dp120ctn-GFP under the control of the ubiquitin promoter (*w*^{1118}*; p120*^{308}*; ubi-p120-GFP*) and measured levels of selected *relish* regulated DIRGs (*AttD, PGRP-LB*, *PGRP-SC2*, *PGRP-SD* and *Sp4*) (Fig 3.17A-E) (De Gregorio et al., 2001, De Gregorio et al., 2002). In *dp120ctn* mutant flies (*w*^{1118}*; p120*^{308}) all targets were significantly unregulated with respect to control flies (*w*^{1118}). As in the case of heat shock expression of dp120ctn-GFP rescued the expression levels of these key targets (Fig 3.17A-E). Most remarkably, halving the genetic dose of *relish* (*w*^{1118}*; p120*^{308}*; Rel*^{E20}/+) rescued the expression of these targets to levels similar to control flies (*w*^{1118}). This data further suggest that *dp120ctn* is required to negatively regulate *relish* dependent transcription in *Drosophila*.

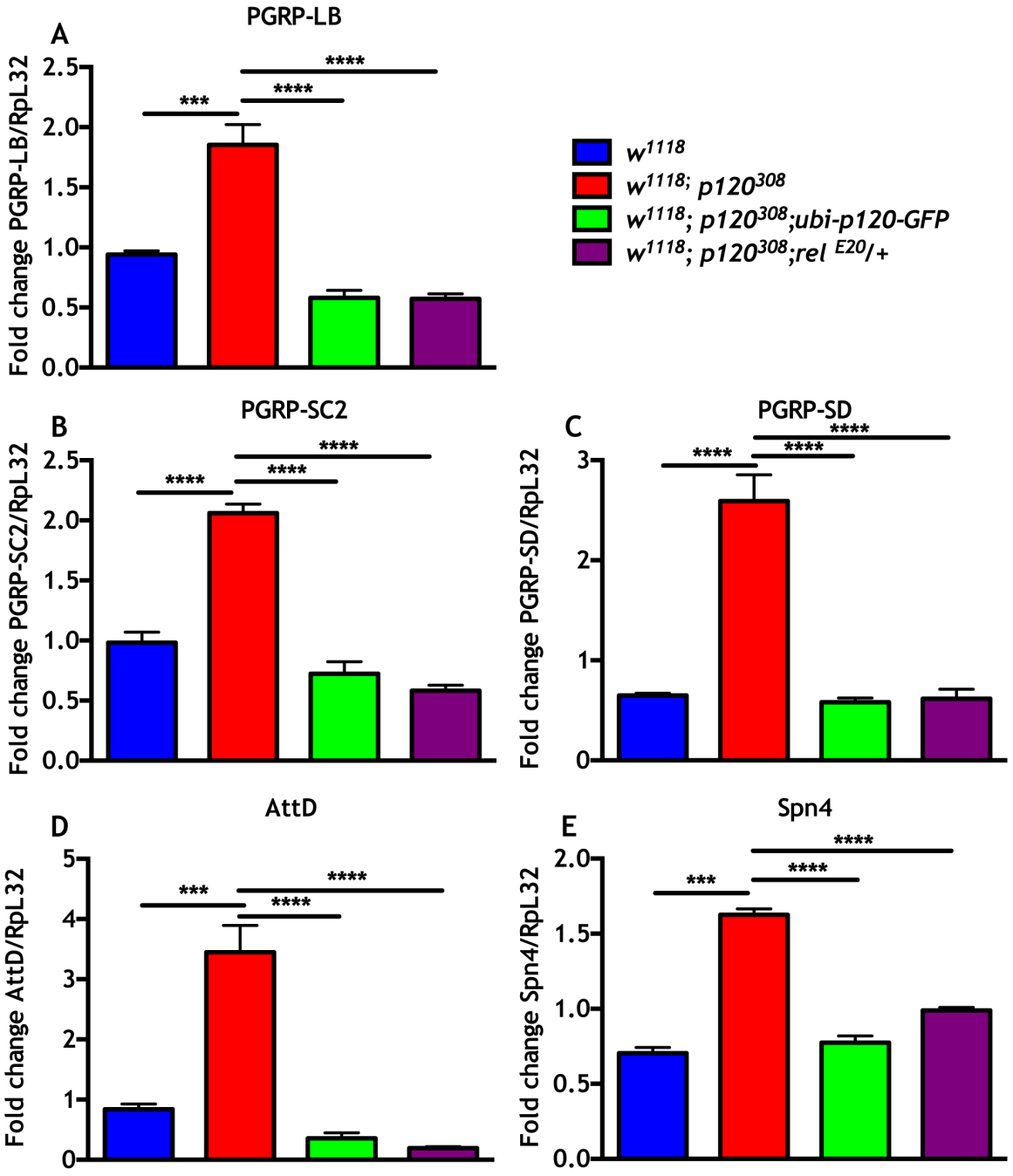

Figure 3.17 Heterozygous loss of *relish* rescues aberrant gene expression in *dp120ctn* flies.

(A-E) qPCR analysis of selected genes in w^{1118}, w^{1118}; $p120ctn^{308}$, w^{1118}; $p120ctn^{308}$; *ubi-p120ctn-GFP* and w^{1118}; $p120ctn^{308}$; $rel^{E20/+}$ flies (one-way ANOVA with Bonferroni post test correction, ***p<0.001****p<0.0001). The targets selected have been reported to be regulated by the *relish* transcription factor in response to infection. This aberrant expression is rescued by heterozygous loss of the transcription factor *relish*.

3.3.14 relish-RFP localization in *dp120ctn* mutants

When the immune response is active, relish is cleaved and translocates to the nucleus where it drives transcription. In order to address whether *relish* was constitutively active in *dp120ctn* mutants I performed a preliminary experiment using an RFP tagged form of relish (Relish-RFP). We combined a UAS transgene for Relish-RFP with the daughterless Gal4 (dauG4) driver, that drives expression ubiquitously, in either a control (*w^{1118}; dauG4-Rel-RFP*) or *dp120ctn* mutant background (*w^{1118}; $p120^{308}$; dauG4-Rel-RFP*). I dissected intestines, which are known to be immune responsive, from control and *dp120ctn* mutant flies and looked at localization of Relish-RFP before and after 1 hour heat shock at 37°C (Fig 3.18). Expression of the transgene was patchy in all the intestines analyzed suggesting that there was not ubiquitous expression using this driver (Fig 3.18). When we looked before heat shock we could observe that in control (*w^{1118}; dauG4-Rel-RFP*) intestines Relish-RFP was diffuse in the cells (Fig 3.18A-A'', white arrows). In *dp120ctn* mutant intestines (*w^{1118}; $p120^{308}$; dauG4-Rel-RFP*), Relish-RFP was more intense but no obvious nuclear localization was observed (Fig 3.18C-C'', white arrows). After heat shock, there was clear nuclear accumulation in control intestines (Fig 3.18B-B'', yellow arrows) and *dp120ctn* mutant intestines (Fig 3.18D-D'', yellow arrows). However, the signal in *dp120ctn* mutant intestines was again more intense and I could observe clear membrane localization (Fig 3.18D-D'', yellow arrows). Although this was a preliminary experiment that will need to be repeated, it suggests that there may indeed be aberrant regulation of *Relish* in *dp120ctn* mutants.

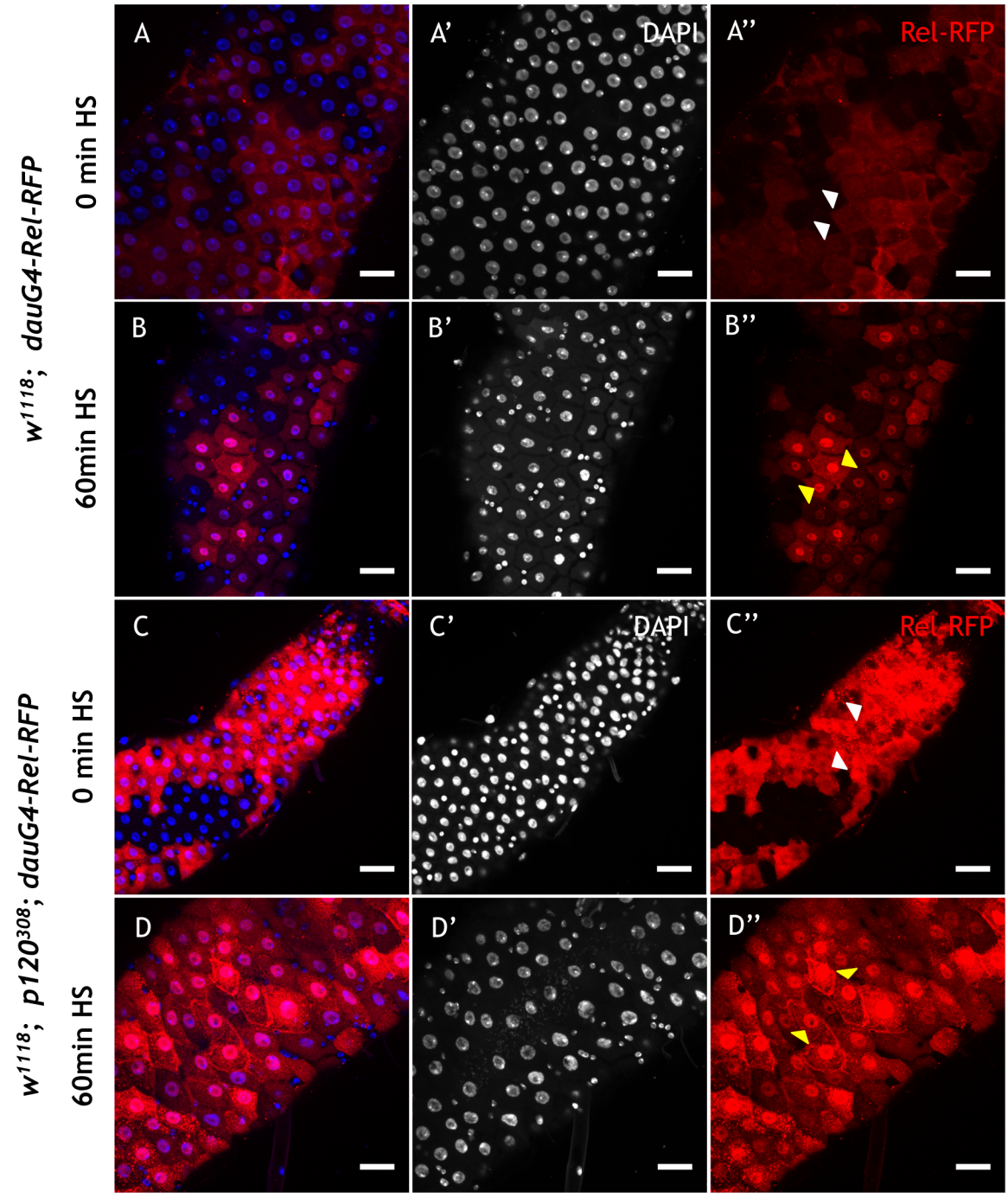

Figure 3.18 Localization of Relish-RFP in *d120ctn* mutants.

(A-D'') Confocal images of 7 day old midguts from *w*^{1118}; *dauG4-Relish-RFP* and *w*^{1118}; *p120*^{308}; *dauG4-Relish-RFP* flies before (A-A'' and C-C'') and after 1 hour Heat-shock (B-B'' and D-D'') stained with DAPI. White arrowheads in A-A'' and C-C'' highlight cytoplasmic localization of Relish-RFP. Yellow arrowheads in B-B'' and D-D'' highlight nuclear localization of Relish-RFP after 1 hour HS. Scale bars 25μm.

3.3.15 Loss of *dp120ctn* enhances tumour burden in *scribble* and *discs large* mutant larvae

As *p120ctn* has been described as potent tumour suppressor (Stairs et al., 2011) and is frequently downregulated or mislocalized in a variety of cancer types (Thoreson and Reynolds, 2002, Talvinen et al., 2010, Miao et al., 2010), I wanted to investigate how *dp120ctn* loss would affect tumour burden in an established model of cancer in *Drosophila*. To do this I utilized null mutants of two polarity tumour suppressors of the *scribble* (*scrib*) group, *scribble* and *discs large*. I first combined the null allele of *dp120ctn* ($p120^{308}$) with a null allele for *scrib* ($scrib^{1}$) to create double mutant larvae ($p120^{308}$; $scrib^{1}$). *scrib* larvae arrest at the larval stage due to transformation of the imaginal tissues. The larvae become giant and bloated (Fig 3.19A-A'). When I looked at *dp120ctn-scrib* mutant larvae I observed that they also arrested in the larval stage and looked to be even more bloated (Fig 3.19A-A''). When I dissected wing imaginal disc tumours from these larvae and stained for DAPI, I could appreciate an increase in tumour size in *dp120ctn-scrib* larvae (Fig 3.19B-C). When I quantified tumour volume for tumours from *scrib* and *dp120ctn-scrib* larvae I found a significant increase in tumour burden (Fig 3.19D).

These results were encouraging but in order to consolidate them I decided to repeat the experiments with another null mutant for the polarity tumour suppressor *discs large* ($dlg^{40.2}$) also part of the *scrib* group. As for *scrib*, I combined the $dlg^{40.2}$ allele with the *dp120ctn* null allele to produce double mutant larvae ($dlg^{40.2}$; $p120^{308}$). Like *scrib*, *dlg* larvae arrest at the larval stage and become bloated as all imaginal tissues become transformed (Fig 3.19E-E'). Double mutant larvae also arrested at the larval stage and became even more bloated (Fig 3.19E-E''). As with tumours dissected from *dp120ctn-scrib* double mutant larvae, tumours from *dlg-dp120ctn* larvae were larger than tumours from *dlg* larvae (Fig 3.19F-G). When I quantified this I found a significant increase in tumour burden in *dlg-dp120ctn* larvae (Fig 3.19H).

These results, although preliminary suggest that *dp120ctn* loss has a positive affect on tumour burden.

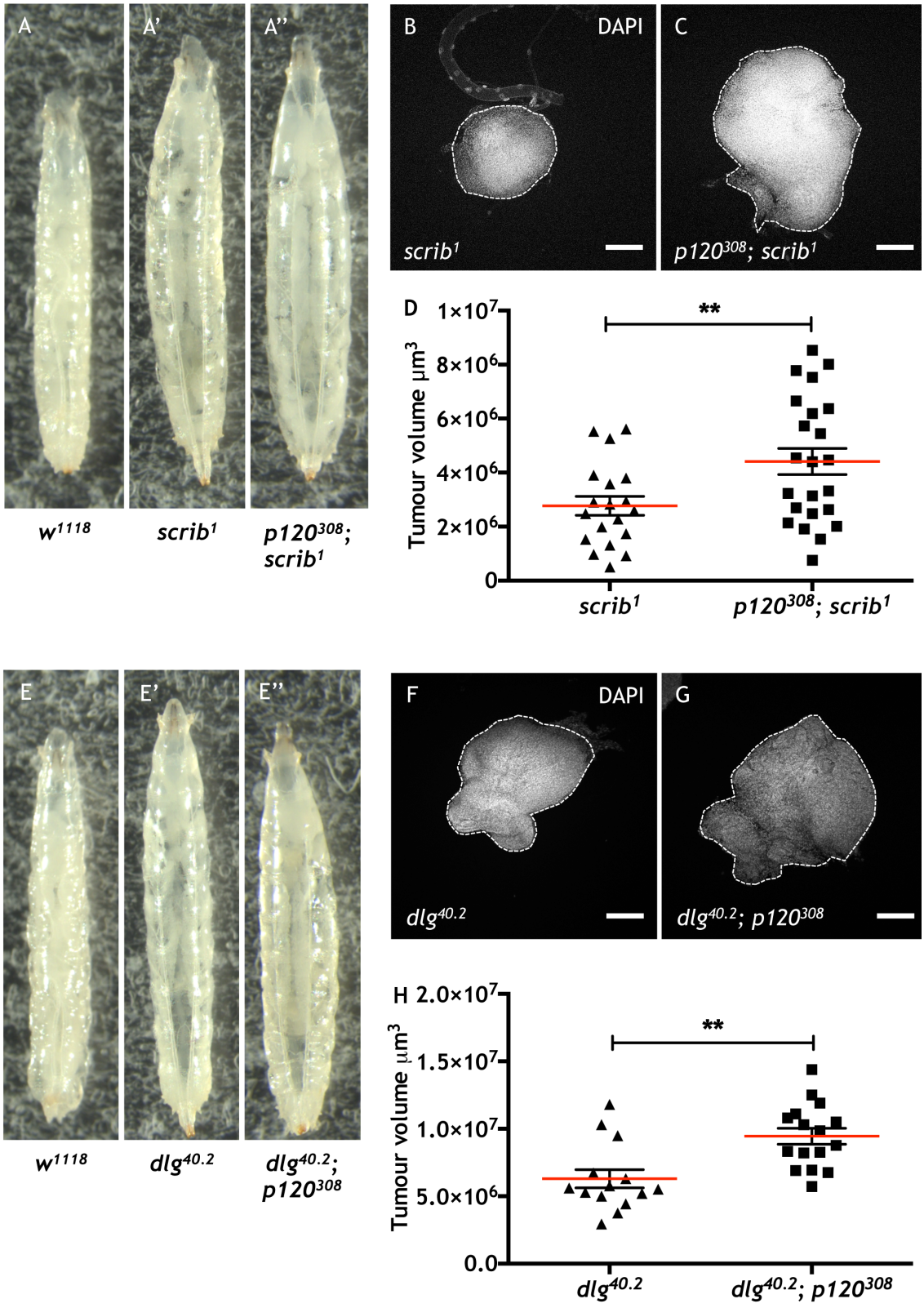

Figure 3.19 Loss of *dp120ctn* enhances tumour burden of *scrib* and *dlg* mutant larvae.

(A-A'' and E-E'') Images of w^{1118} (5 day old), $scrib^{1}$ (11 day old), $p120^{308}$; $scrib^{1}$ (11 AED), $dlg^{40.2}$ (11 AED) and $dlg^{40.2}$; $p120^{308}$ (11 day old) 3rd instar larvae. (B-C and F-G) Immunofluorescence of wing imaginal disc tumours from 11 AED $scrib^{1}$,

p120^{308}; scrib^{1}, *dlg$^{40.2}$* and *dlg$^{40.2}$; p120^{308}* 3rd instar larvae stained for DAPI (dashed outlines mark tumour edges). (D, H) Quantification of Tumour Volume (D, p= 0.0093), (H, p= 0.0015).

3.3.16 Transcriptomic analysis of *dp120ctn* and *scribble* mutant tumours

As I had preliminary evidence that *dp120ctn* could increase tumour burden (Fig 3.19), I wanted to get an unbiased view of transcription in these tumours. I extracted total RNA of wing imaginal disc tumours from *scrib* (*scrib*^{1}) and double mutant larvae (*p120*^{308}*; scrib*^{1}). Samples were purified and then sent to the MIAMI microarray facility at the Paterson Institute where the samples were hybridized to the Affymetrix GeneChip platform. After data collection the Beatson Institute Bioinformatics facility calculated fold change and significance. A cut off of 1.5/-1.5 in fold change and an adjusted p-value of 0.05 was used to select genes for analysis.

When I compared the transcriptional profile of these tumours (*scrib*^{1} vs *p120*^{308}*; scrib*^{1}) I found only around 200 genes were significantly up- or down regulated (Fig 3.20A-B). The Beatson Bioinformatics group performed a gene enrichment analysis on the data set but found no significant enrichment of any biological process or pathway. However, this may be due to our reduced data. For example, there are two genes that code for type VI collagen in *Drosophila* (*Cg25C and Viking*) and both these genes were significantly downregulated in wing disc tumours from double mutant larvae (*p120*^{308}*; scrib*^{1}). However, the gene enrichment analysis failed to detect this as significant despite downregulation of both family members. Additionally, we find several genes that are involved in purine biosynthesis (Fig 3.20B).

More analysis will be needed before we can understand how loss of *dp120ctn* is affecting tumour burden in *Drosophila* but taken together my data suggest that *dp120ctn* may also have tumour suppressor properties in *Drosophila*.

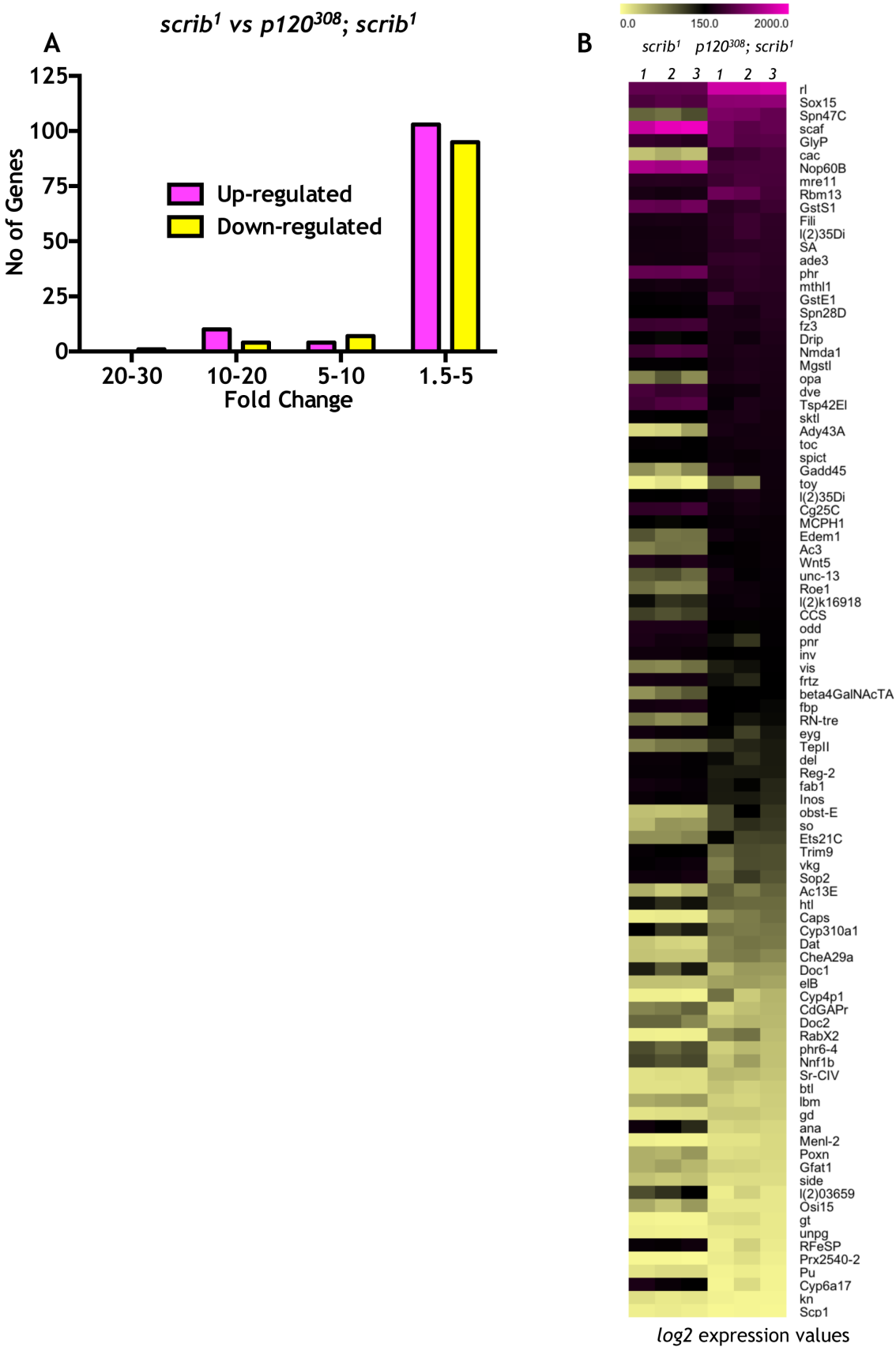

Figure 3.20 Transcriptomic analysis of *dp120ctn - scribble* tumours.

(A) Graph displaying the numbers of genes up-or down regulated in each fold change category between *scrib*^{1} and *p120*^{308}; *scrib*^{1} tumours. (B) Expression

profile (*log2* expression values) of selected genes in biological replicates of *scrib*^{1} and *p120*^{308}; *scrib*^{1} tumours.

3.4 Discussion

3.4.1 *dp120ctn* in the stress response

The generation of a *dp120ctn* null allele unambiguously demonstrated that *dp120ctn* was not required for *Drosophila* adhesion and development (Myster et al., 2003). *dp120ctn* mutant flies are viable and fertile but I hypothesized that as *p120ctn* is well conserved that it may be required in conditions of stress. I found this to be the case, as *dp120ctn* mutant flies (w^{1118}; $p120^{308}$) were more sensitive to Heat shock at 37°C and displayed a reduced median lifespan (Fig 3.4, 3.6 and 3.7). These phenotypes were rescued by ubiquitous overexpression of dp120ctn-GFP (Fig 3.8, 3.10 and 3.11), confirming that they were specific to loss of *dp120ctn*. This is the first demonstration of a systemic requirement for *dp120ctn* in *Drosophila*.

Heat shock stress is an acute stress stimulus while lifespan analysis measures the rate at which an organism becomes unable to deal with environmental stress over a protracted period of time. This suggested two hypotheses; either *dp120ctn* mutant flies (w^{1118}; $p120^{308}$) are more sensitive to stress stimuli or they are inherently more stressed. In order to address this I looked at *dp120ctn* regulation under conditions of stress. dp120ctn-GFP localizes to the plasma membrane in the adult *Drosophila* posterior midgut (Fig 3.12 and 3.13). In midguts, from heat-shocked flies, dp120ctn-GFP became specifically delocalized, diffuse and cytoplasmic while Arm (β-catenin) remained at the plasma membrane (Fig 3.12 and 3.13). Immunoprecipitation and mass spectrometry analysis of dp120ctn-GFP demonstrated that a high molecular weight form of *dp120ctn* was stabilized upon heat shock (Fig 3.14). Unfortunately, from this analysis I was unable to ascertain if the two molecular weights corresponded to cleaved or phosphorylated substrates. In order to clarify and gain further insights I will repeat the immune precipitation and digest with a different protease in order to better understand the differences between the two isoforms I observed. Further analysis will also be needed to understand how *dp120ctn* is regulated under different conditions in *Drosophila* (Fig 3.21).

3.4.2 *dp120ctn* regulation of immune signalling

The Imd signalling pathway is one arm of innate immune signalling in *Drosophila* (Kim and Kim, 2005). Its activation is highly controlled and then rapidly downregulated after infection to prevent a prolonged immune response (Kim and Kim, 2005). As such many negative regulators of the pathway have been identified (Bischoff et al., 2006, Zaidman-Remy et al., 2006, Kleino et al., 2008). Using Microarray analysis I found that adult *dp120ctn* null flies aberrantly express several targets of the transcription factor *relish* before and after heat shock treatment (Fig 3.15 and 3.16). Ubiquitous expression of dp120ctn-GFP or heterozygous loss of *Relish* rescued this aberrant expression (Fig 3.17). These results suggest that dp120ctn may play a role in the negative regulation of immune signalling in *Drosophila*. Preliminary experiments using an RFP labeled Relish (Relish-RFP) suggest that *Relish* localization maybe be disrupted in *dp120ctn* mutant flies (Fig 3.18, Fig 3.21).

Together these data strongly support a role for *dp120ctn* in the negative regulation of the immune response as *dp120ctn* mutants express genes that are normally expressed during an immune response (Fig 3.15, 3.16 and 3.17). This is in accordance with evidence that loss of p120ctn in the murine epidermis, intestine, oral and esophageal tract results in acute inflammation in these tissues despite no barrier defects (Perez-Moreno et al., 2006, Smalley-Freed et al., 2010, Stairs et al., 2011, Smalley-Freed et al., 2011). These results propose a conserved role for *dp120ctn* in the regulation of immune signalling in *Drosophila*.

To further consolidate these results I would like to address the functional contribution of *relish* to the *dp120ctn* mutant stress sensitive phenotype by examining whether reduction in the genetic dose of *relish* could rescue *dp120ctn* mutant stress sensitivity. Moreover, I would like to address how *dp120ctn* might be regulating *relish* dependent transcription. This would be of great interest, as currently inflammation upon loss of p120ctn has been ascribed to epithelial barrier defects and recruitment of immune cells (Perez-Moreno et al., 2006, Perez-Moreno et al., 2008, Smalley-Freed et al., 2010, Smalley-Freed et al., 2011).

3.4.3 *dp120ctn* and Cancer

p120ctn down-regulation or delocalization in cancer correlates with poor prognosis (Vidal et al., 2010, Talvinen et al., 2010). Loss of *p120ctn* in the murine oral cavity and oesophagus results in Oral squamous cell cancers (OSCCs) and oesophageal squamous cell cancers (ESCCs) (Stairs et al., 2011). There is a growing body of evidence that *p120ctn* loss results in tumourigenesis through the establishment of an inflammatory microenvironment through the recruitment of immune cells (Perez-Moreno et al., 2006, Perez-Moreno et al., 2008, Stairs et al., 2011). Conditional knock down of *p120ctn* in the murine intestine and epidermis results in acute inflammation and immune cell infiltration (Perez-Moreno et al., 2006, Perez-Moreno et al., 2008, Smalley-Freed et al., 2010, Smalley-Freed et al., 2011). Moreover, there are well established links between inflammation and tumourigenesis (Balkwill and Mantovani, 2001, Coussens and Werb, 2002, Hanahan and Weinberg, 2011).

When I combined loss of *dp120ctn* with loss of two members of the *scribble* group of polarity tumour suppressors, *scrib* and *dlg*, I observed an increased tumour burden (Fig 3.19, Fig 3.21). Microarray analysis of tumours revealed a small set of genes that are differentially regulated in double mutant tumours (Fig 3.20). Gene enrichment analysis did not find enrichment of any particular pathways. However, several genes of interest were altered. Of particular note is the down regulation of both type VI collagens (*Cg25C* and *Viking*) in *scrib-p120ctn* double mutant tumours, that have been shown to be important readout of cell invasiveness (Woodhouse et al., 1994) (Fig 3.20).

As my analysis has so far focused on the tumour itself, I cannot discount that loss of *dp120ctn* did not result in an activation of immune signalling in other tissues such as the fat body, as I observed in adult *dp120ctn* mutants (Fig 3.15, 3.16 and 3.17).

In the future I would like to address how *dp120ctn* loss is cooperating with loss of *scrib* to increase tumour burden. I would like to quantify the level of proliferation and cell death in these tumours. I would also like to address if *dp120ctn-scrib* larvae have activated immune signalling as a result of *dp120ctn* loss. To do this I will extract RNA from fat bodies of tumour bearing larvae (TBL) and perform qPCR analysis for DIRGs (De Gregorio et al., 2001, De Gregorio et al., 2002). Additionally, I will also test the effects of *dp120ctn* knockdown

specifically in the tumour by combining RNAi for *dp120ctn* with the *Ras-scrib* model of oncogenic cooperation (*eyRas*^{V12}; *scrib*^{1}) (Brumby and Richardson, 2003, Pagliarini and Xu, 2003). Finally I would like to confirm the microarray hits by qPCR and assess the functional role of select genes in my model. Future experiments will be focused on cultivating this line of research and further investigation of the role of *dp120ctn* in cancer.

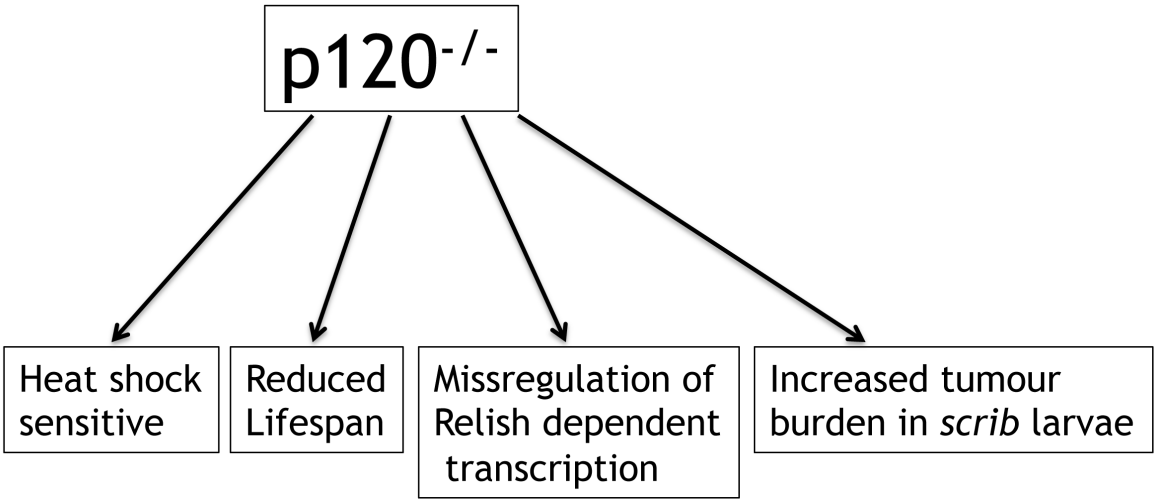

Figure 3.21 *dp120ctn* mutants display a range of phenotypes.

dp120ctn mutant flies display a reduced resistance to 37°C heat shock, a reduced lifespan and posses a unique transcriptional profile before and after heat shock which is *relish* dependent.

4 JAK/STAT and EGFR signalling are required for *Apc1* driven intestinal stem cell hyperplasia

4.1 Summary

Adenomatous polyposis coli (*Apc*) is a negative regulator of the Wnt signalling pathway, which is found frequently mutated in human colorectal cancer. Mouse models have demonstrated that constitutive activation of Wnt signalling upon loss of *Apc* leads to hyperproliferation of intestinal crypts and tumour formation. In this study, we have used the adult *Drosophila* midgut to uncover novel regulators of the *Apc* phenotype. We find a conserved role for *dMyc* and demonstrate the requirement of its transcriptional binding partner *dMax* upon *Apc1* loss. We reduce hyperproliferation and extend survival of *Apc1* null flies through downregulation of *dMyc* and *dMax*. Downstream we detect *dMyc* dependent upregulation of the *upd2/3* cytokines and the *Drosophila* EGF *spitz* upon *Apc1* loss. We establish a role for JAK/STAT signalling in the hyperproliferation of ISCs upon *Apc1* loss that is mediated by *dMyc* dependent production of *upd3* in ECs. Moreover we find a requirement for *Drosophila* EGFR *DER* within ECs for the upregulation of *upd3* and proliferation of ISCs. Altogether our data describe novel mediators of the *Apc* phenotype in *Drosophila* and establishes the adult *Drosophila* midgut as a powerful model to study the molecular signalling underlying the *Apc* phenotype.

4.2 Introduction

4.2.1 Wnt signalling

The Wnt signalling pathways regulate many cellular processes including gene expression, cell adhesion and polarity. Wnt signalling can be divided into canonical and non-canonical and both pathways are activated through ligand receptor binding. Non-canonical Wnt signalling has been shown to regulate cell polarity, cell shape but does not require β-catenin. The work in this thesis relates to the canonical pathway and so I will only introduce this pathway.

Canonical Wnt signalling is well conserved and plays essential roles in cell proliferation, differentiation and determination of cell fate (Seto and Bellen, 2004, Cadigan and Peifer, 2009, Anastas and Moon, 2013) (Fig 4.1). Its misregulation can result in pathologies ranging from embryonic defects to tumourigenesis (Anastas and Moon, 2013). Through its effector β-catenin, Wnt signalling drives transcription of hundreds of genes (Seto and Bellen, 2004, White et al., 2007, Cadigan and Peifer, 2009, Anastas and Moon, 2013). Activation of Wnt signalling is achieved by binding of Wnts, a family of secreted glycoproteins, to the Frizzled (Fz) and LRP-5 receptors (Bhanot et al., 1996, Wehrli et al., 2000). This leads to the stabilization and nuclear translocation of β-catenin that in cooperation with the transcription factor T cell factor (TCF) drives transcription of Wnt targets. When Wnts are not bound, β-catenin is targeted for degradation through the multi-component "destruction" complex (Clevers, 2006). The complex includes Adenomatous polyposis coli (APC), Axin and two kinases, GSK3-β and CK1 which phosphorylate β-catenin targeting it for ubiquitination and subsequent proteasomal degradation (Seto and Bellen, 2004, Clevers, 2006, White et al., 2007, Anastas and Moon, 2013). This complex is inhibited by the dishevelled phosphoprotein that becomes phosphorylated when Wnt signalling is active (Clevers, 2006, White et al., 2007, Anastas and Moon, 2013). Wnt target expression is actively repressed by binding of the transcriptional repressor Groucho together with TCF to DNA (Seto and Bellen, 2004, Clevers, 2006, White et al., 2007, Anastas and Moon, 2013). This picture becomes more complex in mammalian systems due to the presence of several ligands and receptors. This is not surprising considering the many and diverse processes in which both, canonical and non-canonical Wnt signalling is involved

(Seto and Bellen, 2004, Clevers, 2006, White et al., 2007, Anastas and Moon, 2013).

In *Drosophila*, canonical *wingless* (*wg*) signalling although simpler is highly homologous to canonical Wnt signalling in mammals (Seto and Bellen, 2004, Clevers, 2006, White et al., 2007, Anastas and Moon, 2013). *wg* itself was first discovered in a screen for genes required for segment polarity in the embryo (Nusslein-Volhard and Wieschaus, 1980). *wg* signalling has been shown to be essential for cell differentiation and tissue patterning during *Drosophila* development (Cadigan and Nusse, 1997, Wodarz and Nusse, 1998).

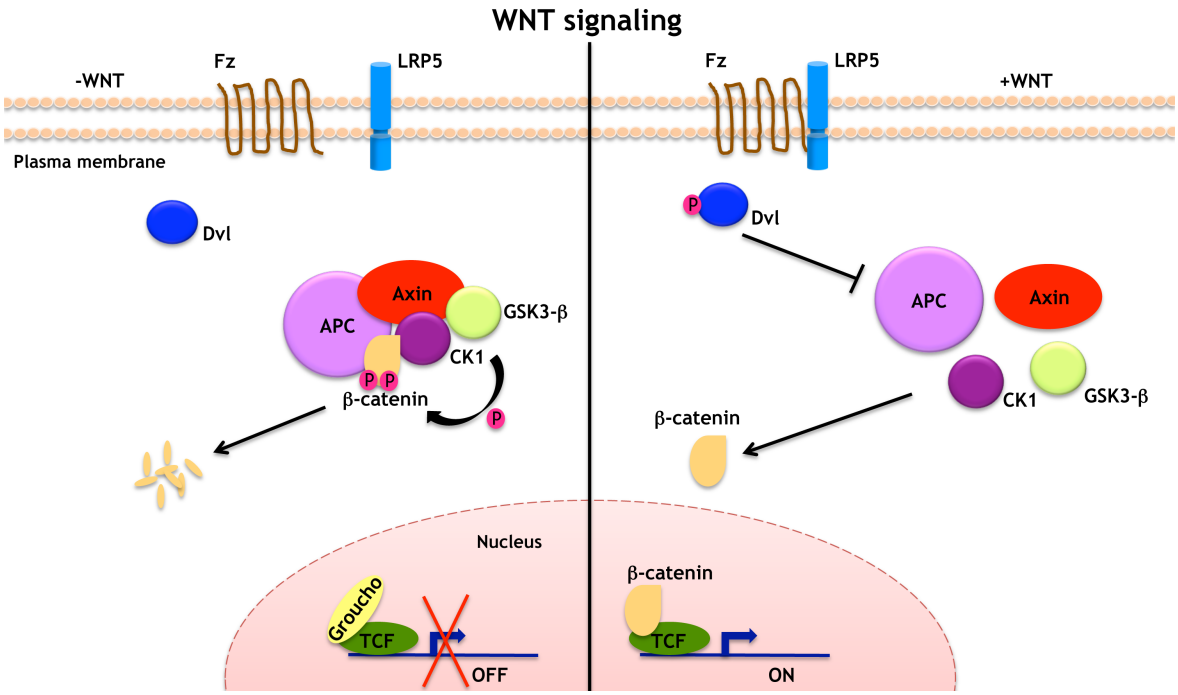

Figure 4.1 Canonical WNT signalling

Upon binding of WNTs to the Frizzled and LRP receptors, disheveled (Dvl) becomes phosphorylated and is able to suppress the formation of the destruction complex made up of APC, Axin, CK1 and GSK3-β allowing β-catenin to translocate to the nucleus and together with TCF drive gene expression. In the absence of WNTs, β-catenin is targeted for degradation through phosphorylation and consequent proteosomal degradation. Gene expression is actively repressed through Groucho and TCF. See text for more details.

4.2.2 The Mammalian small intestine

The mammalian small intestine consists of an epithelial monolayer that carries out digestion and absorption of nutrients. In order to maximize surface area available for nutrient absorption, the epithelium of the small intestine is organized into proliferative crypts and small finger-like protrusions named villi (Radtke and Clevers, 2005). The intestinal epithelium is populated by 5 cell types: the intestinal stem cells (ISCs); the secretory lineage: the paneth cells, goblet cells and the enteroendocrine cells (ee); and the absorptive enterocytes (ECs) (Radtke and Clevers, 2005). The mammalian small intestine undergoes complete turn over once every 4-5 days. The ISCs, which are located at the base of each crypt, are marked by the expression of the Wnt target Lgr5 (Radtke and Clevers, 2005). Once a new cell is produced it will travel up the villus axis until it reaches the tip (Radtke and Clevers, 2005). Due to its rapid turnover and relatively simple architecture, the mammalian small intestine has been often used to investigate stem cell biology (Radtke and Clevers, 2005).

The Adult *Drosophila* midgut bears many similarities with the mammalian intestine (Casali and Batlle, 2009) and as described in detail in section 1.5 it is maintained by dedicated ISCs, which give rise to the differentiated secretory ee cells and absorptive ECs.

4.2.3 Colorectal cancer

In 2010, Colorectal cancer (CRC) diagnosis accounted for around 13% of all cancers diagnosed in the UK (CRUK.org). CRC is characterized by the presence of benign polyps that progress to malignant carcinomas. Around 80% of patients diagnosed with sporadic and inherited forms of CRC will have silencing mutations affecting the *Apc* gene (Kinzler et al., 1991, Kinzler and Vogelstein, 1996, Korinek et al., 1997). In the murine intestine, loss of *Apc* leads to acute activation of Wnt signalling and rapid tissue hyperplasia (Sansom et al., 2004) while targeted deletion of *Apc* in the ISCs leads to the expedited formation of discrete adenomas (Barker et al., 2009). Constitutive activation of Wnt signalling results in the aberrant expression of many genes (Sansom et al., 2004, Holstege and Clevers, 2006, Sansom et al., 2007, Van der Flier et al., 2007). However, the relative contribution of these targets to the *Apc* phenotype and to

intestinal homeostasis needs to be addressed in order to develop novel and effective therapies for CRC.

In the adult *Drosophila* midgut, as in the mammalian small intestine, loss of *Apc* from ISCs leads to hyperproliferation of the intestinal epithelium (Cordero et al., 2009, Lee et al., 2009).

4.2.4 Aims of the project

This project was conducted in collaboration with Dr Julia Cordero, a postdoctoral researcher working in the laboratory of Prof Owen Sansom. When I joined the lab Dr Cordero had recently published data demonstrating the affects of *Apc* downregulation in the adult Drosophila midgut (Cordero et al., 2009). Using this system she was able to demonstrate that *Apc* loss specifically in the ISCs led to a hyperproliferation of the ISCs (Cordero et al., 2009). Using this model we set out to uncover molecular mechanisms that underlie these phenotypes in the adult *Drosophila* midgut in order to gain insights into the mechanisms that mediate Human CRC.

The work presented here is the product of a collaboration with Dr Cordero. Experiments were designed performed and analyzed together with Dr Cordero and this work has been included in a co-first author paper (Cordero et al., 2012a). I also participated in work addressing the role of *wg* in homeostasis and regeneration in the *Drosophila* which was published in *EMBOJ* (Cordero et al., 2012b).

4.3 Results

4.3.1 *Apc1* loss results in ISC hyperproliferation and reduced survival in the adult midgut

Apc mutation in the murine intestine leads to complete disruption of tissue architecture and rapid morbidity (Sansom et al., 2004). In *Drosophila,* there are two *Apc* homologues, *Apc1* and *Apc2*. During development these genes are redundant (Ahmed et al., 2002), but have been shown to have independent functions in the *Drosophila* male germ line (Yamashita et al., 2003). Knockdown of *Apc1* within progenitor cells results in hyperproliferation of the adult *Drosophila* midgut (Cordero et al., 2009). We wanted to examine the effects of *Apc1* loss on ISC proliferation. To do this we combined the null allele of *Apc1* (*Apc1*^{Q8}) (Ahmed et al., 1998), with the ISC/EB Gal4 driver *escargot*-Gal4 driving UAS-GFP (*esg>GFP*) (Brand and Perrimon, 1993, Micchelli and Perrimon, 2006). *Apc1* null flies are viable as *Apc2* is able to take over *Apc1* functions during development. When we compared the posterior midguts of *Apc1* null heterozygotes (*esg>GFP; Apc1*^{Q8}/+) (Ahmed et al., 1998), and homozygotes (*esg>GFP; Apc1*^{Q8}) we found that midguts from *Apc1* null homozygotes were hyperplastic and had increased numbers of ISCs/EBs as we observed an increased number of GFP^{+ve} cells (Fig 4.1A and 4.1B). We measured proliferation in these midguts through staining with phosphohistone H3 (pH3^{+ve}) antibody that marks all mitotic cells. We observed a significant increase in the number of pH3^{+ve} cells (Fig 4.1C) confirming that *Apc1* loss in the adult *Drosophila* midgut results in ISC hyperproliferation (Fig 4.2 A, B and C).

In the mouse, conditional knockout of *Apc* leads to death of the animal in as quickly as 5 days (Sansom et al., 2004). We measured lifespan of flies carrying 3 different *Apc1* null alleles (*Apc1*^{Q8}, *Apc1*^{x1} and *Apc1*^{S76}) as homozygotes, trans-heterozygotes and corresponding heterozygotes (Fig 4.2D). In all combinations, *Apc1* null flies displayed a significantly reduced lifespan when compared to their heterozygous controls (Fig 4.2D).

In order to discount any developmental effects of *Apc1* loss and confirm ISC proliferation upon *Apc1* loss, we used the MARCM system to create GFP marked control (*Lac*-Z) and *Apc1* null (*Apc1*^{Q8}) clones (Lee and Luo, 2001). As we had observed in the midguts of *Apc1* null flies, 14 day old *Apc1* null clones

(*Apc1*^{Q8}) had an increased number of cells per clone when compared to control clones (*Lac*-Z) (Fig 4.2E, 4.2F and 4.2G).

These results demonstrate that, as is the case in the mammalian intestine, *Apc1* loss in the adult *Drosophila* midgut results in a hyperplastic epithelium and *Apc1* loss is sufficient to induce ISC hyperproliferation in the adult *Drosophila* midgut. These phenotypes are consistent with what has been observed in the mammalian intestine and suggests a significant degree of conservation between these two tissues. Therefore the adult *Drosophila* midgut is a useful model to probe the molecular signature underlying the *Apc* phenotype.

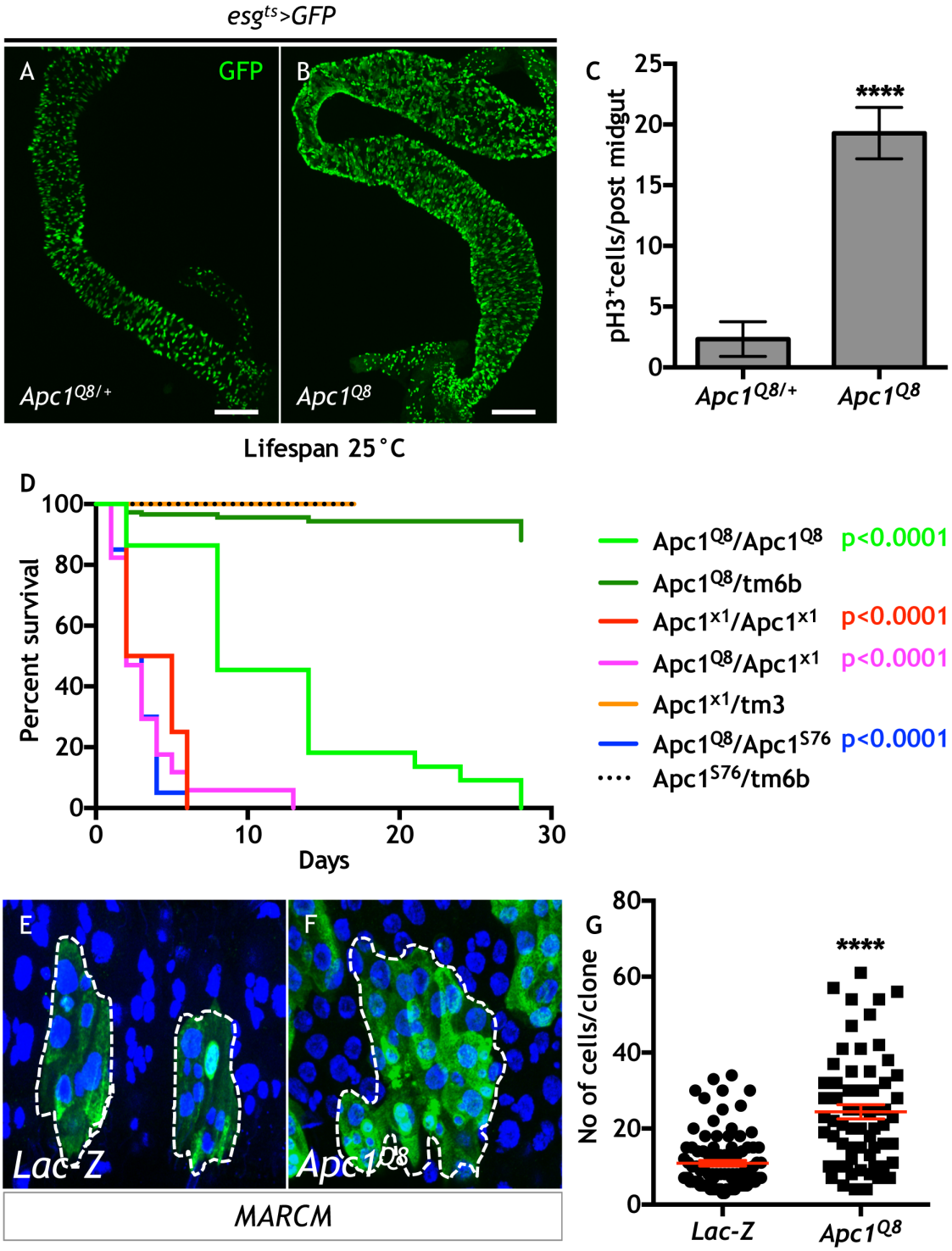

Figure 4.2 *Apc1* loss results in ISC hyperproliferation in the *Drosophila* midgut.

(A-B) Immunofluorescence of 5 day old midguts from $Apc1^{Q8}$/+ (A) and $Apc1^{Q8}$ (B) flies with stained for GFP (Green) and DAPI (blue), Scale bar 20μm. (C) Quantification of the number of $pH3^{+ve}$ cells per posterior midgut. (D) Survival of *Apc1* null allele homo and heterozygotes at 25°C (Log-rank tests, *p* values correspond to comparison between homo and trans-heterozygotes versus

appropriate heterozygotes) (E, F) Confocal images of 14 day old GFP MARCM clones stained for GFP (Green) and DAPI (blue). (G) Quantification of number of cells/clone (t-test ****$p<0.0001$).

4.3.2 dMyc is upregulated and required for the *Apc1* phenotype in the adult *Drosophila* midgut.

The Myc family of transcription factors regulate cell division, differentiation and apoptosis (Johnston et al., 1999, Trumpp et al., 2001). They are well defined proto-oncogenes and are frequently deregulated in many different cancers (Henriksson and Luscher, 1996). c-Myc has been shown to be required for the *Apc* phenotype in the murine intestine as its deletion completely suppressed tissue hyperplasia (Sansom et al., 2007, Athineos and Sansom, 2010).

In *Drosophila*, *dMyc* (*diminutive-dm*) is known to act downstream of *wg* in several contexts (Smith-Bolton et al., 2009). To further validate our model we wanted to test if *dMyc* would be required for the *Apc1* phenotype in the adult *Drosophila* midgut. We first stained midguts from control ($Apc1^{Q8}$/+) and *Apc1* null ($Apc1^{Q8}$) flies with an antibody against dMyc (Fig 4.3A and 4.3B). dMyc levels were elevated in *Apc1* null midguts suggesting that *dMyc* may be required in this context (Fig 4.3A and 4.3B). To more directly access the role of *dMyc* in hyperplasia associated with *Apc1* loss in the adult *Drosophila* midgut we created control (*Lac-Z*), *Apc1* null ($Apc1^{Q8}$) and *Apc1* null ($Apc1^{Q8}$) clones expressing RNA interference (RNAi) for either *dMyc* (*myc-IR,* $Apc1^{Q8}$) or its transcriptional binding partner *dMax* (*max-IR,* $Apc1^{Q8}$) (Steiger et al., 2008) (Fig 4.3C-G). We observed a significant decrease in the number of cells per clone in 14 day old *dMyc* knockdown (*myc-IR,* $Apc1^{Q8}$) and *dMax* knockdown *Apc1* null (*max-IR,* $Apc1^{Q8}$) clones compared with *Apc1* null only clones ($Apc1^{Q8}$) (Fig 4.3H). This confirms that *dMyc* is required for hyperproliferation upon *Apc1* loss in the adult *Drosophila* midgut. Moreover, it demonstrates the conservation of the *Apc* phenotype between the *Drosophila* and mouse intestine.

We next wanted to address if down-regulation of *dMyc* or *dMax* could revert an already established *Apc1* phenotype, an experiment that is technically difficult to perform in the mouse. We combined RNAi for *dMyc* and *dMax* with a temperature sensitive Gal4 repressor, Gal80 ($Gal80^{ts}$) fused to the promoter region of tubulin (*tub-*$Gal80^{ts}$*, UAS-myc-IR* and tub-$Gal80^{ts}$, UAS-max-IR, respectively) in order to control the expression of the RNAis using temperature. Using these tools we assayed the effect of *dMyc* and *dMax* knockdown in *Apc1* null clones and midguts of *Apc1* null flies ($Apc1^{Q8}$).

For clones the experimental setup was as follows: clones for all genotypes were induced and allowed to grow at the non-permissive temperature (22°C) for 14 days (Fig 4.4A). Flies were then transferred to the permissive temperature (29°C) to allow de-repression of the Gal4 and therefore expression of the RNAis within the clones (Fig 4.4A). Midguts were dissected at different time points (Fig 4.4A, * denotes time points when flies were taken) and the number of cells per clone was quantified. We observed no difference between *Apc1* null (*Apc1*^{Q8}) clones, *dMyc* knockdown (*myc-IR, Apc1*^{Q8}) and *dMax* knockdown *Apc1* null (*max-IR, Apc1*^{Q8}) clones after one day at the permissive temperature (15 day) (Fig 4.4C, 4.4D and 4.4E). However, both after 7 and 14 days at the permissive temperature (21 and 28 days total respectively) we observed a significant decrease in clone size in both *dMyc* knockdown (*myc-IR, Apc1*^{Q8}) and *dMax* knockdown *Apc1* null (*max-IR, Apc1*^{Q8}) clones (Fig 4.4C', 4.4D', 4.4D'', 4.4E' and 4.4E'').

We also combined these tools with *Apc1* null flies (*Apc1*^{Q8}) and the ISC/EB Gal4 driver *escargot*-Gal4 driving UAS-GFP (*esg>GFP*). This again allowed us to control when the RNAi was active and allowed us to downregulate *dMyc* and *dMax* specifically in the ISCs/EBs. As in the previous experiment, flies were kept at the non-permissive (22°C) for 5 days before being transferred to the permissive temperature (29°C) for a further 7 days (Fig 4.5A). Midguts were dissected at 5 and 7 days (Fig 4.5A, * denotes time points when flies were taken) and the number of pH3^{+ve} cells was quantified (Fig 4.5B-G). We observed significantly fewer pH3^{+ve} cells in *Apc1* null midguts expressing RNAi for *dMyc* and *dMax* in ISCs/EBs (*myc-IR*^{ts}*; Apc1*^{Q8} and *max-IR*^{ts}*;Apc1*^{Q8}) (Fig 4.5G).

Finally we wanted to examine if the suppression of *Apc1* driven hyperplasia we observed could translate into increased survival. For this we measured the lifespan of *Apc1* null flies expressing RNAi for either *dMyc* or *dMax* in the ISCs/EBs. Strikingly, we observed a significant increase in lifespan in *Apc1* null flies expressing RNAi interference for either *dMyc* or *dMax* when compared to *Apc1* null flies (Fig 4.6A-B).

These results demonstrate that *dMyc* and *dMax* are required for the *Apc1* phenotype in the adult *Drosophila* midgut and down-regulation of these genes suppresses and regresses hyperproliferation associated with *Apc1* loss.

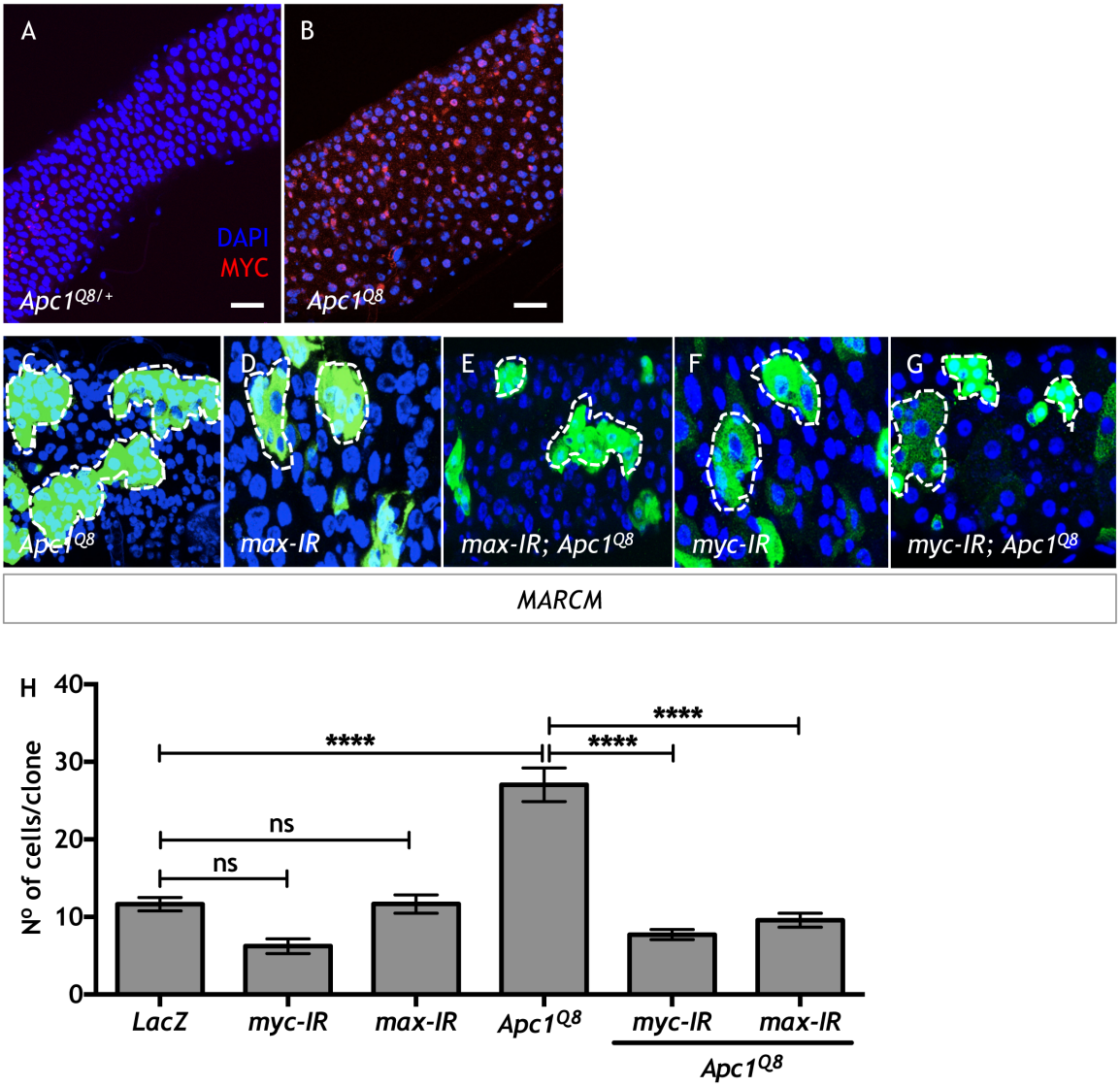

Figure 4.3 *dMyc* is required for *Apc1* associated hyperplasia.

(A-B) Immunofluorescence of 5 day old midguts from $Apc1^{Q8}$/+ (A) and $Apc1^{Q8}$ (B) flies with stained for dMyc (red) and DAPI (blue), Scale bar 20μm. (E, F) Confocal images of 14 day old GFP MARCM clones of the indicated genotypes stained for GFP (Green) and DAPI (blue). (H) Quantification of the number of cells per clone (one-way ANOVA with Bonferroni post test correction, ****p<0.0001, ns-non significant).

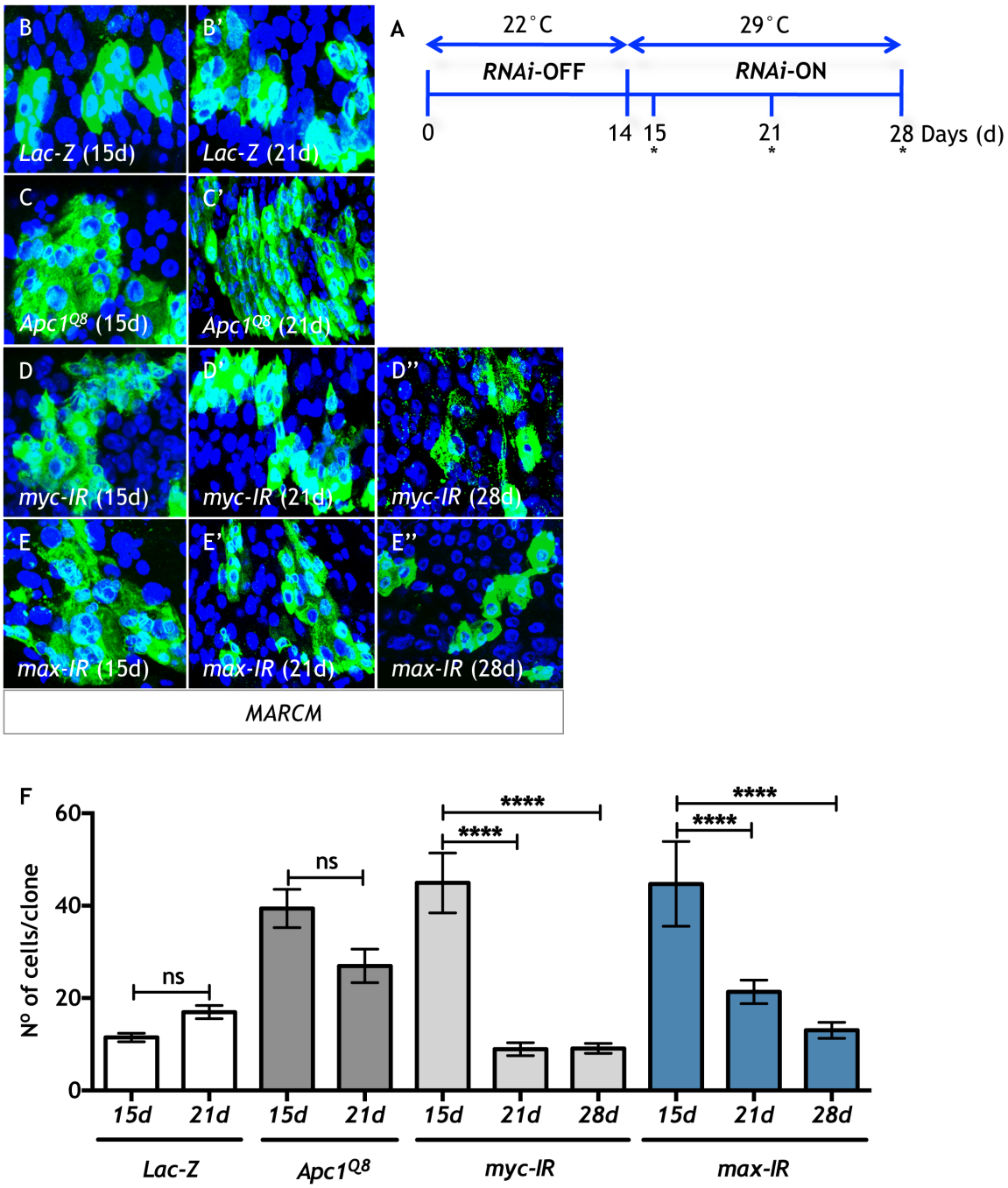

Figure 4.4 *dMyc* or *dMax* downregulation regresses *Apc1* clones.

(A) Schematic representation of experimental setup. (B-E'') Confocal images of GFP MARCM clones of the indicated genotypes and ages stained for GFP (green) and DAPI (blue). (F) Quantification of the number of cells per clone (one-way ANOVA with Bonferroni post test correction, ****p<0.0001, ns-non significant).

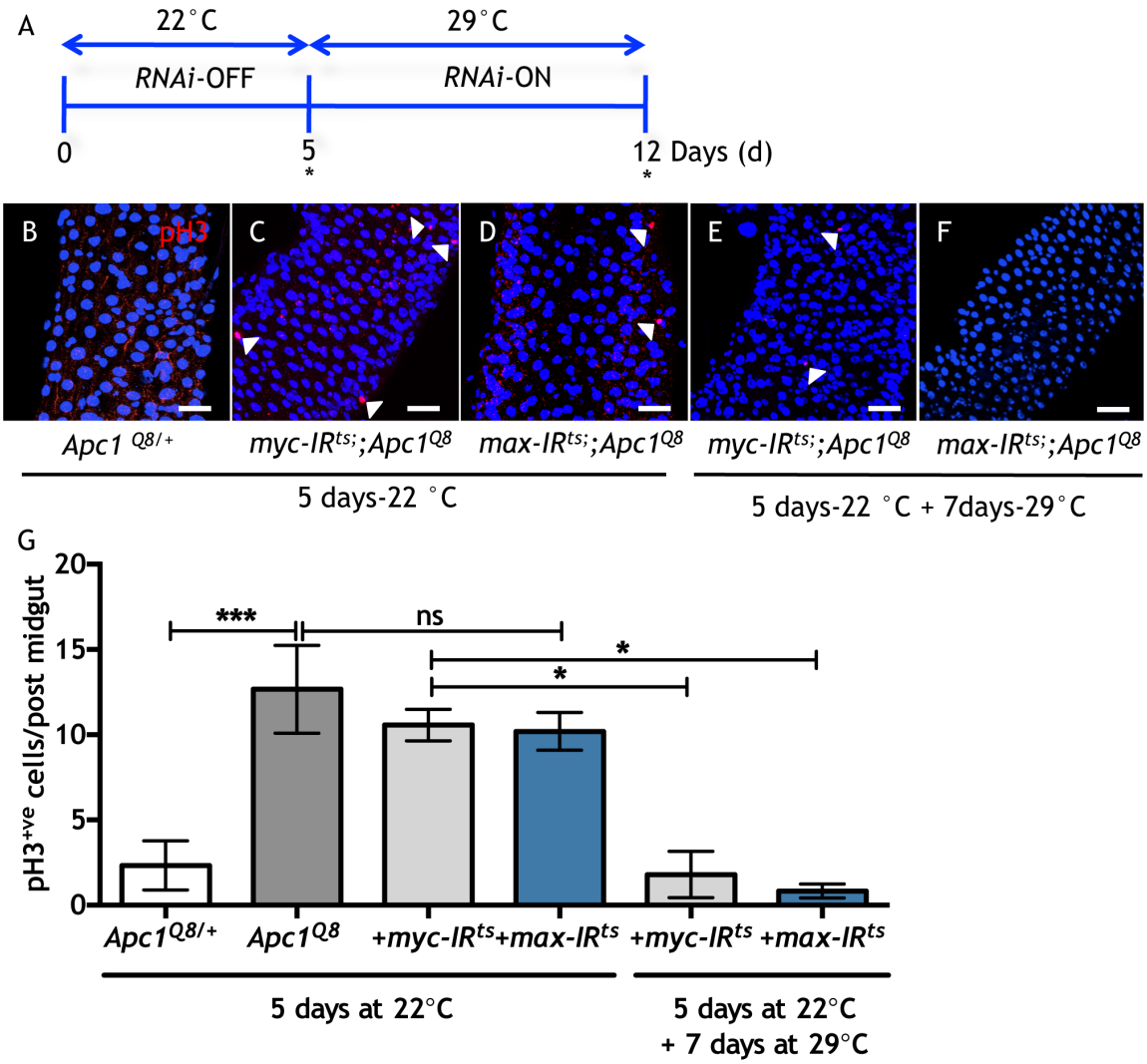

Figure 4.5 *dMyc* or *dMax* downregulation in ISCs of *Apc1* null midguts reverts *Apc1* null midgut phenotype.

(A) Schematic representation of experimental setup. (B-F) Immunofluorescence of midguts of the indicated genotypes and ages stained for pH3 (red) and DAPI (blue). (G) Quantification of the number of $pH3^{+ve}$ per posterior midgut (one-way ANOVA with Bonferroni post test correction, * $p<0.05$, ***$p<0.001$ and ns-non significant).

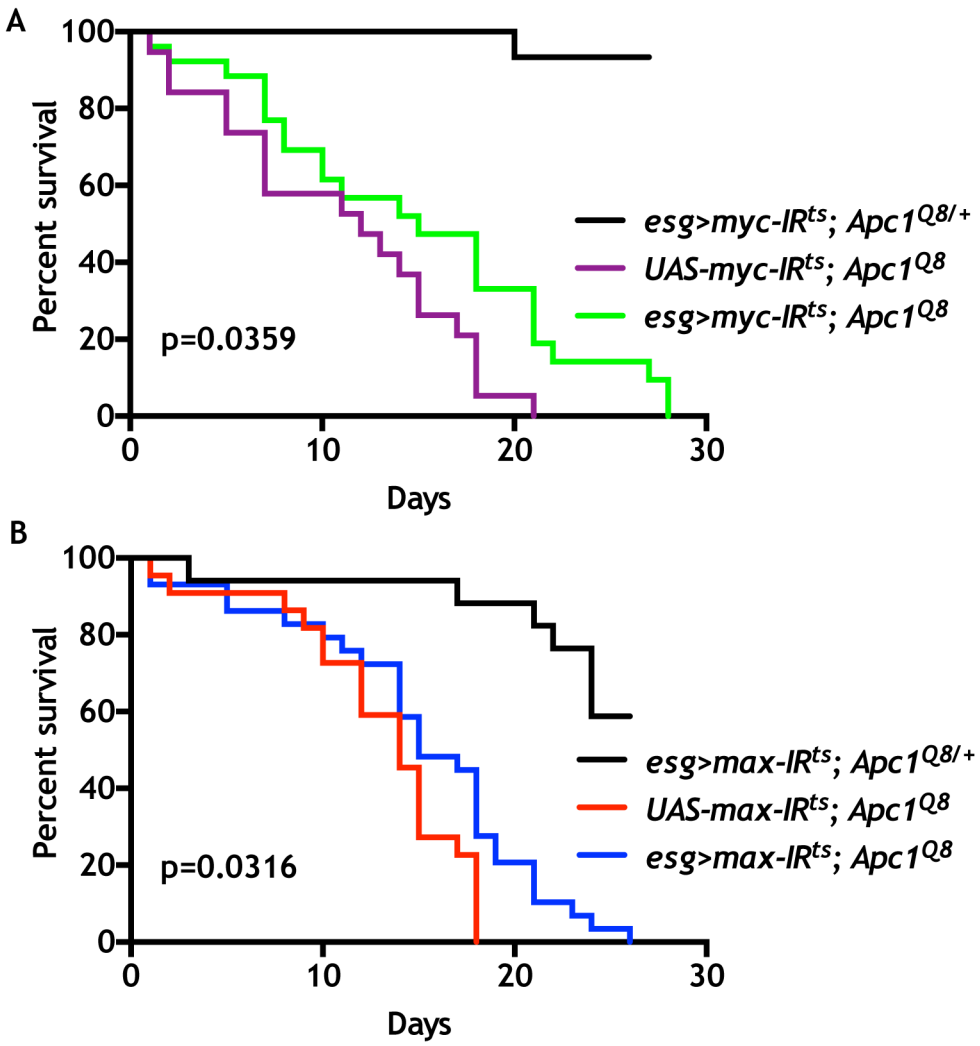

Figure 4.6 Survival of *Apc1* null flies rescued by *dMyc* or *dMax* downregulation.

(A-B) Lifespan analysis of *Apc1* null flies ($Apc1^{Q8}$) expressing RNAi for either *dMyc* (A) or *dMax* (B) under the control of *esgGal4*. *p* values generated using log-rank tests (*p* values correspond to comparison between $Apc1^{Q8}$ homozygotes expressing RNAi for *myc* (A- Purple versus Green) or *max* (B- Red versus Blue).

4.3.3 Loss of *Apc1* leads to JAK/STAT pathway activation

Many studies have examined the contribution of different signalling pathways on the regulation of ISC proliferation in the adult *Drosophila* midgut (Beebe et al., 2009, Buchon et al., 2009b, Jiang and Edgar, 2009, Jiang et al., 2009, Shaw et al., 2010, Ren et al., 2010, Karpowicz et al., 2010, Jiang and Edgar, 2011). We wanted to ascertain which if any of these pathways might also be required for the hyperproliferation of ISCs upon loss of *Apc1*.

The highly conserved JAK/STAT signalling pathway has been shown to be required for homeostasis and proliferation of the ISCs in response to damage in the adult *Drosophila* midgut (Beebe et al., 2009, Buchon et al., 2009b, Jiang et al., 2009) and is an important mediator of hyperproliferation induced as a result of hyperactivation of EGFR and Hippo/Yorkie signalling (Jiang et al., 2009, Shaw et al., 2010, Ren et al., 2010, Karpowicz et al., 2010, Jiang and Edgar, 2011). In *Drosophila,* the pathway is activated when secreted cytokines known as *upds* (*upd, upd2, upd3*) bind the receptor *domeless* (*dome*). This leads to the phosphorylation of the receptor associated Janus Kinase – JAK, *hopscotch* (*hop*). Inactive monomers of *Stat92E* (signal transducer and activator of transcription-STAT) are recruited and phosphorylated which results in the formation of active dimers. *Stat92E* dimers translocate the nucleus where they activate transcriptional targets of the JAK/STAT pathway (Arbouzova and Zeidler, 2006).

Upds are known to be upregulated upon tissue damage. In order to understand if *upds* were upregulated in *Apc1* (*Apc1*^{Q8}) null midguts, we performed qPCR on total RNA from control (*Canton-S*) and *Apc1* null (*Apc1*^{Q8}) midguts for all three *upds* (*upd, upd2, upd3*) and for the negative regulator of JAK/STAT signalling *socs36E*, an established target of the pathway (Fig 4.7A). We detected a significant increase in expression of *upd2, upd3* and *socs36E* but not *upd* in *Apc1* null midguts suggesting a strong activation of JAK/STAT signalling upon loss of *Apc* (Fig 4.7A)

We next combined the *Apc1* null allele (*Apc1*^{Q8}) with a *lacZ* reporter for *upd3* expression (*upd3-lacZ*) (Jiang et al., 2009) to investigate the pattern of expression within the midgut (Fig 4.7B-D'). When we looked at control (*Apc1*^{Q8}/+) midguts we rarely detected *lacZ* expression, this was in stark contrast to what we observed in *Apc1* null (*Apc1*^{Q8}) midguts, where *lacZ* expression could be detected throughout the midgut (Fig 4.7B-C). When we looked more closely

we detected *lacZ* only in the large absorptive ECs, marked by the lack of Delta and Prospero staining, which mark the ISC and ee cell respectively, (Fig 4.7D-D', white arrows). We further confirmed JAK/STAT activation upon *Apc1* loss by using a reporter of JAK/STAT pathway activation, *10xStat-GFP* (Bach et al., 2007). When we combined this reporter with the *Apc1* null allele ($Apc1^{Q8}$) we found that in midguts from *Apc1* null ($Apc1^{Q8}$) flies had increased STAT activation within ISCs whereas in control ($Apc1^{Q8}$/+) midguts only a few ISCs were GFP positive (Fig 4.7E-F, white arrowheads).

These results suggest that upon loss of *Apc1*, *Upd3* is secreted by ECs activating JAK/STAT signalling in ISCs.

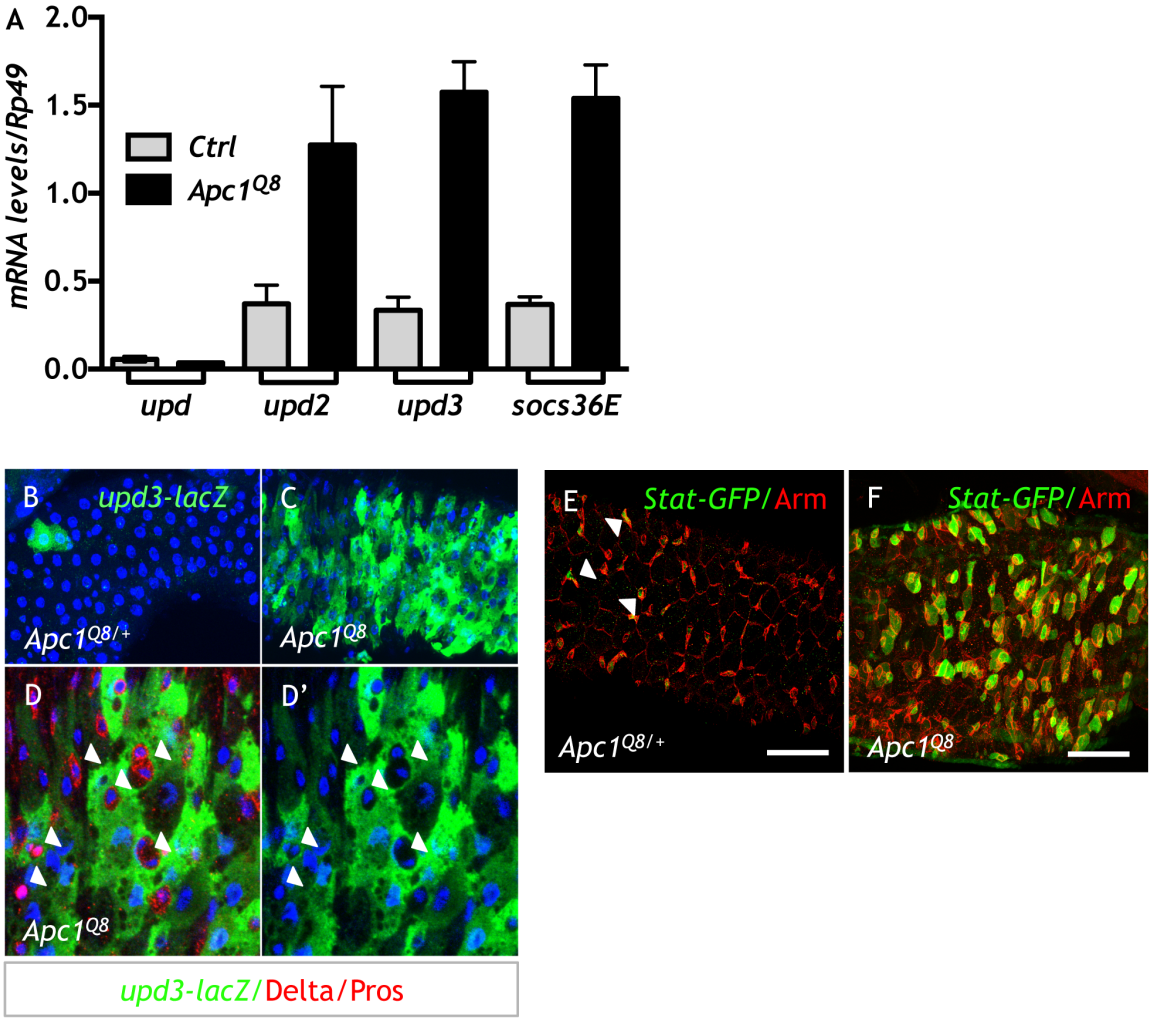

Figure 4.7 JAK/STAT signalling is activated upon *Apc1* loss.

(A) qPCR analysis for *upd*, *upd2* and *upd3* in control and $Apc1^{Q8}$ midguts. (B-D') Immunofluorescence of 5 day old midguts from $Apc1^{Q8}$/+ (B) and $Apc1^{Q8}$ (C-D') flies carrying the *upd3-lacZ* reporter stained for Delta/Prospero to mark ISCs/ee (red-membrane/nuclear) and lacZ (green) – white arrowheads point to small delta and prospero positive cells not expressing *upd3-lacZ*. (E-F) Immunofluorescence of 5 day old midguts from $Apc1^{Q8}$/+ (E) and $Apc1^{Q8}$ (F) flies carrying the *10xSTAT-GFP* reporter stained with Armadillo (red) and GFP (green) – white arrowheads point to small ISCs positive for GFP. Scale bars 50μm.

4.3.4 JAK/STAT signalling is functionally required for hyperproliferation upon *Apc1* loss

As we had now established that JAK/STAT signalling was activated downstream of *Apc1* loss, we next wanted to address the functional relevance of JAK/STAT signalling for the hyperproliferation of ISCs in *Apc1* midguts. Importantly, downregulation of STAT signalling does affect ISC proliferation but rather results in differentiation defects (Beebe et al., 2009, Jiang et al., 2009). We used the MARCM system to induce *Apc1* null ($Apc1^{Q8}$) clones, *dome* knockdown (*dome-IR;* $Apc1^{Q8}$) and *Stat92E* knockdown *Apc1* null clones (*stat-IR;* $Apc1^{Q8}$) (Lee and Luo, 2001). We quantified the number of cells per clone and the percentage number of clones with $pH3^{+ve}$ cells (Fig 4.8A-E). We observed a significant decrease in the size of *dome* knockdown (*dome-IR;* $Apc1^{Q8}$) and *Stat92E* knockdown *Apc1* null clones (*stat-IR;* $Apc1^{Q8}$) (Fig 4.8A-D). Moreover, the percentage number of clones with $pH3^{+ve}$ cells was also reduced when JAK/STAT signalling was downregulated within *Apc1* clones (Fig 4.8E).

These data clearly demonstrate that JAK/STAT signalling is essential for hyperproliferation of ISCs upon loss of *Apc1* in the adult *Drosophila* midgut.

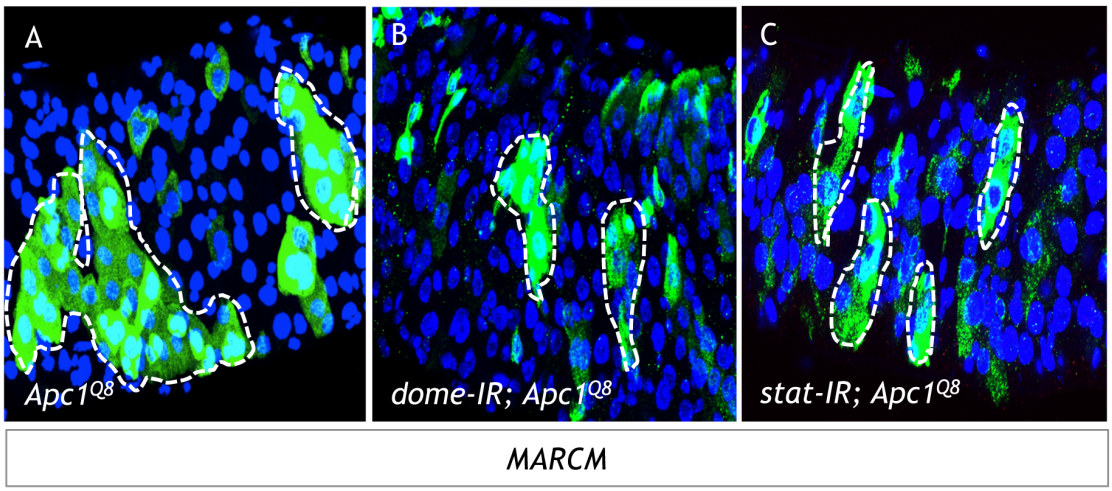

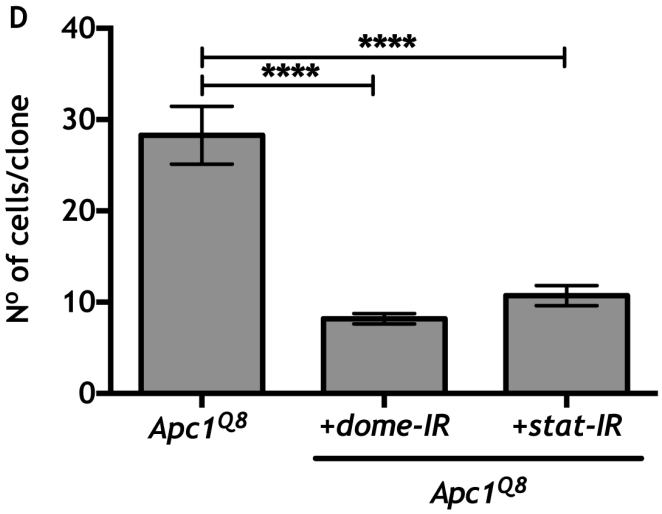

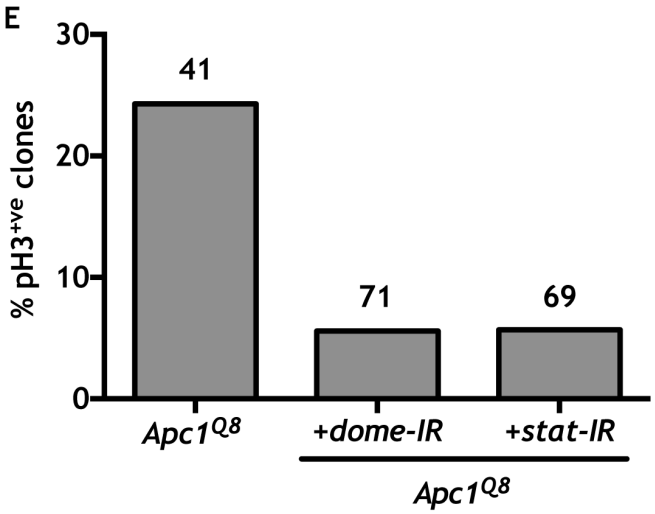

Figure 4.8 JAK/STAT signalling is required for ISC hyperproliferation upon *Apc1* loss.

(A-C) Confocal images of 14 day old GFP MARCM clones of the indicated genotypes and ages stained for GFP (Green) and DAPI (blue). (D) Quantification

of the number of cells per clone (one-way ANOVA with Bonferroni post test correction, ****$p<0.0001$). (E) Quantification of the percentage number of clones with $pH3^{+ve}$ cells.

4.3.5 Activation of JAK/STAT signalling and dMyc upregulation are both required for *Apc1* associated hyperproliferation

Loss of *Apc1* leads to hyperproliferation of ISCs as a result of *dMyc* upregulation and the activation of JAK/STAT signalling. We wanted to address whether these pathways were working in parallel or in epistasis to one another.

To address this we examined if JAK/STAT activation upon *Apc1* loss was dependent on the levels of *dMyc*. We performed qPCR analysis for levels of *upd3* and *socs36E* on control (*Canton-S*), *Apc1* null ($Apc1^{Q8}$) and dMyc knockdown *Apc1* null flies (*esg>myc-IR^{ts}; $Apc1^{Q8}$*) (Fig 4.9A). We observed a significant reduction in *upd3* and *socs36E* levels in *dMyc* knockdown *Apc1* null midguts (*esg>myc-IR^{ts}; $Apc1^{Q8}$*) (Fig 4.9A). This suggested that *dMyc* upregulation was required for JAK/STAT activation upon *Apc1* loss. If this were the case we would expect to see dMyc up-regulation even in the absence of JAK/STAT activation in *Apc1* null midguts. We tested this hypothesis using the previously described (section 4.3.4) *Apc1* null MARCM clones together knockdown for JAK/STAT signalling components *dome* and *Stat92E*. When we stained these midguts for dMyc we observed a significant decrease in dMyc upregulation in *dome* knockdown *Apc1* null clones compared to *Apc1* ($Apc1^{Q8}$) null clones (Fig 4.9B-C'). However, downregulation of *Stat92E* in *Apc1* null clones did not significantly affect dMyc levels (Fig 4.9B-B' and 4.9D-D'). This suggested the existence of a cross talk between these pathways rather than a direct epistatic relationship.

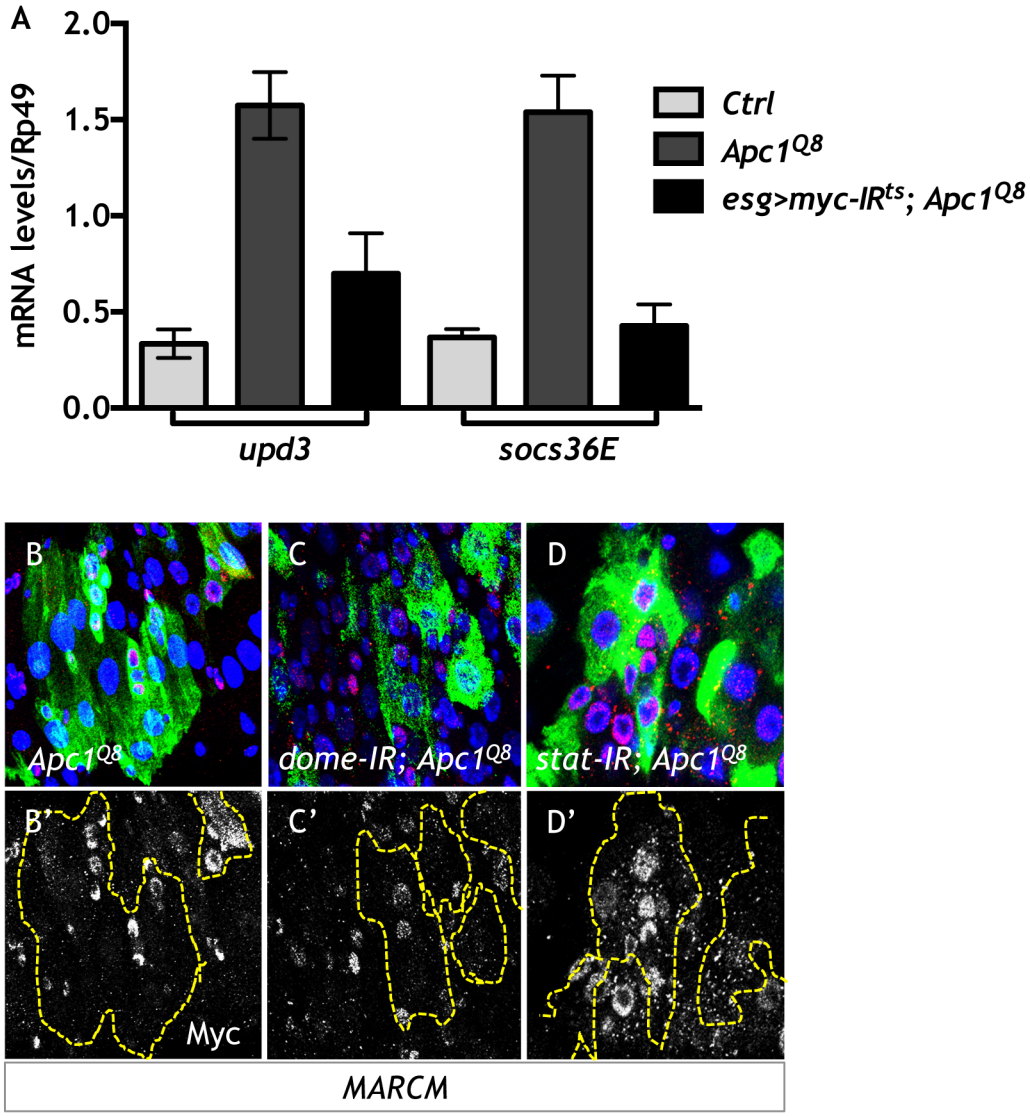

Figure 4.9 JAK/STAT signalling activation upon *Apc1* loss requires *dMyc*.

(A) qPCR analysis for *upd3* and *socs36E* in control, *Apc1*^{Q8} and *esg>myc-IR*^{ts}; *Apc1*^{Q8} midguts. (B-D') Immunofluorescence of 14 day old MARCM clones from *Apc1*^{Q8}, *dome-IR; Apc1*^{Q8} and *stat-IR; Apc1*^{Q8} flies stained with GFP (green), dMyc (red/grey) and DAPI (blue).

4.3.6 EGFR signalling links dMyc and JAK/STAT signalling upon loss of *Apc1*

When we examined the relationship between the levels of *dMyc* and JAK/STAT signalling we found that JAK/STAT activation was dependent on *dMyc* (Fig4.9A). However, we also found that downregulation of *dome* reduced *dMyc* levels (Fig4.9B-C') while downregulation of *Stat92E* did not significantly affect *dMyc* levels (Fig 4.9B-B' and 4.9D-D'). Moreover, *upd3* is produced by ECs upon *Apc1* loss (Fig 4.7) and JAK/STAT activation is absolutely required for ISC proliferation upon *Apc1* loss (Fig 4.8). These results suggested a paracrine cross talk from ECs to ISCs upon loss of *Apc1* which results in hyperproliferation.

It was previously shown that JAK/STAT signalling is activated by overexpression of the *Drosophila* EGF-like ligands and that EGF-R signalling can be activated through over expression of *upds* (Buchon et al., 2010, Jiang et al., 2011, Biteau and Jasper, 2011). We hypothesized that EGFR signalling could be involved in this paracrine signalling and possibly link these two pathways.

We first examined whether EGF ligands were upregulated upon *Apc1* loss in the adult *Drosophila* midgut. We performed qPCR analysis on midguts from control (*Canton-S*) and *Apc1* null ($Apc1^{Q8}$) flies for the EGF-like ligands *vein*, *keren* and *spitz*. We observed upregulation of *vein* and *spitz* upon *Apc1* loss while *keren* levels were unchanged (Fig 4.10A). We repeated the analysis on *Apc1* null flies also expressing RNAi for *dMyc* in ISCs/EBs (*esg>myc-IR^{ts}; $Apc1^{Q8}$*). We found a strong *dMyc* dependency of *spitz* expression in midguts upon *Apc1* loss (Fig 4.10A). These experiments suggested that *spitz* might be involved in the induction of *upd3* downstream of *dMyc* upon *Apc1* loss.

To test the functional requirement of *spitz* in ISCs upon *Apc1* loss we combined RNAi for *Apc1* (*Apc1-IR*) with RNAi for *spitz* (*spitz-IR*) specifically in ISCs/EBs using the *esgGal4* driver (Fig 4.10B-E). We quantified the number of $pH3^{+ve}$ cells to measure proliferation of ISCs in these conditions. Knockdown of *Apc1* (*Apc1-IR*) resulted in a significant increase in ISC proliferation while midguts expressing GFP (*esg>GFP*) alone and knockdown of *spitz* (*esg>spitz-IR*) had similar levels of proliferation. In double knockdown midguts (*esg>spitz-IR; Apc1-IR*) we observed a significant decrease in ISC proliferation when compared to *Apc1* knockdown alone (*esg>Apc1-IR*) (Fig 4.10F). Therefore, knockdown of *spitz* was able to suppress hyperproliferation of ISCs.

To test if EGFR signalling was required for the upregulation of *upd3* in ECs we utilized a dominant negative form of *Drosophila* EGFR (DER^{DN}) in combination with ectopic expression of *wg* (DER^{DN}*; wg*) specifically in ECs using an enterocyte specific Gal4 driver ($MyoIA^{ts}$*Gal4, myosin IA*) (Jiang et al., 2009). Expression of *wg* ($MyoIA^{ts}$>*wg*) in the ECs led to hyperproliferation of ISCs and a significant increase in the number of $pH3^{+ve}$ cells (Fig 4.11B and 4.11E) while very few $pH3^{+ve}$ cells were observed in midguts expressing DER^{DN} ($MyoIA^{ts}$>DER^{DN}) or GFP ($MyoIA^{ts}$>*GFP*) alone (Fig 4.11A, C and 4.11E). In midguts were *wg* and DER^{DN} were overexpressed together ($MyoIA^{ts}$>DER^{DN}; *wg*) the increase in $pH3^{+ve}$ cells observed in *wg* overexpression midguts ($MyoIA^{ts}$>*wg*) was completely suppressed (Fig 4.11D and 4.11E). We next performed qPCR analysis for *upd3* on $MyoIA^{ts}$ >*GFP*, $MyoIA^{ts}$ >*wg* and $MyoIA^{ts}$ >DER^{DN}*; wg* midguts. We observed an increase in *upd3* expression upon *wg* overexpression that was suppressed when *wg* was overexpressed together with a dominant negative form of *Drosophila* EGFR ($MyoIA^{ts}$ >DER^{DN}*; wg*) (Fig 4.11F).

These data demonstrate that EGFR signalling is required within the ECs for production of *upd3* upon activation of *wg* signalling.

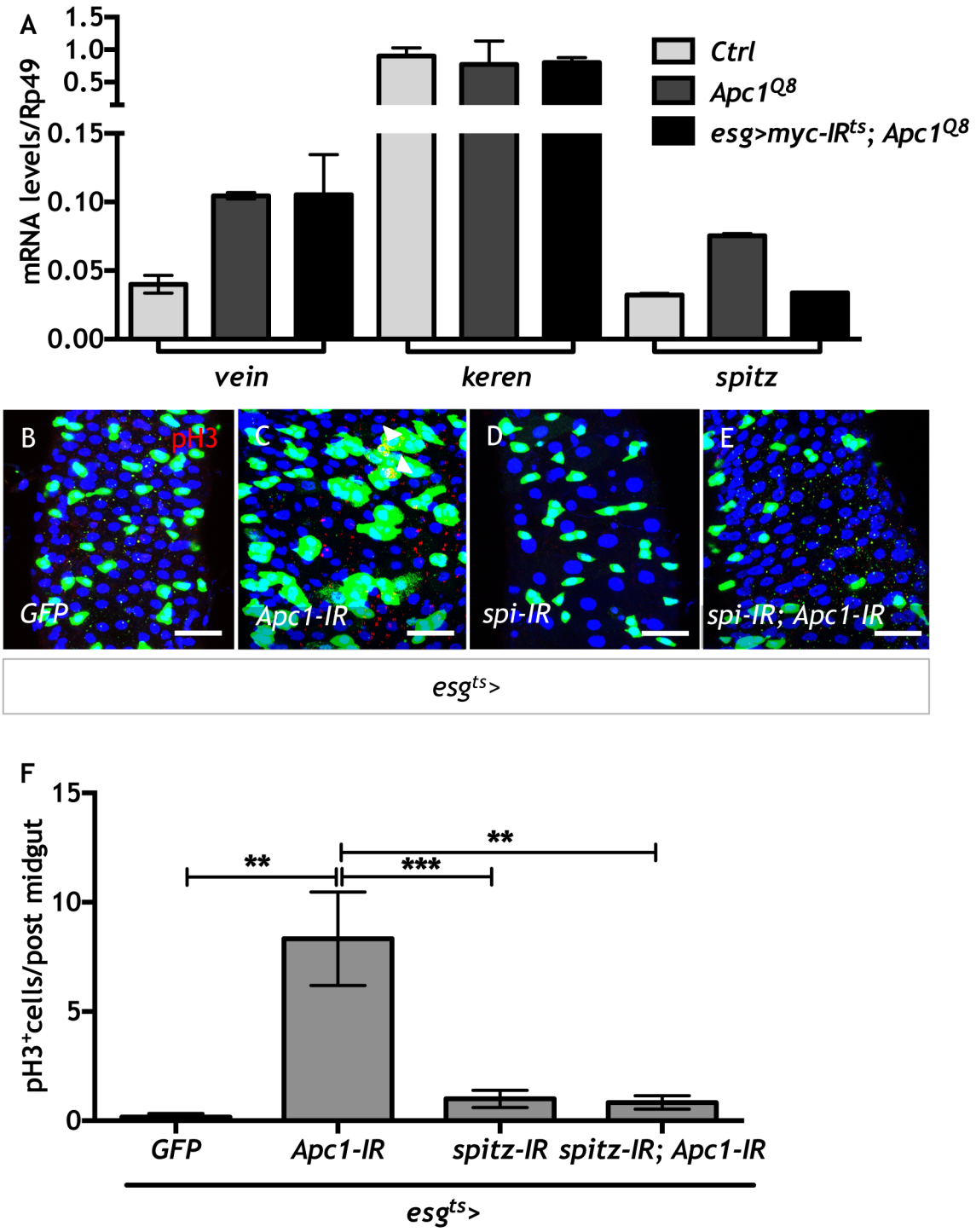

Figure 4.10 *spitz* is required within ISCs for hyperproliferation upon *Apc1* loss.

(A) qPCR analysis for the EGF-like ligands *vein*, *keren* and *spitz* in control, $Apc1^{Q8}$ and *esg>myc-IR*^{ts}; $Apc1^{Q8}$ midguts. (B-E) Immunofluorescence of 14 day old midguts from *esg>GFP* (B), *esg>Apc1-IR* (C), *esg>spitz-IR* (D) and *esg> spitz-IR; Apc1-IR* (E) flies stained with GFP (green), pH3 (red) and DAPI (blue). (F)

Quantifications of the number of $pH3^{+ve}$ cells per posterior midgut (one-way ANOVA with Bonferroni post test correction, ***$p<0.001$ and **$p<0.01$).

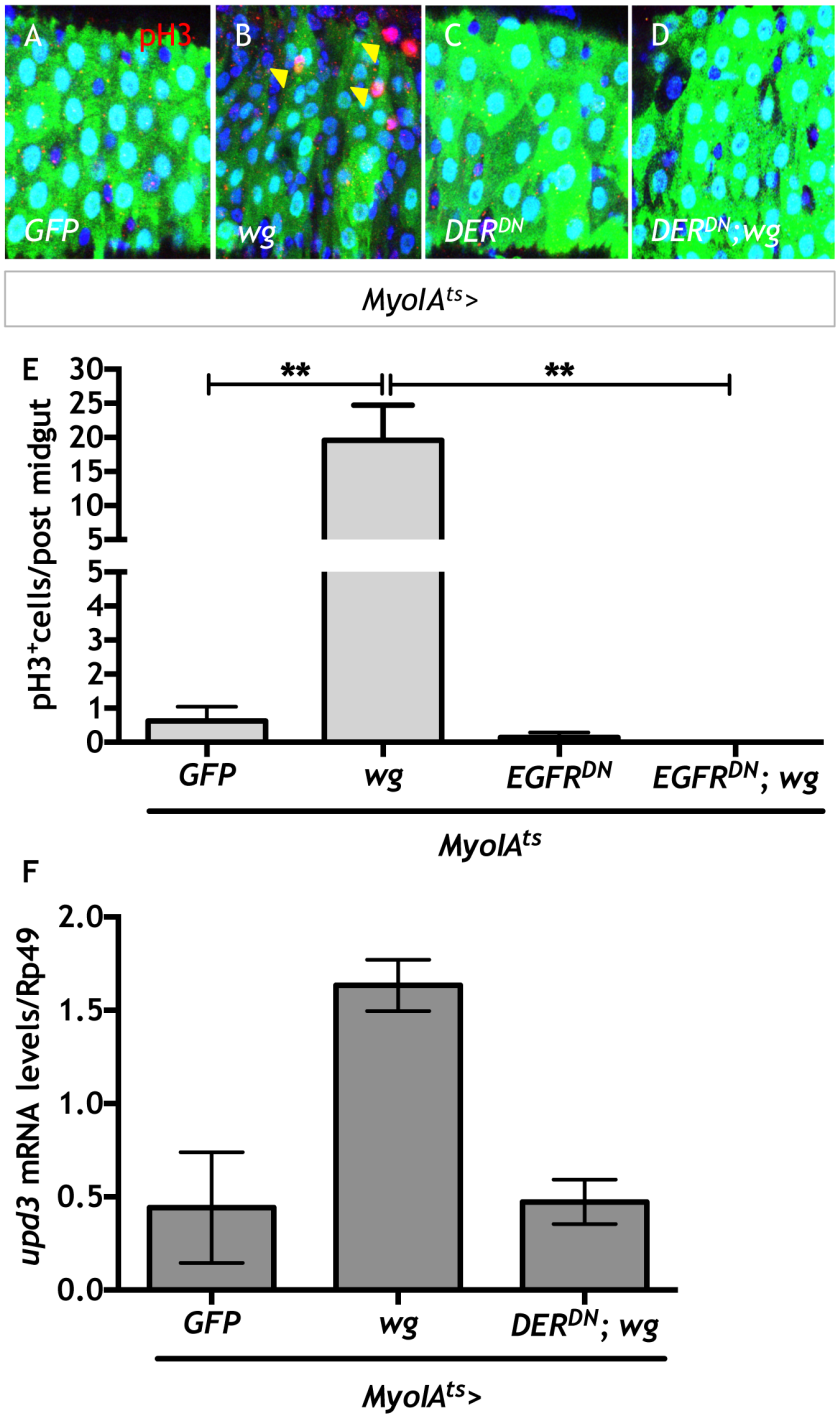

Figure 4.11 EGFR signalling is required within the ECs for ISC proliferation upon activation of *wg* signalling.

(A-D) Immunofluorescence of 14 day old midguts from *MyoIA^{ts}>GFP* (A), *MyoIA^{ts}>wg* (B), *MyoIA^{ts}>DER^{DN}* (C) and *MyoIA^{ts}>DER^{DN}; wg* (D) flies stained for GFP (green), pH3 (red) and DAPI (blue). (E) Quantifications of the number of pH3^{+ve} cell per posterior midgut (one-way ANOVA with Bonferroni post test correction, **p<0.01). (F) qPCR analysis for *upd3* in *MyoIA^{ts}>GFP*, *MyoIA^{ts}>DER^{DN}* and *MyoIA^{ts}>DER^{DN}; wg* midguts.

4.4 Discussion

4.4.1 *dMyc* and *dMax* are required for *Apc1* driven hyperproliferation in the adult *Drosophila* midgut.

Myc is an essential mediator of the *Apc* phenotype in the mammalian intestine (Sansom et al., 2007, Athineos and Sansom, 2010). This work demonstrates the conservation of this interaction in the adult *Drosophila* midgut. Moreover, knockdown of *dMyc* or its transcriptional binding partner *dMax* was able to regress *Apc1* driven hyperplasia and extend survival of *Apc1* mutant flies. These data reinforce the therapeutic potential of *Myc*/*Max* targeted therapies in CRC.

4.4.2 JAK/STAT signalling is activated upon *Apc1* loss and is required for hyperplasia of ISCs in the adult *Drosophila* midgut.

Activation of JAK/STAT signalling is a common feature of CRC (Kusaba et al., 2005). The role of JAK/STAT in the mammalian intestine is not completely understood. *Stat3* is activated in adenomas from $Apc^{Min/+}$ mice and deletion of *Stat3* in this model retarded tumourigenesis but later resulted in the formation of invasive tumours and upregulation of other *Stat* family members (Musteanu et al., 2010). In the adult *Drosophila* intestine, JAK/STAT signalling has been shown to be fundamental for homeostasis and damage induced proliferation (Jiang et al., 2009). Upon damage ECs produce *upds* which activate JAK/STAT signalling within the ISCs (Jiang et al., 2009).

Using a model of *Apc1* loss in the adult *Drosophila* midgut we have demonstrated a *dMyc* dependent activation of JAK/STAT signalling in ISCs and a fundamental requirement of JAK/STAT signalling for *Apc1* driven hyperplasia. Moreover, we describe the production of *upds* by the ECs upon loss of *Apc1*. Our data establish JAK/STAT signalling as an important mediator of *Apc1* driven hyperplasia (Fig 4.12).

4.4.3 EGFR signalling is required to mediate the crosstalk between the *wg* and JAK/STAT signalling pathways.

EGFR signalling is required for ISC proliferation in homeostasis and damaged induced regeneration in the adult *Drosophila* midgut (Jiang and Edgar, 2009,

Jiang et al., 2011, Biteau and Jasper, 2011). Increased EGFR signalling upon *Apc* loss has been reported in the mammalian intestine (Moran et al., 2004). We find a requirement for the *Drosophila* EGF-like *spitz* within ISCs for proliferation upon *Apc1* loss. Moreover, the EGF receptor *DER* is required in ECs for the expression of *upds* upon *Apc1* loss. How the activation of EGFR signalling within the ECs leads to the upregulation of *upds* is unclear as previous studies have reported that EGFR signalling activation, as measured by pMAPK, occurs solely within the ISCs (Buchon et al., 2010, Biteau and Jasper, 2011, Jiang et al., 2011). One explanation for the data is that EGFR signalling in this context does not involve MAPK activation; this is possible as the MAPK/ERK route is only one of several pathways downstream of EGFR activation. We also cannot discount the possibility that other factors may mediate the upregulation of *upds* upon EGFR activation.

Overall, these results present a novel signalling network that upon *Apc1* loss drives hyperproliferation of ISCs (Fig 4.12).

***Apc1* loss in the midgut**

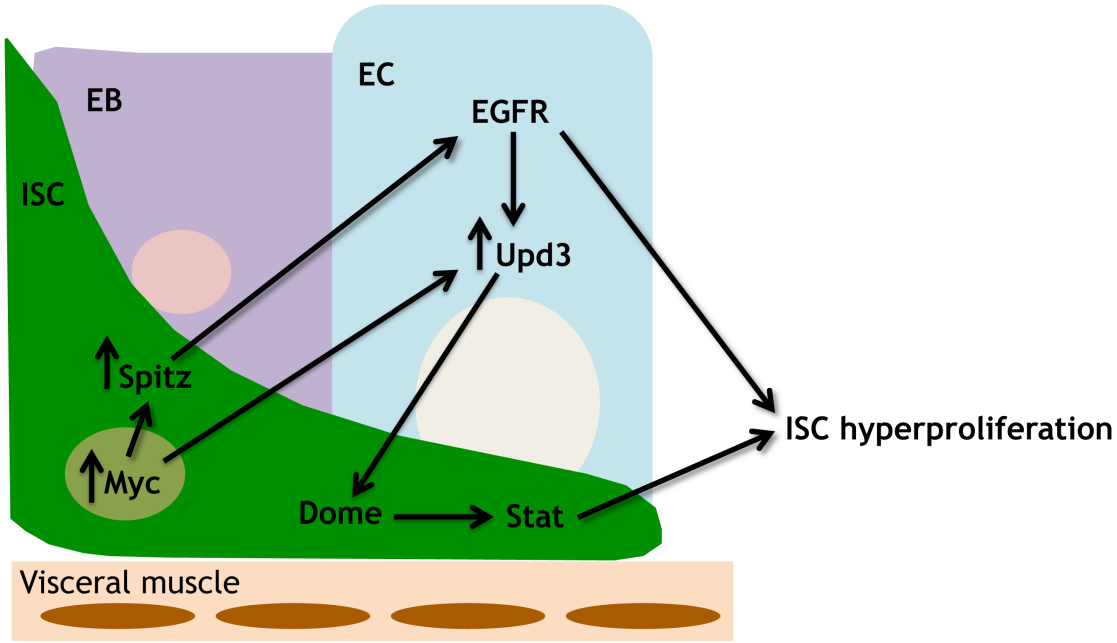

Figure 4.12 Intestinal hyperproliferation upon *Apc1* loss is mediated through crosstalk of the EGFR and JAK/STAT signalling pathways.

Loss of *Apc1* results in activation of MYC production of spitz in the ISCs and upd3 in the ECs. This leads to activation of the EGFR and JAK/STAT signalling pathways driving hyperproliferation of the ISCs.

5 Activation of Toll signalling in the fat body and expression of Eiger/TNF in haemocytes of tumour bearing larvae restricts tumour growth via apoptosis

5.1 Summary

The systemic response of the body to a growing tumour is poorly understood. We show for the first time that the *Drosophila* fat body is able to respond to the presence of a growing tumour by activating Toll signalling and demonstrate the ability of Toll signalling to restrict tumour growth. We identify the *Drosophila* haemocytes as the source of Spätzle to activate Toll signalling in the fat body and Egr/TNFα to induce tumour cell death. Finally, we describe differential roles for tumour intrinsic *versus* haemocyte-derived Egr/TNFα. We report the requirement of tumour intrinsic Egr/TNFα for haemocyte proliferation *via Pvf*/*Pvr* signalling and haemocyte derived Egr/TNFα for tumour cell death. These results demonstrate the ability of the innate immune response to control tumour burden.

5.2 Introduction

5.2.1 Cancer related inflammation

The existence of a connection between chronic inflammation and tumourigenesis has been long proposed. In 1971, Burnet formulated the "cancer immunosurveillance hypothesis". In this, he speculated that the immune system may be able to recognize arising tumour cells as "non-self" and eliminate them (Burnet, 1971). Cancer related inflammation is now an accepted hallmark of cancer and is appreciated as both a cause and a consequence of tumourigenesis. Cancer related inflammation is thought to contribute to tumour cell proliferation, angiogenesis and metastasis and can arise from extrinsic factors that establish a chronic inflammatory response and intrinsic factors such as the nature of genetic lesions present within a tumour, which can result in the upregulation of inflammatory signalling (Balkwill and Mantovani, 2001, Coussens and Werb, 2002, Balkwill and Coussens, 2004, Mantovani et al., 2008, Balkwill, 2009, Balkwill and Joffroy, 2010, Balkwill and Mantovani, 2010, Hanahan and Weinberg, 2011). Studies examining the role of tumour related inflammation in cancer progression have established that inflammation can both promote and hinder a cancer progression. However, due to genetic redundancy and the complexity of cytokine and immune signalling in mammals many open questions remain.

5.2.1.1 Tumour necrosis factor α

Tumour necrosis factor (TNF; also named TNFα) was first isolated in the 1970's from the serum of bacterially infected mice (Carswell et al., 1975). When TNF was administered to tumour bearing mice it induced rapid necrosis of the tumours and hence it was named TNF (Carswell et al., 1975). Since then, TNF has been shown to be a key inflammatory cytokine with many family members (Locksley et al., 2001). There are two receptors for TNF, TNFR1 and TNFR2. TNFR1 is more generally expressed while TNFR2 is mostly expressed within the hematopoietic lineage (Locksley et al., 2001). Once activated TNF/TNFR signalling can induce cell death or the expression of inflammatory and survival factors (Balkwill and Mantovani, 2010, Balkwill and Mantovani, 2012). Thus, mammalian TNF/TNFR signalling can result in both cell death and cell survival.

It is now clear that TNF can act as both anti and pro tumour factor depending on the cellular and genetic context (Balkwill and Joffroy, 2010). TNF is often detected in biopsies of human tumours both within the tumour and the surrounding stroma. Moreover, TNF has been detected in plasma from patients with advanced cancer (Beissert et al., 1989, Naylor et al., 1990, Karayiannakis et al., 2001, Yoshida et al., 2002, Ferrajoli, 2002, Bozcuk et al., 2004). In fact, TNF knockout mice are actually more resistant to chemical carcinogenesis than wild type mice (Moore et al., 1999). These context dependent roles of TNF suggest that correctly harnessed in the right situation TNF may still be able to induce tumour cell death.

5.2.2 *Drosophila* Eiger/TNF

Eiger (eda-like cell death trigger, Egr) is the only homologue of the mammalian cytokine TNF in *Drosophila* (Moreno et al., 2002, Igaki et al., 2002). Overexpression of Egr leads to activation of JNK signalling and JNK dependent apoptosis (Moreno et al., 2002, Igaki et al., 2002). Egr mutant flies are viable and develop normally, but have been shown to be more sensitive to infection from extracellular pathogens suggesting a role for Egr in the *Drosophila* immune response (Schneider et al., 2007). Conversely, Egr secretion has been shown to be required for organismal death in response to *salmonella* infection (Brandt et al., 2004). This suggests that like its mammalian counterpart, Egr has roles in mounting an appropriate inflammatory response but can also contribute to the pathology of infection in *Drosophila* (Brandt et al., 2004, Schneider et al., 2007). In the context of cancer work from our laboratory has shown that Egr is required for elimination of clones of transformed cells through the induction of JNK dependent apoptosis and that Egr can have both anti and pro tumour effects depending on the genetic context (Cordero et al., 2010).

5.2.3 Mammalian Toll-like receptor signalling in Cancer

Mammalian Toll-like receptor signalling is strikingly similar to *Drosophila* Toll signalling (described in detail in 1.6.1). However, unlike in *Drosophila*, the family of mammalian Toll-like receptors (TLRs) are pattern recognition receptors (PRRs) that activate the TLR signalling cascade upon binding of conserved

molecular patterns of pathogenic origin which can be both self or non self (Takeda et al., 2003). The mammalian family of TLRs contains 9 members that are expressed in different subcellular localizations. Activation of TLR signalling leads to the activation of several signalling pathways including the NF-κB and JNK pathways (Lee and Kim, 2007). Activation of these signalling pathways is required for TLR dependent regulation of innate and adaptive immune responses (Akira, 2003, Beutler et al., 2003).

TLRs have also been shown to be required within tissues for homeostasis and repair (Rakoff-Nahoum et al., 2004, Seki et al., 2005, Zhang and Schluesener, 2006, Larsen et al., 2007, Michelsen and Arditi, 2007). Activation of TLRs is also thought to have anti-cancer effects (Salaun et al., 2006, Sfondrini et al., 2006, Krieg, 2007). However, MYD88 knockout mice have been shown to have a reduced tumour burden when combined with heterozygous loss of *Apc* and chemical carcinogenesis in the skin, suggesting that TLR signalling can also positively modulate cancer progression (Rakoff-Nahoum and Medzhitov, 2007, Swann, 2008). Given that TLR signalling can have both positive and negative effects on cancer progression more research is needed to understand the molecular context in which TLR signalling activation could be used to kill tumours.

5.2.4 Aims of the project

This project was conducted in collaboration with Dr Federica Parisi, a postdoctoral researcher working in our laboratory. When I joined the laboratory in October 2009 my supervisor Dr Marcos Vidal was working on a project to delineate the role of Egr/TNF in a larval tumour model in *Drosophila*. I was able to contribute to this project and we demonstrated that Egr/TNF played context dependent roles that could both positively and negatively influence tumour progression (Cordero et al., 2010). In this project Dr Parisi and I aimed to further characterize the interaction between tumours and the innate immune response in larval models of cancer in *Drosophila*.

Experiments were designed, performed and analysed together with Dr Parisi and this work has been included in a co-first author paper with Dr Parisi.

5.3 Results

5.3.1 Toll signalling is activated in the fat bodies of tumour bearing larvae

The *scribble* (*scrib*) group of tumour suppressors, which includes the *l(2)gl, discs large* (*dlg*) and *scrib* genes, has been extensively characterized for its role in the establishment of apical basal polarity in epithelial cells (Bilder, 2004). Homozygous loss of function mutations of any of these genes is sufficient to disrupt epithelial architecture and leads to neoplastic transformation of the mitotic imaginal discs. For this reason they have been used extensively in the field of *Drosophila* cancer research (Potter et al., 2000, Brumby and Richardson, 2005, Stefanatos and Vidal, 2011, Rudrapatna et al., 2012, Gonzalez, 2013).

Cancer associated inflammation requires the activation of the innate immune system (Hanahan and Weinberg, 2011). Using this model we wanted to understand the relationship between the tumour and the immune system in Tumour bearing larvae (TBL). Previous work has demonstrated that the haemocytes, one branch of the *Drosophila* innate immune system, are recruited to imaginal disc neoplasia and have the ability to influence tumour biology (Cordero et al., 2010, Pastor-Pareja et al., 2008).

The fat body is a key tissue in *Drosophila* innate immunity and is the site of AMP production upon pathogenic infection (Hoffmann, 1995, Lemaitre and Hoffmann, 2007). We hypothesized that the fat body may respond to the presence of a growing tumour. In order to characterise this response further we performed qPCR analysis for known readouts of signalling pathways which have been previously implicated in immunity (Hoffmann, 1995, Lemaitre et al., 1996, Pastor-Pareja et al., 2008, Lemaitre and Hoffmann, 2007, Hetru and Hoffmann, 2009, Karpac et al., 2011). We collected fat bodies from control (w^{1118}), *scrib* ($scrib^{1}$) null mutant, and *Ras-scrib* ($eyRas^{V12}$; $scrib^{1}$) larvae. We included *Ras-scrib* ($eyRas^{V12}$; $scrib^{1}$) larvae in our experiment to control for tissue autonomous effects of *scrib* loss, as they carry eye imaginal disc tumours created through the MARCM system meaning that the rest of the larval tissues are wild type in these animals. Therefore, we only considered pathways that were upregulated in fat bodies from both *scrib* and *Ras-scrib* larvae (Fig 5.1).

The JAK/STAT signalling pathway has been shown to have important roles in the regulation of the immune response (Arbouzova and Zeidler, 2006). In

Drosophila, it is important for resistance to viral infection (Lemaitre and Hoffmann, 2007). JAK/STAT signalling was previously reported to be activated systemically in TBL (Pastor-Pareja et al., 2008). Although we did observe an upregulation of the negative regulator and target of the pathway *socs36E* in *scrib* fat bodies (*scrib*^{1}) this upregulation was not mirrored in *eyRas*^{V12}*-scrib* fat bodies (*eyRas*^{V12}*; scrib*^{1}) (Fig 5.1A). This suggests that upregulation of this pathway may be a tissue autonomous effect of *scrib* loss in the fat body (Fig 5.1A). Therefore the role of JAK/STAT signalling in this model was not investigated further.

Many studies have addressed the cross talk between metabolism and Inflammation (Hotamisligil and Erbay, 2008). The *Drosophila* fat body is both a metabolically and immunologically active tissue and since Insulin/FOXO signalling has been shown to regulate the expression of AMPs in response to starvation in *Drosophila* we wanted to examine if this pathway was altered in fat bodies of TBL (Becker et al., 2010). We observed an increase in levels of Insulin receptor (InR) in *scrib* (*scrib*^{1}) fat bodies but again this was not mirrored in *eyRas*^{V12}*-scrib* fat bodies (*eyRas*^{V12}*; scrib*^{1}) (Fig5.1A). We also examined levels of the FOXO target *thor* (homologous to mammalian 4E-BP1) but did not observe any significant change in expression in these samples indicating that Insulin/FOXO signalling was not deregulated in the fat bodies of TBL (Fig5.1A).

Mammalian Toll signalling has been heavily implicated in cancer related inflammation (Rakoff-Nahoum and Medzhitov, 2009, Maruyama et al., 2011). In *Drosophila*, the Toll signalling pathway is activated in the fat body upon infection and drives expression of AMPs. These AMPs include *Drosomycin* (Drs), *Defensin* (*Def*) and *Metchnikowin (*Mtk) (Lemaitre et al., 1996, Lemaitre et al., 1997, Lemaitre and Hoffmann, 2007). We found that all three AMPs were upregulated in fat bodies of TBL (Fig5.1B, *w*^{1118} vs *scrib*^{1}). Moreover, this upregulation was also present in fat bodies of *eyRas*^{V12}*-scrib* larvae (*eyRas*^{V12}*; scrib*^{1}) (Fig5.1B). This indicated that the activation of Toll signalling in the fat body occurs as a response to the presence of tumours.

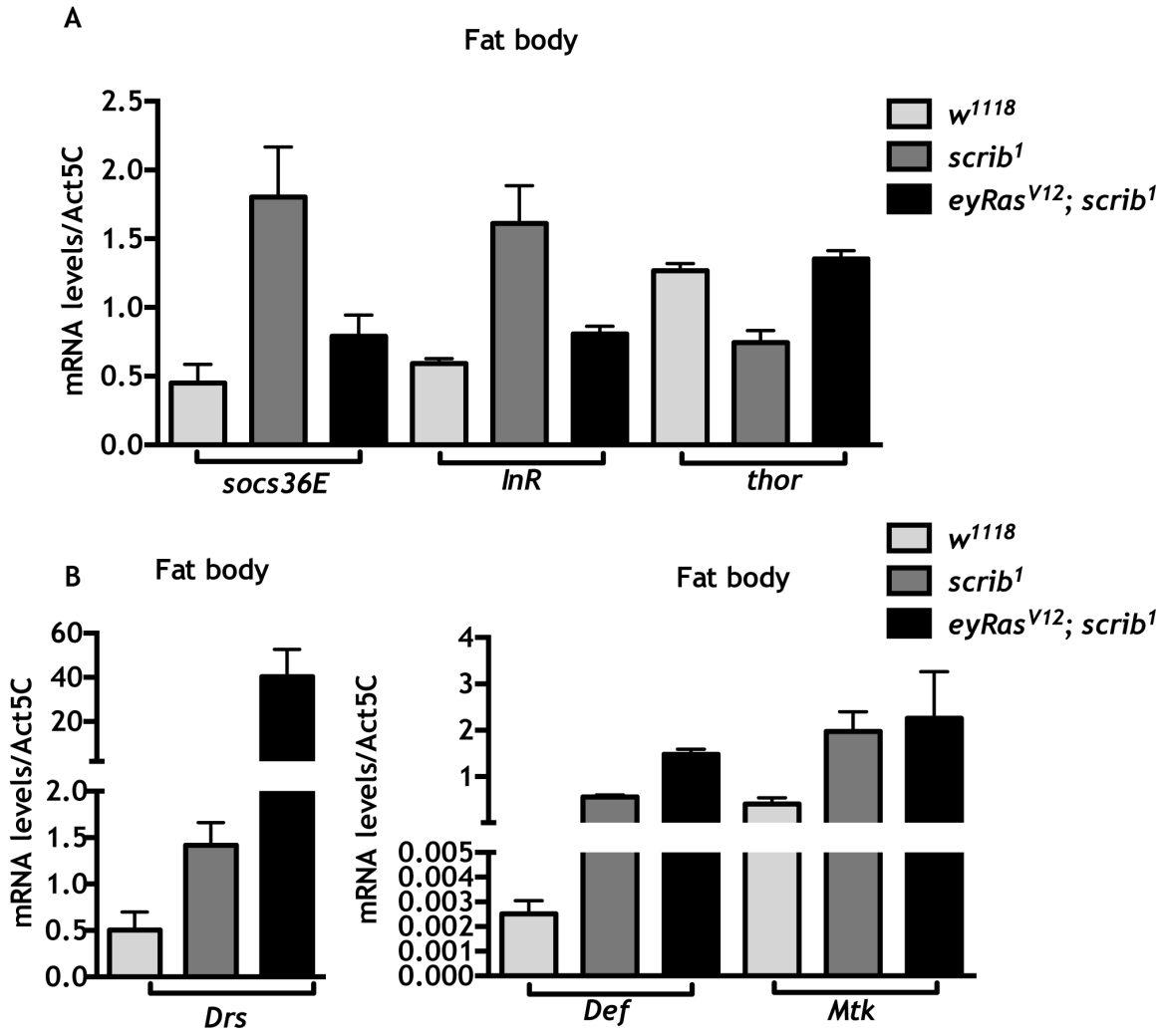

Figure 5.1 Toll signalling is activated in the fat body of tumour bearing larvae.

(A-B) qPCR analysis from fat bodies dissected from w^{1118}, $scrib^{1}$ and $eyRas^{V12}$; *scrib* larvae for the indicated targets. Note the upregulation of *Drs* (*Drosomycin*) and *Def* (*Defensin*) two Toll Antimicrobial peptides (AMPs).

5.3.2 Toll signalling is required within the fat body to restrain tumour growth.

In order to address directly the functional relevance of Toll activation in the fat body of TBL, we combined a null allele of the *scrib* group polarity tumour suppressor *discs large* ($dlg^{40.2}$), which also carries imaginal disc tumours, with the fat body specific Gal4 driver *pumpless-Gal4* (*ppl>*) ($dlg^{40.2}$*; ppl>toll*) (Bilder et al., 2000, Woods and Bryant, 1991, Zinke et al., 1999).

We utilized this mutant, as *dlg* is located on the X-chromosome and this left the 2nd and 3rd chromosome free to be combined with transgenes that would allow us to genetically dissect the effects of Toll signalling in the fat body on tumour growth.

We upregulated Toll activation in the fat body by expressing a UAS transgene for the Toll receptor ($dlg^{40.2}$*; ppl>toll*) and we inhibited Toll activation by expressing an RNAi transgene for the Toll adaptor Myd88 ($dlg^{40.2}$*; ppl>Myd88-IR*) which is required downstream of Toll receptor binding for Toll activation. We expressed a GFP transgene as a control.

At 11 days after egg deposition (AED) we dissected wild type wing discs (w^{1118}) and wing imaginal disc tumours from control ($dlg^{40.2}$*; ppl>GFP*), Myd88 knockdown ($dlg^{40.2}$*; ppl>Myd88-IR*) and Toll overexpressing larvae ($dlg^{40.2}$*; ppl>Toll*) and measured their volume (Fig 5.2). Wild type (w^{1118}) wing imaginal discs are highly folded structures while wing imaginal disc tumours had a more rounded morphology and the folds are completely lost (Fig 5.2A-D). We found that tumours from larvae with impaired Toll activation were significantly bigger than those from control larvae ($dlg^{40.2}$*; ppl>GFP*) (Fig 5.2B-E). In contrast, upregulated Toll activation achieved by overexpression of the Toll receptor ($dlg^{40.2}$*; ppl>Toll*) resulted in a significant decrease in tumour volume (Fig 5.2B, 5.2D and 5.2E).

Taken together, these data indicate that activating Toll signalling in the fat body of TBL restricts tumour growth.

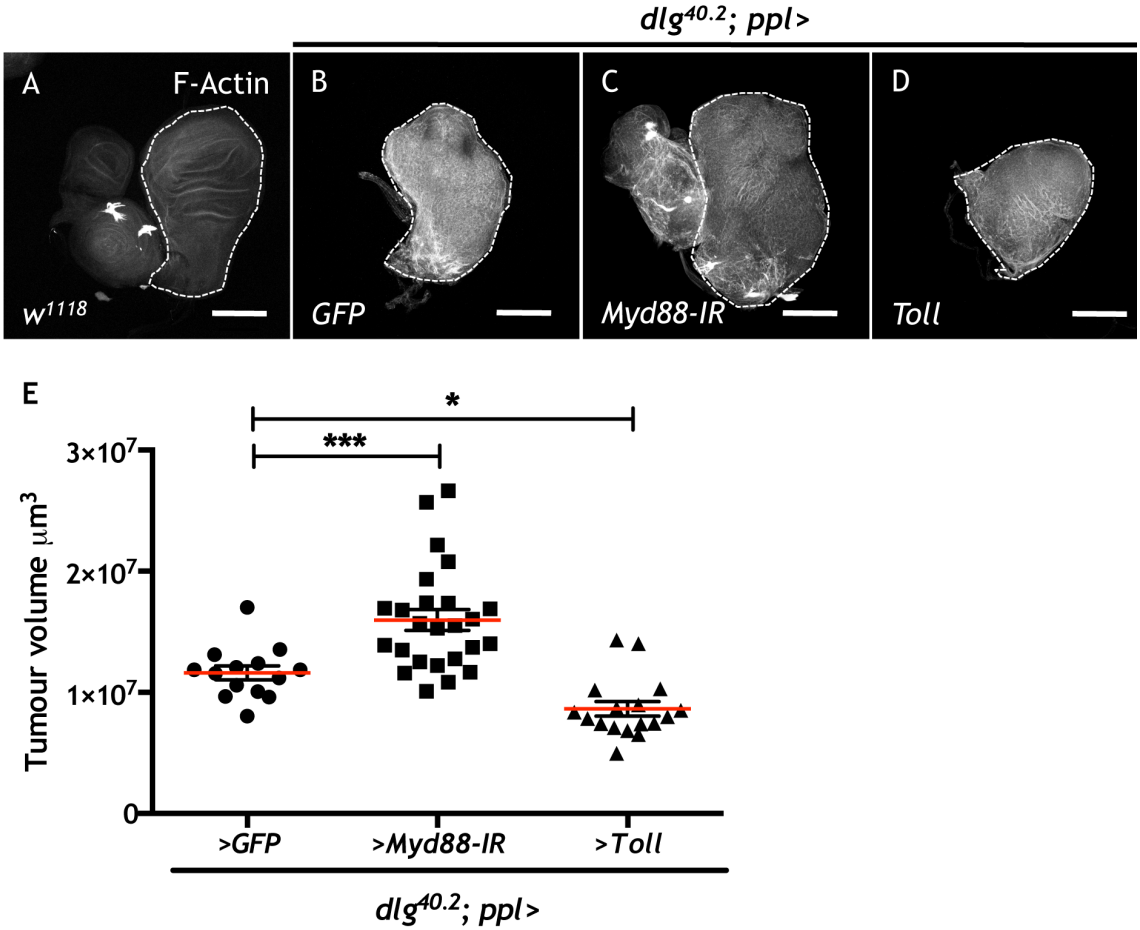

Figure 5.2 Toll signalling is required within the fat body to restrain tumour growth.

(A-D) Immunofluorescence of a wild type wing imaginal disc (outlined with dashed white line) (A) and wing imaginal disc tumours from *dlg$^{40.2}$; ppl* larvae expressing *GFP* (B), *Myd88-IR* (C) and *Toll* (D) in the fat body stained for Actin (outlined with dashed white line). Scale bars 100µm. (E) Quantification of tumour volume of tumours dissected from *dlg$^{40.2}$; ppl* larvae expressing *GFP*, *Myd88-IR* and *Toll* in the fat body (one-way ANOVA with Bonferroni post-test correction, * $p<0.05$, *** $p<0.001$).

5.3.3 Spätzle is required within the haemocytes for activation of Toll signalling in the fat body.

The *Drosophila* haemocytes are required for activation of Toll signalling in the fat body during infection through the production of the Toll receptor ligand *Spätzle* (*spz*) (Shia et al., 2009)(see section 1.6.1).

To clarify whether *spz* is required for Toll activation in the fat body of TBL we tested the requirement of *spz* within the haemocytes of TBL. We used a haemocyte specific Gal4, *hemolectin-Gal4* (*hml>*) (Goto et al., 2001) together with an RNAi transgene for *spz* (*spz-IR*) to specifically downregulate *spz* within the haemocytes ($dlg^{40.2}$*; hml> spz-IR*). We also expressed a GFP transgene as a control ($dlg^{40.2}$*; hml> GFP*).

As previously, we dissected tumours from 11 AED control ($dlg^{40.2}$*; hml>GFP*) and Spz knockdown ($dlg^{40.2}$*; hml>spz-IR*) and measured their volume. Haemocyte-specific knockdown of *spz* ($dlg^{40.2}$*; hml>spz-IR*) resulted in a significant increase in tumour volume compared to tumours dissected from control larvae ($dlg^{40.2}$*; hml>GFP*) (Fig 5.3A-C). Additionally when we performed qPCR analysis on fat bodies from control ($dlg^{40.2}$*; hml>GFP*) and Spz knockdown larvae ($dlg^{40.2}$*; hml>spz-IR*) we observed a significant decrease in *Drosomycin* expression demonstrating a decrease in Toll activation. These results indicate that tumour-driven activation of Toll signalling in the fat body is mediated by the haemocytes via Spätzle secretion.

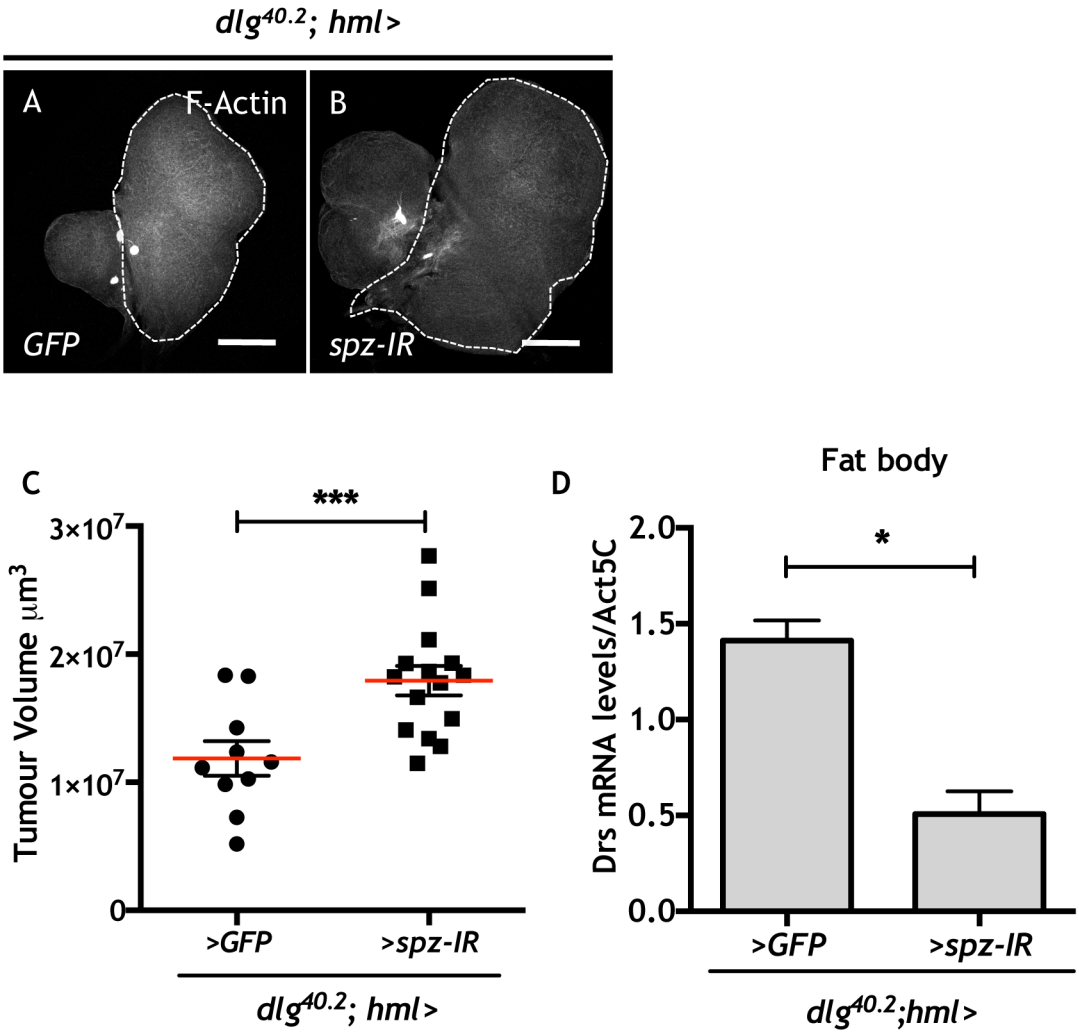

Figure 5.3 Spätzle is required within the haemocytes for activation of Toll signalling in the fat body.

(A-B) Immunofluorescence of wing imaginal disc tumours from *dlg*$^{40.2}$*; hml* larvae expressing *GFP* (A) and *spz-IR* (B) in the haemocytes stained for Actin (outlined with dashed white line). Scale bars 100µm. (C) Quantification of tumour volume of tumours dissected from *dlg*$^{40.2}$*; hml* larvae expressing *GFP* and *spz-IR* in the fat body (t-test *spz-IR* *** p=0.0005). (D) qPCR analysis for *Drosomycin* in fat bodies from *dlg*$^{40.2}$*; hml* larvae expressing *GFP* and *spz-IR* in the haemocytes (t-test *spz-IR* * p=0.0112).

5.3.4 Toll activation in the fat body of TBL restricts tumour growth through tumour cell death

As we had established that Toll activation in the fat body of TBL was negatively affecting tumour size, we hypothesized that this may a result of increased cell death.

To examine cell death in these tumours, we dissected wing imaginal discs from 5 AED wild type (w^{1118}) larvae and tumours from 11 AED control ($dlg^{40.2}$; *ppl>GFP*), Myd88 knockdown ($dlg^{40.2}$; *ppl>Myd88-IR*) and Toll overexpressing ($dlg^{40.2}$; *ppl>Toll*) larvae and stained them for cleaved caspase 3 (CC3) as a read out of apoptotic cell death (Fig 5.4). Wild type (w^{1118}) imaginal discs displayed low or undetectable levels of apoptotic cell death (Fig 5.4A-A') while tumours from control ($dlg^{40.2}$; *ppl>GFP*) and Toll overexpressing larvae ($dlg^{40.2}$; *ppl>Toll*) were regionally positive for CC3 (Fig 5.4B and 5.4D). In tumours from Myd88 knockdown larvae ($dlg^{40.2}$; *ppl>Myd88-IR*) CC3 positivity was similar to wild type wing discs (w^{1118}) (Fig 5.4A-A' and 5.4C-C').

In order to quantify CC3 in these tumours I developed a protocol using the Volocity 3D imaging analysis package (described in 2.3.1.4). Using this protocol we were able to express % tumour cell death (Volume of CC3 positivity *versus* the total tumour volume) of wing imaginal disc tumours. When we quantified the % Tumour cell death in tumours from control ($dlg^{40.2}$; *ppl>GFP*), Myd88 knockdown ($dlg^{40.2}$; *ppl>Myd88-IR*) and Toll overexpressing ($dlg^{40.2}$; *ppl>Toll*) larvae, we observed a significant decrease in % tumour cell death in tumours from Myd88 knockdown ($dlg^{40.2}$; *ppl>Myd88-IR*), while tumours from Toll overexpressing ($dlg^{40.2}$; *ppl>Toll*) larvae had a significant increase in % tumour cell death when compared to tumours from control ($dlg^{40.2}$; *ppl>GFP*) larvae (Fig 5.4F).

As we had shown a requirement for haemocyte derived Spz for Toll activation we wanted to confirm that tumours from Spz knockdown ($dlg^{40.2}$; *hml>spz-IR*) larvae phenocopied tumours from Myd88 knockdown ($dlg^{40.2}$; *ppl>Myd88-IR*) larvae. We dissected tumours from 11 AED control ($dlg^{40.2}$; *hml>GFP*) and Spz knockdown ($dlg^{40.2}$; *hml>spz-IR*) larvae and stained for CC3. As we had observed in tumours from Myd88 knockdown ($dlg^{40.2}$; *ppl>Myd88-IR*) larvae CC3 positivity was similar to wild type wing discs (Fig 5.4A-A', 5.4D-D' and 5.4E-E'). When we measured % tumour cell death we observed a significant

decrease in % tumour cell death in tumours from Spz knockdown (*dlg*$^{40.2}$; *ppl>spz-IR*) larvae. Thus, these data demonstrate the requirement of Toll signalling in the control of tumour burden through the induction of tumour cell death.

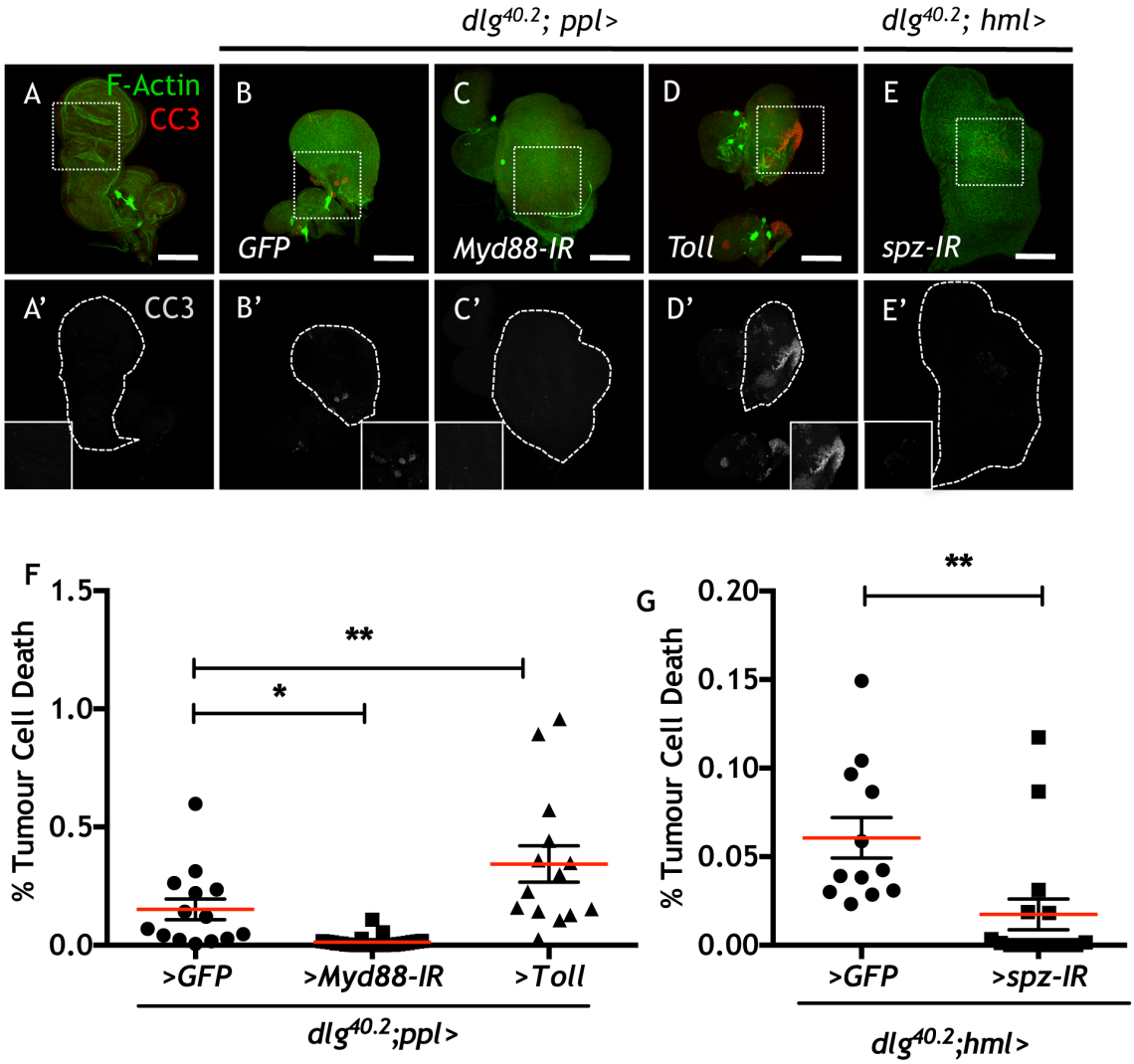

Figure 5.4 Toll activation in the fat body of TBL restricts tumour growth through tumour cell death.

(A-E') Immunofluorescence of a wild type (w^{1118}) wing imaginal disc (A), tumours from $dlg^{40.2}$; *ppl* larvae expressing GFP (B, B'), *Myd88-IR* (C, C') and *Toll* (D, D') and tumours from $dlg^{40.2}$; *hml* larvae expressing *spz-IR* (E, E') stained for actin and anti-cleaved caspase 3 (CC3) (outlined with dashed white line). Scale bars 100µm. (F) Quantification of % Tumour cell death in tumours from $dlg^{40.2}$; *ppl* larvae expressing GFP (B, B'), *Myd88-IR* (C, C') and *Toll* (D, D') (one-way ANOVA with Bonferroni post-test correction, * $p<0.05$, ** $p<0.005$). (G) Quantification of % Tumour cell death in tumours from $dlg^{40.2}$; *hml* larvae expressing *GFP* and *spz-IR* (t-test ** $p=0.0013$)

5.3.5 Egr/TNF is required in the haemocytes to execute Toll dependent tumour cell death

We next wanted to address how tumour cell death was being executed downstream of Toll activation. Eiger/TNF (Egr/TNF) is a potent inducer of cell death and previous work from our laboratory has demonstrated that systemic loss of Egr/TNF was able to ameliorate some of the hallmarks of *scrib* mutants and that haemocytes recruited to tumours produced Egr/TNF (Cordero et al., 2010). Moreover, Egr/TNF depletion specifically in the haemocytes using RNAi prevented the death of *lgl* mutant clones, suggesting a role for Egr/TNF in the removal of transformed cells (Cordero et al., 2010). It has also been shown that TBL have an increased number of haemocytes and that reducing their number through expression of the pro-death protein Hid leads to an increase in tumour volume. We hypothesized that Egr/TNF may be playing a role in the execution of tumour cell death downstream of Toll.

In order to address directly the role of haemocyte-derived Egr/TNF on tumour burden, we knocked down or overexpressed Egr/TNF specifically in haemocytes of TBL. We dissected tumours from 11 AED control (*dlg*$^{40.2}$*; hml>GFP*), Egr/TNF knockdown (*dlg*$^{40.2}$*; hml>egr-IR*) and Egr/TNF overexpressing (*dlg*$^{40.2}$*; hml>egr*) larvae and measured tumour volume and % tumour cell death (Fig 5.4). We found that tumours dissected from haemocyte Egr/TNF knockdown (*dlg*$^{40.2}$*; hml>egr-IR*) larvae had a significantly larger tumour volume than tumours from control (*dlg*$^{40.2}$*; hml>GFP*) larvae (Fig 5.5A-D). Moreover, % tumour cell death was almost completely suppressed in Egr/TNF knockdown (*dlg*$^{40.2}$*; hml>egr-IR*) larvae when compared to control (*dlg*$^{40.2}$*; hml>GFP*) larvae (Fig 5.5E). Conversely, tumours from Egr/TNF overexpressing (*dlg*$^{40.2}$*; hml>egr*) larvae had a significantly reduced tumour volume and a significant increase in % tumour cell death (Fig 5.5A-E). Together these results indicate that haemocyte-derived Egr/TNF is required for tumour cell death in TBL.

Egr/TNF protein has been observed as intracellular puncta within tumour cells and at the plasma membrane of tumour-associated haemocytes (TAHs) (Igaki et al., 2009, Cordero et al., 2010). To visualise haemocyte-derived Egr/TNF in our system we expressed a venus-tagged form of Egr/TNF specifically in the haemocytes of tumour-free animals (*he>egr*^{venus}) or TBL (*dlg*$^{40.2}$*; he>egr*^{venus}) using the haemocyte specific Gal4 driver *hemese-Gal4* (*he>*) (Kurucz

et al., 2003) (Fig 5.6). We readily observed *egr*^{venus} expressing haemocytes associated to both control wing imaginal discs (*he>egr*^{venus}) from tumour-free larvae and to wing imaginal disc tumours (Fig 5.6). In control wing imaginal discs (*he>egr*^{venus}) Egr^{venus} was confined within the associated haemocytes, however in TBL, Egr^{venus} was detected in both associated haemocytes and within the tumour itself (Fig 5.6 compare A'' with B'', white and yellow arrowheads). These results suggest that haemocytes secrete Egr/TNF when associated with transformed tissues in order to induce apoptosis.

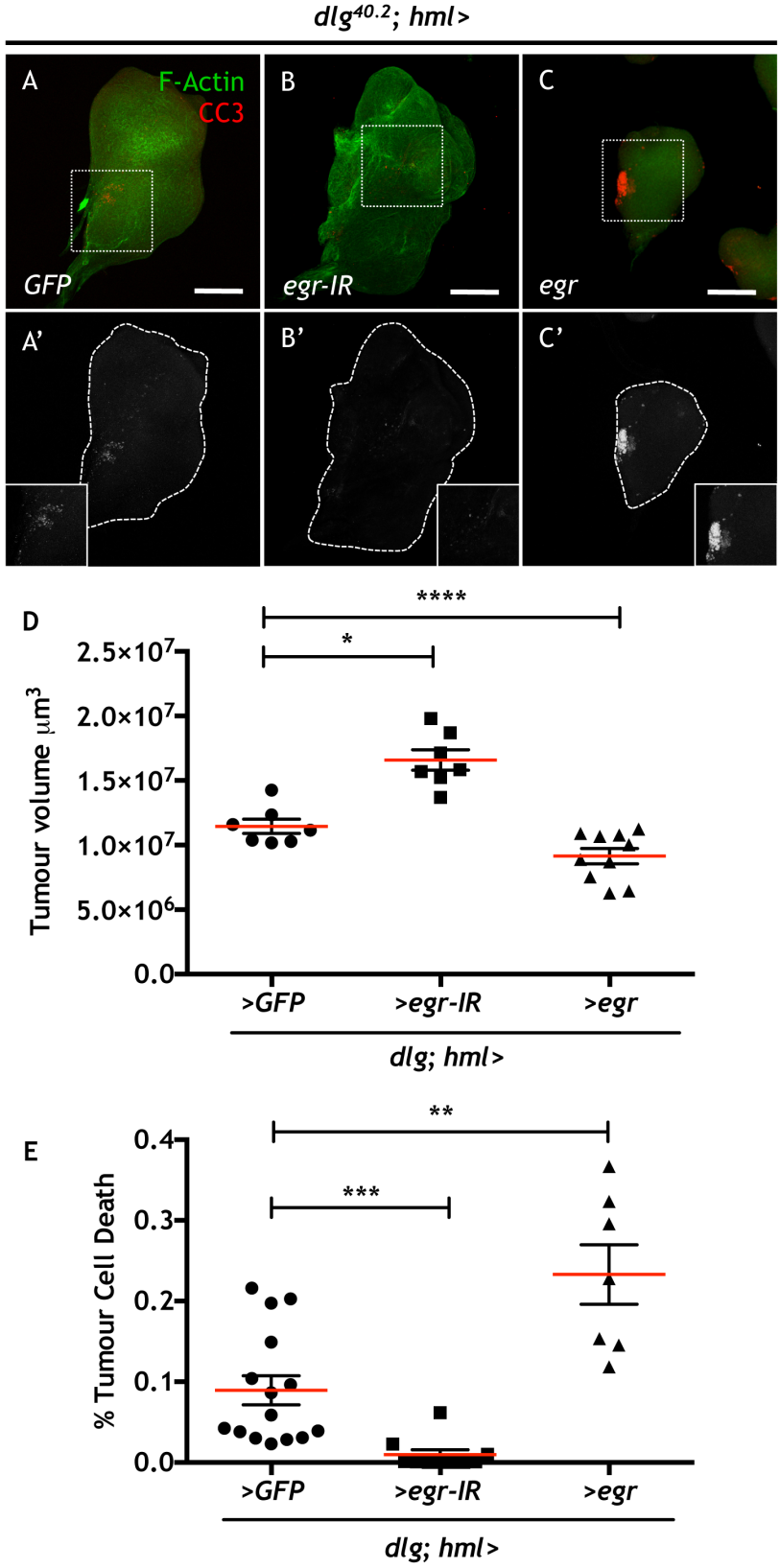

Figure 5.5 Egr/TNF is required in the haemocytes to execute Toll dependent tumour cell death.

(A-C') Immunofluorescence of tumours from *dlg*$^{40.2}$*; hml* larvae expressing either GFP (A, A'), *egr-IR* (B, B') or *egr* (C, C') stained for Actin and anti-cleaved

caspase 3 (CC3) (outlined with dashed white line). Scale bars 100μm. (F) Quantification of tumour volume of tumours from *dlg*$^{40.2}$*; hml* larvae expressing *GFP*, *egr-IR* or *egr* (E) Quantification of % tumour cell death in tumours from *dlg*$^{40.2}$*; hml* larvae expressing GFP, *egr-IR* or *egr* (one-way ANOVA with Bonferroni post test correction, *p<0.05, **p<0.005, ***p<0.001, ****p<0.0001).

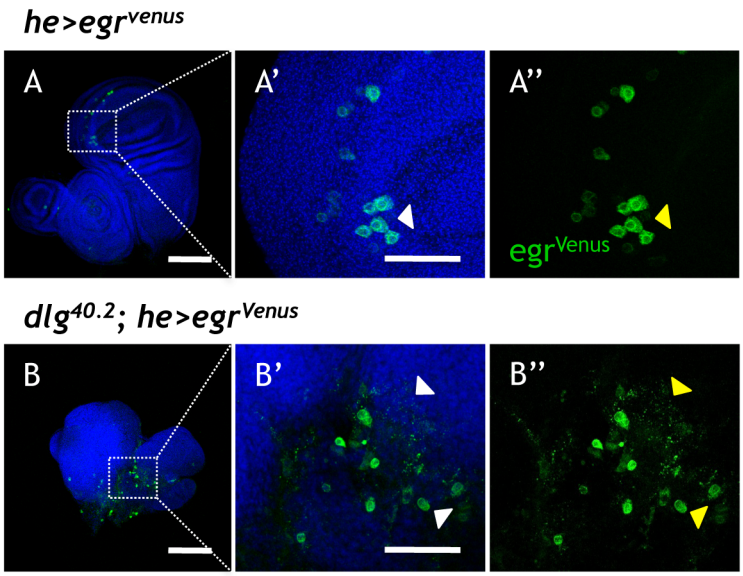

Figure 5.6 Egr/TNFα is deposited by tumour associated haemocytes.

(A-B'') Confocal images of a wing imaginal disc from a *he>egr*^{venus} larva (A-A'') and a tumour from a *dlg*$^{40.2}$*; he>egr*^{venus} larva (B-B''). Scale bars are 100μm and 50μm respectively. White and yellow arrows highlight *egr*^{venus} expressing TAHs

5.3.6 Egr/TNF is required in the haemocytes downstream of Toll activation in the fat body to induce tumour cell death

Given that we observed a correlation between Toll signalling activation in the fat body and tumour cell death, we next wanted to understand whether a haemocyte source of Egr/TNF was required to execute tumour cell death downstream of Toll activation.

To address the relationship between Toll and Egr/TNF signalling in TBL, we used the *cg*-Gal4 driver (Asha et al., 2003), which drives expression in both the haemocytes and fat body in *Drosophila*, to enhance Toll activation and simultaneously knock down Egr/TNF in both the haemocytes and fat body. We dissected tumours from larvae expressing GFP (*dlg$^{40.2}$; cg>GFP*) , overexpressing *Toll* (*dlg$^{40.2}$; cg>Toll*) and larvae overexpressing *Toll* and RNAi for Egr/TNF (*dlg$^{40.2}$; cg>Toll, egr-IR*) under the control of *cg*-Gal4. We found that tumours from larvae overexpressing both *Toll* and RNAi for Egr/TNF (*dlg$^{40.2}$; cg>Toll, egr-IR*) had a significantly larger tumour volume when compared to tumours from larvae expressing GFP (*dlg$^{40.2}$; cg>GFP*) and overexpressing *Toll* alone (*dlg$^{40.2}$; cg>Toll*) (Fig 5.7A-D). Moreover, there was a significant decrease in % Tumour cell death in tumours from larvae overexpressing both *Toll* and RNAi for Egr/TNF (*dlg$^{40.2}$; cg>Toll, egr-IR*) when compared to tumours from larvae expressing GFP (*dlg$^{40.2}$; cg>GFP*) or overexpressing *Toll* alone (*dlg$^{40.2}$; cg>Toll*) (Fig 5.7E). As we were using two transgenes by overexpressing both *Toll* and RNAi for Egr/TNF and only one copy of Gal4 we performed qPCR analysis on fat bodies from control (*dlg$^{40.2}$; cg>GFP*), Toll overexpressing (*dlg$^{40.2}$; cg>Toll*) and Toll overexpression - Egr/TNF knockdown (*dlg$^{40.2}$; cg>Toll, egr-IR*) larvae for *Drosomycin*. We performed this analysis to ensure that the observed increase in tumour volume and decrease in % tumour cell death was not a result of Gal4 titration. *Drosomycin* levels were equally increased in fat bodies from both Toll overexpressing (*dlg$^{40.2}$; cg>Toll*) and Toll overexpression- Egr/TNFα knockdown larvae (*dlg$^{40.2}$; cg>Toll, egr-IR*) when compared with fat bodies from control larvae (*dlg$^{40.2}$; cg>GFP*) (Fig 5.7F).

Additionally, we wanted to examine if Egr/TNFα knockdown (*dlg$^{40.2}$; cg>egr-IR*) or Egr/TNFα overexpression (*dlg$^{40.2}$; cg>egr*) in both the haemocytes and fat body affected the level of *Toll* activation. We performed qPCR analysis for *Drosomycin* on fat bodies from control (*dlg$^{40.2}$; cg>GFP*), Egr/TNF knockdown

(*dlg*$^{40.2}$*; cg>egr-IR*) and Egr/TNF overexpression (*dlg*$^{40.2}$*; cg>egr*) larvae (Fig 5.7G). We did not observe any effect on levels of *Drosomycin* in fat bodies from Egr/TNF knockdown (*dlg*$^{40.2}$*; cg>egr-IR*) or Egr/TNF overexpression (*dlg*$^{40.2}$*; cg>egr*) larvae when compared to levels in fat bodies from control larvae (*dlg*$^{40.2}$*; cg>GFP*). These data suggesting Egr/TNF is required to induce tumour cell death downstream of Toll activation in the fat body but is not required in the haemocytes or fat body to modulate Toll activation.

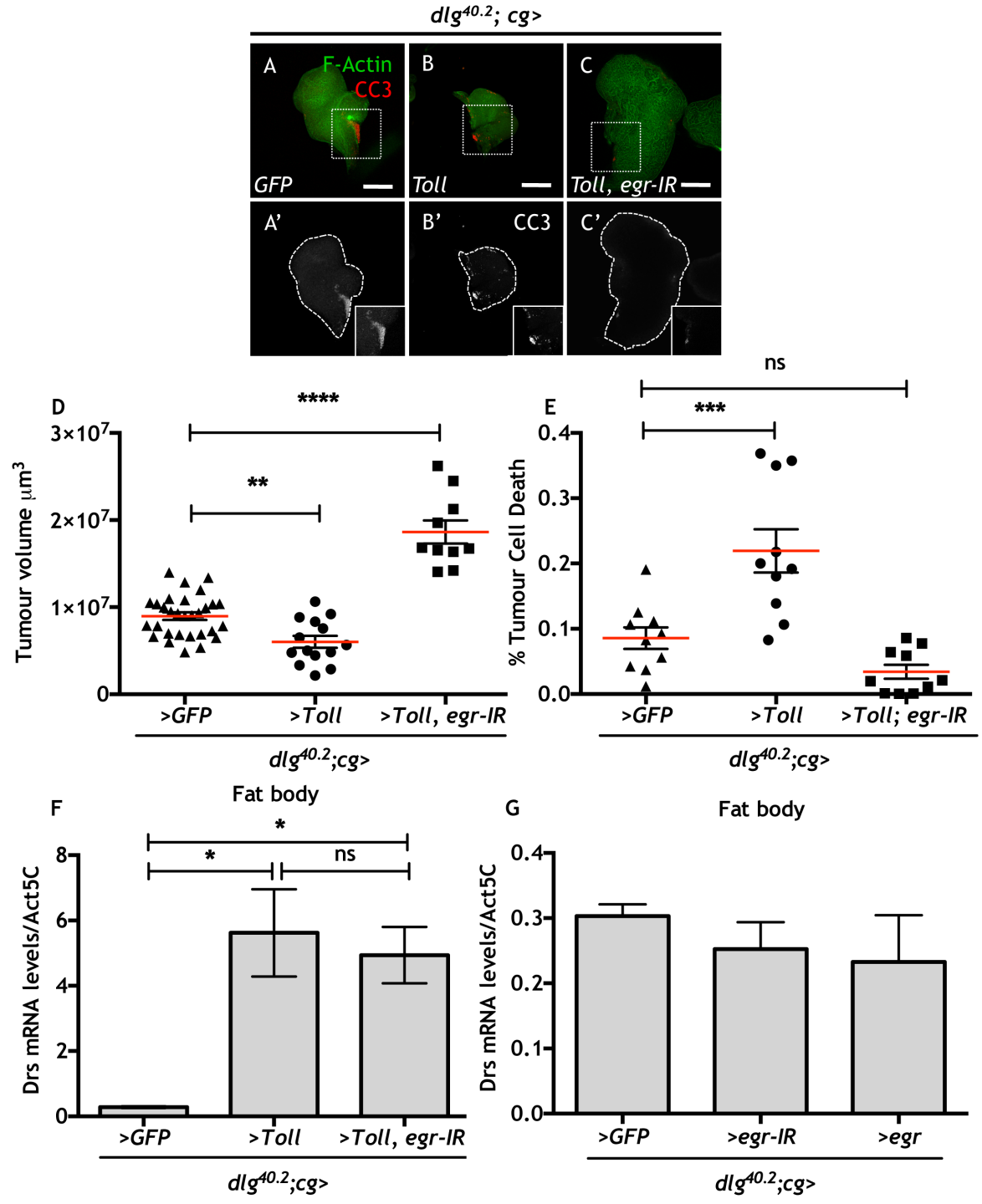

Figure 5.7 Egr/TNF is required in the haemocytes downstream of Toll activation in the fat body to induce tumour cell death.

(A-C') Immunofluorescence of tumours from *dlg*$^{40.2}$*; cg* larvae expressing GFP (A, A') *Toll* (B, B') or *Toll, egr-IR* (C, C') stained for Actin and anti-cleaved caspase 3 (CC3) (outlined with dashed white line). Scale bars 100µm. (D) Quantification of Tumour volume of tumours from *dlg*$^{40.2}$*; cg* larvae expressing either *Toll* or *Toll, egr-IR* (one-way ANOVA with Bonferroni post-test correction, **p<0.01, ****p<0.0001). (E) Quantification of % Tumour cell death in tumours from *dlg*$^{40.2}$*;*

cg larvae expressing either *Toll* or *Toll, egr-IR* (one-way ANOVA with Bonferroni post-test correction, ***p<0.001, ns-no significance) (F) qPCR analysis of fat bodies from $dlg^{40.2}$*; cg* larvae expressing either *Toll* (A, A') or *Toll, egr-IR* for *Drosomycin* (one-way ANOVA with Bonferroni post test correction, ns-no significance *p<0.05). (G) qPCR analysis of fat bodies from $dlg^{40.2}$*; cg* larvae expressing either *GFP*, *egr-IR* or *egr* for *Drosomycin* (one-way ANOVA with Bonferroni post-test correction, ns-no significance).

5.3.7 Egr/TNF is required within transformed cells to activate Toll signalling in the fat body.

Depletion of Egr/TNF from the haemocytes or inhibition of Toll activation in the fat body of TBL results in an increased tumours burden as a consequence of decreased tumours cell death. These observations suggest that the relationship between these two pathways is important for a systemic immunosuppressive response.

To examine the relationship between Egr/TNF and Toll signalling further and to test whether Egr/TNF was required for activation of Toll signalling, we combined a reporter for Toll signalling, *Drosomycin*-GFP (*drs-GFP)*, with larvae mutant for *scrib* (*scrib*^{1}) and larvae mutant for *scrib* and *egr* (*egr*^{3}*; scrib*^{1}). *drs-GFP* reporter activation was observed in the fat body of *scrib* mutant larvae (*scrib*^{1}) but not in double mutant *egr-scrib* larvae (*egr*^{3}*; scrib*^{1}) (Fig 5.8A-B). This suggests that Egr/TNF is required for Toll activation in the fat body of TBL. As we had excluded a role for Egr/TNF in both the fat body and haemocytes for Toll activation in TBL, we next considered whether tumour-intrinsic expression of Egr/TNF (Igaki et al., 2009) could mediate the activation of Toll signalling in the fat body.

To test this possibility we induced the formation of wing imaginal disc dysplasia by driving RNAi for *dlg* (*dlg-IR*) under the control of *scalloped-Gal4* (*sd>dlg-IR*), which drives expression specifically in the wing pouch, in larvae carrying the *drs-GFP* reporter. We observed activation of Toll signalling in the fat body of *sd>dlg-IR* larvae (Fig 5.8C-C'). We repeated this experiment but combined RNAi for *dlg* with RNAi for Egr/TNF (*sd>dlg-IR; egr-IR*). Using this system we could knockdown Egr/TNF specifically within *dlg* transformed cells. We did not observe activation of Toll signalling in these larvae (Fig 5.8D-D'). These results suggest that Egr/TNFα is required within transformed cells for activation of Toll signalling in the fat body.

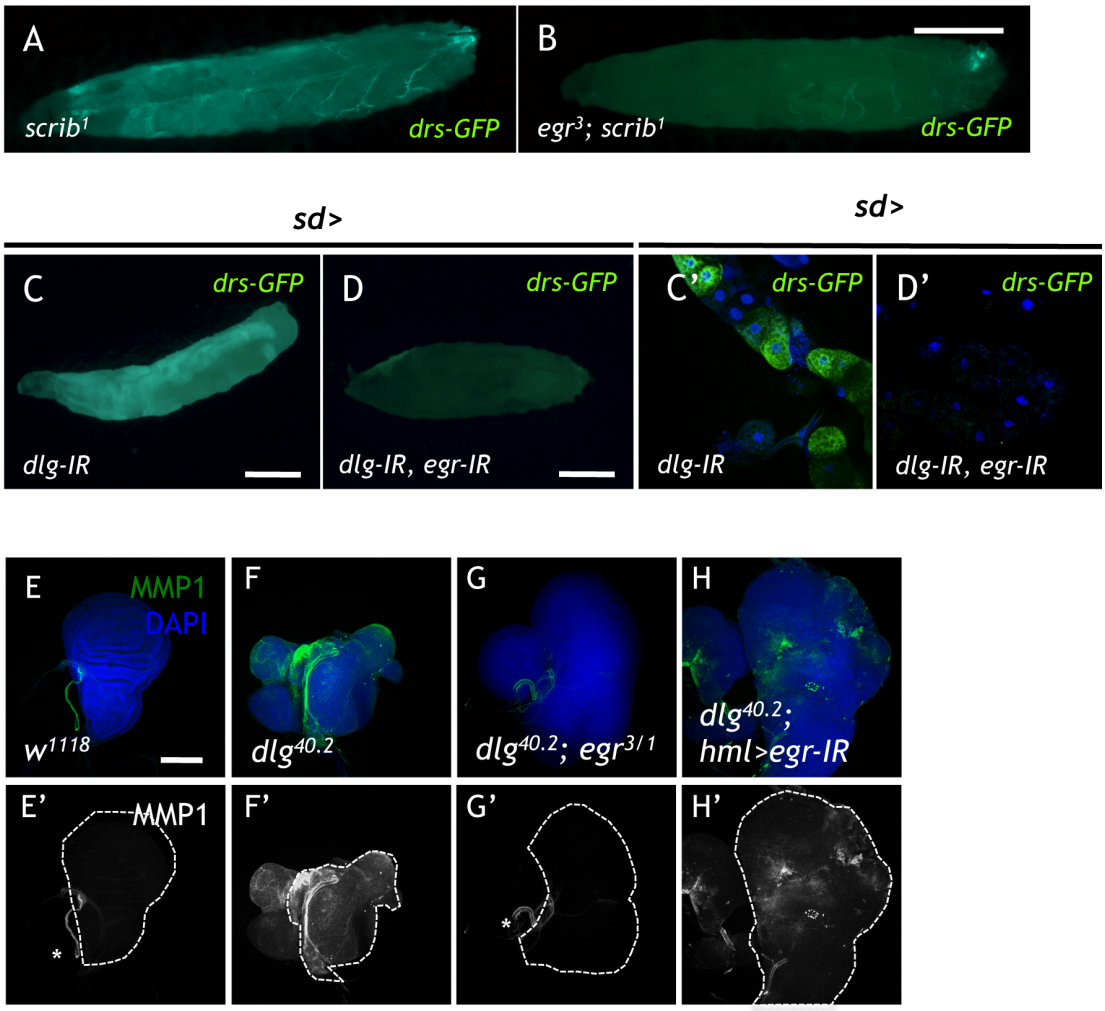

Figure 5.8 Egr/TNF is required within transformed cells to activate Toll signalling in the fat body

(A-B) Fluorescent light microscopy images of *scrib*^{1} and *egr*^{3}*; scrib*^{1} 3rd instar larvae expressing the Toll reporter *drosomycin-GFP* (*drs-GFP*). (C-D') Fluorescent light microscopy images of 3rd instar larvae (C', D') and immunofluorescence of fat bodies (C', D') from larvae expressing the Toll reporter *drosomycin-GFP* (*drs-GFP*) and either *dlg-IR* or *dlg-IR; egr-IR* under the control of *sd-Gal4*. Scale bars 1mm. (E-H') Immunofluorescence a wild type (*w1118*) wing disc and tumours from *dlg*$^{40.2}$, *dlg*$^{40.2}$; *egr*$^{3/1}$ and *dlg*$^{40.2}$; *hml>egr-IR* stained for MMP1 and DAPI (outlined with dashed white line). Scale bars 100µm.

5.3.8 Egr/TNF is required within transformed cells for expression of MMP1

Our results indicate that different sources of Egr/TNF play distinct roles in TBL. Tumour-intrinsic Egr/TNF is required to activate Toll signalling in the fat body while haemocyte-derived Egr/TNF is required to execute the tumour cell death program. Since disruption of the basement membrane has been reported to trigger haemocyte recruitment (Pastor-Pareja et al., 2008), we hypothesized that tumour intrinsic Egr/TNF might be required for the expression of matrix metalloproteinase 1 (*Mmp1*) which is known to promote the degradation of the basement membrane (Cordero et al., 2010, Pastor-Pareja et al., 2008). To address this we dissected wild type (w^{1118}) wing imaginal discs and tumours from *dlg* mutant ($dlg^{40.2}$), *dlg-egr* mutant larvae ($dlg^{40.2}$; $egr^{3/1}$) and *dlg* mutant larvae expressing RNAi for Egr/TNF specifically in the haemocytes ($dlg^{40.2}$;*hml>egr-IR*) and stained for MMP1. In wild type imaginal discs, we only observed MMP1 staining in associated trachea (Fig 5.8E-E', * marks associated trachea). Tumours from *dlg* mutant and *dlg* mutant larvae expressing RNAi for Egr/TNF specifically in the haemocytes, stained strongly for MMP1 (Fig 5.8F-F' and 5.8H-H') while tumours from *dlg-egr* mutant larvae ($dlg^{40.2}$; $egr^{3/1}$) were only positive for MMP1 in the associated trachea (Fig 5.8G-G'). These data demonstrate a requirement for tumour-intrinsic Egr/TNF for MMP1 expression in transformed epithelia.

Together these results point to a correlation between Egr/JNK signalling in the tumour and Toll activation in the fat body, as systemic loss of Egr/TNF prevents Toll activation in response to tumour burden and MMP1 production within the tumour. The haemocytes could link these two tissues as we have demonstrated a requirement for haemocyte derived Spätzle for Toll activation in the fat body and it has been shown that numbers of haemocytes increase in the presence of a tumour (Pastor-Pareja et al., 2008). Thus, we wanted to test whether Egr/TNF expression within the tumour affected haemocyte proliferation. We hypothesized that a higher number of haemocytes could enhance Toll signalling activation in the fat body through the increased production of Spätzle.

5.3.9 *Pvr* signalling is required for increased haemocyte numbers to restrict tumour burden.

Drosophila Pvfs are homologous to vertebrate VEGF/PDGF and have been shown to drive haemocyte migration and proliferation in different contexts (Munier et al., 2002, Wood et al., 2006, Parisi and Vidal, 2011). Mammalian VEGF and PDGF play important roles in both wound healing and tumourigenesis as they are required for angiogenesis and inflammatory infiltrate recruitment (Arwert et al., 2012).

In order to test if Pvfs were responsible for the increased number of haemocytes in TBL, we performed qPCR analysis on wild type (w^{1118}) wing imaginal discs as well as wing imaginal disc tumours from either *scrib* mutant ($scrib^{1}$) or *egr-scrib* double mutant larvae (egr^{3}; $scrib^{1}$). We observed an upregulation of *pvf1* in tumours from *scrib* mutant ($scrib^{1}$) larvae when compared to wild type (w^{1118}) wing imaginal discs (Fig 5.9A). This upregulation was reduced in tumours from *egr-scrib* double mutant larvae (egr^{3}; $scrib^{1}$). These results were encouraging and so we proceeded to test the functional role of *pvf* expression within the tumour.

First we wanted to test if Pvf/Pvr signalling was required for the previously reported tumour associated increase in haemocytes. To address this we expressed *GFP* as a control or RNAi for the *pvf* Receptor *Pvr* specifically in the haemocytes of TBL ($dlg^{40.2}$; *hml>GFP* and $dlg^{40.2}$; *hml>Pvr-IR* respectively). We quantified the number of circulating haemocytes in control ($dlg^{40.2}$; *hml>GFP*) and Pvr knockdown larvae ($dlg^{40.2}$; *hml>Pvr-IR*). We found that Pvr knockdown larvae ($dlg^{40.2}$; *hml>Pvr-IR*) had significantly fewer haemocytes than control larvae ($dlg^{40.2}$; *hml>GFP*) (Fig 5.9B). These data demonstrate the requirement of Pvr for increased numbers of haemocytes in TBL.

We next wanted to examine if this had implications for tumour burden. To assess this we dissected tumours from control ($dlg^{40.2}$; *hml>GFP*) and Pvr knockdown larvae ($dlg^{40.2}$; *hml>Pvr-IR*) and stained for CC3 and measured tumour volume and % tumour cell death (Fig 5.9C-D'). We found that tumours from Pvr knockdown larvae ($dlg^{40.2}$; *hml>Pvr-IR*) had a significantly larger tumour volume when compared to tumours from control larvae ($dlg^{40.2}$; *hml>GFP*) (Fig 5.9E). Additionally, % tumour cell death in tumours from Pvr knockdown larvae ($dlg^{40.2}$; *hml>Pvr-IR*) was significantly reduced (Fig 5.9F).

Taken together, these data indicate that tumour intrinsic Egr/TNF is required for a tumour related increase in haemocyte number *via* an upregulation of *pvf1*.

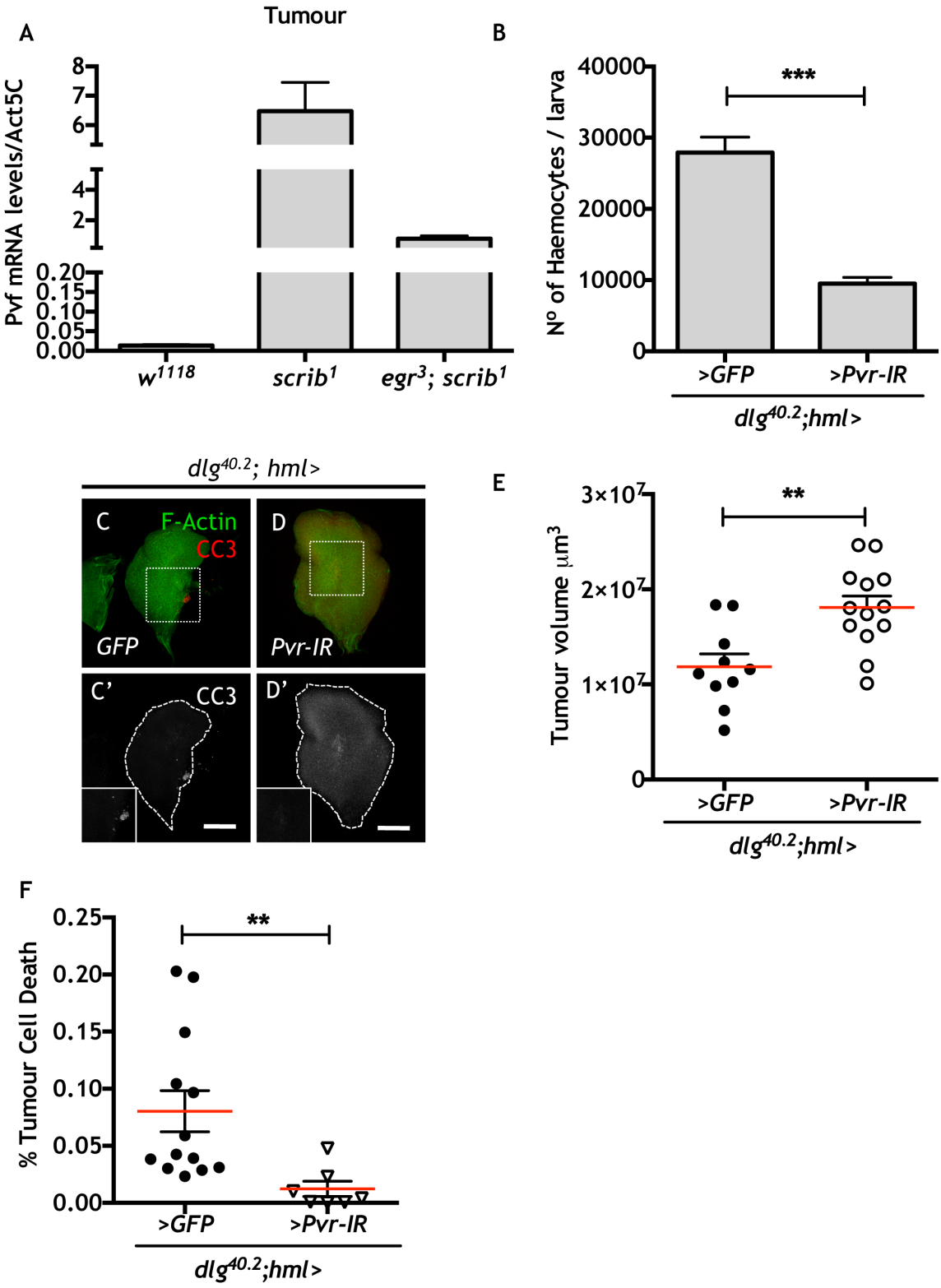

Figure 5.9 *Pvr* signalling is required for increased haemocyte numbers to restrict tumour burden.

(A) qPCR analysis for *pvf1* in wild type (w^{1118}) wing imaginal discs and tumours from *scrib* ($scrib^{1}$) mutant and *egr-scrib* (egr^{3}; $scrib^{1}$) double mutant larvae. (B) Quantification of haemocyte number in $dlg^{40.2}$; *hml* larvae expressing either *GFP*

or *Pvr-IR* (t-test, ***p=0.0079) (C-D') Immunofluorescence of tumours from *dlg$^{40.2}$; hml* larvae expressing either *GFP* (C, C') or *Pvr-IR* (D, D') stained for actin and anti–cleaved caspase 3 (CC3) (outlined with dashed white line). Scale bars 100μm. (E) Quantification of Tumour volume of tumours from *dlg$^{40.2}$; hml* larvae expressing either *GFP* or *Pvr-IR* (t-test, **p=0.0026). (F) Quantification of % Tumour cell death in tumours from rom *dlg$^{40.2}$; hml* larvae expressing either *GFP* or *Pvr-IR* (t-test, **p=0.0030).

5.4 Discussion

Tumours are not isolated entities; they grow within tissues and have complex relationships with both the micro- and macro-environment (Gonda et al., 2009, Hanahan and Weinberg, 2011). Cancer treatment itself is rapidly evolving and clinical studies are now assessing the therapeutic potential of therapies that do not directly target tumour cells (e.g. using anti-angiogenic drugs). Cancer-related inflammation has been shown to act as both a tumour suppressor and tumours promoter (Karin and Greten, 2005, Mantovani et al., 2008, Gonda et al., 2009, Balkwill and Mantovani, 2012).

The results so far presented demonstrate a pivotal role of the *Drosophila* innate immune response in the control of tumour burden (Fig 5.10). Moreover, we have made observations that suggest that haemocytes are able to recognize and eliminate transformed cells.

5.4.1 The Fat body restricts tumour burden via Toll signalling

Research in *Drosophila* has made seminal contributions to the understanding of innate immune signalling. The discovery of the role of Toll-like receptors (TLRs) in innate immunity was first made in the fruit fly and was rapidly followed by the characterization of their relationship with NFκB signalling (Lemaitre, 2004). These remarkable studies led to the identification of mammalian TLRs and to the delineation of their function in the control of numerous aspects of both the innate and adaptive immune responses (Akira, 2003, Beutler et al., 2003).

Mammalian TLRs are important mediators of cancer-related inflammation (Karin and Greten, 2005, Maruyama et al., 2011). Nevertheless, the mechanisms that activate TLR signalling in cancers are still not well understood. It has been proposed that injured or necrotic cells release molecules not normally found in the extracellular milieu (e.g. DNA and nuclear proteins) that can act as endogenous ligands (Kim and Karin, 2011)

During pathogen infection in *Drosophila*, the haemocytes produce the Toll ligand Spätzle to activate Toll signalling in the fat body (Shia et al., 2009). We show that haemocyte derived Spätzle is also required to activate Toll signalling in the presence of a growing tumour (Fig 5.1, 5.2 and 5.3). Furthermore, inhibition of Toll signalling within the fat body resulted in increased tumour

burden through a suppression of tumour cell death (Fig 5.4). These data unequivocally demonstrate that activation of Toll signalling restricts tumour burden in *Drosophila*.

5.4.2 The role of Haemocytes in the restriction of tumour burden.

Tumour-associated macrophages (TAMs) perform a wide array of activities such as engulfing cellular debris from regions of tumour necrosis, remodelling blood vessels and further boosting the inflammatory response via cytokine production. This could result either in tumour suppression or promotion, depending on the context (Balkwill and Mantovani, 2001).

It has been established that TBL have an increased number of haemocytes and that reducing the number of haemocytes in TBL results in an increased tumour burden (Pastor-Pareja et al., 2008). In addition, work from our laboratory has shown that tumour-associated haemocytes (TAHs) are recruited to imaginal disc tumours and express Egr/TNF (Cordero et al., 2010). In this study, we have demonstrated the requirement of a haemocyte source of Egr/TNF for tumour cell death as depletion of Egr/TNF specifically in the haemocytes resulted in increased tumour burden and suppression of tumour cell death (Fig 5.5). Additionally, when we expressed a venus tagged form Egr/TNF we observed Egr/TNF particles in the tumour (Fig 5.6).

Our results demonstrate a requirement of Egr/TNF in haemocytes of TBL to restrict tumour growth through tumour cell death (Fig 5.10).

5.4.3 Egr/TNF plays tissue specific roles in TBL

Previous work from our laboratory demonstrated that systemic loss of Egr/TNF modifies the nature of *scrib* and *dlg* tumours and described a context-dependent role of Egr/TNF in tumours with and without oncogenic Ras (Cordero et al., 2010). Our results presented here suggest that Egr/TNF plays tissue-specific roles that result in specific outcomes. Egr/TNF knockdown in haemocytes fully suppressed tumour cell death but did not affect Toll activation in the fat body (Fig 5.7). In contrast, tumour intrinsic Egr/TNF was required to activate JNK signalling within transformed epithelia and for the induction of Toll activation in

the fat body (5.8). Taken together our data suggest that Egr/TNF is required in epithelial tumours for activation of the immune response and in haemocytes for tumour cell death downstream of Toll activation. One question that I would like to address further is if Egr/TNF dependent cell death is also dependent on Toll activation in the fat body. To do this I would overexpress Egr/TNF and concomitantly inhibit Toll activation. This could be very interesting and if Egr/TNF dependent cell death is also dependent on Toll activation in the fat body this would explain why we do not observe Egr/TNF particles within normal epithelia.

5.4.4 Egr/TNF dependent *pvf1* expression is required for haemocyte proliferation

Haemocyte number has been shown to modulate tumour burden (Pastor-Pareja et al., 2008). Pvf1 is the *Drosophila* homologue of the vertebrate VEGF/PDGF and activation of Pvr signalling has been shown to induce haemocyte proliferation (Zettervall et al., 2004). We have demonstrated that wing imaginal disc tumours produce *pvf1* and that this is dependent on the presence of Egr/TNF (5.9). Functionally, we show that loss of Pvr signalling in haemocytes leads to a decrease in haemocyte numbers and tumour cell death, coupled with an increase in tumour volume. These results demonstrate that tumour associated increase in haemocyte number (Pastor-Pareja et al., 2008), is dependent on Pvr signalling within the haemocytes. We hypothesized that the tumour associated increase in haemocyte number may mediate Toll activation in the fat body through increased production of the Toll ligand Spätzle. In order to address this directly I would like to investigate the effect of modulation of haemocyte number on Toll activation in the fat body.

5.4.5 Overall conclusions and impact

In this study, we have used mutant larvae systemically deficient for polarity tumour suppressor genes. This experimental setup does not allow us to take into account the contribution of wild type untransformed cells. Many studies have shown that mosaic clones of *scrib, lg(2)l* and *dlg* mutant cells are eliminated by wild type cells through cell competition in an *Egr/TNF*, *myc* and *hippo* pathway

dependent fashion (Igaki et al., 2009, Froldi et al., 2010, Menendez et al., 2010, Chen et al., 2012). Previous work from our laboratory has demonstrated a role for Egr/TNF in haemocytes for the elimination of *lg(2)l* mutant clones (Cordero et al., 2010). However, there have been reports that wild type cells can induce apoptosis of transformed cells but haemocytes are still required to remove apoptotic corpses of mutant cells (Lolo et al., 2012). While the normal epithelial neighbours could eliminate small clones of tumorous cells, the data presented here suggests the *Drosophila* innate immune system is indispensable for the elimination of already established tumours. In this context the haemocytes and fat body play essential roles in promoting tumour cell death. Our results also suggest that Egr/TNF plays epithelial intrinsic and extrinsic roles (Fig 5.10).

In order to further consolidate this work I would like to develop a new experimental system where I could examine the conclusions we have made here in the context of oncogenic cooperation between *Ras* and *scrib* (*eyRas^{V12}; scrib^{1}*) (Brumby and Richardson, 2003, Pagliarini and Xu, 2003, Cordero et al., 2010). I would do this by creating transgenic flies that form *Ras-scrib* tumours in the eye or wing imaginal discs and combine them with the Gal4/UAS system to address the role of Egr/TNF in the tumour, haemocytes and fat body. In previous work from our lab we demonstrated a context dependent role for Egr/TNF in *Ras-scrib* oncogenic cooperation (*eyRas^{V12}; scrib^{1}*), however these experiments were performed with systemic loss of Egr/TNF (Cordero et al., 2010). We have now demonstrated differential roles of Egr/TNF in the tumour and haemocytes and I would like to address how these roles are affected in larvae carrying *Ras-scrib* tumours (*eyRas^{V12}; scrib^{1}*).

As the fundamental mechanisms of innate immunity are evolutionary conserved from *Drosophila* to humans, this work could provide important insights into the relationship between tumours and the immune system in higher organisms.

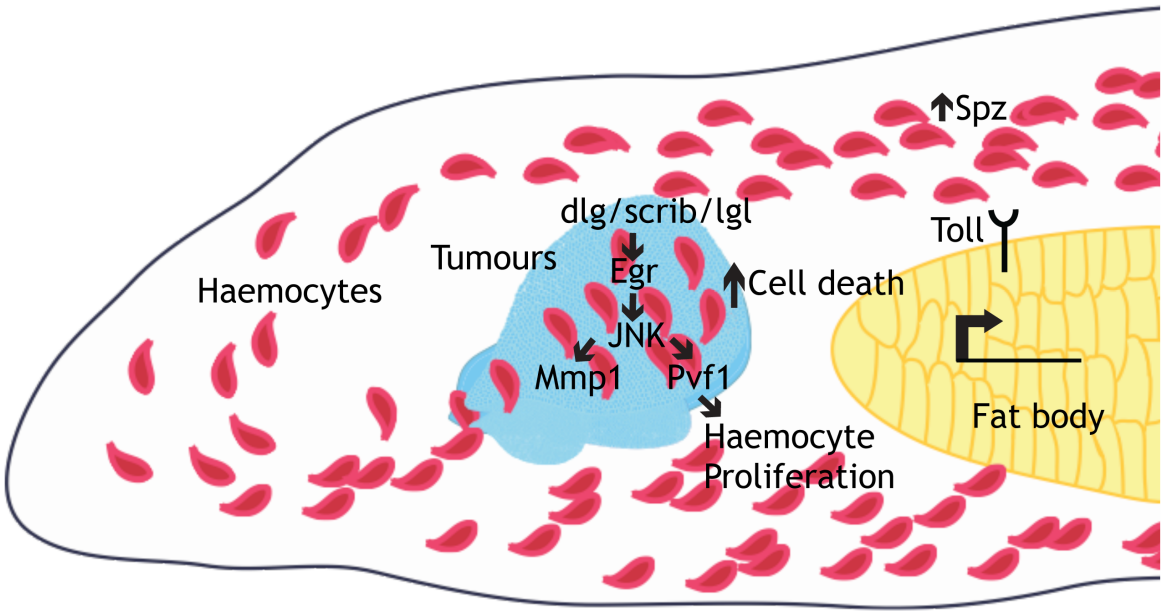

Figure 5.10 Toll and EGR/TNF signalling restricts tumour burden in *dlg* mutant larvae.

In *dlg/scrib/lgl* mutant larvae the imaginal discs have become neoplastic lesions that induce an immune response in the growing larvae. This is characterized by an increased number of haemocytes and activation of Spätzle dependent Toll signalling within the fat body. EGR/TNF signalling is required in the haemocytes for tumour cell death and in the tumour for the production of Pvf1 and Mmp1 and activation of Toll signalling in the fat body.

6 General Discussion

6.1 General Conclusions

The role of inflammation and immunity in tumourigenesis and cancer progression is well established (Balkwill and Mantovani, 2001, Balkwill and Coussens, 2004, Balkwill et al., 2005, Balkwill, 2006, Mantovani et al., 2008, Balkwill, 2009, Balkwill and Joffroy, 2010, Balkwill and Mantovani, 2010, Balkwill and Mantovani, 2012). However, what factors regulate its context dependent effects are unknown. When are inflammation and an activated immune response good and when are they bad? How does a tumour use, what are essentially the host defense systems to its advantage?

In this thesis, I present data from three different projects that highlight the role of host immunity and inflammation in stress and tumourigenesis. In this thesis I describe the effects and requirement of the innate immune pathways in *Drosophila*, the Toll, IMD and JAK/STAT pathways in three different genetic contexts.

I have presented and discussed data focused on uncovering novel adhesion independent roles of *dp120ctn* (see Chapter 3). I find that *dp120ctn* mutant flies are sensitive to heat shock, have a reduced lifespan. Transcriptional analysis of these mutants uncovered a unique transcriptional profile that included upregulation of several IMD/*relish* dependent DIRGs suggesting that *dp120ctn* might be required as a negative regulator of IMD signalling, a major arm of the *Drosophila* immune response. Most interestingly, when I combined loss of *dp120ctn* with loss of the polarity tumour suppressor *scrib* I found that tumour burden was increased. This could suggest in this context that deregulated IMD signalling may contribute to increased tumour burden.

In the *Drosophila* intestine, we have shown that *Apc1* dependent hyperproliferation requires active JAK/STAT signalling as knocking down this pathway completely blocks hyperproliferation (see Chapter 4). We also observe an increased expression of the IL-6 like, *upd3* upon *Apc1* loss. Moreover, the *Drosophila* intestine together with the trachea are two tissues that possess epithelial immunity and as such are able to mount local immune responses in order to maintain epithelial integrity (Lemaitre and Hoffmann, 2007). This is

very interesting when you consider that in the mammalian gut there is evidence that many inflammatory conditions such as Crohn's disease predispose individuals to intestinal and colon cancer. In the *Drosophila* intestine an age-associated dysplasia can be observed as a result of hyperproliferation that has been suggested to be dependent on an age associated increase bacterial load (Buchon et al., 2009a, Buchon et al., 2009b). It would be interesting to address the contribution of systemic as well as local immunity to dysplasia and transformation in the *Drosophila* intestine.

Finally, we demonstrated a non-autonomous tumour suppressive role of Toll and EGR/TNF signalling in *Drosophila* tumour bearing larvae. In previous work in our laboratory had been able to show that haemocytes were recruited from the circulation to the site of tumours and that they expressed EGR/TNF (Cordero et al., 2010). However, in this context due to the genetics we could not directly test the role of EGR/TNF in the haemocytes in this system. In order to do this we utilized whole mutants for the *scribble* group of polarity tumour suppressors in combination with tissue specific Gal4 drivers to overexpress and knockdown Toll and EGR/TNF signalling in the fat body and haemocytes respectively. We observed a significant increase in tumour burden when either Toll or EGR/TNF signalling was inhibited and a decrease in tumour burden when these signalling pathways were enhanced. These results describe tumour suppressive roles for both Toll and EGR/TNF signalling however we also show that EGR/TNF signalling is also required within the tumour for the activation of Toll signalling. Moreover, in our previous paper we have shown a context dependent role of systemic EGR/TNF. In the presence of oncogenic Ras we found that the presence of systemic EGR/TNF was in fact tumour promoting. These context dependent and likely tissue dependent roles of both EGR/TNF and Toll signalling will need to be investigated in order to understand how we can tip the balance in favor of tumour suppression and to uncover novel mediators of these context dependent effects.

The immune system and inflammatory response can be both, a help and a hindrance to tumourigenesis and cancer progression. We know that in *Drosophila* immunity a controlled and measured response to any stimulus is key as a chronic activation of the immune response is detrimental to the host (see Chapter 3) (Brandt et al., 2004, Buchon et al., 2009a, Buchon et al., 2009b). Perhaps the tumour promoting affects that are observed are a result of the acute

immunogenicity of growing tumours which elicit a equally acute but prolonged activation of a host defense system which has evolved to find, eradicate the threat and return to equilibrium. If this is the case maybe we need to focus on how we first limit chronic inflammation that increases the risk of tumourigenesis as well as, how do we shut down a damaging response without causing any further harm to the host.

6.2 Limitations of *Drosophila* as a Cancer Model

Drosophila melanogaster is a well characterized model organism that possesses a powerful genetic tool kit to address fundamental biological questions. *Drosophila* models of cancer are growing in number and the power of genetic screening is routinely being used to identify new modifiers of tumour biology.

However, as with all models there are some limitations of *Drosophila* as a cancer model. Firstly, the lack of any vasculature in this system means that metastasis, as it is currently defined, could not occur by this mechanism in *Drosophila* i.e. the processes of intra and extravasation. However, *Drosophila* possesses a tracheal network which carries oxygen around the fly could be a good model to study metastatic dissemination of tumour cells as it has been recently shown that secondary tumours can grow around tracheal branches and that these tumours have upregulated levels of *branchless*, a fly Fibroblast growth factor ortholog (FGF) which is normally expressed during branch formation (Hirabayashi et al., 2013).

Another caveat that is often used to question the validity of *Drosophila* cancer research is how well *Drosophila* models of cancer can be associated to a specific cancer type. With respect to the *Drosophila* midgut, despite the relatively simple structure many signalling pathways that regulate the mammalian intestine regulate intestinal homeostasis in *Drosophila*. More over results presented in this thesis demonstrate the stark conservation of phenotypes associated with loss of the *Apc* tumour suppressor (Chap 4). In the case of the imaginal discs that are developing precursors of adult structures it is more difficult to ascribe a category. However, the imaginal discs are mitotically active epithelia which when transformed show remarkable histopathological similarities with human neoplasia and studies using the imaginal discs have provided insights many into tumour biology (Gateff, 1978, Woodhouse et al., 1994, Woodhouse et al., 1998, Stefanatos and Vidal, 2011).

The ability to create genetically defined tumours in a tissue specific manner in *Drosophila* allows the interrogation of the systemic effects of tumour burden (Hariharan, 2012, Garelli et al., 2012, Colombani et al., 2012, Rudrapatna et al., 2013) (Chap 5).

In conclusion, despite the great differences between *Drosophila* and Humans I believe that cancer research using *Drosophila* has the potential to provide important insights into tumour biology and the tumour-host interaction.

References

ADAMS, M. D., CELNIKER, S. E., HOLT, R. A., EVANS, C. A., GOCAYNE, J. D., AMANATIDES, P. G., SCHERER, S. E., LI, P. W., HOSKINS, R. A., GALLE, R. F., GEORGE, R. A., LEWIS, S. E., RICHARDS, S., ASHBURNER, M., HENDERSON, S. N., SUTTON, G. G., WORTMAN, J. R., YANDELL, M. D., ZHANG, Q., CHEN, L. X., BRANDON, R. C., ROGERS, Y. H., BLAZEJ, R. G., CHAMPE, M., PFEIFFER, B. D., WAN, K. H., DOYLE, C., BAXTER, E. G., HELT, G., NELSON, C. R., GABOR, G. L., ABRIL, J. F., AGBAYANI, A., AN, H. J., ANDREWS-PFANNKOCH, C., BALDWIN, D., BALLEW, R. M., BASU, A., BAXENDALE, J., BAYRAKTAROGLU, L., BEASLEY, E. M., BEESON, K. Y., BENOS, P. V., BERMAN, B. P., BHANDARI, D., BOLSHAKOV, S., BORKOVA, D., BOTCHAN, M. R., BOUCK, J., BROKSTEIN, P., BROTTIER, P., BURTIS, K. C., BUSAM, D. A., BUTLER, H., CADIEU, E., CENTER, A., CHANDRA, I., CHERRY, J. M., CAWLEY, S., DAHLKE, C., DAVENPORT, L. B., DAVIES, P., DE PABLOS, B., DELCHER, A., DENG, Z., MAYS, A. D., DEW, I., DIETZ, S. M., DODSON, K., DOUP, L. E., DOWNES, M., DUGAN-ROCHA, S., DUNKOV, B. C., DUNN, P., DURBIN, K. J., EVANGELISTA, C. C., FERRAZ, C., FERRIERA, S., FLEISCHMANN, W., FOSLER, C., GABRIELIAN, A. E., GARG, N. S., GELBART, W. M., GLASSER, K., GLODEK, A., GONG, F., GORRELL, J. H., GU, Z., GUAN, P., HARRIS, M., HARRIS, N. L., HARVEY, D., HEIMAN, T. J., HERNANDEZ, J. R., HOUCK, J., HOSTIN, D., HOUSTON, K. A., HOWLAND, T. J., WEI, M. H., IBEGWAM, C., et al. 2000. The genome sequence of Drosophila melanogaster. *Science,* 287**,** 2185-95.

AHMED, Y., HAYASHI, S., LEVINE, A. & WIESCHAUS, E. 1998. Regulation of Armadillo by a Drosophila APC Inhibits Neuronal Apoptosis during Retinal Development. *Cell,* 93**,** 1171-1182.

AHMED, Y., NOURI, A. & WIESCHAUS, E. 2002. Drosophila Apc1 and Apc2 regulate Wingless transduction throughout development. *Development,* 129**,** 1751-1762.

AKIRA, S. 2003. Mammalian Toll-like receptors. *Curr Opin Immunol,* 15**,** 5-11.

ANASTAS, J. N. & MOON, R. T. 2013. WNT signalling pathways as therapeutic targets in cancer. *Nature Reviews Cancer,* 13**,** 11-26.

ANASTASIADIS, P. Z., MOON, S. Y., THORESON, M. A., MARINER, D. J., CRAWFORD, H. C., ZHENG, Y. & REYNOLDS, A. B. 2000. Inhibition of RhoA by p120 catenin. *Nat Cell Biol,* 2**,** 637-44.

ANASTASIADIS, P. Z. & REYNOLDS, A. B. 2000. The p120 catenin family: complex roles in adhesion, signalling and cancer. *J Cell Sci,* 113 (Pt 8)**,** 1319-34.

ANASTASIADIS, P. Z. & REYNOLDS, A. B. 2001. Regulation of Rho GTPases by p120-catenin. *Curr Opin Cell Biol,* 13**,** 604-10.

ARBOUZOVA, N. I. & ZEIDLER, M. P. 2006. JAK/STAT signalling in Drosophila: insights into conserved regulatory and cellular functions. *Development,* 133**,** 2605-2616.

ARWERT, E. N., HOSTE, E. & WATT, F. M. 2012. Epithelial stem cells, wound healing and cancer. *Nature Reviews Cancer,* 12**,** 170-180.

ASHA, H., NAGY, I., KOVACS, G., STETSON, D., ANDO, I. & DEAROLF, C. R. 2003. Analysis of Ras-induced overproliferation in Drosophila hemocytes. *Genetics,* 163**,** 203-215.

ATHINEOS, D. & SANSOM, O. J. 2010. Myc heterozygosity attenuates the phenotypes of APC deficiency in the small intestine. *Oncogene,* 29**,** 2585-90.

BACH, E. A., EKAS, L. A., AYALA-CAMARGO, A., FLAHERTY, M. S., LEE, H., PERRIMON, N. & BAEG, G.-H. 2007. GFP reporters detect the activation of the Drosophila JAK/STAT pathway in vivo. *Gene Expr Patterns,* 7**,** 323-31.

BALKWILL, F. 2006. TNF-alpha in promotion and progression of cancer. *Cancer Metastasis Rev,* 25**,** 409-16.

BALKWILL, F. 2009. Tumour necrosis factor and cancer. *Nature reviews. Cancer,* 9**,** 361-371.

BALKWILL, F., CHARLES, K. A. & MANTOVANI, A. 2005. Smoldering and polarized inflammation in the initiation and promotion of malignant disease. *Cancer Cell,* 7**,** 211-217.

BALKWILL, F. & COUSSENS, L. 2004. Cancer: an inflammatory link. *Nature,* 431**,** 405-406.

BALKWILL, F. & JOFFROY, C. 2010. TNF: a tumor-suppressing factor or a tumor-promoting factor? *Future Oncology,* 6**,** 1833-1836.

BALKWILL, F. & MANTOVANI, A. 2001. Inflammation and cancer: back to Virchow? *Lancet,* 357**,** 539-45.

BALKWILL, F. & MANTOVANI, A. 2010. Cancer and Inflammation: Implications for Pharmacology and Therapeutics. *Clin Pharmacol Ther,* 87**,** 401-406.

BALKWILL, F. R. & MANTOVANI, A. 2012. Cancer-related inflammation: Common themes and therapeutic opportunities. *Semin Cancer Biol,* 22**,** 33-40.

BANGHAM, J., JIGGINS, F. & LEMAITRE, B. 2006. Insect Immunity: The Post-Genomic Era. *Immunity,* 25**,** 1-5.

BARKER, N., RIDGWAY, R., VAN ES, J., VAN DE WETERING, M., BEGTHEL, H., VAN DEN BORN, M., DANENBERG, E., CLARKE, A., SANSOM, O. & CLEVERS, H. 2009. Crypt stem cells as the cells-of-origin of intestinal cancer. *Nature,* 457**,** 608-11.

BATE, M. & MARTINEZ-ARIAS, A. 1993. *The Development of Drosophila melanogaster,* New York, Cold Spring Harbor.

BECKER, T., LOCH, G., BEYER, M., ZINKE, I., ASCHENBRENNER, A. C., CARRERA, P., INHESTER, T., SCHULTZE, J. L. & HOCH, M. 2010. FOXO-dependent regulation of innate immune homeostasis. *Nature,* 463**,** 369-373.

BEEBE, K., LEE, W. & MICCHELLI, C. 2009. JAK/STAT signalling coordinates stem cell proliferation and multilineage differentiation in the Drosophila intestinal stem cell lineage. *Dev Biol,* 338**,** 28-37.

BEISSERT, S., BERGHOLZ, M., WAASE, I., LEPSIEN, G., SCHAUER, A., PFIZENMAIER, K. & KRONKE, M. 1989. Regulation of tumor necrosis factor gene expression in colorectal adenocarcinoma: in vivo analysis by in situ hybridization. *Proc Natl Acad Sci U S A,* 86**,** 5064-8.

BEUTLER, B., HOEBE, K., DU, X. & ULEVITCH, R. J. 2003. How we detect microbes and respond to them: the Toll-like receptors and their transducers. *Journal of Leukocyte Biology,* 74**,** 479-485.

BHANOT, P., BRINK, M., SAMOS, C. H., HSIEH, J.-C., WANG, Y., MACKE, J. P., ANDREW, D., NATHANS, J. & NUSSE, R. 1996. A new member of the frizzled family from Drosophila functions as a Wingless receptor. *Nature,* 382**,** 225-230.

BILDER, D. 2004. Epithelial polarity and proliferation control: links from the Drosophila neoplastic tumor suppressors. *Genes Dev,* 18**,** 1909-25.

BILDER, D., LI, M. & PERRIMON, N. 2000. Cooperative regulation of cell polarity and growth by Drosophila tumor suppressors. *Science,* 289**,** 113-6.

BILDER, D. & PERRIMON, N. 2000. Localization of apical epithelial determinants by the basolateral PDZ protein Scribble. *Nature,* 403**,** 676-80.

BISCHOFF, V., VIGNAL, C., DUVIC, B., BONECA, I. G., HOFFMANN, J. A. & ROYET, J. 2006. Downregulation of the Drosophila immune response by peptidoglycan-recognition proteins SC1 and SC2. *PLoS Pathog,* 2**,** e14.

BITEAU, B. & JASPER, H. 2011. EGF signalling regulates the proliferation of intestinal stem cells in Drosophila. *Development,* 138**,** 1045-55.

BOMAN, H. G., NILSSON, I. & RASMUSON, B. 1972. Inducible Antibacterial Defence System in Drosophila. *Nature,* 237**,** 232-235.

BOUTROS, M., AGAISSE, H. & PERRIMON, N. 2002. Sequential Activation of Signalling Pathways during Innate Immune Responses in Drosophila. *Developmental Cell,* 3**,** 711-722.

BOZCUK, H., USLU, G., SAMUR, M., YILDIZ, M., OZBEN, T., OZDOGAN, M., ARTAC, M., ALTUNBAS, H., AKAN, I. & SAVAS, B. 2004. Tumour necrosis factor-alpha, interleukin-6, and fasting serum insulin correlate with clinical outcome in metastatic breast cancer patients treated with chemotherapy. *Cytokine,* 27**,** 58-65.

BRAND, A. H. & PERRIMON, N. 1993. Targeted gene expression as a means of altering cell fates and generating dominant phenotypes. *Development,* 118**,** 401-15.

BRANDT, S. M., DIONNE, M. S., KHUSH, R. S., PHAM, L. N., VIGDAL, T. J. & SCHNEIDER, D. S. 2004. Secreted Bacterial Effectors and Host-Produced Eiger/TNF Drive Death in a Salmonella Infected Fruit Fly. *PLoS Biol,* 2**,** e418.

BRIDGES, C. B. & BREHME, K. S. 1944. The mutants of Drosophila melanogaster. 552**,** vii + 257pp.

BRUMBY, A. M. & RICHARDSON, H. E. 2003. scribble mutants cooperate with oncogenic Ras or Notch to cause neoplastic overgrowth in Drosophila. *EMBO J,* 22**,** 5769-79.

BRUMBY, A. M. & RICHARDSON, H. E. 2005. Using Drosophila melanogaster to map human cancer pathways. *Nat Rev Cancer,* 5**,** 626-39.

BUCHON, N., BRODERICK, N. A., CHAKRABARTI, S. & LEMAITRE, B. 2009a. Invasive and indigenous microbiota impact intestinal stem cell activity through multiple pathways in Drosophila. *Genes Dev,* 23**,** 2333-44.

BUCHON, N., BRODERICK, N. A., KURAISHI, T. & LEMAITRE, B. 2010. Drosophila EGFR pathway coordinates stem cell proliferation and gut remodeling following infection. *BMC Biol,* 8**,** 152.

BUCHON, N., BRODERICK, N. A., POIDEVIN, M., PRADERVAND, S. & LEMAITRE, B. 2009b. Drosophila intestinal response to bacterial infection: activation of host defense and stem cell proliferation. *Cell Host Microbe,* 5**,** 200-11.

BUCHON, N., OSMAN, D., DAVID, F. P. A., YU FANG, H., BOQUETE, J.-P., DEPLANCKE, B. & LEMAITRE, B. 2013. Morphological and molecular characterization of adult midgut compartmentalization in Drosophila. *CellReports,* 3**,** 1725-38.

BURNET, F. M. 1971. Immunological surveillance in neoplasia. *Transplant Rev,* 7**,** 3-25.

CADIGAN, K. M. & NUSSE, R. 1997. Wnt signalling: a common theme in animal development. *Genes & Development,* 11**,** 3286-3305.

CADIGAN, K. M. & PEIFER, M. 2009. Wnt Signalling from Development to Disease: Insights from Model Systems. *Cold Spring Harbor Perspectives in Biology,* 1.

CAMPOS-ORTEGA, J. A. A. V. H. 1985. . The embryonic development of Drosophila melanogaster. .

CARNAHAN, R. H., ROKAS, A., GAUCHER, E. A. & REYNOLDS, A. B. 2010. The molecular evolution of the p120-catenin subfamily and its functional associations. *PLoS One,* 5**,** e15747.

CARSWELL, E. A., OLD, L. J., KASSEL, R. L., GREEN, S., FIORE, N. & WILLIAMSON, B. 1975. An endotoxin-induced serum factor that causes necrosis of tumors. *Proc Natl Acad Sci U S A,* 72**,** 3666-70.

CASALI, A. & BATLLE, E. 2009. Intestinal Stem Cells in Mammals and Drosophila. *Cell Stem Cell,* 4**,** 124-127.

CHAN, H. Y. & BONINI, N. M. 2000. Drosophila models of human neurodegenerative disease. *Cell Death Differ,* 7**,** 1075-80.

CHARROUX, B. & ROYET, J. 2010. Drosophila immune response: From systemic antimicrobial peptide production in fat body cells to local defense in the intestinal tract. *Fly (Austin),* 4**,** 40-7.

CHEN, C. L., SCHROEDER, M. C., KANGO-SINGH, M., TAO, C. & HALDER, G. 2012. Tumor suppression by cell competition through regulation of the Hippo pathway. *Proc Natl Acad Sci U S A,* 109**,** 484-9.

CLEVERS, H. 2006. Wnt/β-Catenin Signalling in Development and Disease. *Cell,* 127**,** 469-480.

COGNIGNI, P., BAILEY, A. P. & MIGUEL-ALIAGA, I. 2011. Enteric neurons and systemic signals couple nutritional and reproductive status with intestinal homeostasis. *Cell Metabolism,* 13**,** 92-104.

COLOMBANI, J., ANDERSEN, D. S. & LÉOPOLD, P. 2012. Secreted peptide Dilp8 coordinates Drosophila tissue growth with developmental timing. *Science,* 336**,** 582-5.

CORDERO, J. B., MACAGNO, J., STEFANATOS, R. K. A., STRATHDEE, K., CAGAN, R. & VIDAL, M. 2010. Oncogenic Ras diverts a host TNF tumor suppressor activity into tumor promoter. *Developmental cell,* 18**,** 999-1011.

CORDERO, J. B. & SANSOM, O. J. 2012. Wnt signalling and its role in stem cell-driven intestinal regeneration and hyperplasia. *Acta Physiol (Oxf),* 204**,** 137-43.

CORDERO, J. B., STEFANATOS, R. K. A., MYANT, K., VIDAL, M. & SANSOM, O. J. 2012a. Non-autonomous crosstalk between the Jak/Stat and Egfr pathways mediates Apc1-driven intestinal stem cell hyperplasia in the Drosophila adult midgut. *Development,* 139**,** 4524-35.

CORDERO, J. B., STEFANATOS, R. K. A., SCOPELLITI, A., VIDAL, M. & SANSOM, O. J. 2012b. Inducible progenitor-derived Wingless regulates adult midgut regeneration in Drosophila. *EMBO J,* 31**,** 3901-17.

CORDERO, J. B., VIDAL, M. & SANSOM, O. 2009. APC as a master regulator of intestinal homeostasis and transformation: from flies to vertebrates. *Cell Cycle,* 8**,** 2926-31.

COUSSENS, L. M. & WERB, Z. 2002. Inflammation and cancer. *Nature,* 420**,** 860-7.

COX, J. & MANN, M. 2008. MaxQuant enables high peptide identification rates, individualized p.p.b.-range mass accuracies and proteome-wide protein quantification. *Nat Biotechnol,* 26**,** 1367-72.

DAI, S.-D., WANG, Y., ZHANG, J.-Y., ZHANG, D., ZHANG, P.-X., JIANG, G.-Y., HAN, Y., ZHANG, S., CUI, Q.-Z. & WANG, E.-H. 2011. Upregulation of δ-catenin is associated with poor prognosis and enhances transcriptional activity through Kaiso in non-small-cell lung cancer. *Cancer Sci,* 102**,** 95-103.

DAI, S. D., WANG, Y., JIANG, G. Y., ZHANG, P. X., DONG, X. J., WEI, Q., XU, H. T., LI, Q. C., ZHAO, C. & WANG, E. H. 2010. Kaiso is expressed in lung cancer: its expression and localization is affected by p120ctn. *Lung Cancer,* 67**,** 205-15.

DANG, D. T. & PERRIMON, N. 1992. Use of a yeast site-specific recombinase to generate embryonic mosaics in Drosophila. *Dev Genet,* 13**,** 367-75.

DANIEL, J. M. 2007. Dancing in and out of the nucleus: p120(ctn) and the transcription factor Kaiso. *Biochim Biophys Acta,* 1773**,** 59-68.

DANIEL, J. M. & REYNOLDS, A. B. 1995. The tyrosine kinase substrate p120cas binds directly to E-cadherin but not to the adenomatous polyposis coli protein or alpha-catenin. *Molecular and Cellular Biology,* 15**,** 4819-24.

DANIEL, J. M. & REYNOLDS, A. B. 1999. The catenin p120(ctn) interacts with Kaiso, a novel BTB/POZ domain zinc finger transcription factor. *Molecular and Cellular Biology,* 19**,** 3614-23.

DAVIS, M. A. & REYNOLDS, A. B. 2006. Blocked acinar development, E-cadherin reduction, and intraepithelial neoplasia upon ablation of p120-catenin in the mouse salivary gland. *Dev Cell,* 10**,** 21-31.

DE GREGORIO, E., SPELLMAN, P. T., RUBIN, G. M. & LEMAITRE, B. 2001. Genome-wide analysis of the Drosophila immune response by using oligonucleotide microarrays. *Proc Natl Acad Sci U S A,* 98**,** 12590-5.

DE GREGORIO, E., SPELLMAN, P. T., TZOU, P., RUBIN, G. M. & LEMAITRE, B. 2002. The Toll and Imd pathways are the major regulators of the immune response in Drosophila. *EMBO J,* 21**,** 2568-79.

DEL VALLE-PÉREZ, B., CASAGOLDA, D., LUGILDE, E., VALLS, G., CODINA, M., DAVE, N., DE HERREROS, A. G. & DUÑACH, M. 2011. Wnt controls the transcriptional activity of Kaiso through CK1{varepsilon}-dependent phosphorylation of p120-catenin. *J Cell Sci,* 124**,** 2298-309.

DOW, L. E., BRUMBY, A. M., MURATORE, R., COOMBE, M. L., SEDELIES, K. A., TRAPANI, J. A., RUSSELL, S. M., RICHARDSON, H. E. & HUMBERT, P. O. 2003. hScrib is a functional homologue of the Drosophila tumour suppressor Scribble. *Oncogene,* 22**,** 9225-30.

ELIA, L. P., YAMAMOTO, M., ZANG, K. & REICHARDT, L. F. 2006. p120 catenin regulates dendritic spine and synapse development through Rho-family GTPases and cadherins. *Neuron,* 51**,** 43-56.

FANG, X., JI, H., KIM, S.-W., PARK, J.-I., VAUGHT, T. G., ANASTASIADIS, P. Z., CIESIOLKA, M. & MCCREA, P. D. 2004. Vertebrate development requires ARVCF and p120 catenins and their interplay with RhoA and Rac. *The Journal of Cell Biology,* 165**,** 87-98.

FEI, Y., CHENG, Z., LIU, S., LIU, X., GE, Z., WANG, F., ZONG, G. & WANG, W. 2009. Expression and clinical significance of p120 catenin mRNA and protein in pancreatic carcinoma. *Bosn J Basic Med Sci,* 9**,** 191-7.

FERRAJOLI, A. 2002. The clinical significance of tumor necrosis factor-a plasma level in patients having chronic lymphocytic leukemia. *Blood,* 100**,** 1215-1219.

FROLDI, F., ZIOSI, M., GAROIA, F., PESSION, A., GRZESCHIK, N. A., BELLOSTA, P., STRAND, D., RICHARDSON, H. E., PESSION, A. & GRIFONI, D. 2010. The lethal giant larvae tumour suppressor mutation requires dMyc oncoprotein to promote clonal malignancy. *BMC Biol,* 8**,** 33.

FUJITA, Y., KRAUSE, G., SCHEFFNER, M., ZECHNER, D., LEDDY, H. E. M., BEHRENS, J., SOMMER, T. & BIRCHMEIER, W. 2002. Hakai, a c-Cbl-like protein, ubiquitinates and induces endocytosis of the E-cadherin complex. *Nat Cell Biol,* 4**,** 222-31.

GARELLI, A., GONTIJO, A. M., MIGUELA, V., CAPARROS, E. & DOMINGUEZ, M. 2012. Imaginal Discs Secrete Insulin-Like Peptide 8 to Mediate Plasticity of Growth and Maturation. *Science,* 336**,** 579-582.

GATEFF, E. 1978. Malignant neoplasms of genetic origin in Drosophila melanogaster. *Science,* 200**,** 1448-59.

GONDA, T. A., TU, S. P. & WANG, T. C. 2009. Chronic inflammation, the tumor microenvironment and carcinogenesis. *Cell Cycle,* 8**,** 2005-2013.

GONZALEZ, C. 2013. Drosophila melanogaster: a model and a tool to investigate malignancy and identify new therapeutics. *Nat Rev Cancer,* 13**,** 172-83.

GOTO, A., KUMAGAI, T., KUMAGAI, C., HIROSE, J., NARITA, H., MORI, H., KADOWAKI, T., BECK, K. & KITAGAWA, Y. 2001. A Drosophila haemocyte-specific protein, hemolectin, similar to human von Willebrand factor. *Biochemical Journal,* 359**,** 99-108.

GOTTAR, M., GOBERT, V., MICHEL, T., BELVIN, M., DUYK, G., HOFFMANN, J. A., FERRANDON, D. & ROYET, J. 2002. The Drosophila immune response against Gram-negative bacteria is mediated by a peptidoglycan recognition protein. *Nature,* 416**,** 640-644.

GREENWALD, I. 1998. LIN-12/Notch signalling: lessons from worms and flies. *Genes & Development,* 12**,** 1751-1762.

GU, D., SATER, A. K., JI, H., CHO, K., CLARK, M., STRATTON, S. A., BARTON, M. C., LU, Q. & MCCREA, P. D. 2009. Xenopus delta-catenin is essential in early embryogenesis and is functionally linked to cadherins and small GTPases. *J Cell Sci,* 122**,** 4049-61.

HANAHAN, D. & WEINBERG, R. A. 2011. Hallmarks of cancer: the next generation. *Cell,* 144**,** 646-74.

HARIHARAN, I. K. 2012. How growth abnormalities delay "puberty" in Drosophila. *Science Signalling,* 5**,** pe27.

HARSHBARGER, J. C. & TAYLOR, R. L. 1968. Neoplasms of Insects. *Annual Review of Entomology,* 13**,** 159-190.

HEDENGREN, M., ASLING, B., DUSHAY, M. S., ANDO, I., EKENGREN, S., WIHLBORG, M. & HULTMARK, D. 1999. Relish, a central factor in the control of humoral but not cellular immunity in Drosophila. *Mol Cell,* 4**,** 827-37.

HENRIKSSON, M. & LUSCHER, B. 1996. Proteins of the Myc network: essential regulators of cell growth and differentiation. *Adv Cancer Res,* 68**,** 109-82.

HETRU, C. & HOFFMANN, J. 2009. NF-kappaB in the immune response of Drosophila. *Cold Spring Harbor perspectives in biology,* 1.

HIRABAYASHI, S., BARANSKI, T. J. & CAGAN, R. L. 2013. Transformed Drosophila Cells Evade Diet-Mediated Insulin Resistance through Wingless Signalling. *Cell,* 154**,** 664-675.

HOFFMANN, J. A. 1995. Innate immunity of insects. *Curr Opin Immunol,* 7**,** 4-10.

HOLSTEGE, F. & CLEVERS, H. 2006. Transcription factor target practice. *Cell,* 124**,** 21-3.

HOTAMISLIGIL, G. S. & ERBAY, E. 2008. Nutrient sensing and inflammation in metabolic diseases. *Nat Rev Immunol,* 8**,** 923-934.

HUANG, D. W., SHERMAN, B. T. & LEMPICKI, R. A. 2008. Systematic and integrative analysis of large gene lists using DAVID bioinformatics resources. *Nat. Protocols,* 4**,** 44-57.

HUMBERT, P. O., GRZESCHIK, N. A., BRUMBY, A. M., GALEA, R., ELSUM, I. & RICHARDSON, H. E. 2008. Control of tumourigenesis by the Scribble/Dlg/Lgl polarity module. *Oncogene,* 27**,** 6888-907.

IGAKI, T., KANDA, H., YAMAMOTO-GOTO, Y., KANUKA, H., KURANAGA, E., AIGAKI, T. & MIURA, M. 2002. Eiger, a TNF superfamily ligand that triggers the Drosophila JNK pathway. *EMBO J,* 21**,** 3009-18.

IGAKI, T., PASTOR-PAREJA, J. C., AONUMA, H., MIURA, M. & XU, T. 2009. Intrinsic tumor suppression and epithelial maintenance by endocytic activation of Eiger/TNF signalling in Drosophila. *Dev Cell,* 16**,** 458-65.

IRETON, R. C., DAVIS, M. A., VAN HENGEL, J., MARINER, D. J., BARNES, K., THORESON, M. A., ANASTASIADIS, P. Z., MATRISIAN, L., BUNDY, L. M., SEALY, L., GILBERT, B., VAN ROY, F. & REYNOLDS, A. B. 2002. A novel role for p120 catenin in E-cadherin function. *The Journal of Cell Biology,* 159**,** 465-76.

ISHIYAMA, N., LEE, S.-H., LIU, S., LI, G.-Y., SMITH, M. J., REICHARDT, L. F. & IKURA, M. 2010. Dynamic and static interactions between p120 catenin and E-cadherin regulate the stability of cell-cell adhesion. *Cell,* 141**,** 117-28.

JIANG, G., WANG, Y., DAI, S., LIU, Y., STOECKER, M., WANG, E. & WANG, E. 2012. P120-Catenin Isoforms 1 and 3 Regulate Proliferation and Cell Cycle of Lung Cancer Cells via ß-Catenin and Kaiso Respectively. *PLoS ONE,* 7**,** e30303.

JIANG, H. & EDGAR, B. A. 2009. EGFR signalling regulates the proliferation of Drosophila adult midgut progenitors. *Development,* 136**,** 483-93.

JIANG, H. & EDGAR, B. A. 2011. Intestinal stem cells in the adult Drosophila midgut. *Exp Cell Res,* 317**,** 2780-8.

JIANG, H., GRENLEY, M. O., BRAVO, M.-J., BLUMHAGEN, R. Z. & EDGAR, B. A. 2011. EGFR/Ras/MAPK Signalling Mediates Adult Midgut Epithelial Homeostasis and Regeneration in Drosophila. *Cell Stem Cell,* 8**,** 84-95.

JIANG, H., PATEL, P. H., KOHLMAIER, A., GRENLEY, M. O., MCEWEN, D. G. & EDGAR, B. A. 2009. Cytokine/Jak/Stat signalling mediates regeneration and homeostasis in the Drosophila midgut. *Cell,* 137**,** 1343-55.

JOHNSTON, L. A., PROBER, D. A., EDGAR, B. A., EISENMAN, R. N. & GALLANT, P. 1999. Drosophila myc regulates cellular growth during development. *Cell,* 98**,** 779-90.

JONES, J., WANG, H., ZHOU, J., HARDY, S., TURNER, T., AUSTIN, D., HE, Q., WELLS, A., GRIZZLE, W. E. & YATES, C. 2012. Nuclear kaiso indicates aggressive prostate cancers and promotes migration and invasiveness of prostate cancer cells. *The American journal of pathology,* 181**,** 1836-46.

KARAYIANNAKIS, A. J., SYRIGOS, K. N., POLYCHRONIDIS, A., PITIAKOUDIS, M., BOUNOVAS, A. & SIMOPOULOS, K. 2001. Serum levels of tumor necrosis factor-alpha and nutritional status in pancreatic cancer patients. *Anticancer Res,* 21**,** 1355-8.

KARIN, M. & GRETEN, F. R. 2005. NF-kappaB: linking inflammation and immunity to cancer development and progression. *Nat Rev Immunol,* 5**,** 749-59.

KARPAC, J., YOUNGER, A. & JASPER, H. 2011. Dynamic coordination of innate immune signalling and insulin signalling regulates systemic responses to localized DNA damage. *Developmental Cell,* 20**,** 841-54.

KARPOWICZ, P., PEREZ, J. & PERRIMON, N. 2010. The Hippo tumor suppressor pathway regulates intestinal stem cell regeneration. *Development,* 137**,** 4135-45.

KIM, S. & KARIN, M. 2011. Role of TLR2-dependent inflammation in metastatic progression. *Year in Immunology,* 1217**,** 191-206.

KIM, T. & KIM, Y.-J. 2005. Overview of innate immunity in Drosophila. *J Biochem Mol Biol,* 38**,** 121-7.

KINZLER, K., NILBERT, M., SU, L., VOGELSTEIN, B., BRYAN, T., LEVY, D., SMITH, K., PREISINGER, A., HEDGE, P., MCKECHNIE, D. & AL., ET 1991. Identification of FAP locus genes from chromosome 5q21. *Science,* 253**,** 661-5.

KINZLER, K. W. & VOGELSTEIN, B. 1996. Lessons from Hereditary Colorectal Cancer. *Cell,* 87**,** 159-170.

KLEINO, A., MYLLYMÄKI, H., KALLIO, J., VANHA-AHO, L.-M., OKSANEN, K., ULVILA, J., HULTMARK, D., VALANNE, S. & RÄMET, M. 2008. Pirk is a negative regulator of the Drosophila Imd pathway. *J Immunol,* 180**,** 5413-22.

KORINEK, V., BARKER, N., MORIN, P., VAN WICHEN, D., DE WEGER, R., KINZLER, K., VOGELSTEIN, B. & CLEVERS, H. 1997. Constitutive transcriptional activation by a beta-catenin-Tcf complex in APC-/- colon carcinoma. *Science,* 275**,** 1784-7.

KRIEG, A. M. 2007. Development of TLR9 agonists for cancer therapy. *J Clin Invest,* 117**,** 1184-94.

KURLEY, S. J., BIERIE, B., CARNAHAN, R. H., LOBDELL, N. A., DAVIS, M. A., HOFMANN, I., MOSES, H. L., MULLER, W. J. & REYNOLDS, A. B. 2012. p120-catenin is essential for terminal end bud function and mammary morphogenesis. *Development,* 139**,** 1754-64.

KURUCZ, É., MÁRKUS, R., ZSÁMBOKI, J., FOLKL-MEDZIHRADSZKY, K., DARULA, Z., VILMOS, P., UDVARDY, A., KRAUSZ, I., LUKACSOVICH, T., GATEFF, E., ZETTERVALL, C.-J., HULTMARK, D. & ANDÓ, I. 2007. Nimrod, a Putative Phagocytosis Receptor with EGF Repeats in Drosophila Plasmatocytes. *Current Biology,* 17**,** 649-654.

KURUCZ, E., ZETTERVALL, C. J., SINKA, R., VILMOS, P., PIVARCSI, A., EKENGREN, S., HEGEDUS, Z., ANDO, I. & HULTMARK, D. 2003. Hemese, a hemocyte-specific transmembrane protein, affects the cellular immune response in Drosophila. *Proceedings of the National Academy of Sciences of the United States of America,* 100**,** 2622-2627.

KUSABA, T., NAKAYAMA, T., YAMAZUMI, K., YAKATA, Y., YOSHIZAKI, A., NAGAYASU, T. & SEKINE, I. 2005. Expression of p-STAT3 in human colorectal adenocarcinoma and adenoma; correlation with clinicopathological factors. *J Clin Pathol,* 58**,** 833-838.

LARSEN, P. H., HOLM, T. H. & OWENS, T. 2007. Toll-like receptors in brain development and homeostasis. *Sci. STKE,* 2007**,** pe47.

LARSON, D. E., LIBERMAN, Z. & CAGAN, R. L. 2008. Cellular behavior in the developing Drosophila pupal retina. *Mech Dev,* 125**,** 223-32.

LEE, M. S. & KIM, Y. J. 2007. Signalling pathways downstream of pattern-recognition receptors and their cross talk. *Annu. Rev. Biochem.,* 76**,** 447-480.

LEE, T. & LUO, L. 2001. Mosaic analysis with a repressible cell marker (MARCM) for Drosophila neural development. *Trends Neurosci,* 24**,** 251-4.

LEE, W.-C., BEEBE, K., SUDMEIER, L. & MICCHELLI, C. A. 2009. Adenomatous polyposis coli regulates Drosophila intestinal stem cell proliferation. *Development,* 136**,** 2255-64.

LEMAITRE, B. 2004. The road to Toll. *Nature reviews. Immunology,* 4**,** 521-527.

LEMAITRE, B. & HOFFMANN, J. 2007. The host defense of Drosophila melanogaster. *Annual review of immunology,* 25**,** 697-743.

LEMAITRE, B., KROMER-METZGER, E., MICHAUT, L., NICOLAS, E., MEISTER, M., GEORGEL, P., REICHHART, J. M. & HOFFMANN, J. A. 1995. A recessive mutation, immune deficiency (imd), defines two distinct control pathways in the Drosophila host defense. *Proceedings of the National Academy of Sciences,* 92**,** 9465-9469.

LEMAITRE, B., NICOLAS, E., MICHAUT, L., REICHHART, J. M. & HOFFMANN, J. A. 1996. The dorsoventral regulatory gene cassette spatzle/Toll/cactus controls the potent antifungal response in Drosophila adults. *Cell,* 86**,** 973-983.

LEMAITRE, B., REICHHART, J.-M. & HOFFMANN, J. A. 1997. Drosophila host defense: Differential induction of antimicrobial peptide genes after infection by various classes of microorganisms. *Proceedings of the National Academy of Sciences,* 94**,** 14614-14619.

LEWIS I. HELD, J. 2002. *Imaginal Discs: The Genetic and Cellular Logic of Pattern Formation*, Cambridge University Press.

LIN, G., XU, N. & XI, R. 2008. Paracrine Wingless signalling controls self-renewal of Drosophila intestinal stem cells. *Nature,* 455**,** 1119-23.

LOCKSLEY, R. M., KILLEEN, N. & LENARDO, M. J. 2001. The TNF and TNF receptor superfamilies: integrating mammalian biology. *Cell,* 104**,** 487-501.

LOHIA, M., QIN, Y. & MACARA, I. G. 2012. The Scribble Polarity Protein Stabilizes E-Cadherin/p120-Catenin Binding and Blocks Retrieval of E-Cadherin to the Golgi. *PLoS ONE,* 7**,** e51130.

LOLO, F.-N., CASAS-TINTÓ, S. & MORENO, E. 2012. Cell Competition Time Line: Winners Kill Losers, which Are Extruded and Engulfed by Hemocytes. *CellReports,* 2**,** 526-39.

LU, Q. 2010. δ-Catenin dysregulation in cancer: interactions with E-cadherin and beyond. *J Pathol,* 222**,** 119-23.

MA, J. & PTASHNE, M. 1987. The carboxy-terminal 30 amino acids of GAL4 are recognized by GAL80. *Cell,* 50**,** 137-42.

MAGIE, C. R., PINTO-SANTINI, D. & PARKHURST, S. M. 2002. Rho1 interacts with p120ctn and alpha-catenin, and regulates cadherin-based adherens junction components in Drosophila. *Development,* 129**,** 3771-82.

MANTOVANI, A., ALLAVENA, P., SICA, A. & BALKWILL, F. 2008. Cancer-related inflammation. *Nature,* 454**,** 436-444.

MARCIANO, D. K., BRAKEMAN, P. R., LEE, C.-Z., SPIVAK, N., EASTBURN, D. J., BRYANT, D. M., BEAUDOIN, G. M., HOFMANN, I., MOSTOV, K. E. & REICHARDT, L. F. 2011. p120 catenin is required for normal renal tubulogenesis and glomerulogenesis. *Development,* 138**,** 2099-109.

MARUYAMA, K., SELMANI, Z., ISHII, H. & YAMAGUCHI, K. 2011. Innate immunity and cancer therapy. *International Immunopharmacology,* 11**,** 350-357.

MATSUMOTO, K., TOH-E, A. & OSHIMA, Y. 1978. Genetic control of galactokinase synthesis in Saccharomyces cerevisiae: evidence for constitutive expression of the positive regulatory gene gal4. *J Bacteriol,* 134**,** 446-57.

MAYERLE, J., FRIESS, H., BÜCHLER, M. W., SCHNEKENBURGER, J., WEISS, F. U., ZIMMER, K.-P., DOMSCHKE, W. & LERCH, M. M. 2003. Up-regulation,

nuclear import, and tumor growth stimulation of the adhesion protein p120 in pancreatic cancer. *Gastroenterology,* 124**,** 949-60.

MCGUIRE, S. E., LE, P. T., OSBORN, A. J., MATSUMOTO, K. & DAVIS, R. L. 2003. Spatiotemporal rescue of memory dysfunction in Drosophila. *Science,* 302**,** 1765-8.

MECHLER, B. M., MCGINNIS, W. & GEHRING, W. J. 1985. Molecular cloning of lethal(2)giant larvae, a recessive oncogene of Drosophila melanogaster. *EMBO J,* 4**,** 1551-7.

MEISTER, M. & LAGUEUX, M. 2003. Drosophila blood cells. *Cellular Microbiology,* 5**,** 573-580.

MENDOZA-TOPAZ, C., URRA, F., BARRÍA, R., ALBORNOZ, V., UGALDE, D., THOMAS, U., GUNDELFINGER, E. D., DELGADO, R., KUKULJAN, M., SANXARIDIS, P. D., TSUNODA, S., CERIANI, M. F., BUDNIK, V. & SIERRALTA, J. 2008. DLGS97/SAP97 Is Developmentally Upregulated and Is Required for Complex Adult Behaviors and Synapse Morphology and Function. *The Journal of Neuroscience,* 28**,** 304-314.

MENENDEZ, J., PEREZ-GARIJO, A., CALLEJA, M. & MORATA, G. 2010. A tumor-suppressing mechanism in Drosophila involving cell competition and the Hippo pathway. *Proceedings of the National Academy of Sciences of the United States of America,* 107**,** 14651-14656.

MIAO, Y., LIU, N., ZHANG, Y., LIU, Y., YU, J.-H., DAI, S.-D., XU, H.-T. & WANG, E.-H. 2010. p120ctn isoform 1 expression significantly correlates with abnormal expression of E-cadherin and poor survival of lung cancer patients. *Med Oncol,* 27**,** 880-6.

MICCHELLI, C. A. & PERRIMON, N. 2006. Evidence that stem cells reside in the adult Drosophila midgut epithelium. *Nature,* 439**,** 475-9.

MICHALSKI, A., DAMOC, E., LANGE, O., DENISOV, E., NOLTING, D., MÜLLER, M., VINER, R., SCHWARTZ, J., REMES, P., BELFORD, M., DUNYACH, J.-J., COX, J., HORNING, S., MANN, M. & MAKAROV, A. 2012. Ultra High Resolution Linear Ion Trap Orbitrap Mass Spectrometer (Orbitrap Elite) Facilitates Top Down LC MS/MS and Versatile Peptide Fragmentation Modes. *Molecular & Cellular Proteomics,* 11.

MICHEL, T., REICHHART, J. M., HOFFMANN, J. A. & ROYET, J. 2001. Drosophila Toll is activated by Gram-positive bacteria through a circulating peptidoglycan recognition protein. *Nature,* 414**,** 756-9.

MICHELSEN, K. S. & ARDITI, M. 2007. Toll-like receptors and innate immunity in gut homeostasis and pathology. *Curr. Opin. Hematol.,* 14**,** 48-54.

MOORE, R. J., OWENS, D. M., STAMP, G., ARNOTT, C., BURKE, F., EAST, N., HOLDSWORTH, H., TURNER, L., ROLLINS, B., PASPARAKIS, M., KOLLIAS, G. & BALKWILL, F. 1999. Mice deficient in tumor necrosis factor-alpha are resistant to skin carcinogenesis. *Nat Med,* 5**,** 828-31.

MORAN, A. E., HUNT, D. H., JAVID, S. H., REDSTON, M., CAROTHERS, A. M. & BERTAGNOLLI, M. M. 2004. Apc Deficiency Is Associated with Increased Egfr Activity in the Intestinal Enterocytes and Adenomas of C57BL/6J-Min/+ Mice. *Journal of Biological Chemistry,* 279**,** 43261-43272.

MORENO, E., YAN, M. & BASLER, K. 2002. Evolution of TNF signalling mechanisms: JNK-dependent apoptosis triggered by Eiger, the Drosophila homolog of the TNF superfamily. *Curr Biol,* 12**,** 1263-8.

MORTAZAVI, F., AN, J., DUBINETT, S. & RETTIG, M. 2010. p120-catenin is transcriptionally downregulated by FOXC2 in non-small cell lung cancer cells. *Mol Cancer Res,* 8**,** 762-74.

MUNIER, A. I., DOUCET, D., PERRODOU, E., ZACHARY, D., MEISTER, M., HOFFMANN, J. A., JANEWAY, C. A. & LAGUEUX, M. 2002. PVF2, a PDGF/VEGF-like growth factor, induces hemocyte proliferation in Drosophila larvae. *Embo Reports,* 3**,** 1195-1200.

MUSTEANU, M., BLAAS, L., MAIR, M., SCHLEDERER, M., BILBAN, M., TAUBER, S., ESTERBAUER, H., MUELLER, M., CASANOVA, E., KENNER, L., POLI, V. & EFERL, R. 2010. Stat3 Is a Negative Regulator of Intestinal Tumor Progression in ApcMin Mice. *Gastroenterology,* 138**,** 1003-1011.e5.

MYSTER, S. H., CAVALLO, R., ANDERSON, C. T., FOX, D. T. & PEIFER, M. 2003. Drosophila p120catenin plays a supporting role in cell adhesion but is not an essential adherens junction component. *The Journal of Cell Biology,* 160**,** 433-49.

NAYLOR, M. S., MALIK, S. T. A., STAMP, G. W. H., JOBLING, T. & BALKWILL, F. R. 1990. In situ detection of tumour necrosis factor in human ovarian cancer specimens. *Eur. J. Cancer,* 26**,** 1027-1030.

NUSSLEIN-VOLHARD, C. & WIESCHAUS, E. 1980. Mutations affecting segment number and polarity in Drosophila. *Nature,* 287**,** 795-801.

O'KEEFE, L. V., SMIBERT, P., COLELLA, A., CHATAWAY, T. K., SAINT, R. & RICHARDS, R. I. 2007. Know thy fly. *Trends Genet,* 23**,** 238-42.

OAS, R. G., XIAO, K., SUMMERS, S., WITTICH, K. B., CHIASSON, C. M., MARTIN, W. D., GROSSNIKLAUS, H. E., VINCENT, P. A., REYNOLDS, A. B. & KOWALCZYK, A. P. 2010. p120-Catenin is required for mouse vascular development. *Circ Res,* 106**,** 941-51.

OHLSTEIN, B. & SPRADLING, A. 2006. The adult Drosophila posterior midgut is maintained by pluripotent stem cells. *Nature,* 439**,** 470-4.

PACQUELET, A., LIN, L. & RORTH, P. 2003. Binding site for p120/delta-catenin is not required for Drosophila E-cadherin function in vivo. *The Journal of Cell Biology,* 160**,** 313-9.

PAGLIARINI, R. A. & XU, T. 2003. A genetic screen in Drosophila for metastatic behavior. *Science,* 302**,** 1227-31.

PARISI, F. & VIDAL, M. 2011. Epithelial delamination and migration: lessons from Drosophila. *Cell Adh Migr,* 5**,** 366-72.

PASTOR-PAREJA, J. C., WU, M. & XU, T. 2008. An innate immune response of blood cells to tumors and tissue damage in Drosophila. *Dis Model Mech,* 1**,** 144-54.

PAULSON, A. F., FANG, X., JI, H., REYNOLDS, A. B. & MCCREA, P. D. 1999. Misexpression of the catenin p120(ctn)1A perturbs Xenopus gastrulation but does not elicit Wnt-directed axis specification. *Developmental Biology,* 207**,** 350-363.

PECE, S. & GUTKIND, J. S. 2002. E-cadherin and Hakai: signalling, remodeling or destruction? *Nat Cell Biol,* 4**,** E72-4.

PEREZ-MORENO, M., DAVIS, M. A., WONG, E., PASOLLI, H. A., REYNOLDS, A. B. & FUCHS, E. 2006. p120-catenin mediates inflammatory responses in the skin. *Cell,* 124**,** 631-44.

PEREZ-MORENO, M., SONG, W., PASOLLI, H. A., WILLIAMS, S. E. & FUCHS, E. 2008. Loss of p120 catenin and links to mitotic alterations, inflammation, and skin cancer. *Proc Natl Acad Sci USA,* 105**,** 15399-404.

PETTITT, J., COX, E. A., BROADBENT, I. D., FLETT, A. & HARDIN, J. 2003. The Caenorhabditis elegans p120 catenin homologue, JAC-1, modulates cadherin-catenin function during epidermal morphogenesis. *The Journal of Cell Biology,* 162**,** 15-22.

POTTER, C. J., TURENCHALK, G. S. & XU, T. 2000. Drosophila in cancer research. An expanding role. *Trends Genet,* 16**,** 33-9.

RADTKE, F. & CLEVERS, H. 2005. Self-renewal and cancer of the gut: two sides of a coin. *Science,* 307**,** 1904-9.

RAFTERY, L. A. & SUTHERLAND, D. J. 1999. TGF-beta family signal transduction in Drosophila development: from Mad to Smads. *Dev Biol,* 210**,** 251-68.

RAKOFF-NAHOUM, S. & MEDZHITOV, R. 2007. Regulation of spontaneous intestinal tumorigenesis through the adaptor protein MyD88. *Science,* 317**,** 124-127.

RAKOFF-NAHOUM, S. & MEDZHITOV, R. 2009. Toll-like receptors and cancer. *Nature Reviews Cancer,* 9**,** 57-63.

RAKOFF-NAHOUM, S., PAGLINO, J., ESLAMI-VARZANEH, F., EDBERG, S. & MEDZHITOV, R. 2004. Recognition of commensal microflora by Toll-like receptors is required for intestinal homeostasis. *Cell,* 118**,** 229-241.

REN, F., WANG, B., YUE, T., YUN, E.-Y., IP, Y. T. & JIANG, J. 2010. Hippo signalling regulates Drosophila intestine stem cell proliferation through multiple pathways. *Proc Natl Acad Sci USA,* 107**,** 21064-9.

REYNOLDS, A. B. 2007. p120-catenin: Past and present. *Biochim Biophys Acta,* 1773**,** 2-7.

REYNOLDS, A. B., DANIEL, J., MCCREA, P. D., WHEELOCK, M. J., WU, J. & ZHANG, Z. 1994. Identification of a new catenin: the tyrosine kinase substrate p120cas associates with E-cadherin complexes. *Molecular and Cellular Biology,* 14**,** 8333-42.

REYNOLDS, A. B., ROESEL, D. J., KANNER, S. B. & PARSONS, J. T. 1989. Transformation-specific tyrosine phosphorylation of a novel cellular protein in chicken cells expressing oncogenic variants of the avian cellular src gene. *Mol Cell Biol,* 9**,** 629-38.

RUDRAPATNA, V. A., BANGI, E. & CAGAN, R. L. 2013. Caspase signalling in the absence of apoptosis drives Jnk-dependent invasion. *EMBO Rep,* 14**,** 172-7.

RUDRAPATNA, V. A., CAGAN, R. L. & DAS, T. K. 2012. Drosophila cancer models. *Dev Dyn,* 241**,** 107-18.

RUTSCHMANN, S., KILINC, A. & FERRANDON, D. 2002. Cutting Edge: The Toll Pathway Is Required for Resistance to Gram-Positive Bacterial Infections in Drosophila. *The Journal of Immunology,* 168**,** 1542-1546.

SALAUN, B., COSTE, I., RISSOAN, M. C., LEBECQUE, S. J. & RENNO, T. 2006. TLR3 can directly trigger apoptosis in human cancer cells. *J. Immunol.,* 176**,** 4894-4901.

SALOMON, R. N. & JACKSON, F. R. 2008. Tumors of the testis and midgut in aging flies. *Fly,* 2**,** 265-268.

SANSOM, O., MENIEL, V., MUNCAN, V., PHESSE, T., WILKINS, J., REED, K., VASS, J., ATHINEOS, D., CLEVERS, H. & CLARKE, A. 2007. Myc deletion rescues Apc deficiency in the small intestine. *Nature,* 446**,** 676-9.

SANSOM, O., REED, K., HAYES, A., IRELAND, H., BRINKMANN, H., NEWTON, I., BATLLE, E., SIMON-ASSMANN, P., CLEVERS, H., NATHKE, I., CLARKE, A. & WINTON, D. 2004. Loss of Apc in vivo immediately perturbs Wnt signalling, differentiation, and migration. *Genes Dev,* 18**,** 1385-90.

SCHNEIDER, D. 2000. Using Drosophila as a model insect. *Nat Rev Genet,* 1**,** 218-26.

SCHNEIDER, D. S., AYRES, J. S., BRANDT, S. M., COSTA, A., DIONNE, M. S., GORDON, M. D., MABERY, E. M., MOULE, M. G., PHAM, L. N. & SHIRASU-HIZA, M. M. 2007. Drosophila eiger Mutants Are Sensitive to Extracellular Pathogens. *PLoS Pathog,* 3**,** e41.

SEKI, E., TSUTSUI, H., IIMURO, Y., NAKA, T., SON, G., AKIRA, S., KISHIMOTO, T., NAKANISHI, K. & FUJIMOTO, J. 2005. Contribution of Toll-like receptor/myeloid differentiation factor 88 signalling to murine liver regeneration. *Hepatology,* 41**,** 443-50.

SETO, E. S. & BELLEN, H. J. 2004. The ins and outs of Wingless signalling. *Trends Cell Biol,* 14**,** 45-53.

SFONDRINI, L., ROSSINI, A., BESUSSO, D., MERLO, A., TAGLIABUE, E., MENARD, S. & BALSARI, A. 2006. Antitumor activity of the TLR-5 ligand flagellin in mouse models of cancer. *J Immunol,* 176**,** 6624-30.

SHAW, R. L., KOHLMAIER, A., POLESELLO, C., VEELKEN, C., EDGAR, B. A. & TAPON, N. 2010. The Hippo pathway regulates intestinal stem cell proliferation during Drosophila adult midgut regeneration. *Development,* 137**,** 4147-58.

SHIA, A., GLITTENBERG, M., THOMPSON, G., WEBER, A., REICHHART, J.-M. & LIGOXYGAKIS, P. 2009. Toll-dependent antimicrobial responses in Drosophila larval fat body require Spätzle secreted by haemocytes. *J Cell Sci,* 122**,** 4505-4515.

SMALLEY-FREED, W. G., EFIMOV, A., BURNETT, P. E., SHORT, S. P., DAVIS, M. A., GUMUCIO, D. L., WASHINGTON, M. K., COFFEY, R. J. & REYNOLDS, A. B. 2010. p120-catenin is essential for maintenance of barrier function and intestinal homeostasis in mice. *J Clin Invest,* 120**,** 1824-35.

SMALLEY-FREED, W. G., EFIMOV, A., SHORT, S. P., JIA, P., ZHAO, Z., WASHINGTON, M. K., ROBINE, S., COFFEY, R. J. & REYNOLDS, A. B. 2011. Adenoma formation following limited ablation of p120-catenin in the mouse intestine. *PLoS One,* 6**,** e19880.

SMITH, A. L., DOHN, M. R., BROWN, M. V. & REYNOLDS, A. B. 2012. Association of Rho-associated protein kinase 1 with E-cadherin complexes is mediated by p120-catenin. *Molecular biology of the cell,* 23**,** 99-110.

SMITH-BOLTON, R. K., WORLEY, M. I., KANDA, H. & HARIHARAN, I. K. 2009. Regenerative Growth in Drosophila Imaginal Discs Is Regulated by Wingless and Myc. *Developmental Cell,* 16**,** 797-809.

STAIRS, D. B., BAYNE, L. J., RHOADES, B., VEGA, M. E., WALDRON, T. J., KALABIS, J., KLEIN-SZANTO, A., LEE, J.-S., KATZ, J. P., DIEHL, J. A., REYNOLDS, A. B., VONDERHEIDE, R. H. & RUSTGI, A. K. 2011. Deletion of p120-Catenin Results in a Tumor Microenvironment with Inflammation and Cancer that Establishes It as a Tumor Suppressor Gene. *Cancer Cell,* 19**,** 470-83.

STARK, M. B. 1918. An Hereditary Tumor in the Fruit Fly, Drosophila. *The Journal of Cancer Research,* 3**,** 279-301.

STEFANATOS, R. K. A. & VIDAL, M. 2011. Tumor invasion and metastasis in Drosophila: a bold past, a bright future. *J Genet Genomics,* 38**,** 431-8.

STEIGER, D., FURRER, M., SCHWINKENDORF, D. & GALLANT, P. 2008. Max-independent functions of Myc in Drosophila melanogaster. *Nat Genet,* 40**,** 1084-91.

STERGIOPOULOS, K., CABRERO, P., DAVIES, S. A. & DOW, J. A. 2009. Salty dog, an SLC5 symporter, modulates Drosophila response to salt stress. *Physiol Genomics,* 37**,** 1-11.

STERN, C. & BRIDGES, C. B. 1926. The mutants of the extreme left end of the second chromosome of Drosophila melanogaster. *Genetics,* 11**,** 503-530.

SWANN, J. B. 2008. Demonstration of inflammation-induced cancer and cancer immunoediting during primary tumorigenesis. *Proc. Natl Acad. Sci. USA,* 105**,** 652-656.

TAKEDA, K., KAISHO, T. & AKIRA, S. 2003. Toll-like receptors. *Annu. Rev. Immunol.,* 21**,** 335-376.

TAKEICHI, M., NAKAGAWA, S., AONO, S., USUI, T. & UEMURA, T. 2000. Patterning of cell assemblies regulated by adhesion receptors of the cadherin superfamily. *Philos Trans R Soc Lond, B, Biol Sci,* 355**,** 885-90.

TALVINEN, K., TUIKKALA, J., NYKÄNEN, M., NIEMINEN, A., ANTTINEN, J., NEVALAINEN, O. S., HURME, S., KUOPIO, T. & KRONQVIST, P. 2010. Altered expression of p120catenin predicts poor outcome in invasive breast cancer. *J Cancer Res Clin Oncol,* 136**,** 1377-87.

THEODOSIOU, N. A. & XU, T. 1998. Use of FLP/FRT system to study Drosophila development. *Methods,* 14**,** 355-65.

THORESON, M. A., ANASTASIADIS, P. Z., DANIEL, J. M., IRETON, R. C., WHEELOCK, M. J., JOHNSON, K. R., HUMMINGBIRD, D. K. & REYNOLDS, A. B. 2000. Selective uncoupling of p120(ctn) from E-cadherin disrupts strong adhesion. *The Journal of Cell Biology,* 148**,** 189-202.

THORESON, M. A. & REYNOLDS, A. B. 2002. Altered expression of the catenin p120 in human cancer: implications for tumor progression. *Differentiation,* 70**,** 583-9.

TRUMPP, A., REFAELI, Y., OSKARSSON, T., GASSER, S., MURPHY, M., MARTIN, G. R. & BISHOP, J. M. 2001. c-Myc regulates mammalian body size by controlling cell number but not cell size. *Nature,* 414**,** 768-73.

TZOU, P., REICHHART, J.-M. & LEMAITRE, B. 2002. Constitutive expression of a single antimicrobial peptide can restore wild-type resistance to infection in immunodeficient Drosophila mutants. *Proc Natl Acad Sci USA,* 99**,** 2152-7.

VALANNE, S., WANG, J.-H. & RÄMET, M. 2011. The Drosophila Toll signalling pathway. *J Immunol,* 186**,** 649-56.

VAN DER FLIER, L., SABATES-BELLVER, J., OVING, I., HAEGEBARTH, A., DE PALO, M., ANTI, M., VAN GIJN, M., SUIJKERBUIJK, S., VAN DE WETERING, M., MARRA, G. & CLEVERS, H. 2007. The Intestinal Wnt/TCF Signature. *Gastroenterology,* 132**,** 628-32.

VAN ROY, F. M. & MCCREA, P. D. 2005. A role for Kaiso-p120ctn complexes in cancer? *Nat Rev Cancer,* 5**,** 956-64.

VIDAL, M. & CAGAN, R. L. 2006. Drosophila models for cancer research. *Curr Opin Genet Dev,* 16**,** 10-6.

VIDAL, M., SALAVAGGIONE, L., YLAGAN, L., WILKINS, M., WATSON, M., WEILBAECHER, K. & CAGAN, R. 2010. A role for the epithelial microenvironment at tumor boundaries: evidence from Drosophila and human squamous cell carcinomas. *Am J Pathol,* 176**,** 3007-14.

WEHRLI, M., DOUGAN, S. T., CALDWELL, K., O'KEEFE, L., SCHWARTZ, S., VAIZEL-OHAYON, D., SCHEJTER, E., TOMLINSON, A. & DINARDO, S. 2000. arrow encodes an LDL-receptor-related protein essential for Wingless signalling. *Nature,* 407**,** 527-530.

WEIGMANN, K., KLAPPER, R., STRASSER, T., RICKERT, C., TECHNAU, G., JÄCKLE, H., JANNING, W. & KLÄMBT, C. 2003. FlyMove a new way to look at development of Drosophila. *Trends in genetics* 19**,** 310-311.

WHITE, B., NGUYEN, N. & MOON, R. 2007. Wnt signalling: it gets more humorous with age. *Curr Biol,* 17**,** R923-5.

WHITE, R., ROSE, K. & ZON, L. 2013. Zebrafish cancer: the state of the art and the path forward. *Nature Reviews Cancer,* 13**,** 624-36.

WODARZ, A. & NUSSE, R. 1998. MECHANISMS OF WNT SIGNALLING IN DEVELOPMENT. *Annual Review of Cell and Developmental Biology,* 14**,** 59-88.

WOOD, W., FARIA, C. & JACINTO, A. 2006. Distinct mechanisms regulate hemocyte chemotaxis during development and wound healing in Drosophila melanogaster. *Journal of Cell Biology,* 173**,** 405-416.

WOOD, W. & JACINTO, A. 2007. Drosophila melanogaster embryonic haemocytes: masters of multitasking. *Nat Rev Mol Cell Biol,* 8**,** 542-51.

WOODHOUSE, E., HERSPERGER, E. & SHEARN, A. 1998. Growth, metastasis, and invasiveness of Drosophila tumors caused by mutations in specific tumor suppressor genes. *Dev Genes Evol,* 207**,** 542-50.

WOODHOUSE, E., HERSPERGER, E., STETLER-STEVENSON, W. G., LIOTTA, L. A. & SHEARN, A. 1994. Increased type IV collagenase in lgl-induced invasive tumors of Drosophila. *Cell Growth Differ,* 5**,** 151-9.

WOODS, D. F. & BRYANT, P. J. 1991. The discs-large tumor suppressor gene of Drosophila encodes a guanylate kinase homolog localized at septate junctions. *Cell,* 66**,** 451-64.

XU, G., CRAIG, A. W. B., GREER, P., MILLER, M., ANASTASIADIS, P. Z., LILIEN, J. & BALSAMO, J. 2004. Continuous association of cadherin with β-catenin requires the non-receptor tyrosine-kinase Fer. *Journal of Cell Science,* 117**,** 3207-3219.

YAMASHITA, Y. M., JONES, D. L. & FULLER, M. T. 2003. Orientation of Asymmetric Stem Cell Division by the APC Tumor Suppressor and Centrosome. *Science,* 301**,** 1547-1550.

YOSHIDA, N., IKEMOTO, S., NARITA, K., SUGIMURA, K., WADA, S., YASUMOTO, R., KISHIMOTO, T. & NAKATANI, T. 2002. Interleukin-6, tumour necrosis factor alpha and interleukin-1 beta in patients with renal cell carcinoma. *British Journal of Cancer,* 86**,** 1396-1400.

ZAIDMAN-REMY, A., HERVE, M., POIDEVIN, M., PILI-FLOURY, S., KIM, M. S., BLANOT, D., OH, B. H., UEDA, R., MENGIN-LECREULX, D. & LEMAITRE, B. 2006. The Drosophila amidase PGRP-LB modulates the immune response to bacterial infection. *Immunity,* 24**,** 463-73.

ZETTERVALL, C.-J., ANDERL, I., WILLIAMS, M. J., PALMER, R., KURUCZ, E., ANDO, I. & HULTMARK, D. 2004. A directed screen for genes involved in Drosophila blood cell activation. *Proc Natl Acad Sci USA,* 101**,** 14192-7.

ZHANG, J., O'DONNELL, J. J., HOLIAN, O., VINCENT, P. A., KIM, K. S. & LUM, H. 2010. P120 catenin represses transcriptional activity through Kaiso in endothelial cells. *Microvasc Res,* 80**,** 233-9.

ZHANG, P.-X., WANG, Y., LIU, Y., JIANG, G.-Y., LI, Q.-C. & WANG, E.-H. 2011. p120-catenin isoform 3 regulates subcellular localization of Kaiso and promotes invasion in lung cancer cells via a phosphorylation-dependent mechanism. *Int J Oncol,* 38**,** 1625-35.

ZHANG, Z. & SCHLUESENER, H. J. 2006. Mammalian Toll-like receptors: from endogenous ligands to tissue regeneration. *Cell. Mol. Life Sci.,* 63**,** 2901-2907.

ZHAO, Z. M., REYNOLDS, A. B. & GAUCHER, E. A. 2011. The evolutionary history of the catenin gene family during metazoan evolution. *BMC Evol Biol,* 11**,** 198.

ZINKE, I., KIRCHNER, C., CHAO, L. C., TETZLAFF, M. T. & PANKRATZ, M. J. 1999. Suppression of food intake and growth by amino acids in Drosophila: the role of pumpless, a fat body expressed gene with homology to vertebrate glycine cleavage system. *Development,* 126**,** 5275-5284.

ZONDAG, G. C., REYNOLDS, A. B. & MOOLENAAR, W. H. 2000. Receptor protein-tyrosine phosphatase RPTPmu binds to and dephosphorylates the catenin p120(ctn). *J Biol Chem,* 275**,** 11264-9.